



**Otago region hazards management
investigation: tsunami modelling study**

**NIWA Client Report: CHC2007-030
September 2007**

NIWA Project: ORC07503

Otago region hazards management investigation: tsunami modelling study

Emily Lane
Roy Walters
Michelle Wild
Jade Arnold
Matt Enright
Helen Roulston
Joshu Mountjoy

Prepared for

Otago Regional Council

NIWA Client Report: CHC2007-030
September 2007
NIWA Project: ORC07503

National Institute of Water & Atmospheric Research Ltd
10 Kyle Street, Riccarton, Christchurch
P O Box 8602, Christchurch, New Zealand
Phone +64-3-348 8987, Fax +64-3-348 5548
www.niwa.co.nz

Contents

Executive summary	iv
1. Introduction	1
2. Literature and data review	5
2.1. Far field tsunamis	5
2.2. Regional and near-field tsunamis	11
2.2.1. Geological setting	11
2.2.2. Potential fault sources	13
2.2.3. Potential submarine landslide sources	18
2.2.4. Potential submarine landslide triggers	19
3. Modelled tsunami events	20
3.1. Far-field tsunamis	20
3.2. Regional and near-field tsunami	21
4. Numerical modelling of tsunamis	22
4.1. Model Grid – Topography and Bathymetry	22
4.2. Numerical model	25
4.3. Submarine landslide model	26
4.4. Initial conditions	26
4.4.1. Puysegur subduction zone fault generation event	27
4.4.2. Landslide generation events	28
4.4.3. Far-Field tsunami	29
5. Numerical modelling results	29
5.1. Near-field	32
5.2. Far-field	37
5.3. In-depth Areas	38
5.3.1. Tautuku	42
5.3.2. Papatowai	53
5.3.3. Catlins	64
5.3.4. Kaka Point and Clutha	75
5.3.5. Toko Mouth	95
5.3.6. Taieri Mouth	106
5.3.7. Brighton	126
5.3.8. Kaikorai and Waldronville	137
5.3.9. South Dunedin	148
5.3.10. Dunedin Harbour	159
5.3.11. Long Beach and Purakanui	170

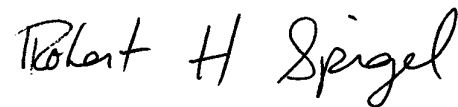
5.3.12	Warrington and Blueskin Bay	181
5.3.13	Karitane	192
5.3.14	Moeraki	203
5.3.15	Hampden	214
5.3.16	Taranui and Kakanui	225
5.3.17	Oamaru	236
6.	Discussion	247
6.1	Near-field	247
6.2	Fair-field	248
7.	Conclusion	248
8.	References	249
Appendix A: Observations from South American Tsunamis		
Appendix B: Background geological information for Otago faults		
Appendix C: RiCOM model description		
Appendix D: Background geological information for Otago submarine landslide		
Appendix E: Velocity vectors for the Clutha Delta		

Reviewed by:



James Goff

Approved for release by:



Bob Spiegel

Executive Summary

Otago Regional Council contracted NIWA to undertake a tsunami inundation study for the Otago region. The particular focus of this work was to identify inundation associated with credible near- and far-field tsunami sources for specific communities along the Otago coastline.

The most likely tsunamigenic sources were first identified. For near-field tsunamis this was a large subduction zone earthquake (around $M_w 8.5$) on the Puysegur fault, which has a return period of approximately 1:600 years and is also the probable maximum frequency earthquake for this region. Submarine landslides were also considered as a source but modelling showed that their effect on the coastline was localised and fairly small.

South America was identified as the source of far-field tsunamis that threaten the Otago coastline. Two tsunamis, corresponding to a 1:100 year tsunami and 1:500 year (also equivalent to the far-field PMF) tsunami originating from a similar region along the Chilean coast were considered.

The numerical model RiCOM was used to produce the results described in this report. Three numerical grids were produced using GridGen to study local submarine landslides, the Puysegur subduction zone and South American remote tsunamis respectively. Inundation grids for the communities of interest were embedded within these larger grids. These inundation grids contain topographic information taken from LIDAR data and were used to quantify the inundation caused by each tsunami.

Results show that a subduction zone earthquake in the Puysegur fault causes the most inundation of the Otago coast as a whole and especially in the southern section. Waves are refracted around the bottom of New Zealand and coastally trapped waves travel as far north as Oamaru.

Remotely generated South American tsunamis can also cause considerable inundation. Furthermore these occur more frequently with the return period for a moderate tsunami being in the order of 1:100 years. Remote tsunamis are the most significant source for the section of coastline north of Otago Peninsula.

Sea level rise scenarios of 30 and 50 cm were also studied for each of the tsunami sources. These showed that both inundation depths and maximum water speeds increased with sea level rise indicating that the risks of inundation and erosion may be even greater in the future.

1. Introduction

The Otago Regional Council contracted NIWA to undertake a hazards management investigation into the risk to coastal and estuarine communities along the Otago coast from storm surge and tsunami events. As storm surge and tsunamis represent independent threats to the Otago coast, this investigation has been separated into two parts with this initial report covering the tsunami component including:

1. The determination of tsunami events to be modelled.
2. Computational modelling of tsunami events, including the effects of sea level rise, and mapping of scenarios for sites of interest.

The Otago coastline investigated in this study extends from the Waitaki Fan in the north, to Wallace Beach in the south (Figure 1.1). The places of interest, where wave run-up, wave speeds and inundation mapping will be specified and mapped include the settlements of:

- Tautuku Peninsula,
- Papatowai,
- Catlins Lake/Catlins River settlements (including Jacks Bay and Surat Bay),
- Kaka Point,
- Clutha delta,
- Toko Mouth and estuary,
- Taieri Mouth and estuary,
- Brighton,
- Kaikorai Mouth and estuary,
- Dunedin Harbour and South Dunedin (including St. Clair, St Kilda, and Tomahawk beaches),
- Long Beach,
- Purakanui and estuary,
- Moeraki,
- Hampden,
- Kakanui/Taranui and,
- Oamaru.

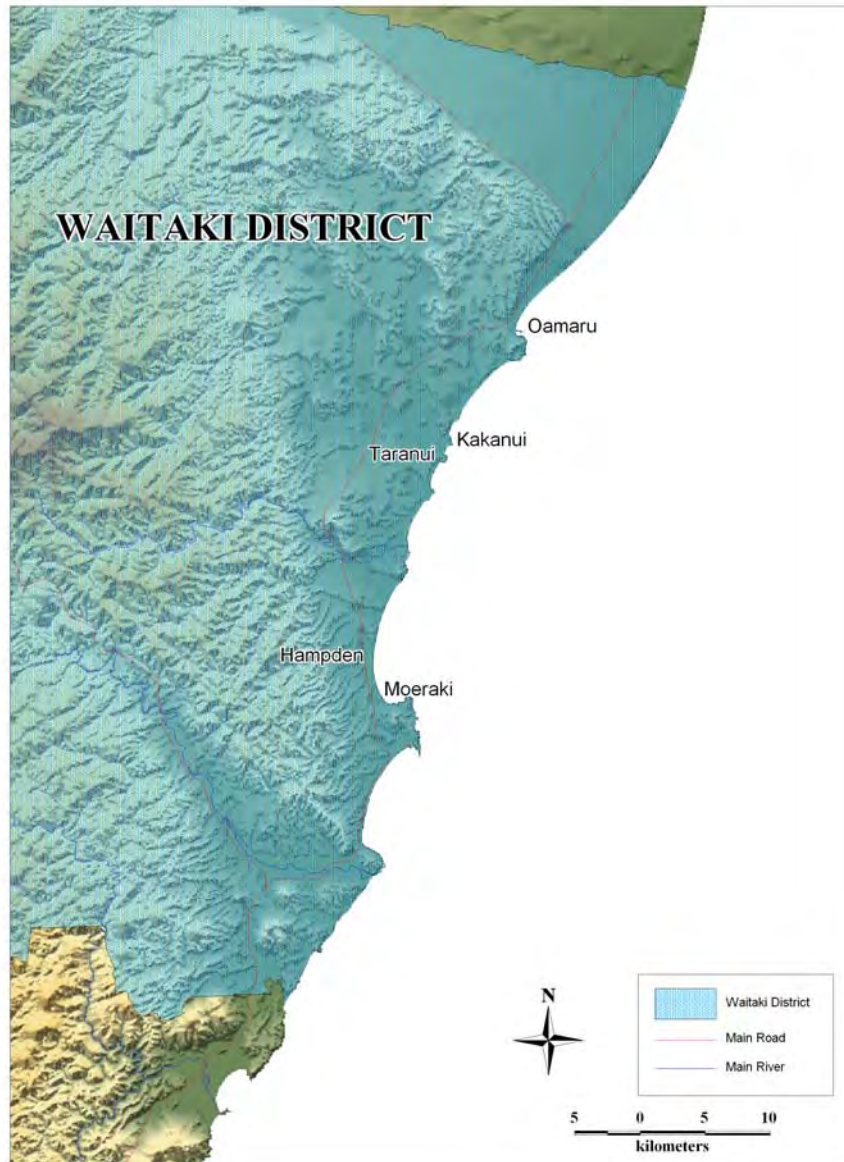






Figure 1.1: Maps of Waitaki District, Dunedin City and Clutha District including study areas. (provided by ORC)

2. Literature and data review

Tsunami events affecting the Otago coastline have been separated into far-field and near-field sources. Near-field tsunami sources (Section 2.2) include the regional Puysegur subduction zone (see Glossary), while other more distant, regional sources have been included with far-field ones (Section 2.1).

2.1. Far field tsunamis

Earthquakes with magnitude $M > 8$ are the most common source of damaging tsunamis worldwide. Approximately 80% of these earthquakes occur around the perimeter of the Pacific Ocean (Berryman, 2005). Figure 2.1 shows earthquake source locations for tsunamis dated between 1840 and 2007 (National Geographic Data Center (NGDC) tsunami database).

For a far-field tsunami to have a significant impact on the Otago coastline, the outgoing wave (generated at the source) needs to be orientated directly towards the Otago coast. Table 2.1 summarises earthquake source features and tsunami propagation for the various regions around the Pacific that have an impact on New Zealand. Most of this data was summarised from Berryman (2005). Figure 2.2 also highlights tsunami sources that have had the greatest impact on the Otago coastline.

The regions that potentially have the largest impact on the Otago coastline are South America, Cascadia, Alaska & Aleutians, and Kurile Islands (Table 2.1). Figure 2.2 shows that of these areas, South American sources have historically had the greatest impact along the Otago coast. Berryman (2005) supports South American sources as being the most likely risk for Dunedin by assigning 83% and 93% contributions to total risk for 100 year and 500 year return periods, respectively, from South America. The Aleutians were the only other far field region included with a 2% contribution to total risk for Dunedin for a 100-year return period (the remaining % contributions were assigned to the 'regional' Puysegur subduction zone source).

Significant tsunamis from South America in the last 150 years were:

- 13 August 1868 at 4:45pm - northern Chile (21 m local maximum water height) (see Glossary under 'Tsunami Height')

In New Zealand the tsunami occurred from 15-17 August. It is the most widespread tsunami reported in New Zealand, and the only tsunami to have directly caused the loss of human life in New Zealand (de Lange & Healy, 1986).

Table 2.1: Summary of earthquake source characteristics and tsunami propagation in relation to impacts on New Zealand (Berryman, 2005; and other sources) (See Glossary for definition of M_w)

Source region	Earthquake magnitudes and frequency	Tsunami propagation
South America	Historical records indicate large earthquakes and tsunamis occur relatively frequently (approximately every 50 years there is an earthquake with $M_w > 8.5$). Earthquake magnitudes of M_w 9.4-9.5 (for example, 1960 earthquake) are likely to represent the upper limit of magnitude for the whole of South America (and worldwide).	The orientation of the faults, together with the seabed bathymetry between South America and NZ, combine to generate tsunamis that are often well directed towards NZ. There are also few islands to dissipate the tsunami wave energy. Fluctuations in water level of over 2.5m have been observed at Oamaru for 3 events originating in South America (1868, 1877 & 1960)
Mexico & Central America	Maximum historical earthquakes in this area have been $M_w < 8.5$, which is not likely to generate damaging tsunamis. Potential for larger earthquakes is small.	Not orientated towards NZ.
Cascadia	Fault rupture thought to occur either as whole-region ruptures of $\sim M_w$ 9.0 at recurrence intervals of ~ 800 years or in earthquakes with $M_w < 9.0$ which may occur more frequently.	Research suggests that this source could result in wave heights of ~ 3 m in places along the north and east coasts of NZ. The smaller earthquakes would probably not pose a significant risk.
Alaska & Aleutians	Highly active source with 3 historical earthquakes of significant magnitude (1964 = M_w 9.4 Alaska, 1957 = M_w 8.7-9.1 Rat Is, 1946 = M_w 7.9 Aleutian).	Not very well directed towards NZ, except for the area around the source zone of the 1957 Rat Island earthquake. Run-ups of up to 2m have been observed along the NZ north and east coasts, but Tonkin & Taylor (1997) do not document any observations for the 1946 or 1957 events for Otago. For the 1964 event 0.5m fluctuations were observed at the Clutha Mouth.
Kurile Islands, Kamchatka	In 1952 a M_w 9 earthquake occurred south of Kamchatka Peninsula producing a maximum local run-up of 19m. A 1737 earthquake of M 8.3 produced a local run-up of 63m, and a 15m run-up over 1000km away.	No observed effects from the 1952 tsunami were noted for the Otago coast, although there was a 0.1-0.3m fluctuation on the Otago Harbour tide record (Tonkin & Taylor, 1997).
Japan	No events thought to be of magnitude > 9 in long historical local record (of several hundred years), but many greater than 8.	Not orientated towards NZ and the islands along any propagation path also dissipate wave energy. Only very small waves height < 1 m recorded in NZ.
Solomon Islands, PNG	Historically, very few earthquakes from this area have magnitude > 8.5 and it is thought that there is little capacity to do so.	Not orientated towards NZ and the large number of islands along the propagation path also dissipate wave energy. Only small wave heights have been recorded in NZ. The recent M 8.0 Solomon Is tsunami on 2 April 2007 recorded a 1.1m maximum crest-to-trough wave at Charleston. However the maximum wave was significantly smaller on the east coast (Sumner = 0.12m).
South of NZ (excluding Puysegur subduction zone)	Most plate boundary zones are strike-slip and large earthquakes are unlikely to produce large tsunamis.	M 8.1 events along Macquarie Ridge and near Balleny Island have produced small tsunamis (< 0.5 m) in southern NZ.
Southern New Hebrides, Tonga & Kermadec Trench	Earthquakes greater than M 8.5 are probably possible in these regions.	Possible risk to Northland, Auckland and Bay of Plenty areas more so than Otago. Historically, no observed effects along the Otago coast.
Outside Pacific region		Not orientated towards NZ and not likely to generate significant water level fluctuations along NZ coasts. Historical record of tsunami observations for Otago shows that maximum fluctuations of 1m occurred in Oamaru after the 1883 Krakatau volcanic eruption. The Boxing Day 2004 M 9 Sumatra tsunami generated a maximum wave height of 0.27m in Otago Harbour (www.mulgor.co.nz).



Figure 2.1: World map showing tsunami-generating earthquake sources from 1840 to 2007 with magnitude 7.5 or greater. [Source: http://www.ngdc.noaa.gov/seg/hazard/tsevsrch_idb.shtml] (1. South America. 2. Cascadia. 3. Alaska and Aleutian Islands. 4. Kurile Islands.)



Figure 2.2: World map showing far-field tsunami-generating sources (mainly earthquakes) from 1840 to present that may have had an impact on the Otago coastline. Numbers = earthquake magnitude (year of event), ● = observed waves ≥ 1m, ● = observed waves < 1m, ● = no obvious tide record observations or observations up to approximately 0.3m (observed wave heights are as at the Otago coast) [Primary sources: http://www.ngdc.noaa.gov/seg/hazard/tsevsrch_idb.shtml, Tonkin & Taylor (1997)]

- 10 May 1877 at 0:59am - northern Chile (24 m local maximum water height)

This was extensively recorded around New Zealand, although the impact was less significant than the 1868 tsunami.

- 22 May 1960 at 19:11 – southern Chile (25 m local maximum water height)

A giant earthquake of magnitude 9.5 generated this tsunami. Cisternas et al. (2005) suggest that this earthquake ended a recurrence interval that began 385 years earlier with a 1575 earthquake. Earthquakes that followed in 1737 and 1837 appear to have produced negligible subsidence or tsunamis and, as a result, are likely to have left the fault partly loaded with accumulated plate motion. The 1960 earthquake would probably have released this loading, producing a fault slip representative of approximately 200-300 years worth of plate motion.

In New Zealand, the tsunami distribution in 1960 was similar to the 1868 and 1877 tsunamis, but wave heights were generally smaller. Contemporary reports show that the hardest hit areas were tidal estuaries and streams south of Dunedin (de Lange & Healy, 1986), making the effects of 1960 and 1868 tsunamis similar along the Otago coast.

Other large tsunamis from South America (recorded in South America but likely to have impacted the Otago coastline) prior to this time are (based upon the NGDC tsunami database):

- 20 February 1835 at 16:22 – central Chile (24 m local maximum water height)
- 29 October 1746 at 3:30 – Peru (24 m local maximum water height)
- 8 July 1730 – central Chile (16 m local maximum water height)
- 24 November 1604 – Peru (16 m local maximum water height)
- 10 July 1586 - Peru (24 m local maximum water height)
- 16 December 1575 – central Chile ('high tsunami', Cisternas et al. (2005))
- 28 October 1562 – central Chile (16 m local maximum water height)

Therefore, in the last 445 years there have been at least 10 tsunami events from South America, which could have had a significant impact on the Otago coastline. This indicates that, on average, approximately every 45-50 years we are likely to observe a relatively large event (compared to the smaller events like the 2001 Peru tsunami that

had a 7 m local maximum water height, but was only observed in tide records in New Zealand as fluctuations significantly less than 1 m).

It is also important to note that bays and inlets around the New Zealand coast have specific natural frequencies. If the natural frequency of the bay matches that of the tsunami waves, amplification of the waves will occur. This can often explain variations in tsunami height experienced along the coast for each event, and also between different tsunamis. For example, widespread shallow mudflats in Otago Harbour can quickly dampen any waves. This means that tsunamis are not often observed in the harbour (Heath, 1976).

Table A.1 (Appendix A) summarises the observations from the three large South American tsunamis that have inundated the Otago coast since European settlement. This information shows that, although these tsunamis all came from South America, the observations for each event do not necessarily vary linearly for different locations along the Otago coast. The time of arrival also means that if the tsunami arrives at night, less visual observations can be made. This all combines to make it complicated in determining which event is more severe for the Otago coast (especially since the characteristics of the incoming waves mean that they may cause amplification on different areas of the coast).

One advantage of the main far-field source of potentially damaging tsunamis originating in South America is that travel times to the Otago coast are well over 12 hours. This gives sufficient time for evacuation, unlike near-field tsunamis where it may only be a matter of minutes between feeling an earthquake and the tsunami arriving.

Other potential sources of far-field tsunamis for the Otago coast include:

- Volcanoes

The 1883 Krakatau eruption generated tsunami-like water level oscillations that were observed in New Zealand. The wave is thought to have been created by the coupling of an atmospheric pressure wave with the ocean.

- Sector collapse landslides

Large tsunamis could be generated in New Zealand from failure along the sides of the Hawaiian volcano chain - there is potential for sector collapses of 1000-5000 km³ to occur. Return periods from any one source are large (Berryman, 2005).

- Asteroids

There is evidence of at least one large impact of an asteroid. This was the late Pliocene (see Glossary) impact of the Eltanin asteroid into the Bellingshausen Sea (Gersonde *et. al.*, 1997).

Although such events are possible, the return periods for sector collapse landslide or asteroid scenarios are extremely large, and the effect of a volcanic eruption (1883 Krakatau eruption) observed in New Zealand was less extreme than the South American tsunamis of 1868, 1877 & 1960. Therefore, none of these events have been included in the modelled scenarios.

2.2. Regional and near-field tsunamis

2.2.1. Geological setting

New Zealand is located on the boundary between the Pacific and Australian plates (Figure 2.3). This plate boundary includes subduction zones (the Hikurangi and Puysegur) a strike-slip fault (see Glossary) system (the Marlborough faults), and a transform plate boundary fault (the Alpine Fault), see figure 2.4 for locations.

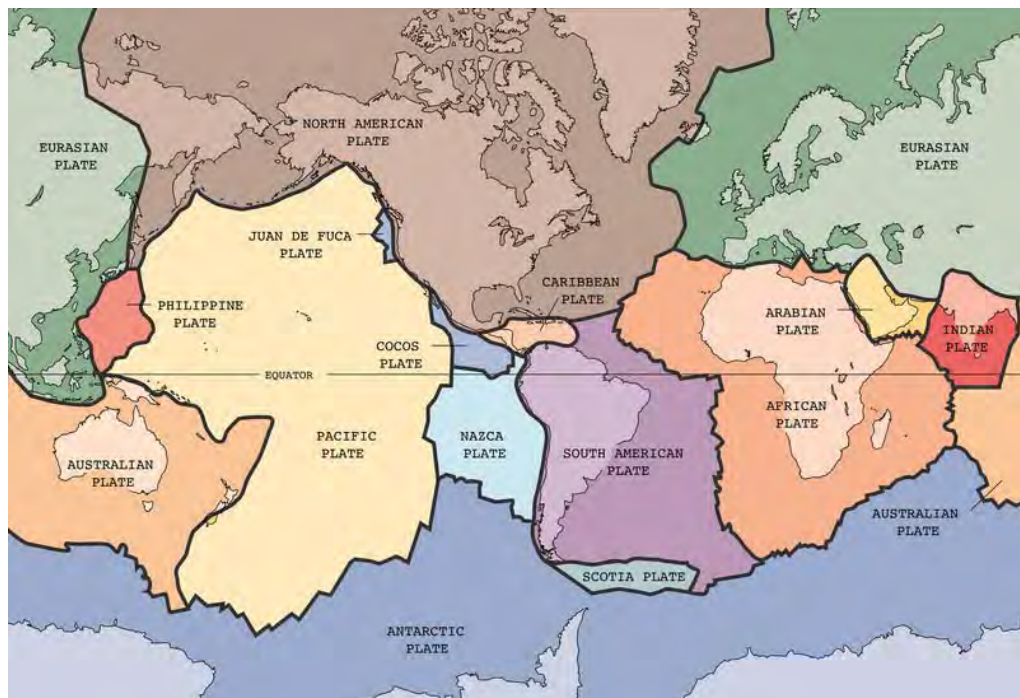


Figure 2.3: Tectonic plate boundaries (http://en.wikipedia.org/wiki/Image:Tectonic_plates.png)

The above tectonic features (along with the transitions between these features) are all either potential direct or indirect tsunami sources for the Otago coastal region. Of particular interest, with regards to tsunamis, are fault ruptures that lie within the local coastal/marine environment, as well as more distant faults that are capable of generating significant groundshaking in the Otago region (i.e. submarine landslide triggers). Areas investigated for this study include the Akatore Fault, Takapu Fault, Puysegur subduction zone and the Otago submarine fan complex (potential submarine landslide source).

Figure 2.4 shows that most, but not all, of the active faults in the Otago region are located on land. This means that fault ruptures are unlikely to directly generate a tsunami. However, as some of these faults are capable of producing MM VII+ intensity earthquakes in the Dunedin City area, they may be able to trigger submarine landslides along the edge of the continental shelf.

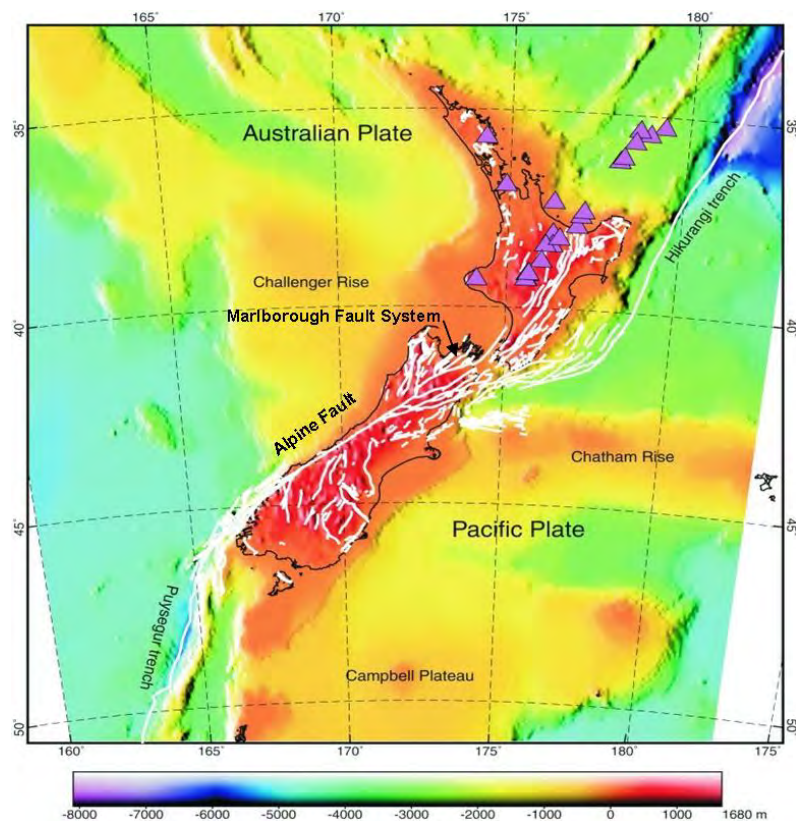


Figure 2.4: The tectonic environment of New Zealand overlying shaded-relief topography. White lines = active and potentially active fault traces, triangles = active volcanoes (Liu & Bird, 2002). Note that the Puysegur trench lies to the South West of New Zealand and this region includes the Puysegur Bank and other related areas.

Therefore, the potential near-field tsunami sources for the Otago coastline are likely to be either:

- a fault rupture from a local or regional offshore source (Section 2.2.2), or
- a submarine landslide along the edge of the continental shore, triggered by an earthquake (Section 2.2.3).

2.2.2. Potential fault sources

For a fault rupture to directly generate a tsunami, the fault must:

- produce significant vertical deformation of the sea bed, and
- be orientated in a direction so that any resulting wave will be directed towards the coastline.

As we are interested in deriving 1:100 year, 1:500 year, and probable maximum frequency (PMF) events, the faults also need to be active (i.e. events with return periods of a million years will not be relevant for 1:100 and 1:500 year events).

It is also important to note that, in some cases, locally generated tsunamis may only have a significant impact on a part of the Otago coastline. This may be due to, for example, the orientation of the fault or submarine landslide. Potential regional and near-field tsunami sources have therefore been separated into sources north and south of Otago Peninsula. Potential fault sources for the Otago coast are summarised below.

Potential fault sources south of Otago Peninsula

1 Puysegur subduction zone

At the Puysegur Trench, the Australian Plate moves beneath the Puysegur Bank and the Fiordland Massif (Lamarche & Lebrun, 2000). The Puysegur subduction zone extends approximately 150 km southwest from the southern end of the Alpine Fault, as shown in Figure 2.4.

Table 2.2 summarises large historical earthquakes known to have occurred in the Puysegur Bank region, which includes the Puysegur Bank, Puysegur Trench and Solander Trough. It should be noted that prior to the 1960s when a worldwide seismic network was established, large earthquakes in this area could not be accurately identified and located (Berryman, 2005).

Table 2.2: Summary of recent earthquakes in the Puysegur Bank region

Location	Date	M _w	Depth (km)
Puysegur Bank (-47.13S, 166.27E)	3 Nov 1918	6.7*	8 ± 5*
Puysegur Bank (-46.83S, 165.80E)	1 Sep 1945	7.4-7.7*	28 ± 5*
Solander (-46.49S, 166.68E)	25 Sep 1968	6.3	4
Puysegur (-46.69S, 165.74E)	12 Oct 1979	7.2	12
Resolution Ridge (-46.06S, 165.03E)	31 Jan 1985	6.2	27
Puysegur Trench (-46.68S, 164.72E) #	23 Nov 2004#	7.1#	10#

NGDC Significant Earthquakes Database

* Summarised in Doser et al. (1999).

Although the Puysegur subduction zone is active, since 1918 all earthquakes in this area have had a magnitude of approximately ≤ 7.7 . There have also been no reported observations of tsunamis as a result of these earthquakes along the Otago coastline prior to 1997 (Tonkin & Taylor, 1997), and no tsunami was observed on the Dog Island record (recorded at a 1 minute interval) for the November 2004 event. This suggests that the Puysegur subduction zone would need to generate a fault rupture with a magnitude of the order of 7.7 or greater to generate a significant tsunami. It seems likely that a 7.7+ magnitude event along the Puysegur subduction zone will have a relatively high return period.

South of the Puysegur subduction zone, both the Macquarie Ridge and Balleny Islands areas have produced large M_w 8.1 earthquakes in recent years. However, the earthquakes occurring at Macquarie Ridge (1989 and 2004) and near the Balleny Islands (1998) have all been strike-slip events. As such, these events have not generated large tsunamis due to the lack of significant vertical uplifting of the seabed. The resulting tsunamis that have reached New Zealand have all had a magnitude less than 0.5 m, and it is not expected that significantly larger events are likely due to the fault characteristics of the area. As no highly active subduction zones have been identified to the south of the Puysegur subduction zone area, it is assumed for this study that the Puysegur subduction zone is the most likely tsunami source for the area south of New Zealand.

When Walters and Callaghan (2005) investigated the possible sources of the 1820s Southland tsunami, five separate fault rupture events were modelled:

- Alpine Fault rupture

- Fiordland subduction zone event (with and without surface rupture)
- Puysegur subduction zone event (with and without surface rupture).

Of these events, only the Puysegur subduction zone events caused significant effects on water levels as far east as the south-east coast of the South Island. Both the Puysegur surface rupture case (rupture from 25 km depth to surface, 8.64 M_w event) and no surface rupture case (rupture from 10 – 25 km depth, 8.49 M_w event) generated maximum water level elevations in the vicinity of Bluff and Papatowai of >1 m. In both cases a maximum fault rupture scenario was modelled. This involved fault ruptures along the full length of the zone with 8 m displacement on the fault and a 10 degrees eastward dip.

Berryman (2005) estimates that a M8.7 earthquake is the upper limit for the Puysegur subduction zone, and that the recurrence interval is weighted as:

- 300 year (0.25)
- 600 year (0.5)
- 1500 year (0.25),

where the number in brackets is the probability of the given return period. Thus the most likely return period according to Berryman (2005) is 600 years.

2 *Akatore Fault*

The Akatore Fault (Figure 2.5) is a reverse fault (see Glossary) that is approximately 65 km long. The fault is orientated northeast-southwest to north-south, and the onshore section of the fault can be identified by scarps passing along hillsides and across marine and fluvial terraces (Litchfield and Norris, 2000). The northern offshore section of the Akatore Fault extends from south of the Taieri River mouth to Otago Peninsula, where the fault extends onshore north of Waldronville (heading in the direction of Dunedin City). The southern offshore section of the fault extends from south of the Tokomairiro River mouth to offshore from the Clutha River mouth. As the fault approaches the Clutha River mouth it divides into 3 fault structures. The offshore sections of the Akatore Fault were mapped by Johnstone (1990).

Litchfield & Norris (2000) concluded that:

- The onshore section of the Akatore Fault has a scarp dating from the last major uplift event that occurred around 1150-1000 yr BP [Geoarchaeological

evidence along the coast, has revised these dates to most likely be in the period 1350-1370 AD (B. McFadgen, pers. Comm.. 2006; Goff et al., 2006)]. Evidence suggests that the whole fault ruptured during this event with a vertical change of 2-4 m.

- The previous uplift event is likely to have been post-3800 yr BP. This is based on a radiocarbon date from the base of Bull Creek swamp, and evidence of localised rupture at the southern end of the fault. Uplift of a 6 m marine terrace may have been caused by this event.
- There is no evidence of fault movement in the period between formation of the terrace (80 ka) and the post-3800 yr BP event. If this is the case, then the Akatore Fault is not behaving in a characteristic fashion.

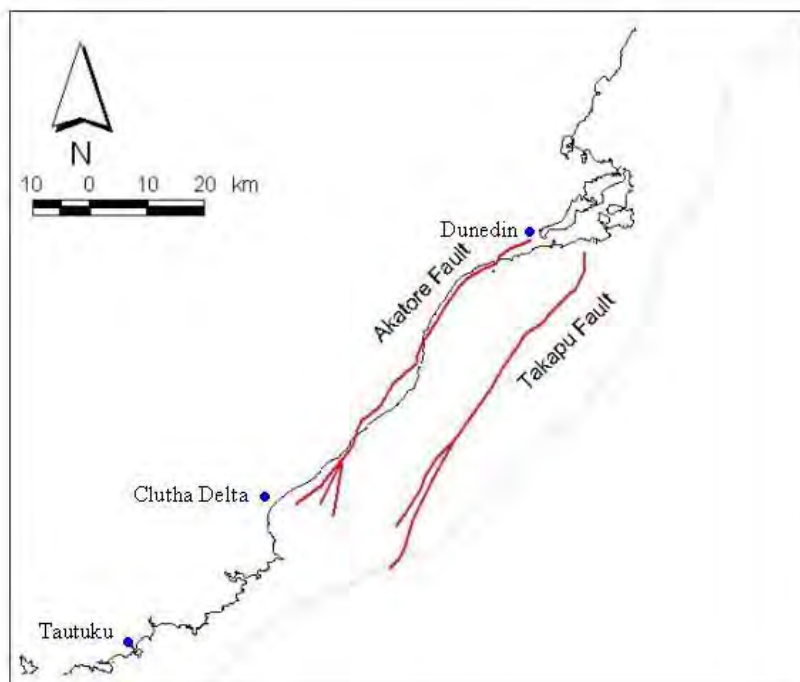


Figure 2.5: Indicative location of the Akatore and Takapu Faults (location of faults estimated from Norris & Litchfield, 1996) which lie on the northern end of the Waipounamou Fault System. (Note: black line = coastline, grey line = 100 m depth contour).

Norris & Litchfield (1996) estimated that the Akatore Fault had displacement upwards on the southeast, a likely vertical uplift of 2 m (magnitude 7-7.3), and a frequency of 5-10,000 years.

The Dunedin City Lifelines Project Report (December 1998) identified the potential source for a maximum credible earthquake for Dunedin City to be a surface breaking event on a fault of the Akatore system. It is thought that this could produce a probable maximum bedrock intensity in the city area of MM IX. The source used as the maximum credible event is described as a single continuous rupture along 40 km of the Akatore Fault, with rupture extending to within 20 km from the centre of Dunedin. The epicentre was taken to be offshore, just north of the Taieri River mouth, with the earthquake magnitude estimated as M7.0. The frequency of this event was estimated as approximately 7,000 years (5,000-10,000 years).

3 Takapu Fault Zone - Waipounamou Fault System

The Takapu fault zone is located at the northern limit of the Waipounamou Fault System, and contains the only northeast orientated, continuous, fault structures identified on seismic profiles for this area (Norris & Litchfield, 1996). The Takapu Fault (Figure 2.5) is the main fault within the Takapu fault zone, and is considered comparable to the Akatore Fault as it has displacement up on the southeast, a likely vertical uplift of 2 m (magnitude 7-7.3) and a frequency in the order of 5-10,000 years (Norris & Litchfield, 1996). Two other faults, with the same orientation, lie between the Akatore and Takapu Faults and have been identified as having similar characteristics (Norris & Litchfield, 1996).

The predicted slip rate in this region (as described by Liu & Bird (2002)) is estimated to be up to 4.7 mm/yr (Liu & Bird, 2002). Since the onshore Akatore Fault has a slip rate under 2 mm/yr (Litchfield & Norris, 2000), the Akatore Fault may not have been the cause of M4+ events that occurred around Dunedin in 1974, 1982, 1989 and 1991. Instead, the offshore faults may contribute a significant proportion of the local seismic hazard (Liu & Bird, 2002). Liu & Bird (2002) conclude that the offshore SE coastal fault needs to be included in seismic hazard estimates. A more detailed description of the location of the modelled SE coastal fault, and the derivation of the slip rates, are given in Appendix B.

4 Castle Hill fault zone

The Castle Hill fault zone runs offshore in a NW-SE direction from the Clutha River mouth area. The offshore section of the fault is approximately 35 km in length. The activity is roughly estimated as being reverse uplift on the NE side, with uplift of about 1 m (magnitude 6.5-7) with a frequency of approximately 10,000 years (Norris & Litchfield, 1996). It is stated that this is 'at best an educated guess'.

Potential fault sources north of Otago Peninsula

1 Waihemo Fault System

The Waihemo Fault System extends offshore for at least 8 km from Shag Point. Norris & Litchfield (1996) estimate activity as being an upwards displacement on the northeast of about 1 m per event (magnitude 6.5-7) with an uncertain, estimated, frequency in the order of 10,000 years.

2 Waitati Fault System

The Waitati fault system runs parallel to the coast from approximately Shag Point in the north, to Warrington in the south. As the fault passes very close to the shore it is difficult to identify. Norris & Litchfield (1996) estimate activity as being an upwards displacement on the southeast, with a probable displacement of 1-2 m per event (magnitude 6.5-7.5) and an uncertain, estimated, frequency in the order of 10,000 years.

2.2.3. Potential submarine landslide sources

Sediments eroded from the Southern Alps travel across the continental shelf and into the Otago fan complex, located at the head of the Bounty Trough (Carter & Carter, 1996). The Otago fan complex is located in water depths of 250-1500 m, and is made up of a series of fans fed by nine major and a large number of minor submarine canyons. These canyons, extending along a 200 km section of the continental slope, merge into North, Centre and South channels which, in turn, combine to form the Bounty Channel (Carter & Carter 1988).

Figure 2.6 shows the transition from the continental shelf to the Bounty Trough. The bathymetry of the Bounty Trough, with slopes of up to 37 m/km (2°) towards the trough head, reducing to approximately 3.5 m/km (0.2°) along the trough axis are dictated by the paths of sediment supply and locations of sediment deposition (Carter & Carter, 1996).

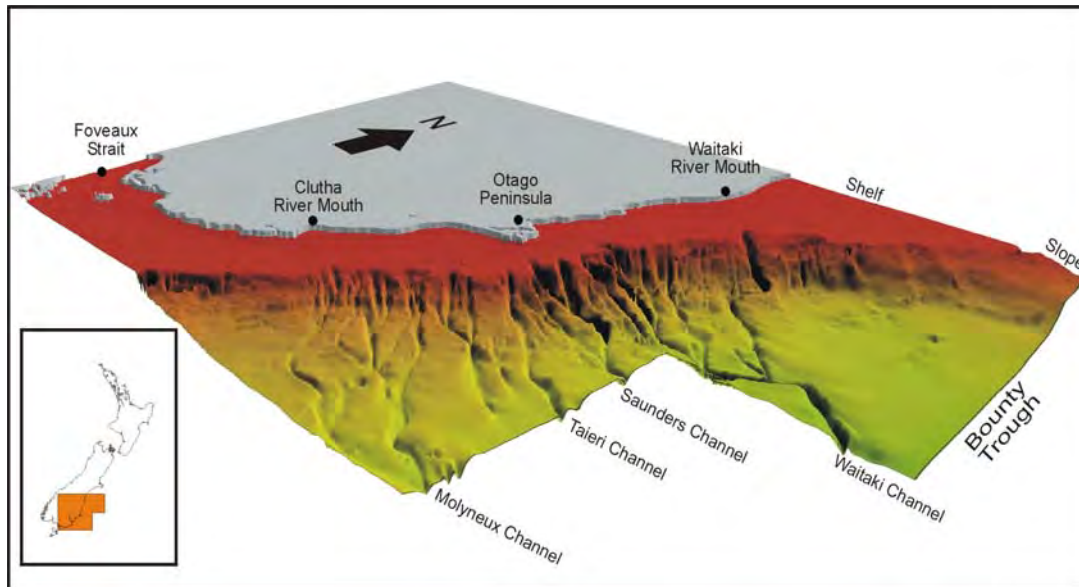


Figure 2.6: Eastern South Island continental margin showing the transition from the continental shelf to the Bounty Trough (source: <http://www.indstate.edu/gomez/margins.html>)

2.2.4. Potential submarine landslide triggers

It is possible that earthquakes with a magnitude 5.1 or greater (Walters, et al 2004) could be sufficient to trigger a submarine landslide.

The Dunedin City Lifelines Project Report (December 1998) identified potential sources for a design earthquake of Modified Mercalli Scale VII (MM VII) for Dunedin City to be:

- Rupture along any one of the longer fault segments in the central and eastern Otago region (not including the Akatore Fault). There are at least 10 faults in a 100 km radius of Dunedin that could potentially generate earthquakes that measure 6 on the Richter Scale (M6). Larger events on any of the western Otago fault zones or eastern Fiordland faults could also generate similar intensities in Dunedin.

Frequency: Of these faults, no single fault segment is highly active. Recurrence intervals are of the order of 5000 years. If it is assumed that an even distribution of events occurs over time, a likely recurrence interval for an M6 earthquake on at least one of these structures is of the order of 300-500 years.

- Earthquakes of magnitude $M > 7.5$ along the Alpine Fault, including the Fiordland onshore and offshore segments.

Frequency: 200-400 years

- Small to moderate ($M_{4.5-5.5}$) earthquakes within 20 km radius of Dunedin Centre. In 1974 Dunedin earthquake ($M_{4.9}$) produced maximum intensities of MM VII in a limited area. Unfortunately fault segments capable of generating these smaller earthquakes are difficult or impossible to recognize in surface geology.

Frequency: Uncertain, probably 150 years at the top of the range.

3. Modelled tsunami events

3.1. Far-field tsunamis

The literature review identified South America as being the most likely source of far-field tsunami able to cause significant damage to the Otago coast. This is due to the tsunami generated by fault rupture sources in South America being:

- Highly likely to be orientated towards New Zealand,
- Uninhibited by islands or other landmasses that may disperse wave,
- Of a magnitude to produce significant wave heights on arrival at the New Zealand coast.

As outlined in section 2.1, large subduction zone tsunamis are generated in South America approximately every 45-50 years. Their impact on the New Zealand coastline depends on the position of the earthquake along the fault. In particular, earthquakes with epicentres around the Peru-Chile border (around 19°S to 8°S) tend to direct tsunamis towards New Zealand. The 1868 tsunami from this border region was generated by a smaller magnitude earthquake than the 1960 event, but produced a tsunami equivalent in size.

Based on this information we propose the 1868 tsunami in reality is representative of both the 1:100 year AND 1:500 year event. For the probable maximum frequency scenario though, we propose an earthquake with a moment magnitude comparable to that of the 1960 but with epicentre at the location of the 1868 event.

3.2. Regional and near-field tsunami

Potential fault rupture sources

The main regional and near-field fault rupture sources, identified in this study as being potentially capable of generating the design events, are summarised in Section 2.2.2.

Of these sources, only the Puysegur subduction zone appears to be regularly active, with a likely upper limit of a M8.7 earthquake that has a 0.5 weighting of having a recurrence interval of 600 years (Berryman 2005). The other offshore faults identified in section 2.2.2 have estimated return periods of $\geq 5,000$ years.

As the return periods for the near-field faults (excluding Puysegur) are all estimated at having long return periods, none of the local faults are capable of generating a 1:100 or 1:500 near-field tsunami event. However, a fault rupture along the Akatore or Takapu fault could potentially be considered for a probable maximum event for the coast south of Otago Peninsula, and Waitati Fault for north of Otago Peninsula. Our studies of these faults however, indicates that they are not probable maximum events, and in reality are more likely to be important for generating groundshaking induced submarine landslides off the continental slope.

Tonkin & Taylor (1997) estimate that the near-field faults (excluding Puysegur) would produce a maximum credible tsunami with a water surface displacement of 2 m, wave periods (see Glossary under 'Tsunami Period') of 9-48 seconds, and a return period of 1,500-2,000 years. The return periods are long, and the tsunamis are small, with only local significance (e.g. for the Taieri River mouth from an Akatore fault rupture).

From the available information, it does not appear that a 1:100 year scenario exists for a near-field tsunami. Berryman (2005) gives an expected mean estimate wave (above mean sea level at the shore) for Dunedin, from local sources, of 0.6m for a 100 year return period, 1.2m for a 500 year return period, and 1.8m for a 2,500 year return period. However, a plausible generating mechanism for a significant near-field tsunami with a return period of 100 years has yet to be identified. All the local tsunamigenic sources we identified had considerably longer return periods than 100 years. A scenario for this return period is therefore not considered.

The two plausible sources for near-field tsunami with return periods on the order of 500 years are the Puysegur subduction zone and submarine landslides. Submarine landslides are a much more local phenomenon, but given that there are a number of potential generating mechanisms (local faults, slope instability) the compounded return period could sit within the 1:500 year framework.

A 1:500 year scenario is dependent on whether potential submarine landslides, located approximately 30 km off the Otago coast at the edge of the continental shelf, would have a significant effect on the coastline. At the beginning of this study it was unknown whether most of the wave energy would dissipate before reaching the shoreline. It was also unknown whether a Puysegur subduction zone fault event would have a significant effect on some or most of the Otago Coast.

By running hydraulic models of the Puysegur subduction zone fault rupture scenario and one of the submarine landslide scenarios, a better indication of the likely impacts on the Otago Coast was obtained (i.e. modelling provided information on the sensitivity of the Otago coast to various near-field tsunami sources). This information was used to confirm which scenario was more severe, and hence, what the design tsunami events are for Otago.

The derived tsunami design events for a near-field tsunami are summarized in Table 3.1.

Table 3.1: Summary of near-field design tsunami events for the Otago coastline

Design event	Valid for ...	Description of tsunami source
1:100		No significant event exists
1:500	Mainly north of Otago Peninsula	Submarine landslide off continental shelf
Probable Maximum Frequency (PMF)	All coast	Puysegur subduction zone fault rupture. $M_w 8.5$ event with no surface rupture

4. Numerical modelling of tsunamis

4.1. Model Grid – Topography and Bathymetry

The model grid has a number of requirements that ensure that the model calculations will be accurate and free of excessive numerical errors (Henry and Walters, 1993). The primary requirements are that the triangular elements of the model grid are roughly equilateral in shape and their grading in size is smooth from areas of high resolution (small elements) in the coastal zone to areas of low resolution (large elements) in the offshore ocean areas.

The shoreline boundary for the model “ocean” grid was obtained by sub-sampling the LINZ shoreline data. An open ocean boundary was also specified. The interior part of the grid was generated using the program GridGen (Henry and Walters, 1993) according to the requirements described above. A combination of a frontal marching

algorithm (Sadek, 1980) and a cluster algorithm described in Henry and Walters (1993) was used. Depths at the vertices were then interpolated from a reference grid comprising all the available seabed bathymetry data. Land inundation grids were developed for each of the settlements described in Section 1. The refined coastal boundary from the larger grid was used as the seaward boundary and a landward boundary was created to encompass potential areas of inundation. The interior of this grid was then generated using the program GridGen, as before giving an approximate spacing between points of 20m. LIDAR data was used to give topographic information.

This report is based on state-of-the-art knowledge and modelling capabilities of tsunamis and tsunami inundation. While every effort is made to provide accurate information, there are many uncertainties involved including knowledge of potential sources, source characteristics, bathymetry and topography. In addition, while RiCOM captures much of the physics involved in tsunami propagation and inundation as with all models, it also includes some simplifying assumptions. The information provided in this report is of a technical nature and should be viewed with the above limitations in mind.

Variations on the above general methodology were required to generate the specific model grid for each of the source scenarios. The model grids are described in more detail below, for each scenario.

South America (far-field)

The grid for the far-field scenarios is built up from a refined version of the EEZ 2005 grid, which spans from approximately 157 to 210 degrees east longitude and 22 to 65 degrees south latitude. The Otago coastline was further refined for the areas of interest. The resultant model grid has 467,784 vertices and 908,814 elements. Details of the grid can be seen in Figure 4.1.

Puysegur subduction zone (near-field)

The Puysegur subduction zone model grid consists of a subsection of the EEZ 2005 grid chosen to include the Puysegur fault and the Otago coast. This subsection was further refined to accommodate the shorter length scales associated with the near-field subduction zone tsunami. The resultant model grid (shown in Figure 4.2) has 336,303 vertices and 660,013 elements.

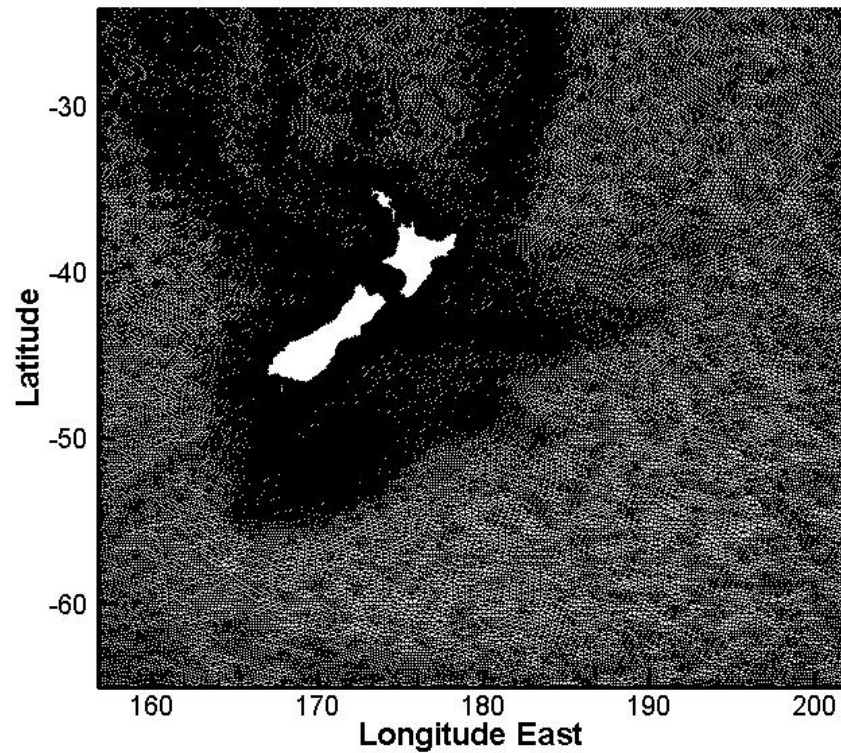


Figure 4.1: Details of the Far-field Tsunami grid. Extra refinement of elements can be seen in shallower coastal areas and areas of rapidly changing bathymetry.

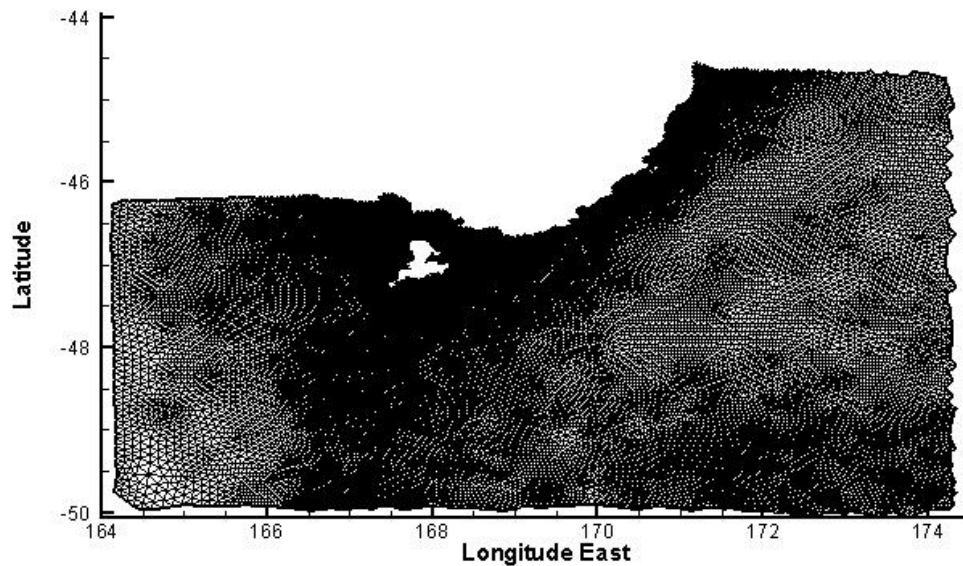


Figure 4.2: The Puysegur Subduction Zone Grid. The subduction zone lies to the SW of Stewart Island. The grid extends well to the east to allow the wave to refract around, and hit, the Otago coastline.

Continental shelf submarine landslide (near-field)

The local submarine landslide grid is also a subsection of the EEZ 2005 grid comprising of the Otago coastline. This grid was refined four times in the area covering the coastline from Oamaru to Brighton, which represents the potential 'cone of impact' of a submarine landslide off the coast of Dunedin. The refinement can be seen in Figure 4.3. This especially fine grid is needed for submarine landslides because of the comparatively small spatial scales involved. The resultant model grid has 596,843 vertices and 1,182,735 elements.

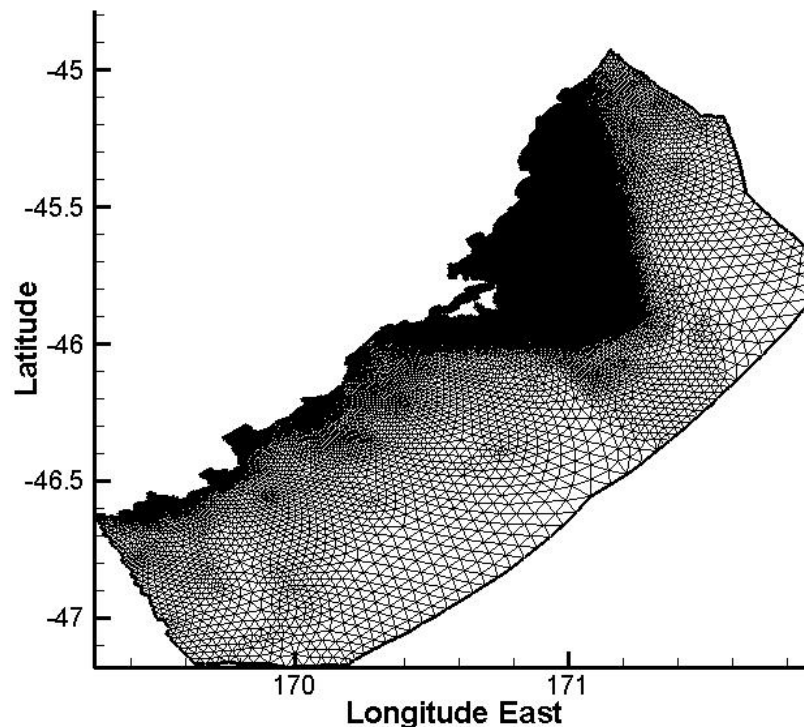


Figure 4.3: The local submarine landslide grid. The darker triangle at the top of the grid shows the very fine resolution covering the submarine canyons and coastline that a landslide generated tsunami may affect.

4.2. Numerical model

The numerical model used in this study is a general-purpose hydrodynamics and transport model known as RiCOM (River and Coastal Ocean Model). The model has been under development for several years and has been evaluated and verified continually during this process (Walters and Casulli, 1998; Walters, 2005; Walters et al., 2006a; 2006b). The hydrodynamics part of this model was used to derive the results described in this report. A more detailed description of the model can be found

in Appendix C and in the references. A general overview is contained in the following paragraphs.

The model is based on a standard set of equations - the Reynolds-averaged Navier-Stokes equation (RANS) and the incompressibility condition. In this study, the hydrostatic approximation is used so the equations reduce to the shallow water equations.

To permit flexibility in the creation of the model grid across the continental shelf, finite elements are used to build an unstructured grid of triangular elements of varying-size and shape. The time intervals that the model solves for are handled by a semi-implicit numerical scheme that avoids stability constraints on wave propagation. The advection scheme is semi-Lagrangian, which is robust, stable, and efficient (Staniforth and Côté, 1991). Wetting and drying of intertidal or flooded areas occurs naturally with this formulation and is a consequence of the finite volume form of the continuity equation and method of calculating fluxes (flows) through the triangular element faces. At open (sea) boundaries, a radiation condition is enforced so that outgoing waves will not reflect back into the study area, but instead are allowed to realistically continue “through” this artificial boundary and into the open sea. The equations are solved with a conjugate-gradient iterative solver. The details of the numerical approximations that lead to the required robustness and efficiency may be found in Walters and Casulli (1998) and Walters (2005b).

4.3. Submarine landslide model

There are two types of landslides that we can model as tsunami sources. The first is a slump. In the time frame of the tsunami this can be thought to occur instantaneously and thus the appropriate initial condition is to specify the sea level at the start of the model run on the assumption that this will follow the surface displacement caused by the slump. The second type of landslide involves fluidised sediments. For this situation the landslide model uses a dynamic, viscous fluid approximation developed under NIWA research project (Marsden Grant, NIW101, Royal Society of New Zealand).

4.4. Initial conditions

For each of the design tsunamis modelled it was assumed that the undisturbed water level was mean high water, spring tide (MHWS). For simplicity this is kept constant throughout the simulation. Thus it represents a sort of worst-case scenario for each of the cases in that all the waves essentially come in on a high tide. In reality the tsunami

waves come in over an interval of several hours during which time the sea level will be at different tidal stages. Obviously if a tsunami wave comes in at a lower tidal level its effect will be less severe. The difference will be roughly proportional to the difference in tides. In the case of Otago, MHWS was taken to be 0.9m above MSL which is the value given by LINZ for the tidal difference both at Oamaru and at the Otago harbour entrance (NZ Nautical Almanac 2006/07).

4.4.1. Puysegur subduction zone fault generation event

The Puysegur event ruptures the length of the trench with 8 m of displacement on a fault and 10 degrees eastward dip. Laura Wallace (personal communication) provided two scenarios: one ruptures from 25 km depth to the surface (surface rupture case), and the other ruptures between 10 and 25 km depth (no surface rupture case, Figure 4.4). The amount of displacement, dips, depth, and other information for the fault were provided by Martin Reyners (personal communication). The surface rupture case corresponds to an 8.64 M_w event and the no surface rupture case corresponds to an 8.49 M_w event. The event that we chose to model was the no surface rupture case rounded up to M_w 8.5 for this study. Although the magnitude of this earthquake is smaller because there is no surface rupture (fault rupture was from 10 to 25 km depth) the surface displacement (i.e. actual change in position of the surface) is greater, causing a larger tsunami.

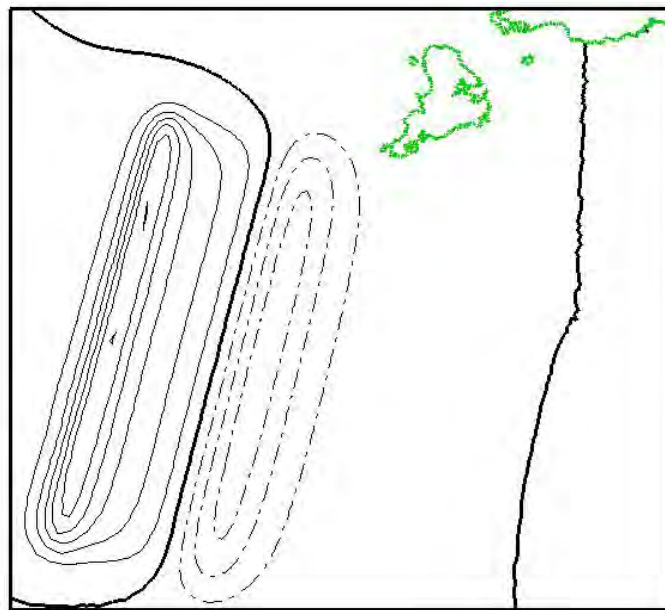


Figure 4.4: Initial water level conditions for Puysegur subduction zone event (trench scenario with no surface rupture). The thick contour line represents the undisturbed level of the sea;

the contour interval is 0.5 metres; dashed lines represent depression of water; solid lines, elevation.

Normally, fault movement is rapid when compared to time scales for wave propagation. Because of the incompressible nature of water, the instantaneous initial conditions on the water surface are the same as the fault displacement. This modelling strategy is adopted for the fault rupture scenario identified above. Essentially, the tsunami starts with zero velocity and a water surface displacement given by the estimates for seabed displacement. The wave then evolves in time as a long gravity wave.

4.4.2. Landslide generation events

To determine potential submarine landslide sources offshore from the Otago coastline, existing landslides were delineated based on geomorphic expression in the high-resolution bathymetric data. Bathymetric data were collected by the NIWA vessel RV Tangaroa during 3 surveys between 2003 and 2004: TAN0306; TAN0307; and, TAN0405. The RV Tangaroa has a hull mounted Simrad EM300 multibeam system operating 135 beams at 30 kHz frequency with approximately 1 degree beam width. Shipboard navigation comprises a POS/MV system with differential GPS. Survey data has been processed together using Hydromap and gridded to 10m x 10m cell size.

Three primary types of failures were identified:

1. Gulley head failures
2. Translational sheet slides in slope mantling sediments.
3. Larger scale canyon wall slumping

Type 1 landslides, gulley head failures, were not considered further as they were expected to be of too small a volume to generate waves of any significance. Types 2 and 3 were considered to be of sufficient volume to be considered in tsunami scenarios.

Several scenarios were inferred for the Type 3 failure style. These failures typically occur on the outside of meander bends and affect steep canyon walls from ridge crest to channel base. This model is backed up by observations from the Cook Strait Canyon systems. One Type 2 scenario is included adjacent to existing failures. Volume estimates are based on simplified geometries measured from bathymetry data. All scenarios occur within the areas surveyed by multibeam sonar (shaded areas of figure D1), however it is reasonable to take a typical geometry from the given

scenarios and locate it within other canyons as defined by the regional bathymetry contours. A summary of the existing and predicted submarine failures is given in Appendix D.

To determine whether a submarine failure could generate a significant tsunami along the Otago coast, “Potential 2” predicted submarine failure (from Appendix D, Table D.1) was modelled. This is a type 2 landslide with a volume of approximately 0.55 km³. It is located approximately 30 km east of Otago Peninsula on the edge of the continental shelf (see Figure D.1). The material is consolidated sands derived from longshore sediment transport and contains entrained water and organic material. The landslide is about 100-120 m thick at its centre.

The pre-landslide topography is identical to the reference seabed topography that was interpolated onto the model grid for all tsunami scenarios. We also have a secondary model grid that contains the post-landslide seabed topography. As little information is known about the likely failure surface, the post-landslide seabed topography was developed by assuming the slope of the failure surface as being 5-10°. These two sets of data were used within the “landslide module” of the model to define the surface displacement caused by the landslide.

4.4.3. Far-Field tsunami

The source of the far-field tsunami occurs well outside the detailed component of the model domain for a South American subduction zone event. As it propagates across the Pacific Ocean away from the source the tsunami approximates a plane wave train. Using an inverse model approach the South American tsunami is modelled by three solitary waves entering the eastern end of the detailed component of the model.

5. Numerical modelling results

The study area extends from the Waitaki Fan in the north to Wallace Beach in the south (Figure 1.1).

The settlements of interest are Tautuku Peninsula, Papatowai, Catlins Lake/Catlins River settlements (including Jacks Bay and Surat Bay), Kaka Point, Clutha delta, Toko Mouth and estuary, Taieri Mouth and estuary, Brighton, Kaikorai Mouth and estuary, Dunedin Harbour and South Dunedin (including St. Clair, St Kilda, and Tomahawk beaches), Long Beach, Purakanui and estuary, Moeraki, Hampden,

Kakanui/Taranui and, Oamaru. In each of these settlements wave run-up, wave speeds and inundation were modelled for each design tsunami scenario.

In the context used here, the amplitude of tsunami waves is the level of the wave crest and trough reached respectively above and below the sea level at the time of the event. The wave height from crest to trough is therefore twice the amplitude. However, in shallower water the wave distorts so, unless stated otherwise, what is reported here is the vertical height above the undisturbed level of the sea (in these cases mean high water spring MHWS) reached by the wave crest. This was considered the most relevant to evaluating the tsunami inundation risk. In this study mean high water spring (MHWS) is at an elevation of 0.9 m. In the event that the tsunami arrives at a lower tidal level, the vertical height of the wave will still be approximately correct. When waves encounter shallow water, the speed of the crests and troughs (phase speed) decreases. Thus the wavelength becomes shorter and the amplitude increases. If the wave encounters a sloping beach, the runup (see Glossary under 'Tsunami Runup') height can be up to four or five times the initial wave amplitude. The wave also undergoes partial reflection from the shoreline. If the wave encounters a vertical cliff, the wave is completely reflected and the amplitude at the cliff is twice the incident wave amplitude. This creates a standing wave where the reflection occurs, and is a common occurrence in many of the coastal inlets and bays.

In addition, wave refraction occurs if the wave front straddles areas with different water depths at each end of the wave front. Because the wave travels more slowly in shallow water, the wave front tends to bend around toward the gradient in depth. For a long straight beach, incident waves coming in at an angle to the coast (obliquely) then tend to become more parallel to the shore. By the same process, waves travelling along the shoreline will tend to be trapped because the offshore component of the wave travels substantially faster and hence keeps refracting back toward the shore.

When a wave is generated, all these processes occur simultaneously along the coast with a complex bathymetry and shoreline platform shape, leading to complicated wave patterns. The coastal-trapped waves are reflected by the irregular coastline and then traverse the entire coast, back and forth, until they fade away. When these waves resonate (slosh back and forth) in small bays, there can be large amplitude waves that occur long after the waves were initially generated. Examples of this can be seen for both the Puysegur subduction zone tsunamis and the remotely generated tsunamis with large waves occurring along the coast for many hours after the initial arrivals.

The rest of this section is structured in the following way. First, some general comments will be made about the near-field and far-field tsunamis and their impact on

the Otago coastline. Time series figures based upon point source data (Figure 5.1) show the progression of these tsunamis along the Otago coast.



Figure 5.1 Points where time series for tsunami arrivals are given (figures 2-3 give the time series for the Puysegur tsunami and figures 6-7 for the 1:100 year remote tsunami).

Following these sections, we will look at each of the specified areas in detail. Inundation depth and maximum water speed maps are shown for each of the scenarios considered. Bullet point comments are made with regards to wave arrivals, runup, inundation and potential for erosion. Estimates of inundation of private land are made based on the coastal parcels provided to NIWA by Otago Regional Council on the assumption that if they are not public land then they must be private land. These coastal parcels do not always line up with the land boundary i.e. sometime parts of them lie in the ocean or in bays. The information provided on the inundation of private land is only as accurate as these parcel boundaries. Furthermore, the model resolution is 15-20 metres and this should be taken into account when interpreting the results.

5.1. Near-field

Puysegur subduction zone fault rupture

The earthquake rupture depth is 10-25 km. There is no surface rupture but the seafloor is displaced more than 2 m upwards on the western side and 1.5 m down on the eastern side (figure 4.4). The sea surface is similarly displaced, causing a trough on the eastern side and a peak on the western side. The initial water velocity is assumed to be zero. This displacement can be considered as a combination of two waves travelling in opposite directions such that the wave velocity sums to zero. Thus the displacement will initially split into two waves – one travelling west and one travelling east, each with about one-half the original amplitude. For a wave with a long and straight wave crest such as those generated by long fault ruptures, the amplitude will be maintained, subject to variations in water depth. Only the ends of the wave will tend to decrease in amplitude as they radiate in circular patterns.

The animation for this event shows the western propagating wave rapidly leaving the area of interest. The peak of the eastward propagating wave, however, catches up with the trough, steepening as it does so. This wave is focussed as it refracts around the high part of the Campbell plateau directly south of Stewart Island. The first wave arrival from the tsunami to reach the Otago coastline actually travels north of this wave, just south of Stewart Island. This is a relatively small wave. The re-radiation of the focussed wave causes the first big arrival.

The tsunami moves northwards up the Otago coastline. Figures 5.2 and 5.3 show time series data for the sites specified in figure 5.1. The sea level recorder at Green Island lies between Brighton and Kaikorai and so the reading at Green Island could be expected to be similar to the time series for Brighton or Kaikorai. The first sign of the tsunami along the Otago coastline is a decrease in the water level between 0.3 and 0.8m below the expected level of sea (i.e. MHWS in the model scenarios). This begins around 70 minutes after the fault rupture for the southernmost sites (Tautuku and Papatowai) up to around 105 minutes (6300 seconds) after fault rupture in Oamaru (Figure 5.3). The water level decreases over around 40 minutes before beginning to rise again. As mentioned above, in most places the first arrival is quite small, sometimes not even reaching the pre-tsunami level of sea. Shortly after this though, the first big wave arrives. Usually this arrival is the biggest wave, although not always. Generally this wave is larger the further south the site is, although this also depends on the specifics of the site. Offshore, the water level increases to its peak height in about 15 minutes. In most places a succession of large waves hit the shoreline with a frequency of around one every 30 minutes. The height of these waves

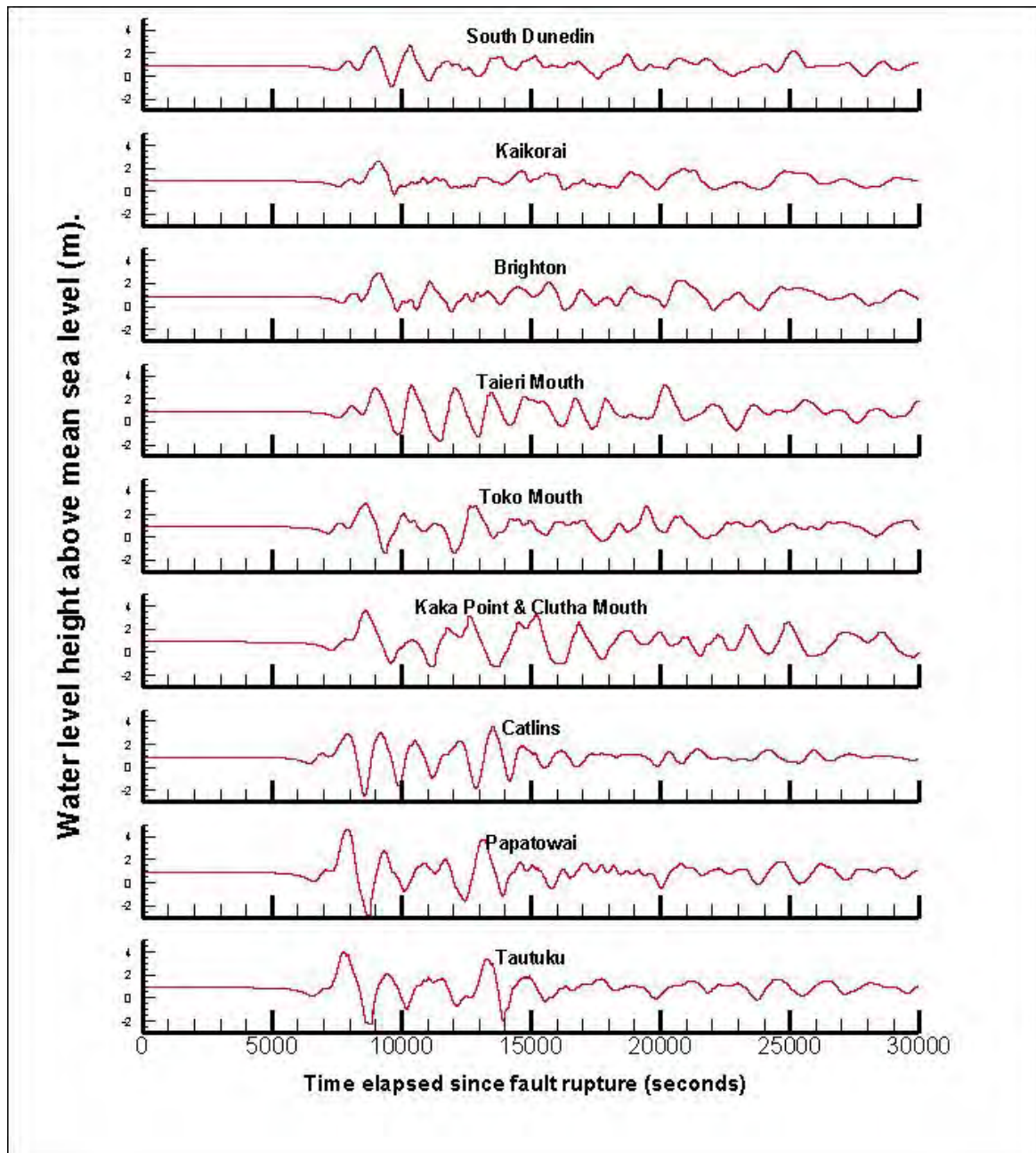


Figure 5.2 Time series for Puysegur tsunami for areas south of Otago Peninsula (note the change in the scale of water level between the northern (figure 5.3) and southern (this figure) sections). The time is given in seconds since fault rupture. Figure 5.1 shows the points where the time series are taken.

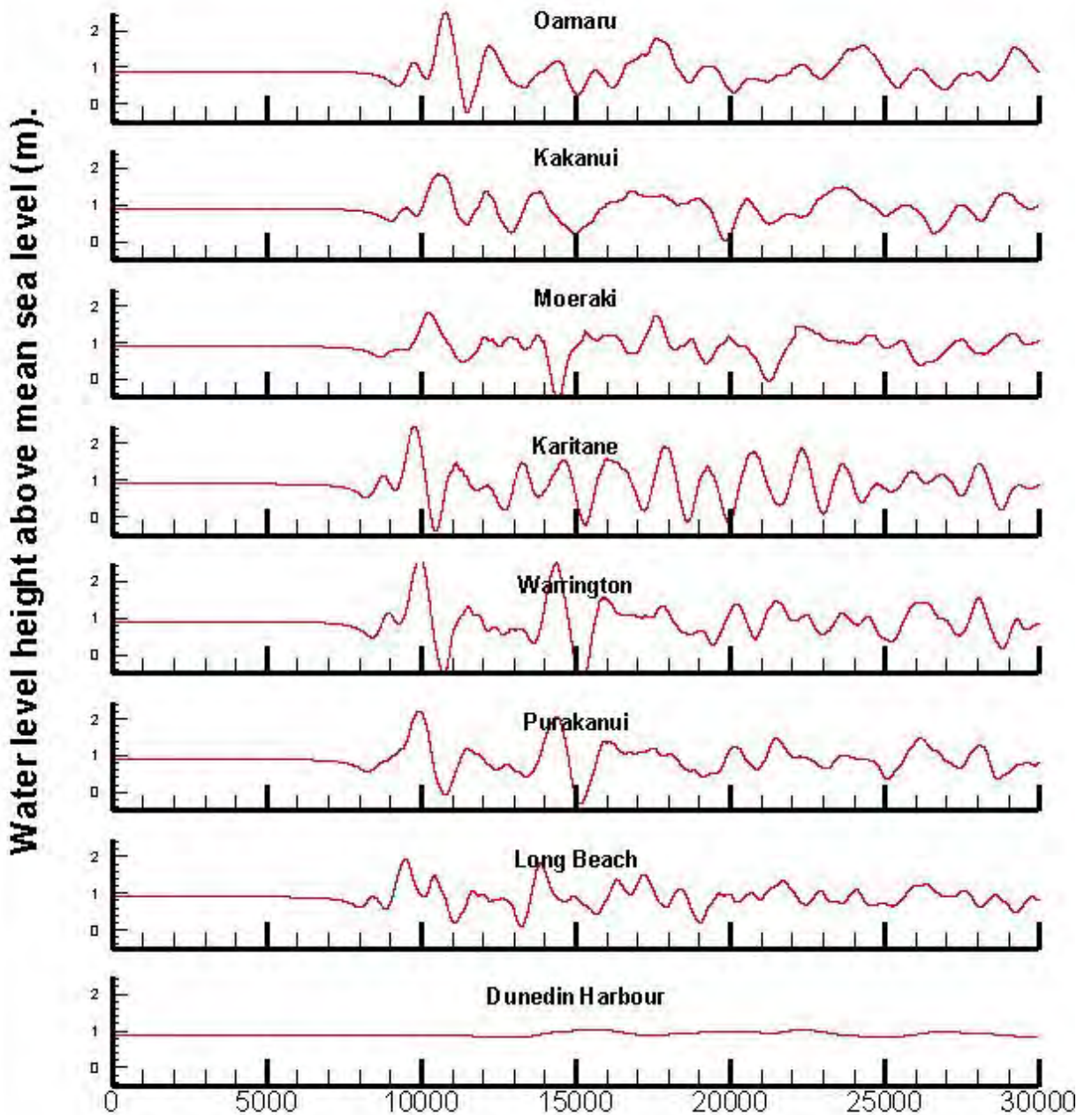


Figure 5.3: Time series for Puysegur tsunami for areas north of Otago Peninsula (note the change in the scale of water level between the northern (this figure) and southern (figure 5.2) sections). The time is given in seconds since fault rupture. Figure 5.1 shows the points where the time series are taken.

varies and often a particularly large wave may come in 4-5 hours after the fault rupture. These waves continue to hit the shoreline for many hours after the fault rupture but generally the largest waves have passed after 10 or so hours. As well as a succession of big waves, the sea level drops dramatically between each of them.

Dunedin Harbour is well protected from the tsunami (Figures 5.3 and 5.4). Although sites further north receive waves over a metre high (the largest wave in Oamaru reaches 1.5 m above sea level), the maximum disturbance within the harbour is no more than 20 cm.

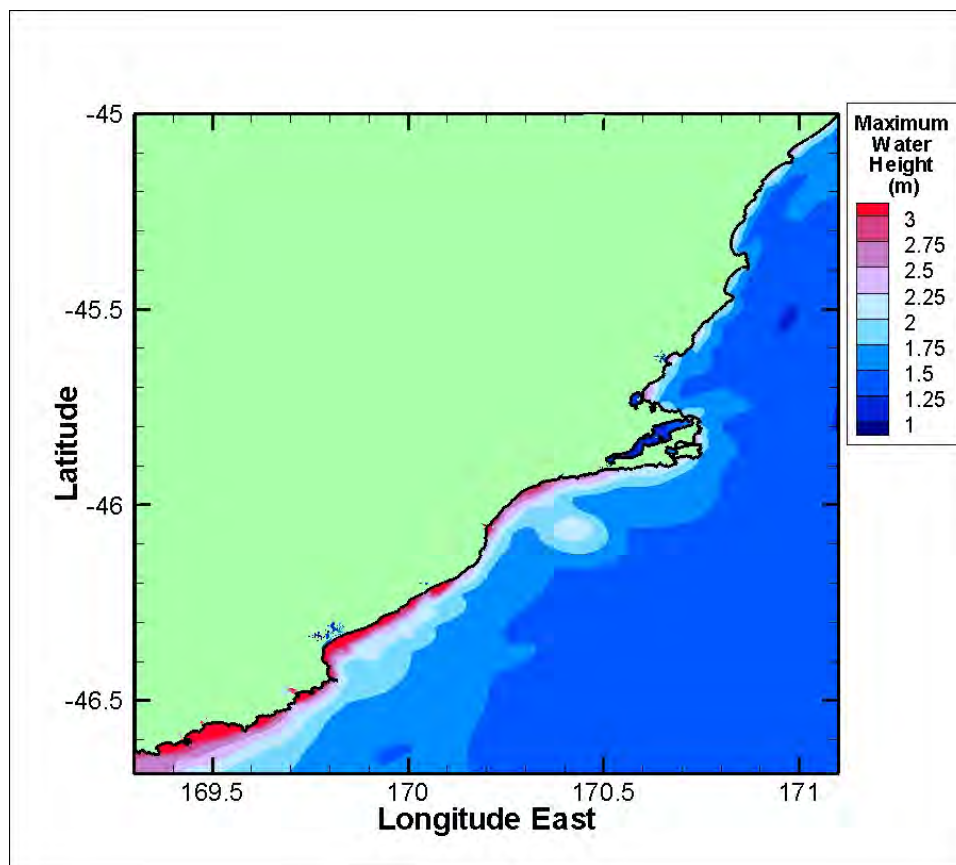


Figure 5.4: Maximum water level for Puysegur tsunami. Note that the undisturbed level of sea is 0.9m representing MHWS.

Predicted submarine landslide “2”

The source area for a submarine landslide scenario is much smaller than for an elongated fault rupture case. Thus the effects are primarily felt locally and the wave dissipates fairly rapidly. When an underwater landslide occurs, the water above it is drawn down by the sinking sediment mass and the water in front forms a forced wave

(bow wake) that is pushed along at the speed of the landslide. When the landslide changes direction or stops, the bow wake continues on as a freely propagating wave.

The scenario modelled is a rotational slump on the northern slope of the submarine canyons feeding the Bounty Trough. Once the forced wave is released it propagates radially outwards and interacts with the bathymetry. The wave refracts inland and is amplified over the submarine ridges creating the three distinct ‘fingers’ of maximum water height seen in Figure 5.5. The tsunami makes landfall at Tairaroa Heads around 20 minutes after the landslide and then hits the coast north of Otago Peninsula 5-10 minutes later. Because the period of these waves is far shorter than for the other tsunamis they attenuate rapidly. By the time the wave has travelled 30 km over the continental shelf to the coast the largest wave amplitude is around one metre above the undisturbed sea level. In addition, the impact from the tsunami is localised to the section of coast between Otago Peninsula and Moeraki.

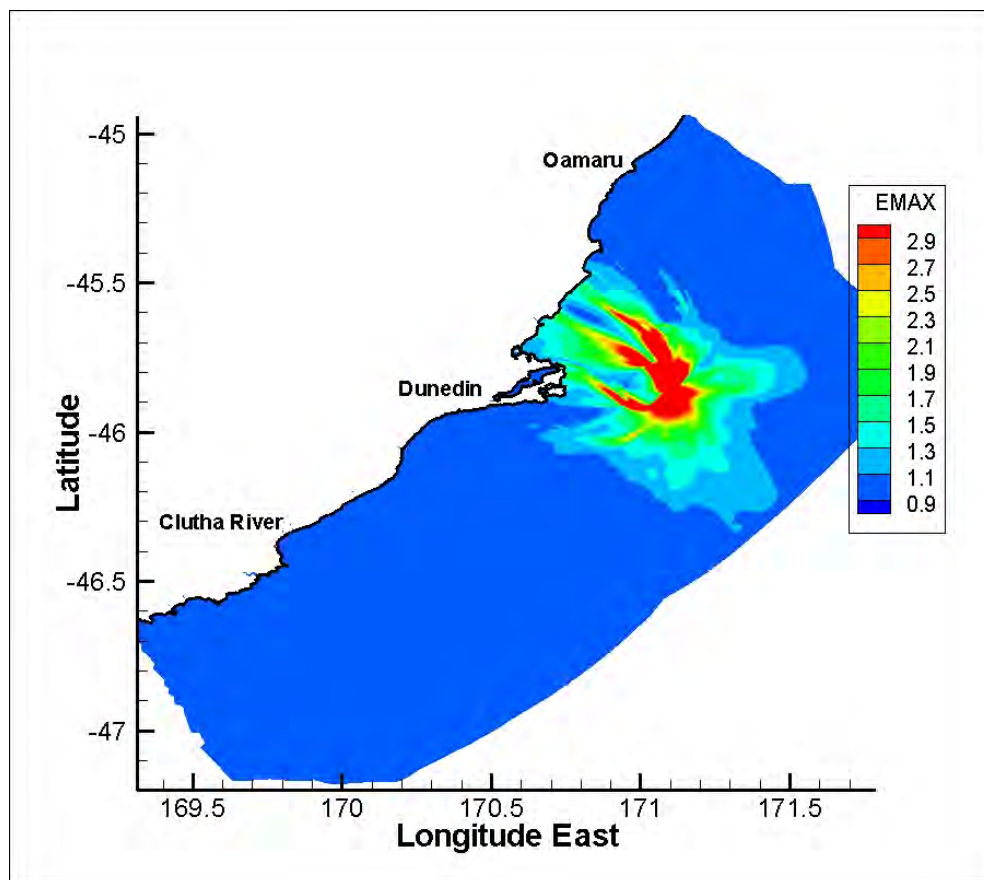


Figure 5.5: Maximum water level for submarine landslide scenario “2”. Note that the undisturbed level of sea is 0.9m representing MHWS.

This scenario is for the largest of all identified potential landslides (all other landslides have less than a third of the volume). It did not cause major inundation and as a result we decided that further landslide generated tsunami scenarios need not be considered.

5.2. Far-field

We focus on two different source scenarios for far-field tsunamis. The first, with a return period of approximately 100 years is equivalent to either the 1868 Chile (originally Peru) earthquake or the 1960 Chilean earthquake. Although the details of the sources of these differ they can be thought of as representative of a similar scale of tsunami because the fault location of the 1868 tsunami directed it straight towards New Zealand even though it was a smaller magnitude earthquake than the 1960 event meaning that the wave that finally arrived in New Zealand was comparable. The second scenario is a hypothetical earthquake with a similar epicentre to the 1868 earthquake but with the same moment magnitude as the 1960 earthquake. This is considered both the one in 500 year far-field tsunami and the Probable Maximum Frequency far-field tsunami as it represents the upper limit in the plausible magnitude of subduction zone earthquakes with the source placement designed to maximise the affect to New Zealand. Because the source area is similar for the two scenarios the wave propagation will likewise be similar. The earthquake in the second scenario however is bigger with larger surface displacement causing a commensurately larger tsunami.

The three main factors that determine the effect in New Zealand of a tsunami generated by a South American subduction zone earthquake are the source characteristics (location, geometry and magnitude), wave transformations occurring during open ocean propagation and the effects of bathymetry in the continental shelf and coastal region.

In the open ocean the tsunami generally follows the great circle route perpendicular to the wave front. This path however is modified by reflection and refraction when the depth of the water changes. Waves may also be diffracted when they pass through island chains, however this does not occur in this instance because there are no significant islands between South America and New Zealand. Over these great distances, tsunami waves are dispersive (meaning that longer wavelengths travel faster than shorter wavelengths) and so single waveforms spread out to become wave trains. This behaviour is important when considering runup and resonances of bays and harbours.

When a tsunami encounters the continental shelf its water speed decreases and it is partially reflected. In addition, the wavelength shortens and the amplitude of the wave increases. In areas where the bathymetry changes very abruptly, such as near the Chatham Islands, the shoaling and amplification can be similarly abrupt causing wave heights several times larger than experienced on the mainland. The final representation of the tsunami at the shoreline is dependent upon the bathymetry and geometry of the coast. A tsunami wave is made up of many different components with differing amplitudes and frequencies. Depending on the geometry of the coastline, especially bays and harbours, different wave frequencies may be amplified if they are in resonance or dampened otherwise. Thus there is a wide range of observed frequencies and amplitude for a single tsunami as it interacts with the coast.

As shown in the animation, the amplitude of the incoming wave is around 15 cm and has a period of around 2 hours. As it approaches the Chatham Rise and the Campbell Plateau the wave is refracted and the amplitude increases as it slows down. The wave is turned so that its crest is approximately parallel to the South Island coastline. Thus the wave arrives nearly simultaneously at all the location of interest along the Otago Coast (Figures 5.6 and 5.7). At the coastline the wave amplitude is approximately 1m although it varies depending upon the geometry of the bays and harbours (Figures 5.8 and 5.9).

The three most significant direct wave arrivals associated with the tsunami arrive approximately two hours apart. In most areas they are the biggest waves of the event although, especially in the North Otago region, waves of comparable size continue to hit the shore for over ten hours. Smaller wave arrivals continue for even longer. Between each arrival the sea level may drop significantly.

5.3 In-depth Areas

Where inundation extends landward of the LIDAR coverage we have added a zone of “potential inundation >50 cm” which represents the estimated maximum limit of inundation for water >50 cm depth. These estimates are based upon the LINZ Topographic Map 260 Series at 1: 50,000, aerial photographs, and consultation with Otago Regional Council.

In some cases there are isolated areas of inundation in the model domain. These are linked to the main inundation areas by flow paths that are too shallow or slow to be recorded in the resolution of the model. The terms amplitude and runup are defined in the glossary.

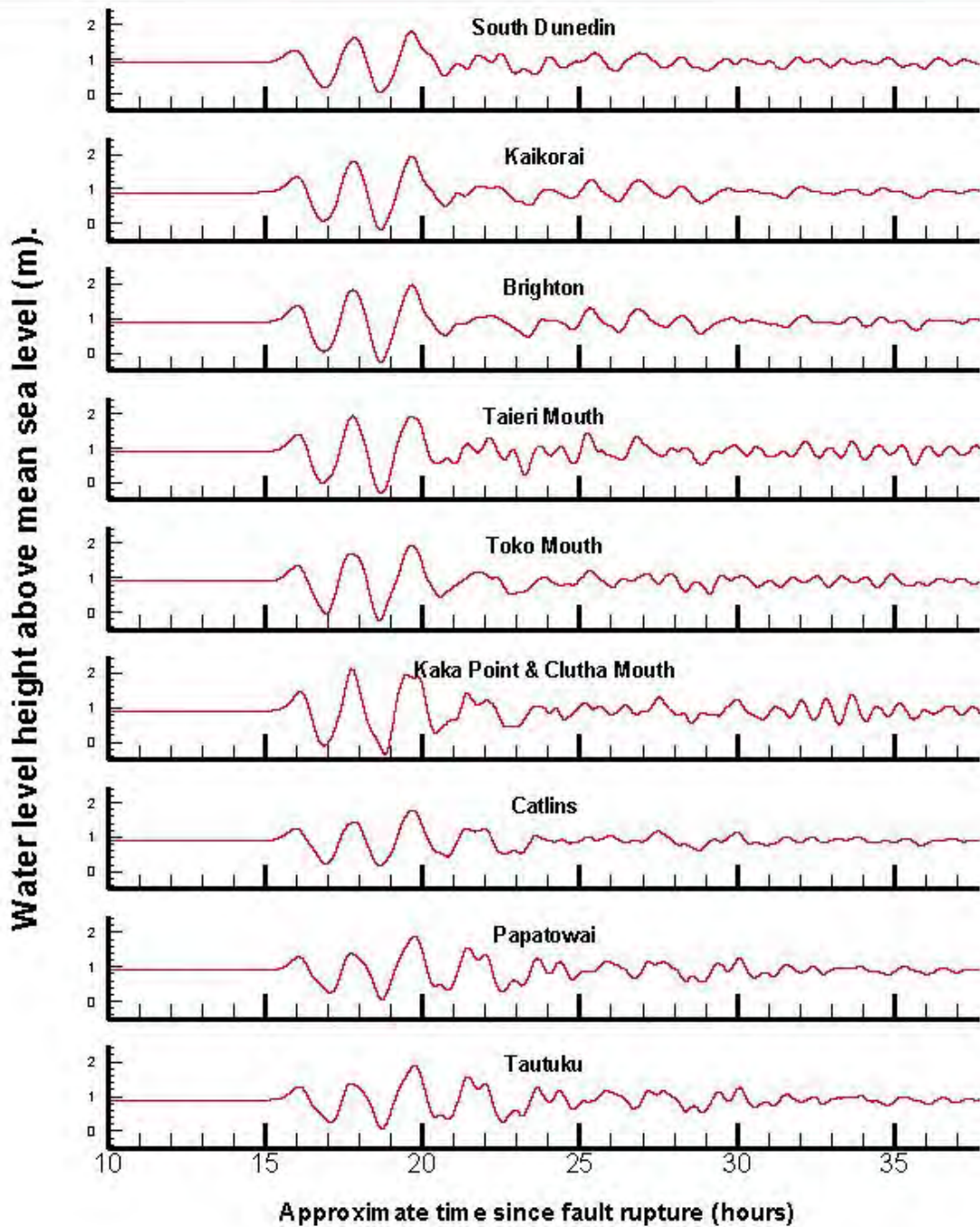


Figure 5.6: Time series for 1:100 remote South American tsunami for areas south of Otago Peninsula. The time is given in approximate hours since fault rupture. Figure 5.1 shows the points where the time series are taken (the same scale is used for both the northern and southern sections for the remote tsunami).

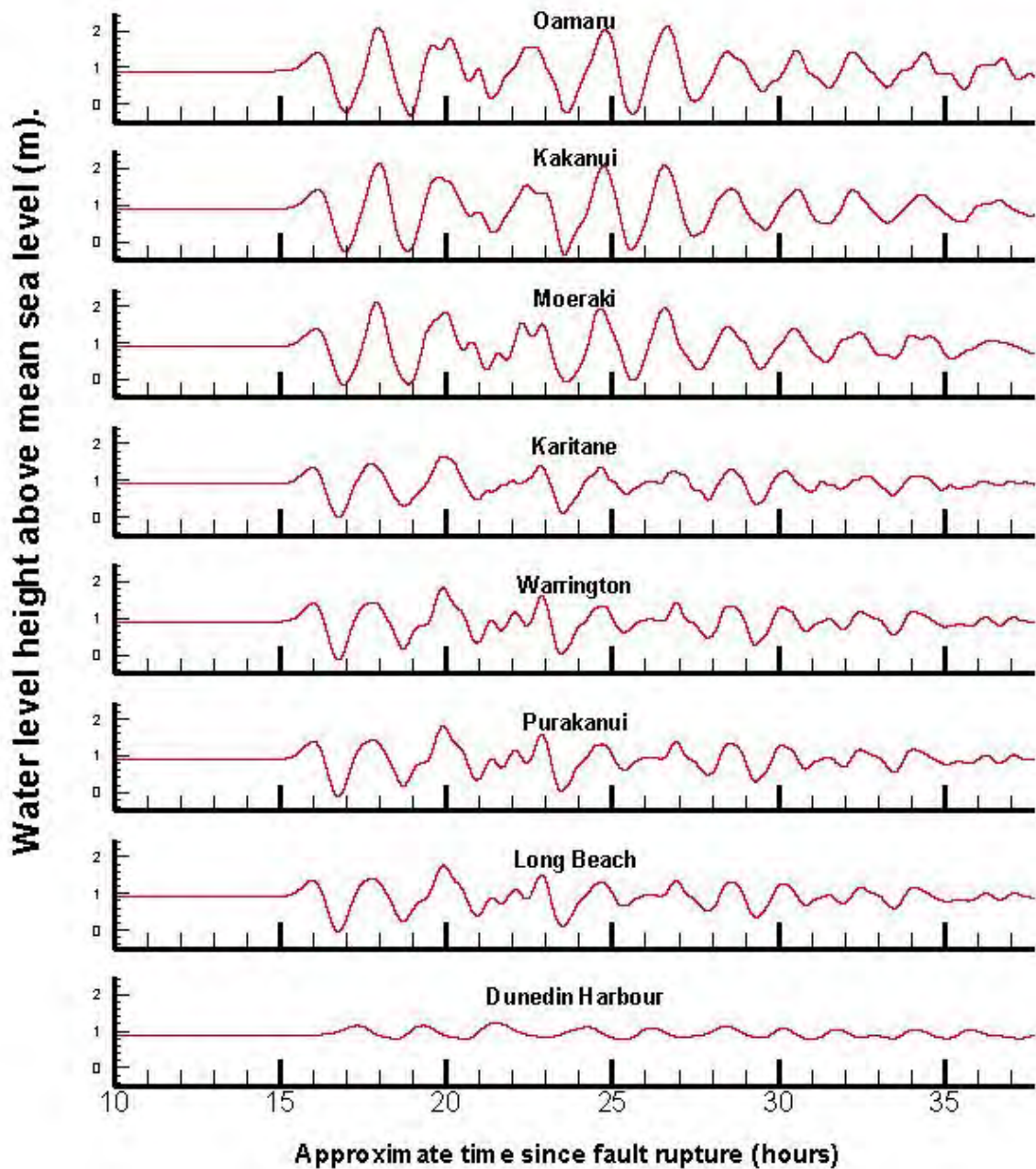


Figure 5.7: Time series for 1:100 remote South American tsunami for areas north of Otago Peninsula. The time is given in approximate hours since fault rupture. Figure 5.1 shows the points where the time series are taken (the same scale is used for both the northern and southern sections for the remote tsunami).

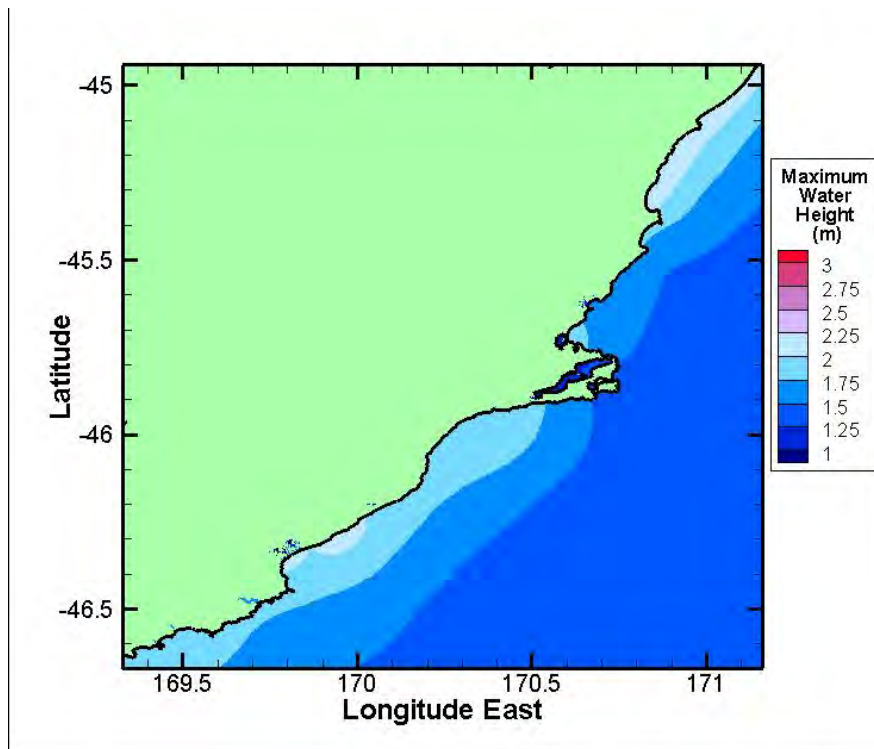


Figure 5.8: Maximum water level for 1:100 South American tsunami. Note that the undisturbed level of sea is 0.9m representing MHWS.

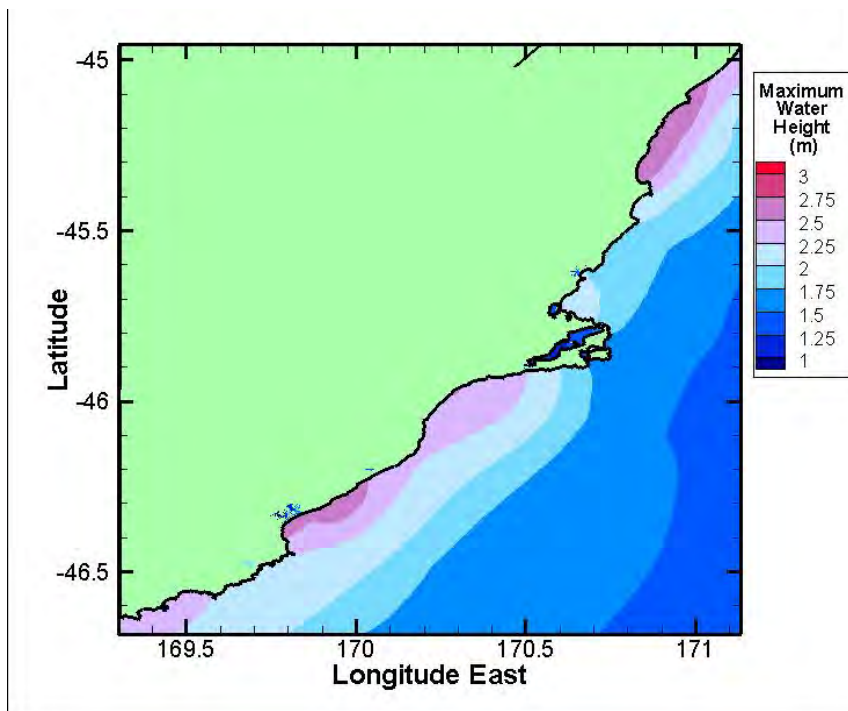


Figure 5.9: Maximum water level for 1:500 (and Probable Maximum Frequency) South American tsunami. Note that the undisturbed level of sea is 0.9m representing MHWS.

Comments for each area are given as bullet points for the near-field and far-field tsunamis. When 1:100 or 1:500 is not specified for the far-field tsunami the comment can be assumed to hold for both the modelled tsunamis.

5.3.1. Tautuku

Figure 5.10 – 5.12 show maximum inundation and water speed for the near-field (Puysegur) tsunami scenarios. Figures 5.13 – 5.18 show maximum inundation and water speed for the far-field (South American) tsunami scenarios.

Tautuku: Near-Field

- Trough arrives first approximately 70 minutes after fault rupture.
- Water level decreases 80 cm over 40 minutes.
- First main wave biggest. Arrives around 2 hours after fault rupture. Increases from undisturbed level of sea to maximum height over 15 mins, amplitude 3.1 m. Second maximum around 3.5 hours after fault rupture, amplitude 2.5 m.
- Predominant period of wave arrivals: 30 minutes. Maximum runup: up to 5m.
- Large amounts of land inundated especially north of Tautuku River up to 1 m depth in places. Also some inundation on the north side of Tautuku Peninsula.
- High maximum speeds in and around the river mouth indicate the possibility of erosion, especially the dunes on Tautuku Beach.
- With projected sea level rises of 30 and 50 cm the inundation is more severe with some coastal areas being inundated up to three metres deep. There is likelihood of erosion, especially of sand dunes on Tautuku Beach near the river mouth. Subsequent waves could cause even more inundation because of the loss of these sand dunes.

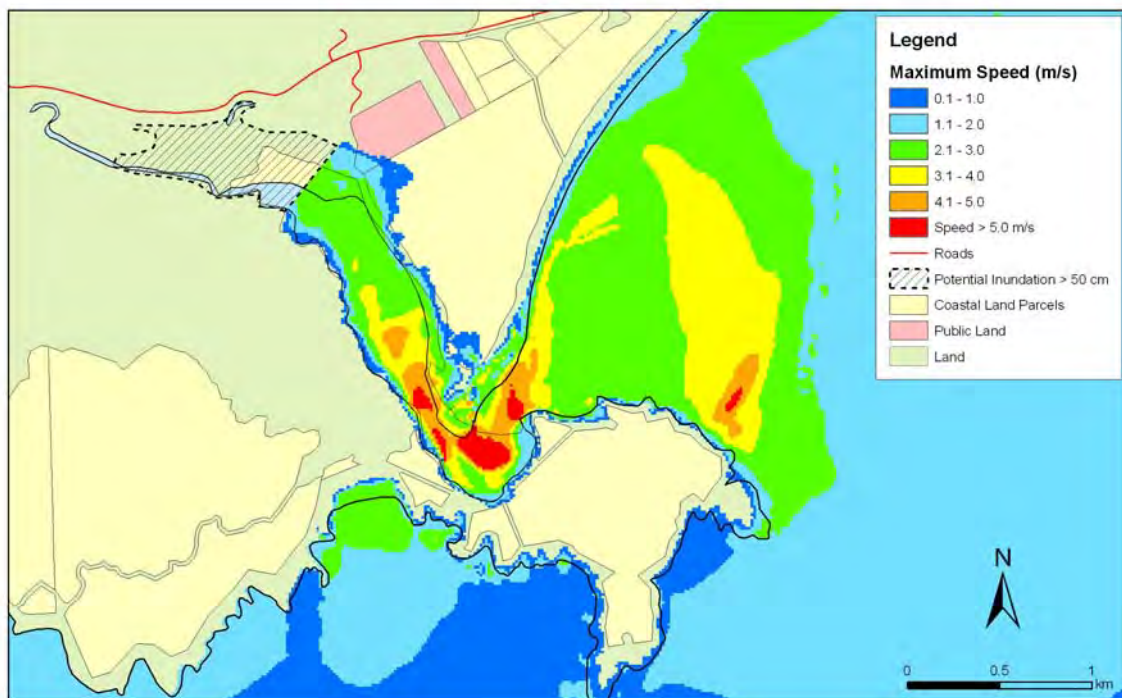
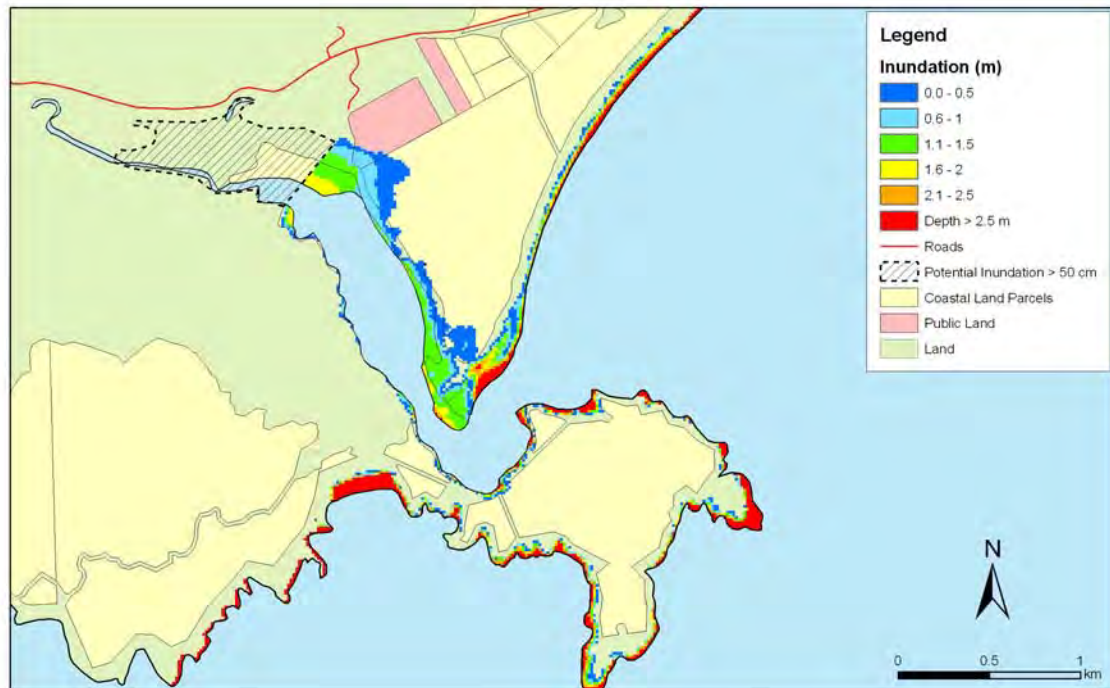


Figure 5.10: Tautuku - Puysegur tsunami: Maximum water depth for inundated land (top) and maximum speed (bottom) at Mean High Water Spring (MHWS).

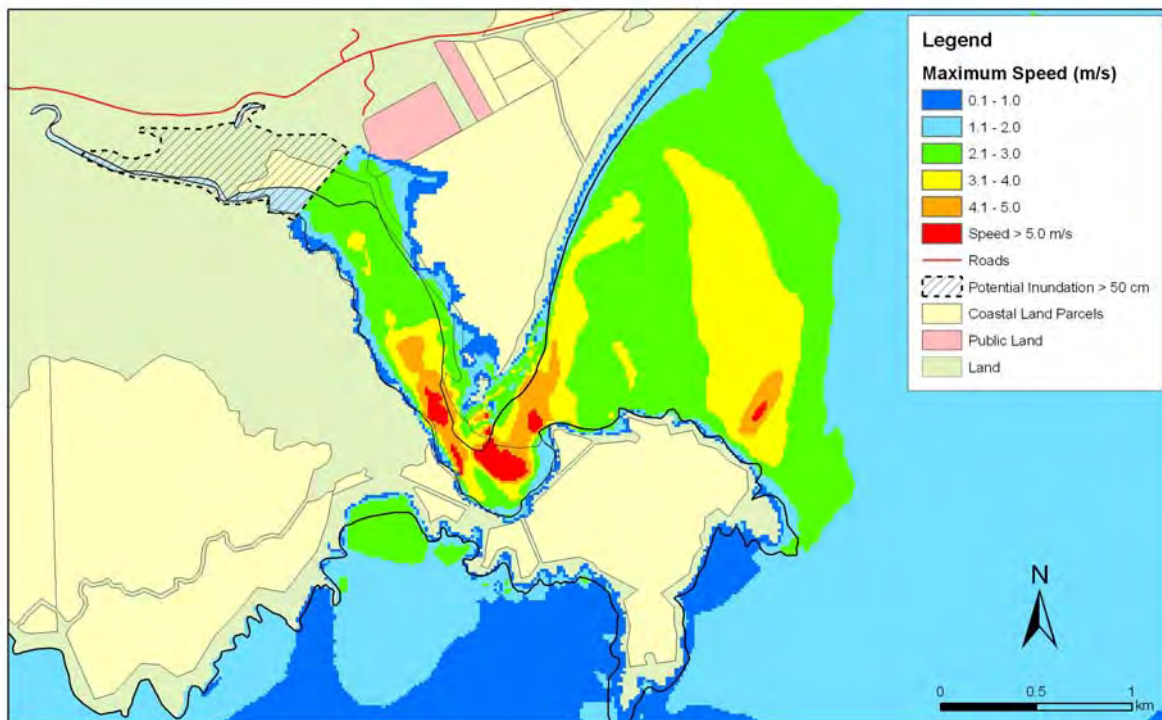
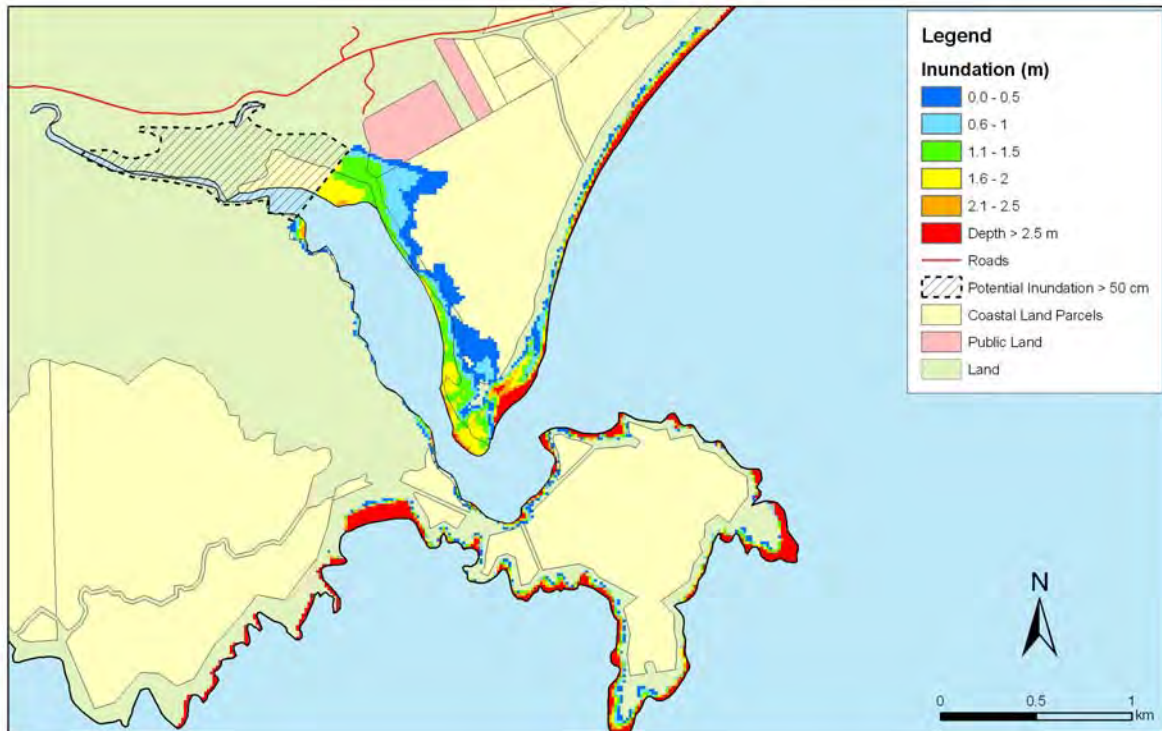


Figure 5.11: Tautuku - Puysegur tsunami: Maximum water depth for inundated land (top) and maximum speed (bottom) at MHWS - with a sea level rise of 30 cm.

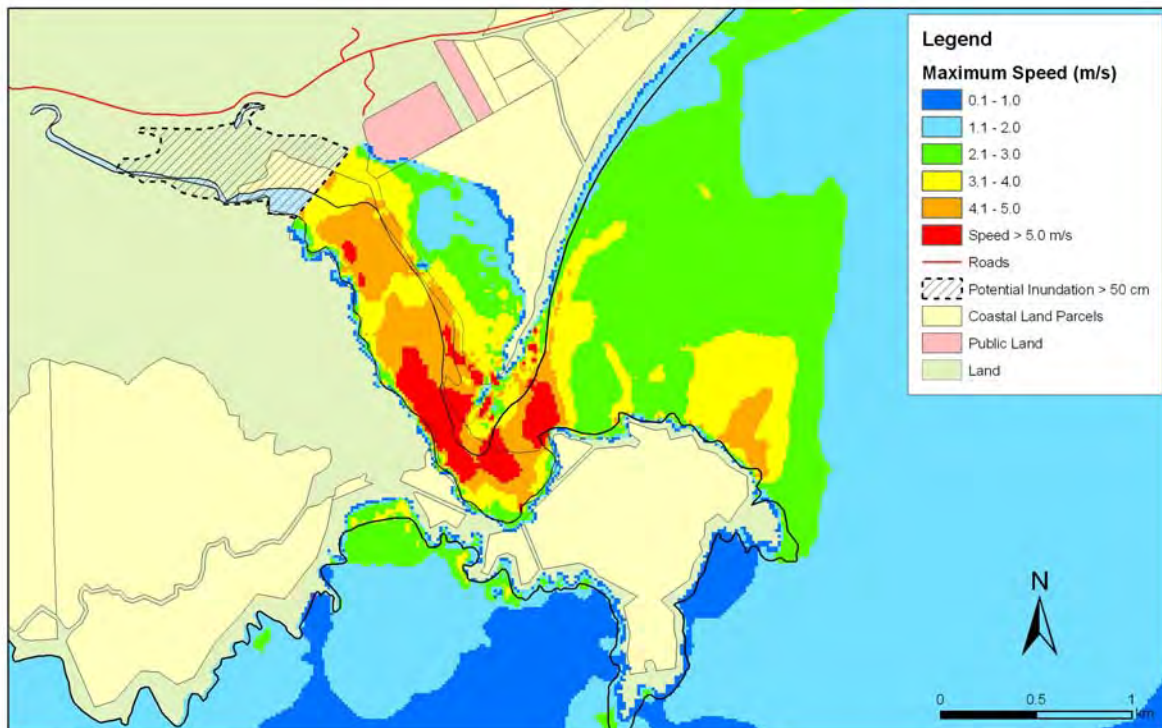
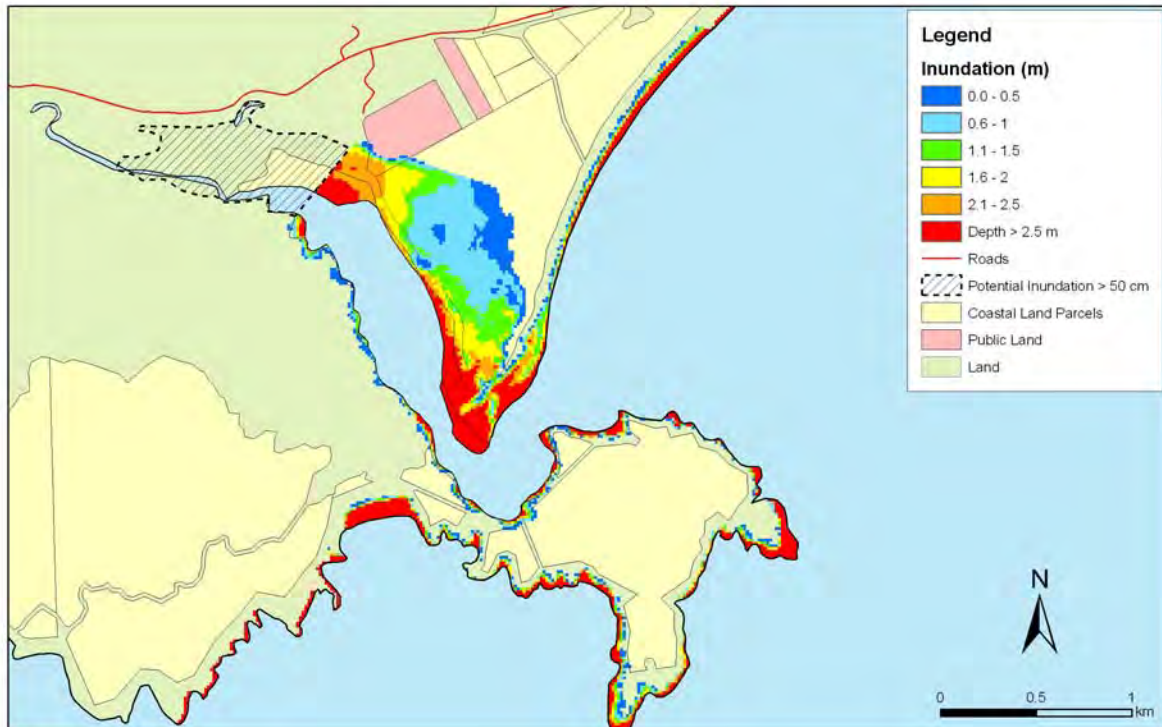


Figure 5.12: Tautuku - Puysegur tsunami: Maximum water depth for inundated land (top) and maximum speed (bottom) at MHWS - with a sea level rise of 50 cm.

Tautuku: Far Field

- Tsunami arrival for both remote scenarios is marked by an increase in the water level.
- Third wave is highest with amplitude 1 m, and wave height of 1.8 m for the 1:100 year tsunami and amplitude 1.5m for the 1:500 year tsunami.
- Large waves continue for around 7 hours after first arrival then many smaller ones.
- Resonance period around 1.5 hours.
- Maximum runup: up to 1.9 metres for the 1:100 year tsunami and 2.4 for the 1:500 year tsunami.
- The inundation and erosion risk is less severe than for the Puysegur tsunami scenario.

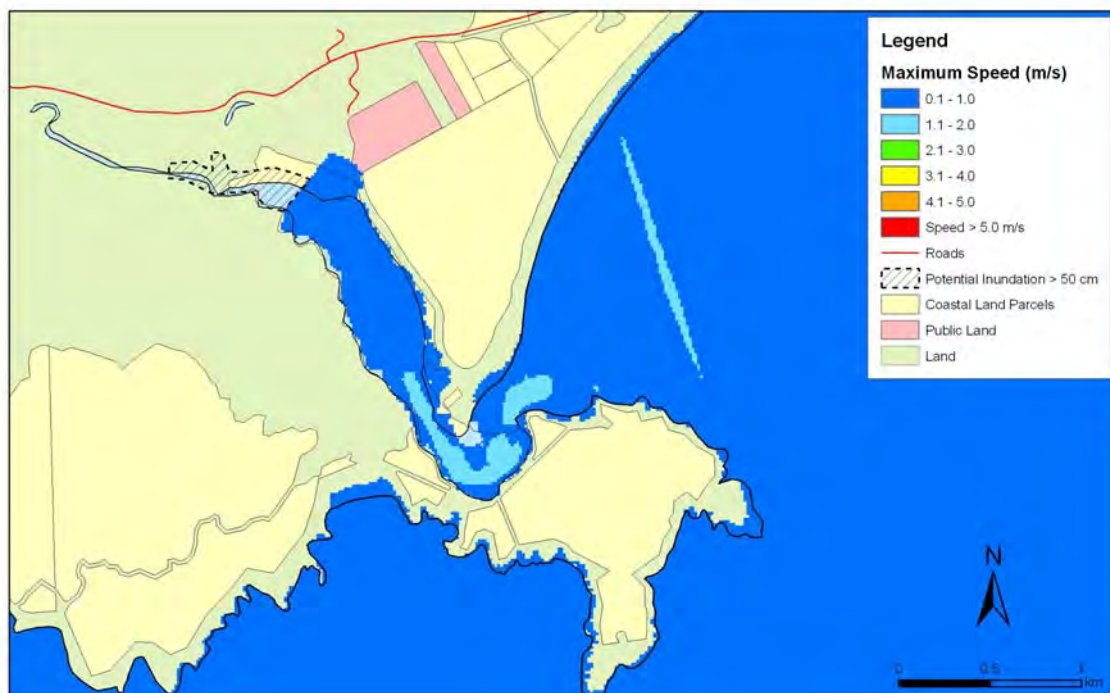
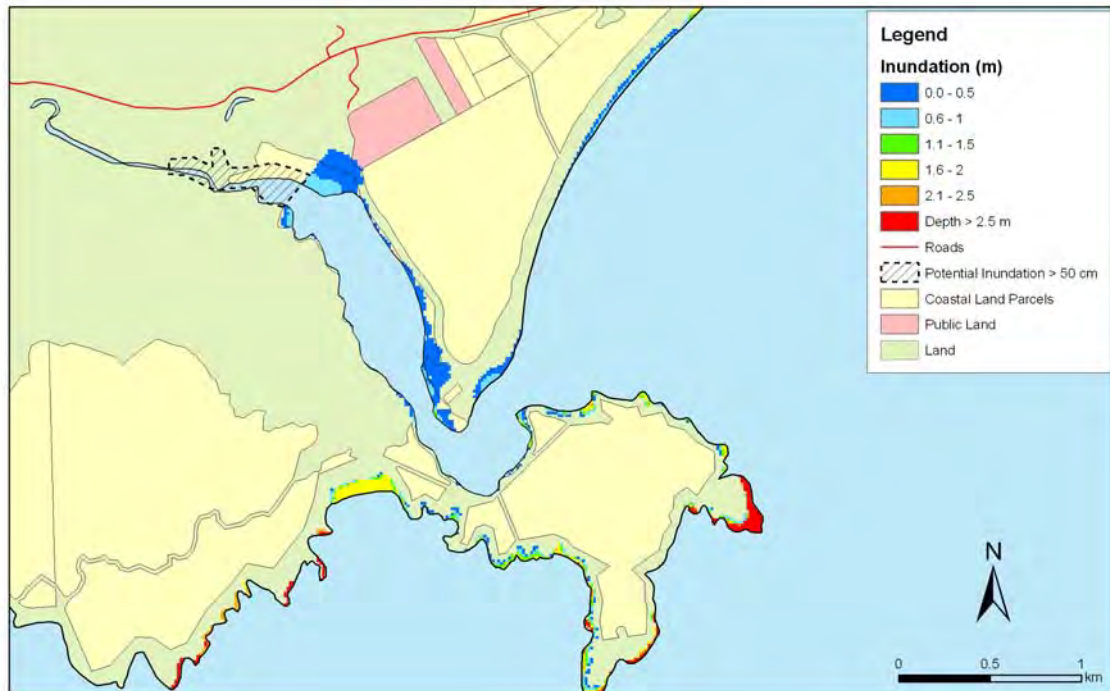


Figure 5.13: Tautuku - 1:100 year remote tsunami: Maximum water depth (top) for inundated land and maximum speed (bottom) for MHWS.

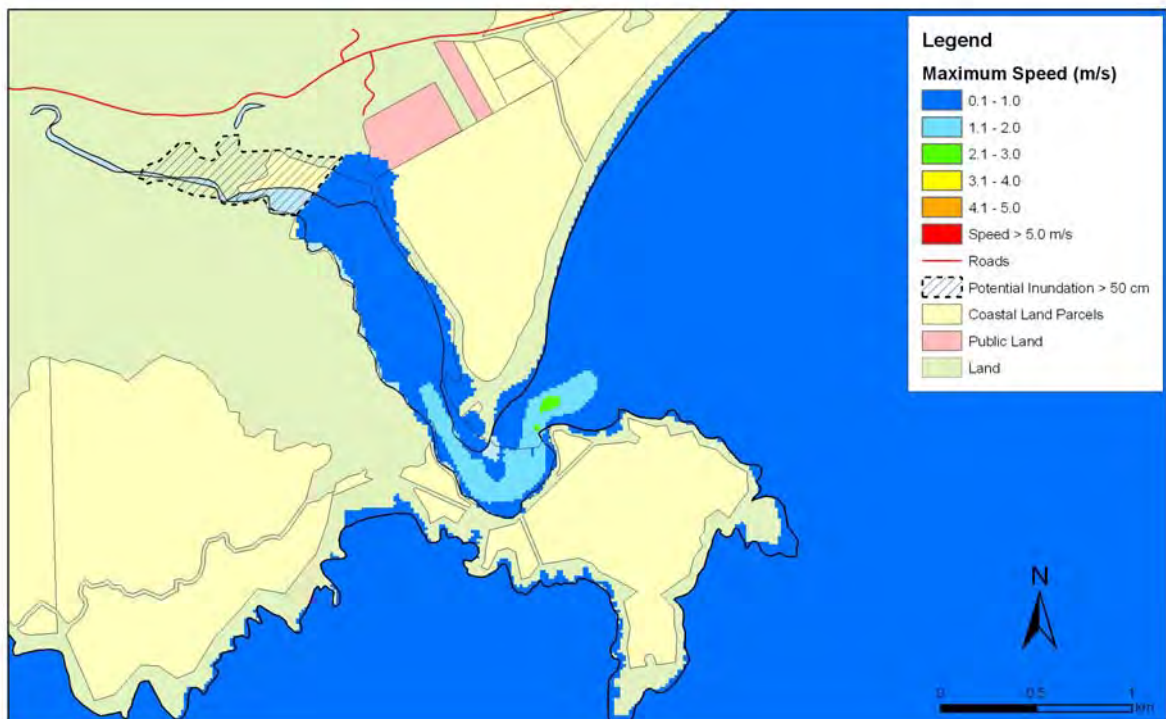
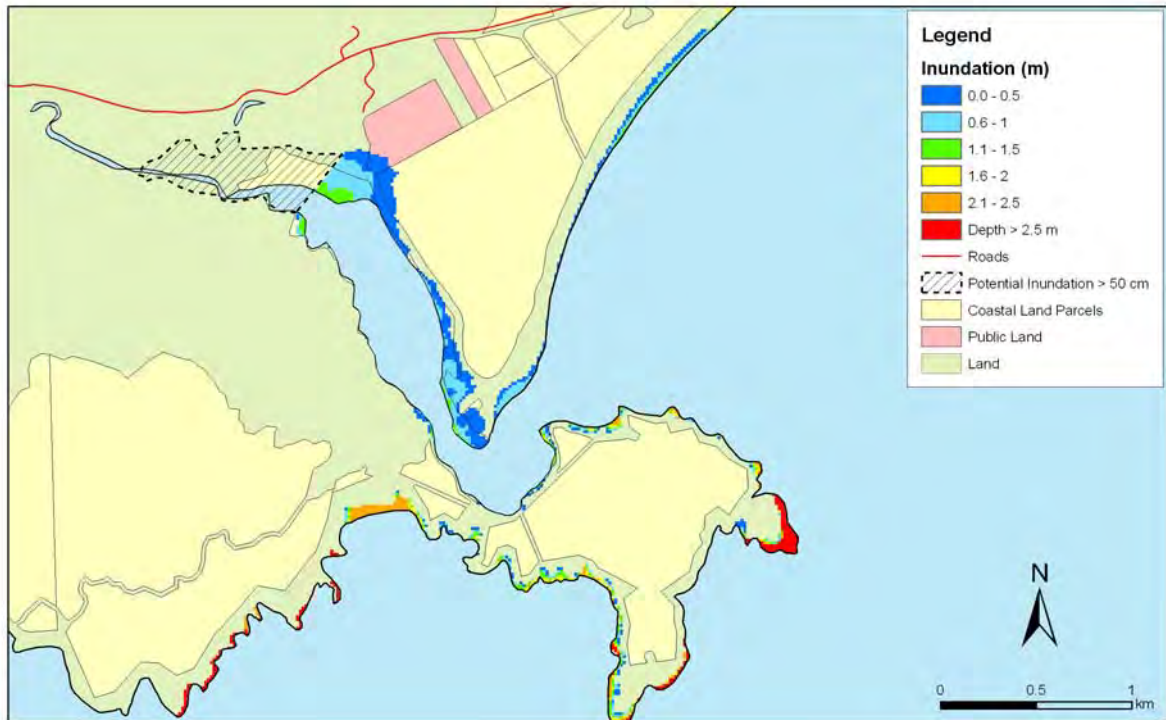


Figure 5.14: Tautuku - 1:100 year remote tsunami: Maximum water depth (top) for inundated land and maximum speed (bottom) for MHWS - with a sea level rise of 30 cm.

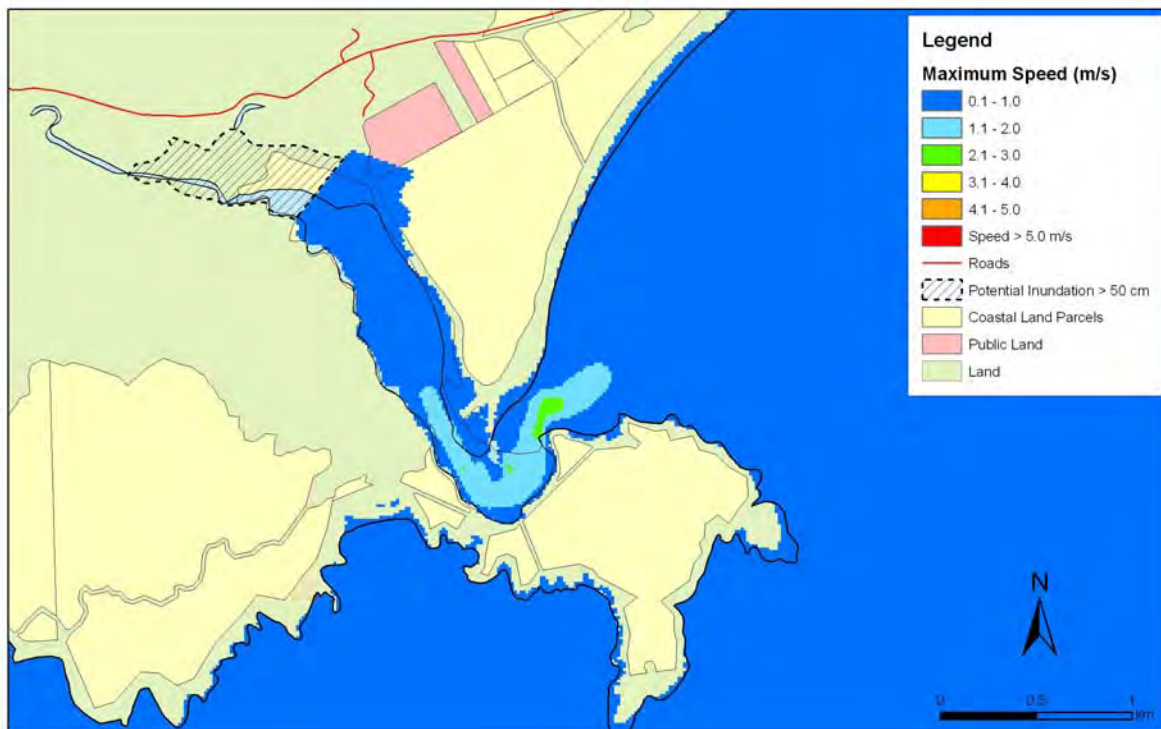
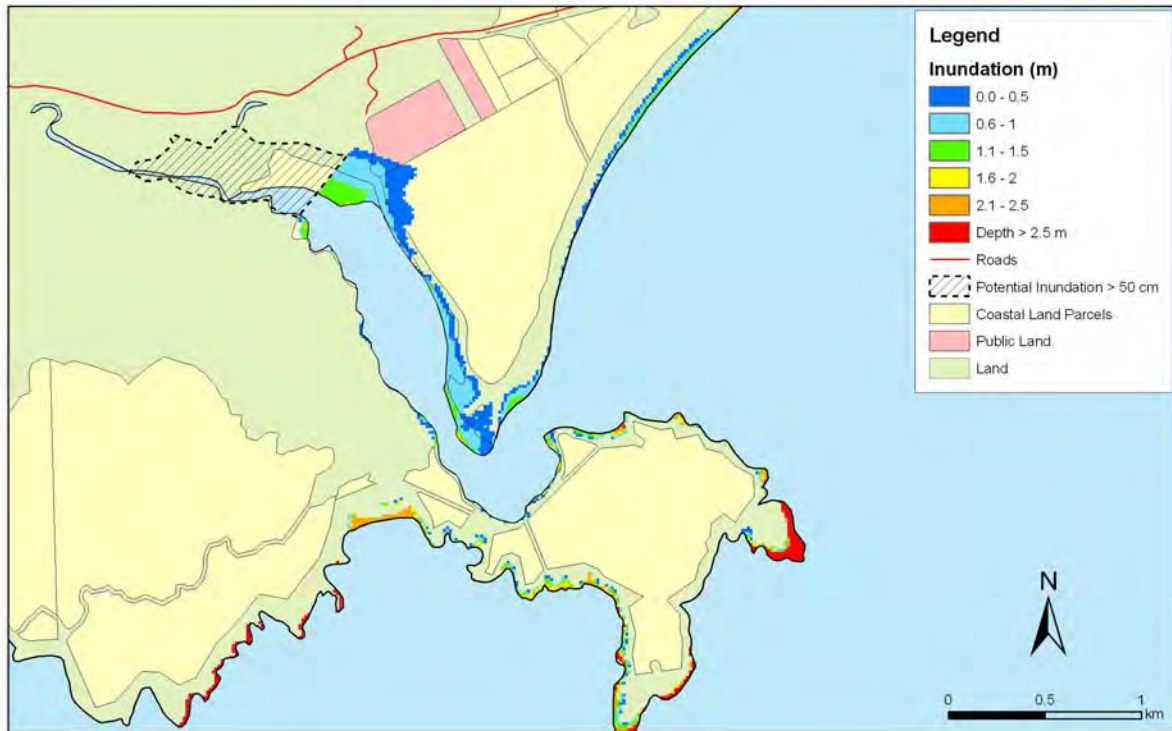


Figure 5.15: Tautuku - 1:100 year remote tsunami: Maximum water depth (top) for inundated land and maximum speed (bottom) for MHWS - with a sea level rise of 50 cm.

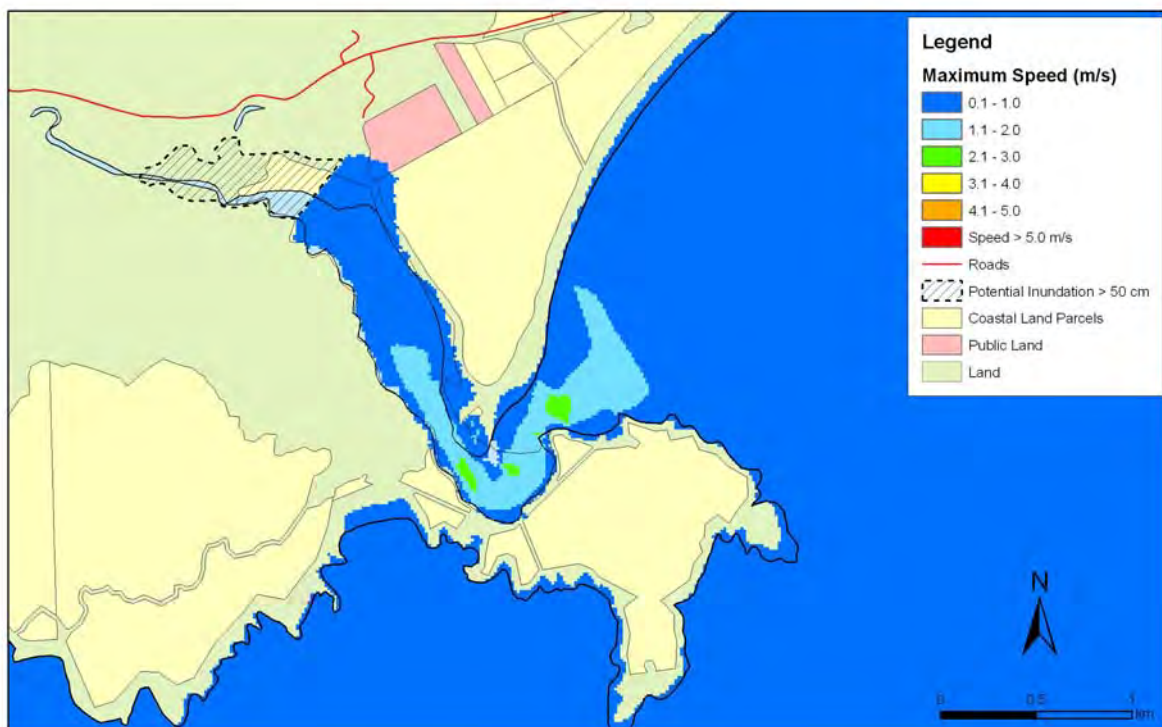
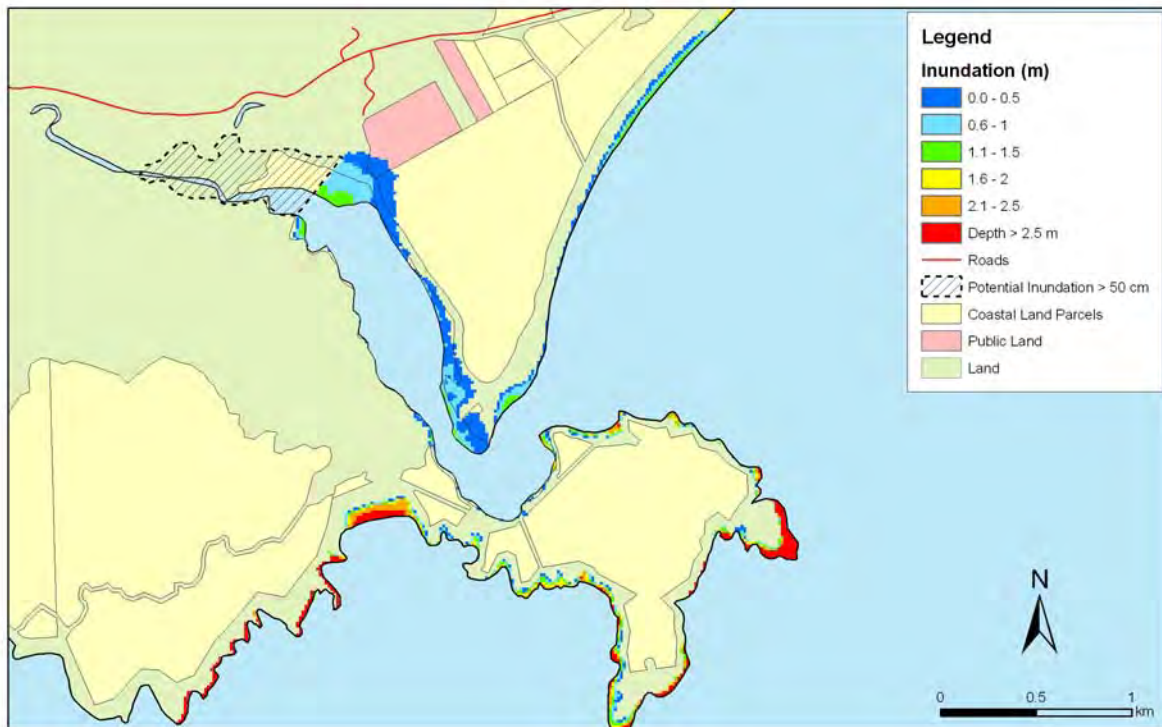


Figure 5.16: Tautuku - 1:500 year remote tsunami: Maximum water depth (top) for inundated land and maximum speed (bottom) for MHWS.

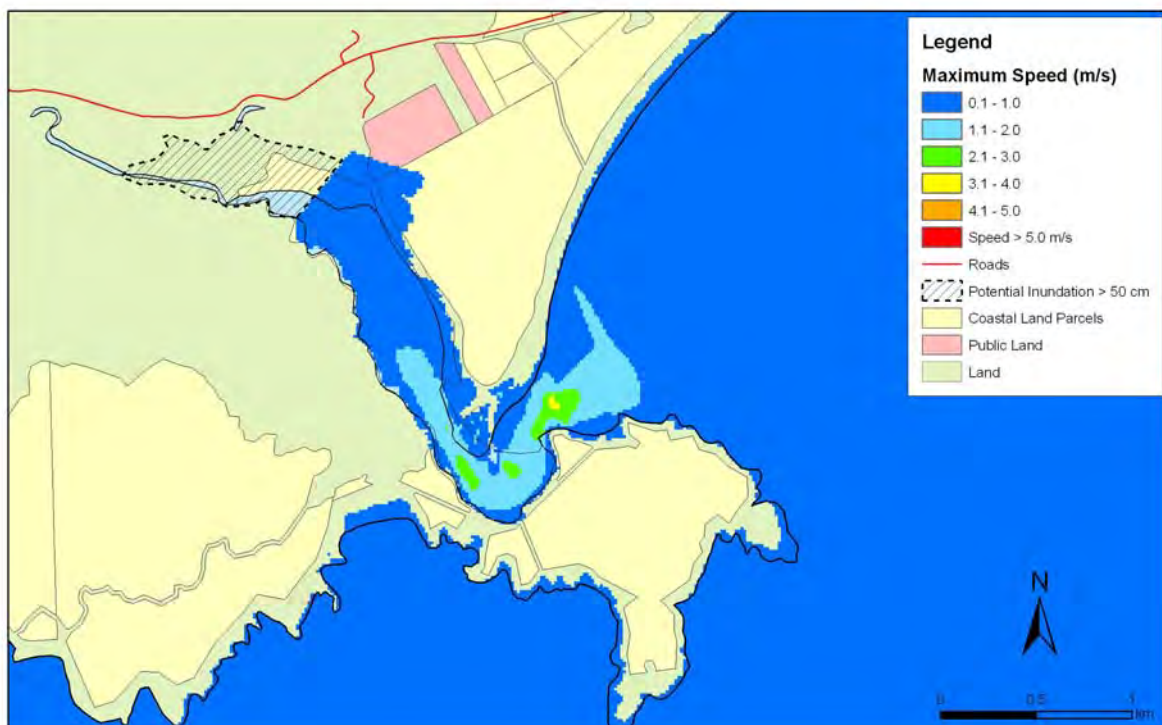
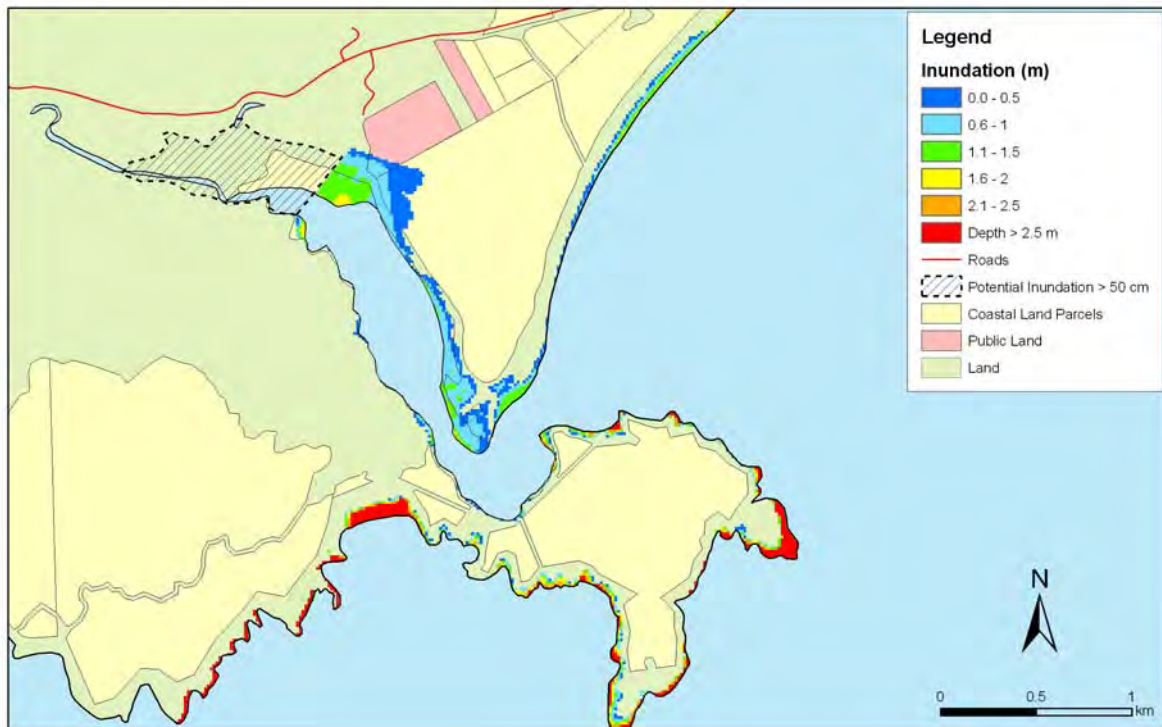


Figure 5.17: Tautuku - 1:500 year remote tsunami: Maximum water depth (top) for inundated land and maximum speed (bottom) for MHWS - with a sea level rise of 30 cm.

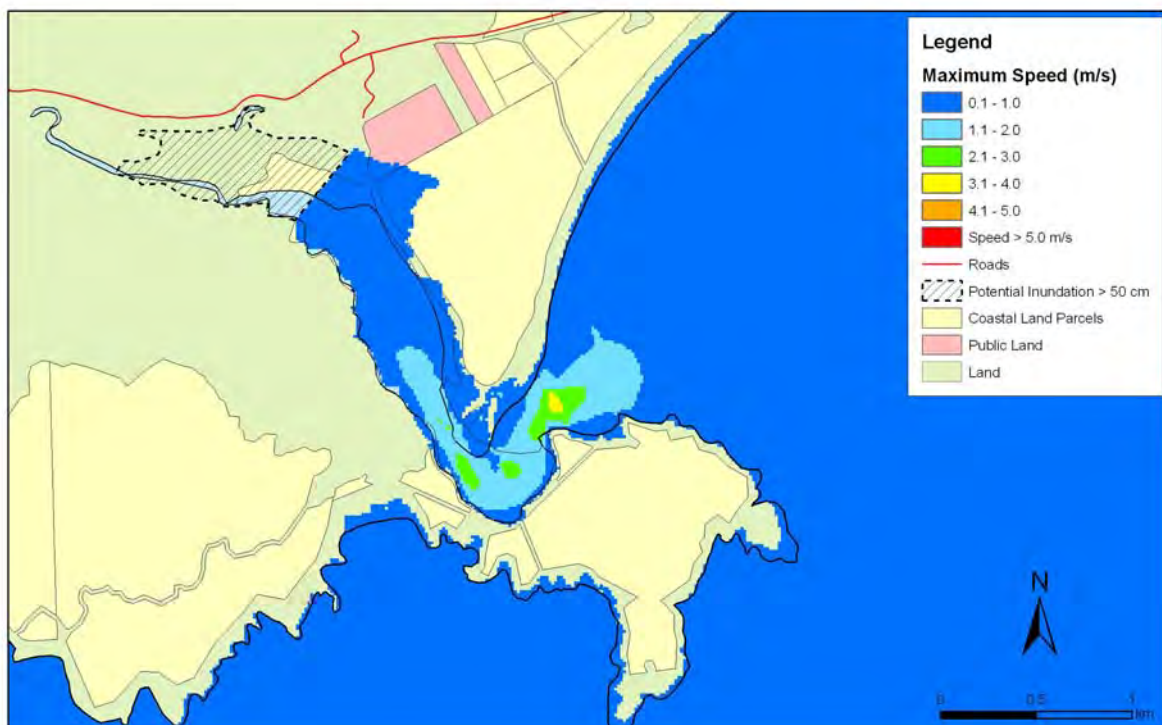
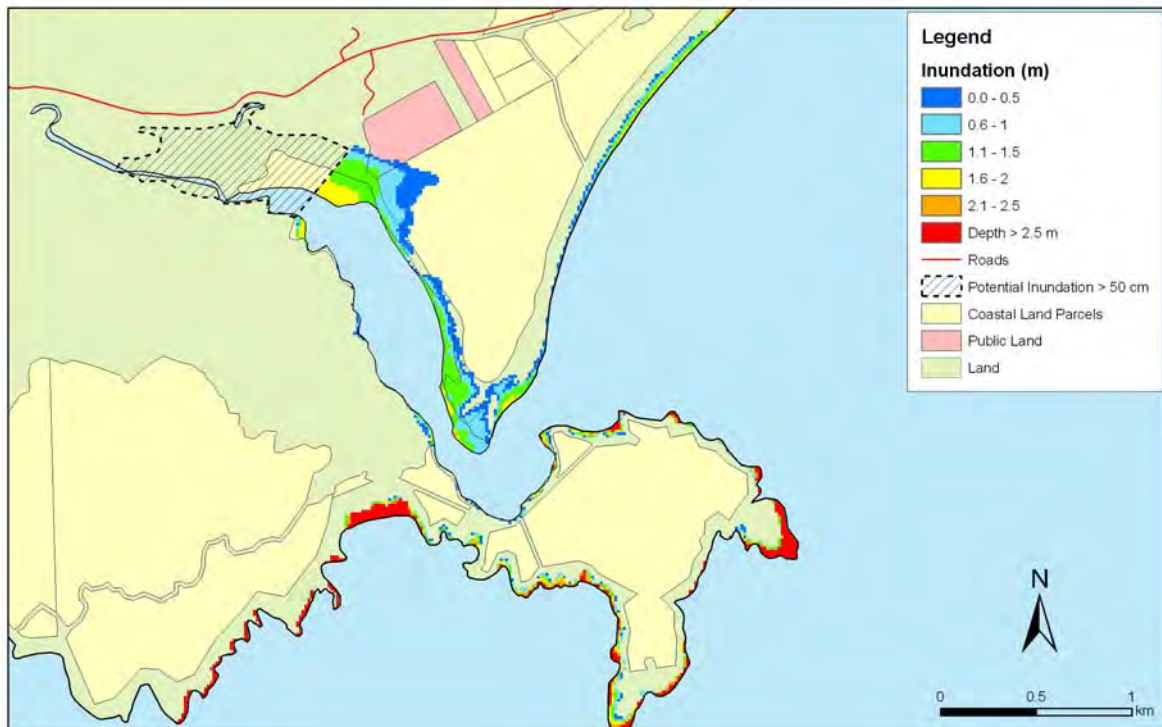


Figure 5.18: Tautuku - 1:500 year remote tsunami: Maximum water depth (top) for inundated land and maximum speed (bottom) for MHWS - with a sea level rise of 50 cm.

5.3.2 Papatowai

Figures 5.19 – 5.21 show maximum inundation and water speed for the near-field (Puysegur) tsunami scenarios. Figures 5.22 – 5.27 show maximum inundation and water speed for the far-field (South American) tsunami scenarios.

Papatowai: Near-Field

- Trough arrives first approximately 70 minutes after fault rupture. Water level decreases 80 cm over 40 minutes.
- First wave is largest. Arrives around 2 hours after fault rupture. Increases from undisturbed level of sea to maximum height over 15 mins. Amplitude 3.7 m.
- Multiple large waves, second highest is 4th with amplitude 2.8 m.
- Predominant period of wave arrivals: 30 minutes.
- Maximum runup: up to 4.5 m
- Private land is inundated on both sides of the Tahakopa River, especially near the mouth. There is inundation upriver to the landward limit of the modelling domain.
- At the current sea level there will only be a small amount of inundation of the township of Papatowai but as sea level rises this will be more pronounced. Additional areas also will risk more serious inundation.
- High maximum velocities at the river mouth and further upstream near the bridge suggest the risk of erosion and scouring at these points. Again, sea level rise exacerbates this risk. Erosion from the Puysegur tsunamis may have implications for the channel infrastructure.

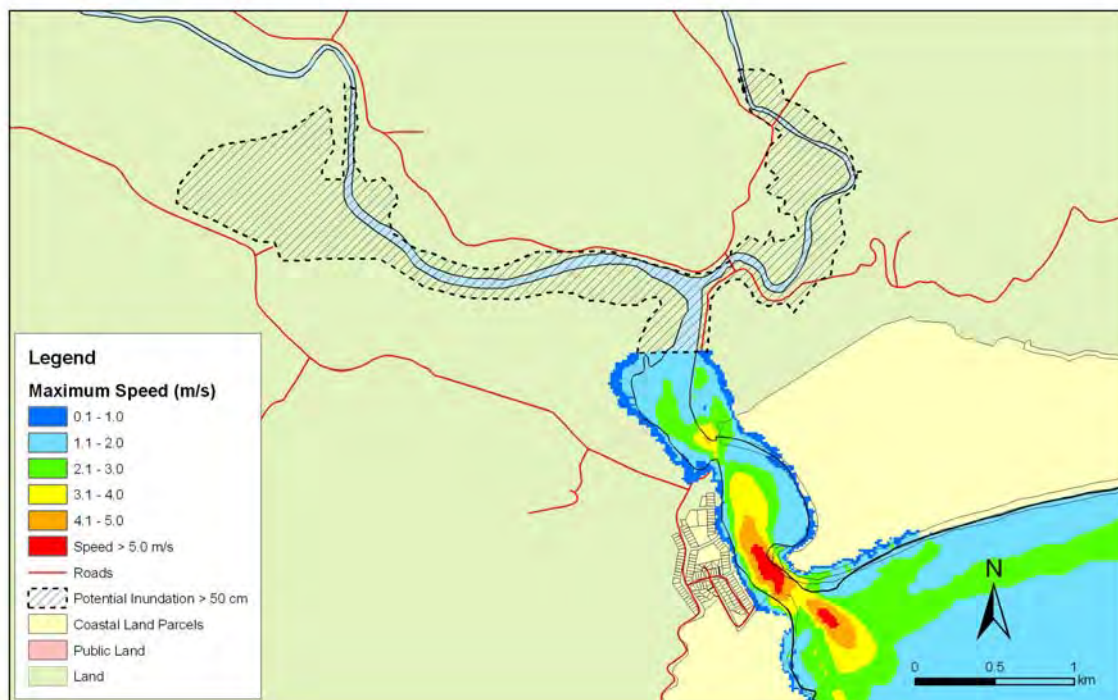
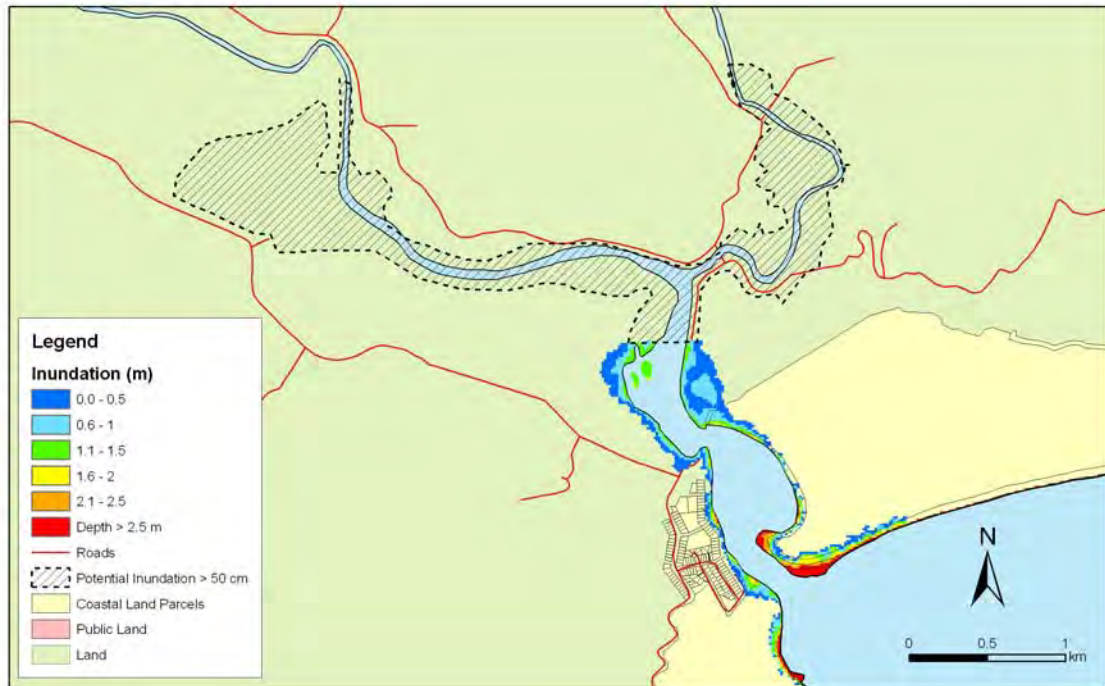


Figure 5.19: Papatowai - Puysegur tsunami: Maximum water depth for inundated land (top) and maximum speed (bottom) - for MHWS.

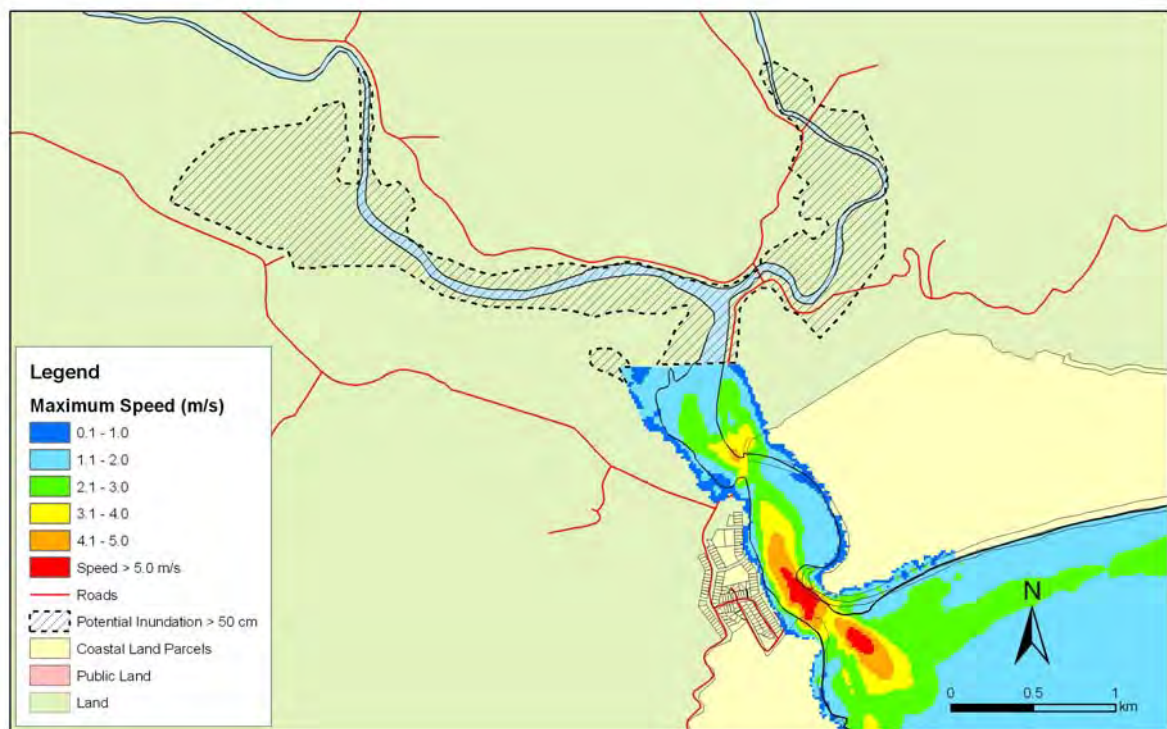


Figure 5.20: Papatowai - Puysegur tsunami: Maximum water depth for inundated land (top) and maximum speed (bottom) - for MHWS with a sea level rise of 30 cm.

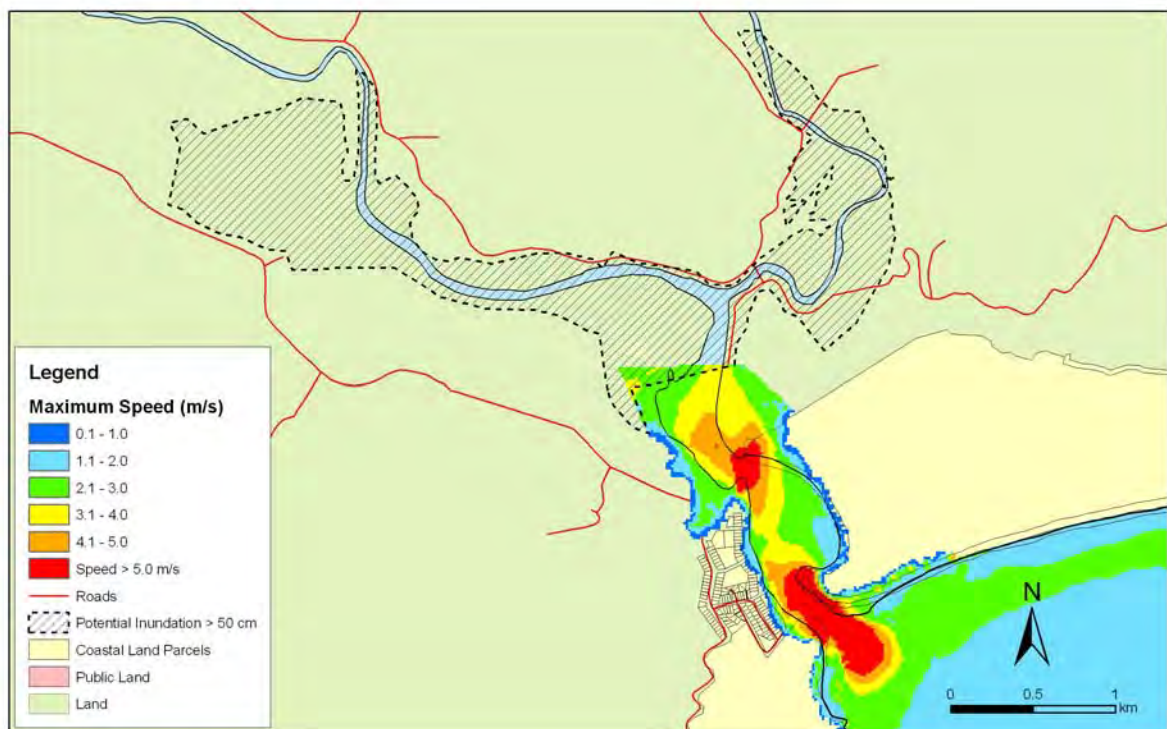
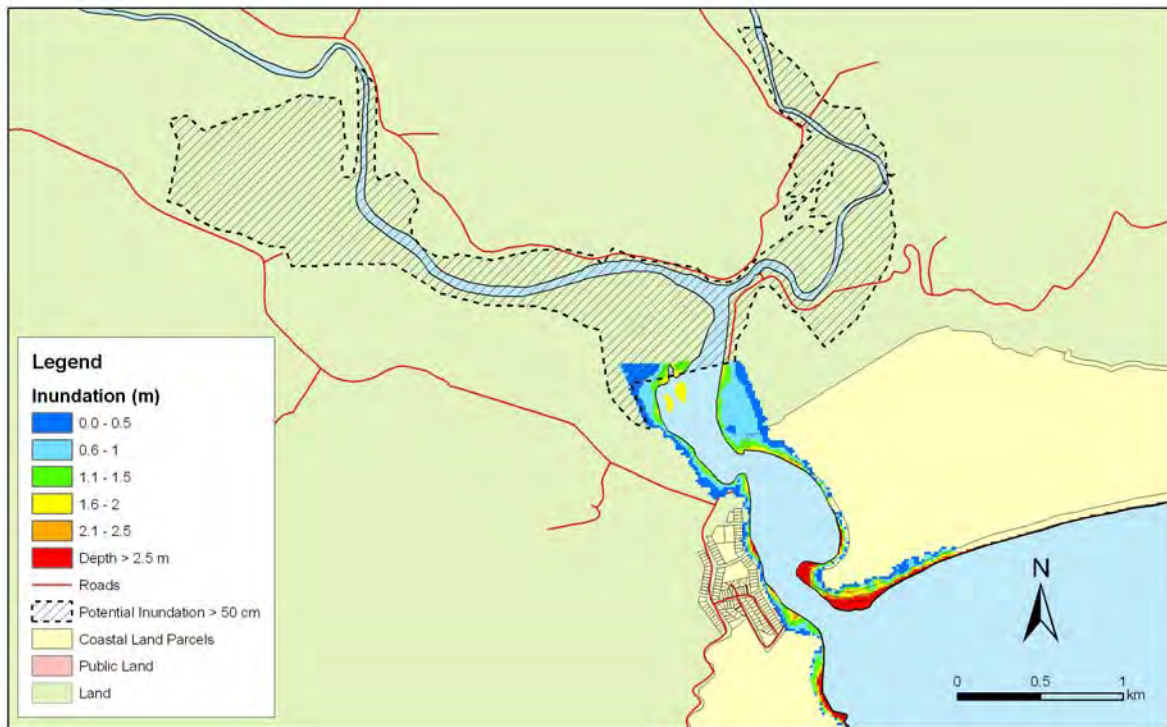


Figure 5.21: Papatowai - Puysegur tsunami: Maximum water depth for inundated land (top) and maximum speed (bottom) - for MHWS with a sea level rise of 50 cm.

Papatowai: Far-Field

- Both remote tsunamis begin with an increase in the water level.
- Third wave is highest with amplitude 1m, and a total height of 1.8m for the 1:100 year tsunami and amplitude 1.6m, total height 2.8m for the 1:500 year tsunami.
- Large waves experienced for around 7 hours after first arrival, with many subsequent smaller waves.
- Resonance period around 1.5 hours.
- Maximum runup: up to 1.9 metres for the 1:100 year tsunami and 2.6 for the 1:500 year tsunami.
- Inundation on either side of the Papatowai River especially near the river mouth.
- The erosion risk is highest at the river mouth and the bend in the river where the bridge crosses. Erosion from the remote tsunami may have implications on the channels and bridge infrastructure.

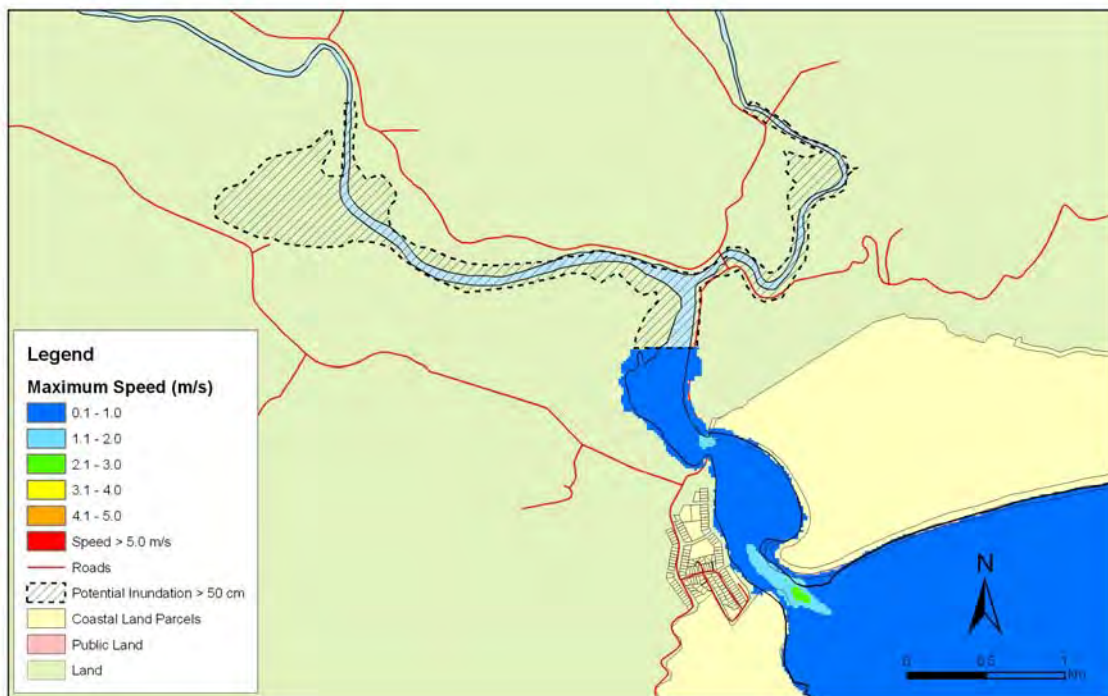


Figure 5.22 Papatowai – 1:100 year remote tsunami: Maximum water depth for inundated land (top) and maximum speed (bottom) - for MHWS.

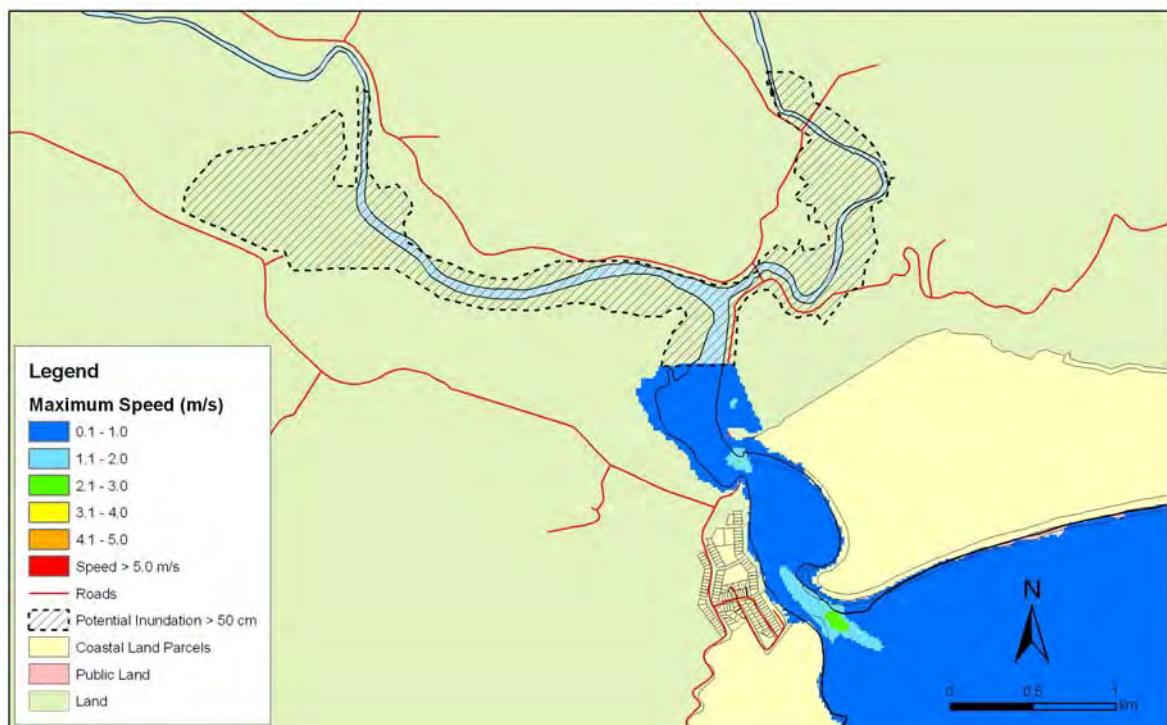


Figure 5.23: Papatowai – 1:100 year remote tsunami: Maximum water depth for inundated land (top) and maximum speed (bottom) - for MHS with a sea level rise of 30 cm.

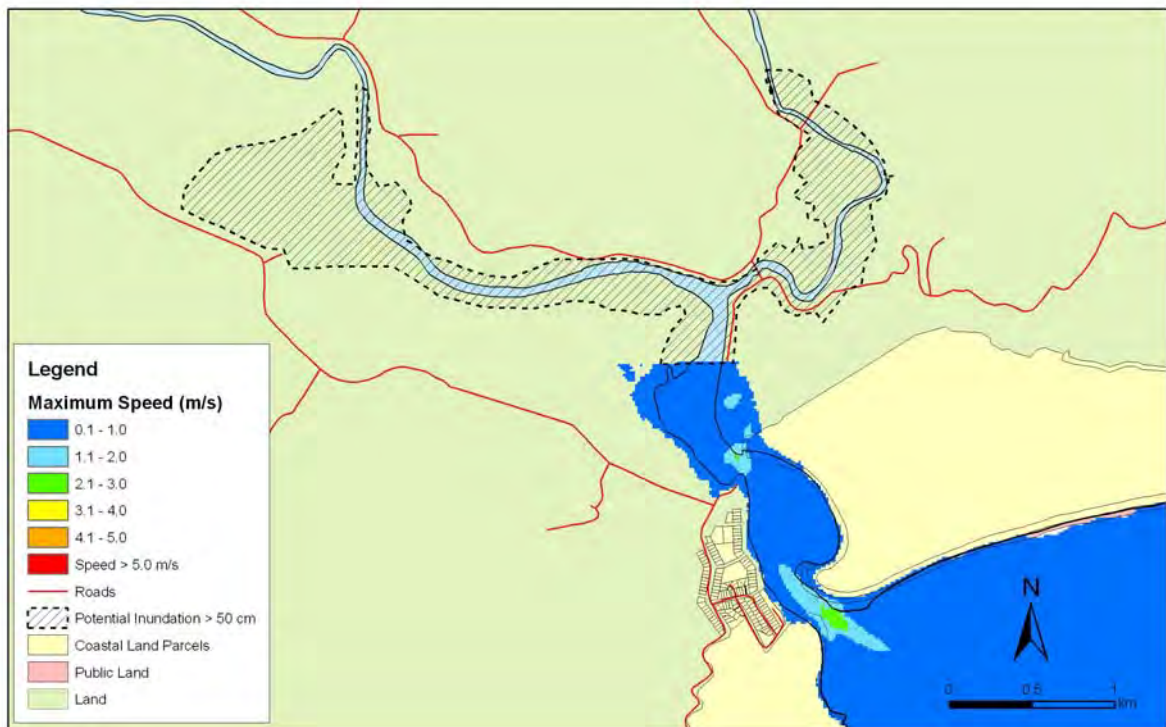


Figure 5.24: Papatowai – 1:100 year remote tsunami: Maximum water depth for inundated land (top) and maximum speed (bottom) - for MHWS with a sea level rise of 50 cm.

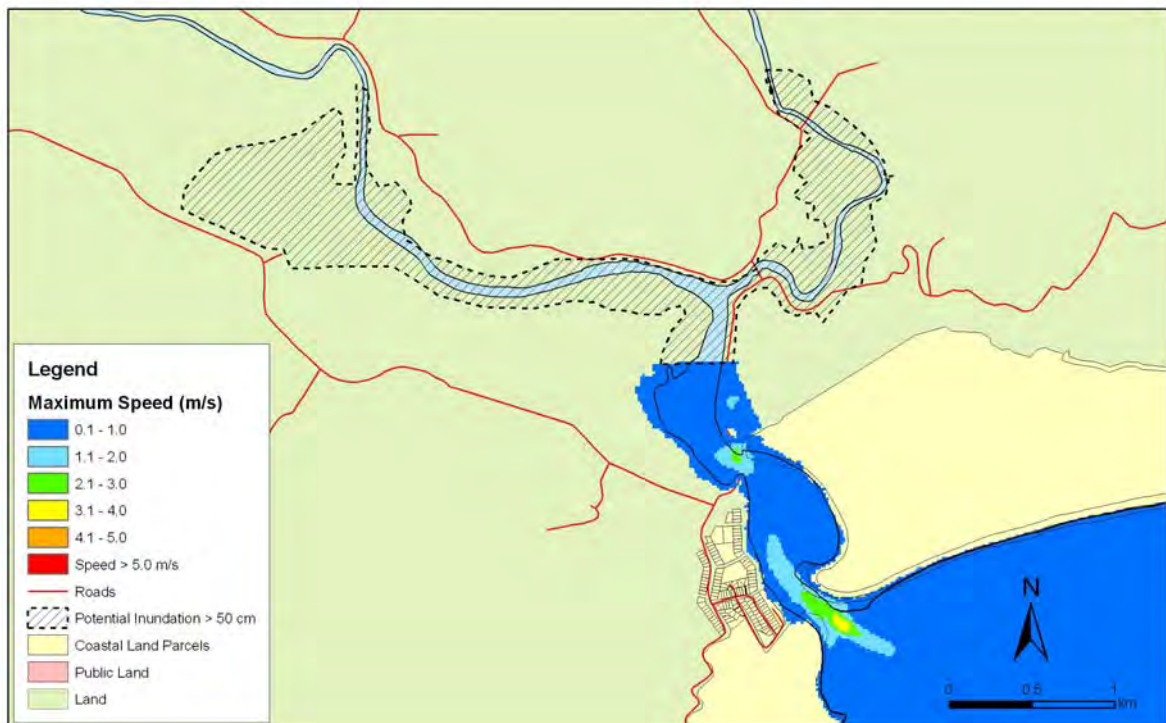


Figure 5.25: Papatowai – 1:500 year remote tsunami: Maximum water depth for inundated land (top) and maximum speed (bottom) - for MHWS.

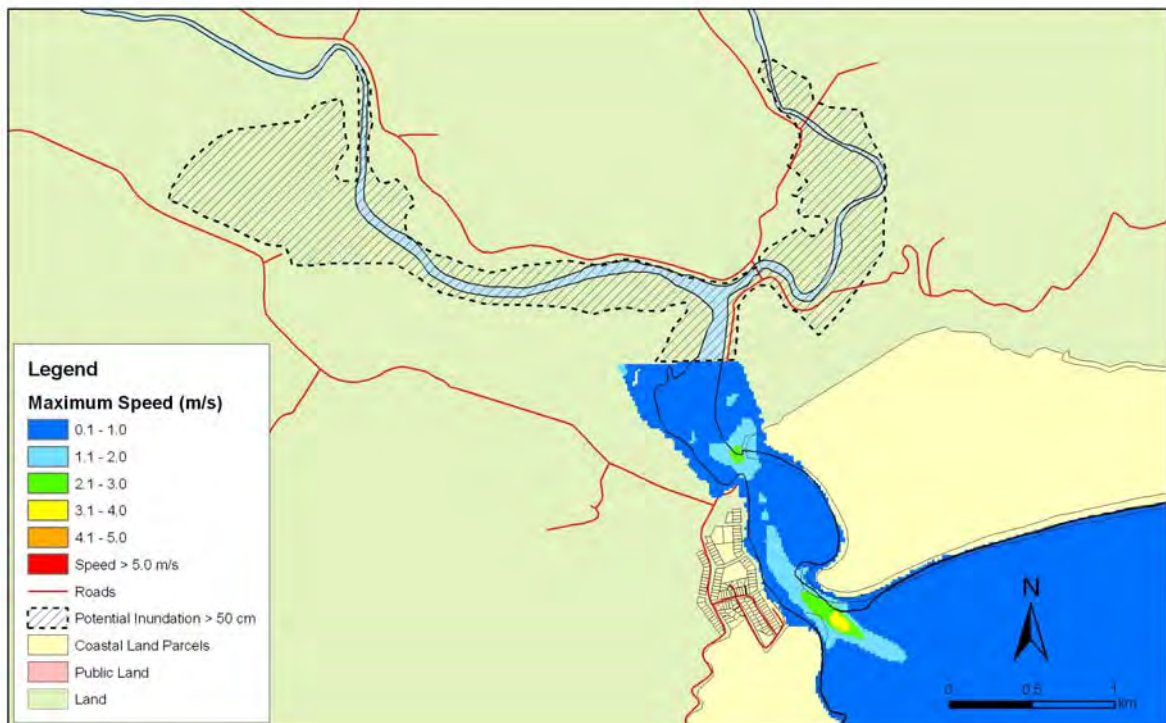
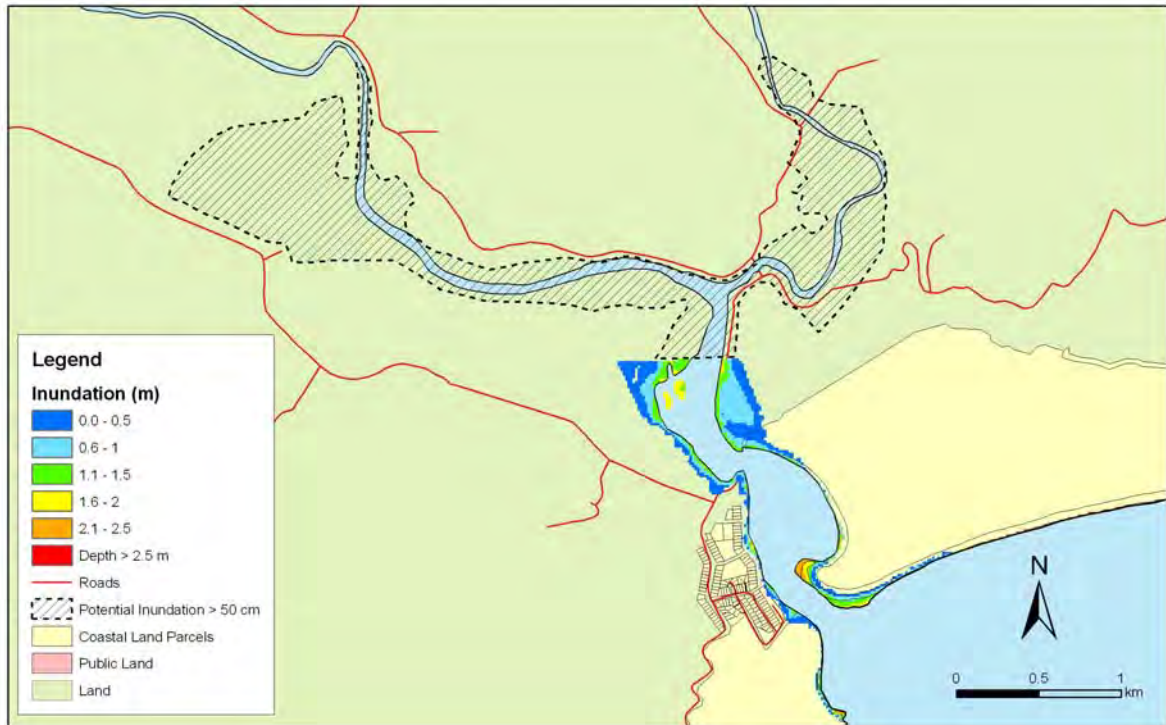


Figure 5.26: Papatowai – 1:500 year remote tsunami: Maximum water depth for inundated land (top) and maximum speed (bottom) - for MHS with a sea level rise of 30 cm.

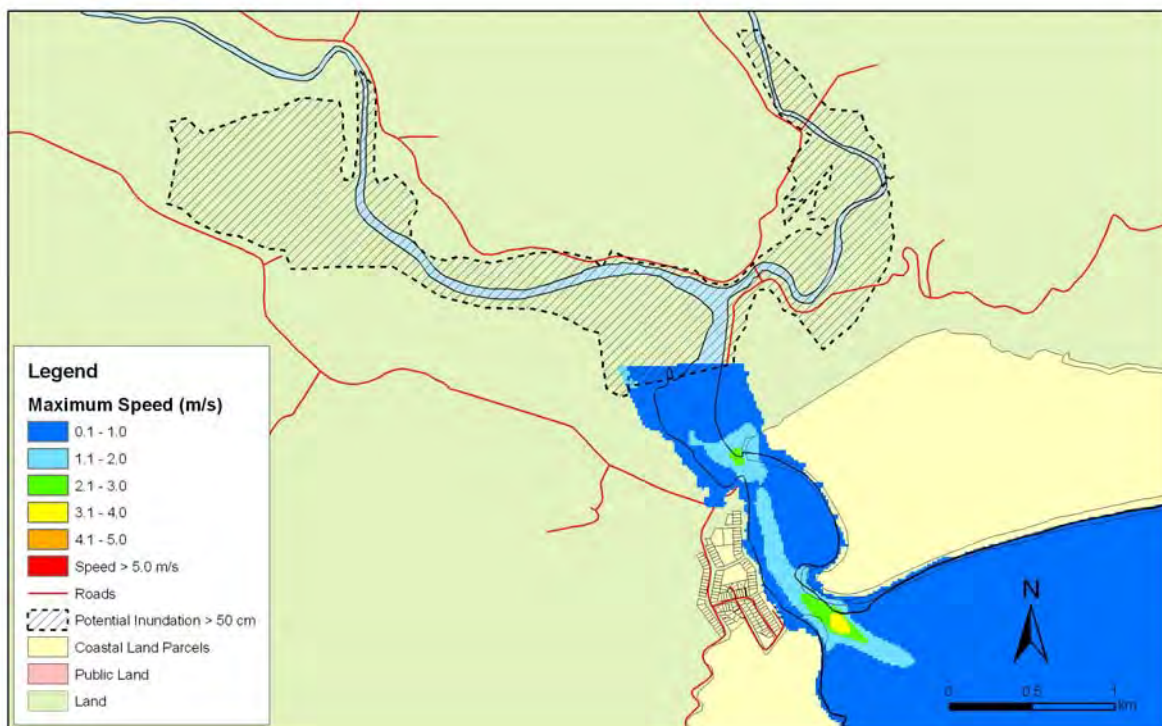
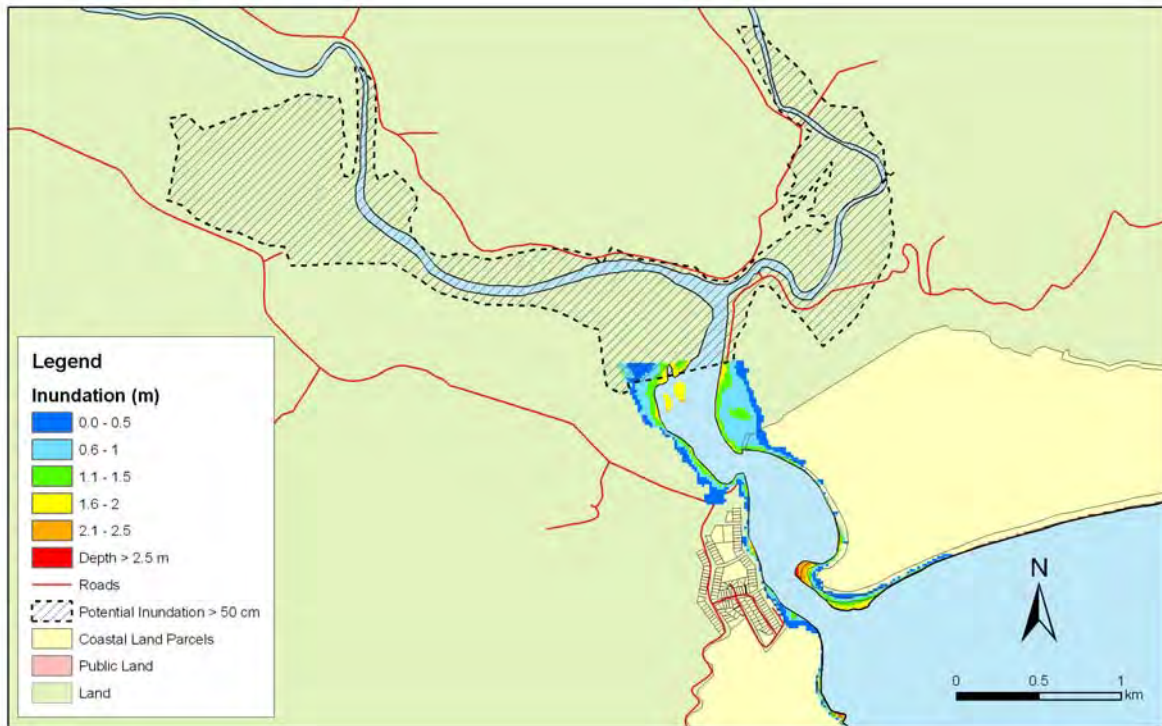


Figure 5.27: Papatowai – 1:500 year remote tsunami: Maximum water depth for inundated land (top) and maximum speed (bottom) - for MHS with a sea level rise of 50 cm.

5.3.3 Catlins

Figures 5.28 – 5.30 show maximum inundation and water speed for the near-field (Puysegur) tsunami scenarios. Figures 5.31 – 5.36 show maximum inundation and water speed for the far-field (South American) tsunami scenarios.

Catlins: Near-Field

- Trough arrives first approximately 70 minutes after fault rupture. Water level decreases 60 cm over 40 minutes.
- A small wave arrives before the first main wave (which is the third biggest). Arrives around 2 hours after fault rupture. Amplitude 2.0 m.
- Second wave has amplitude 2.1 m.
- Biggest wave is fifth wave with amplitude 2.6 m.
- Predominant period of wave arrivals: 20 minutes.
- Maximum runup: up to 4 m in places.
- Significant inundation of Pounaweia and up the Catlins River to the landward extent of the model domain. Inundation up to 2 metres deep at current sea level.
- High velocities on headland and upriver pose extensive erosion risk. Velocities are considerably higher with sea level rise highlighting increased erosion risk.

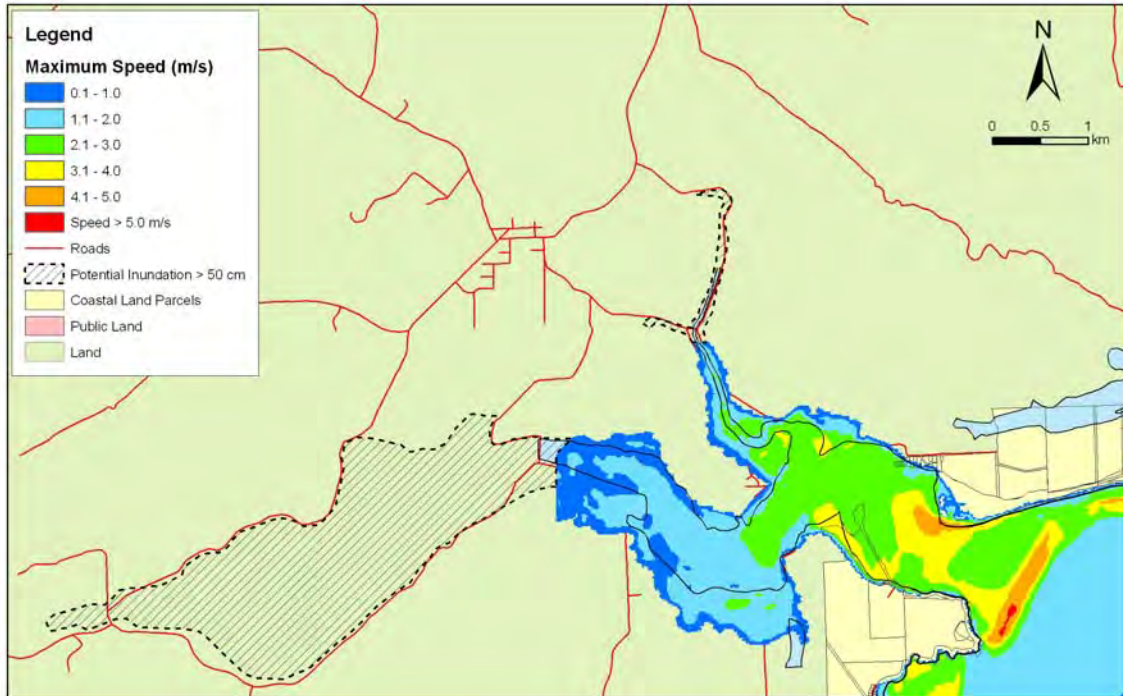
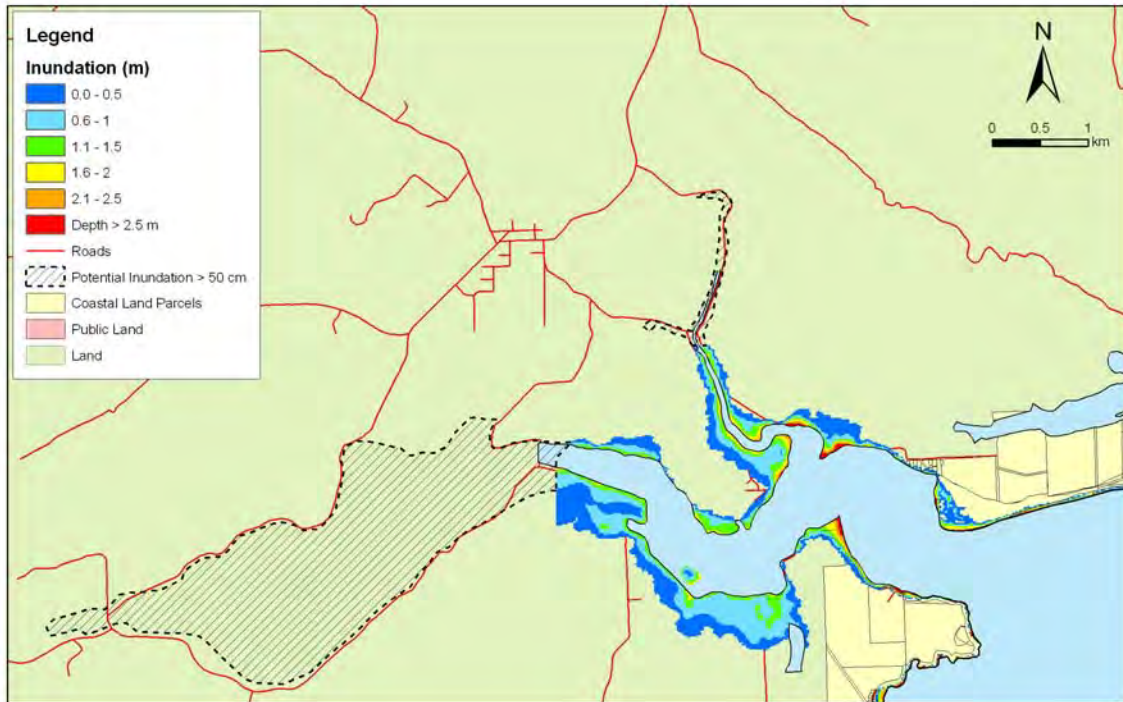


Figure 5.28: Catlins – Puysegur tsunami: Maximum water depth for inundated land (top) and maximum speed (bottom) for MHWS.

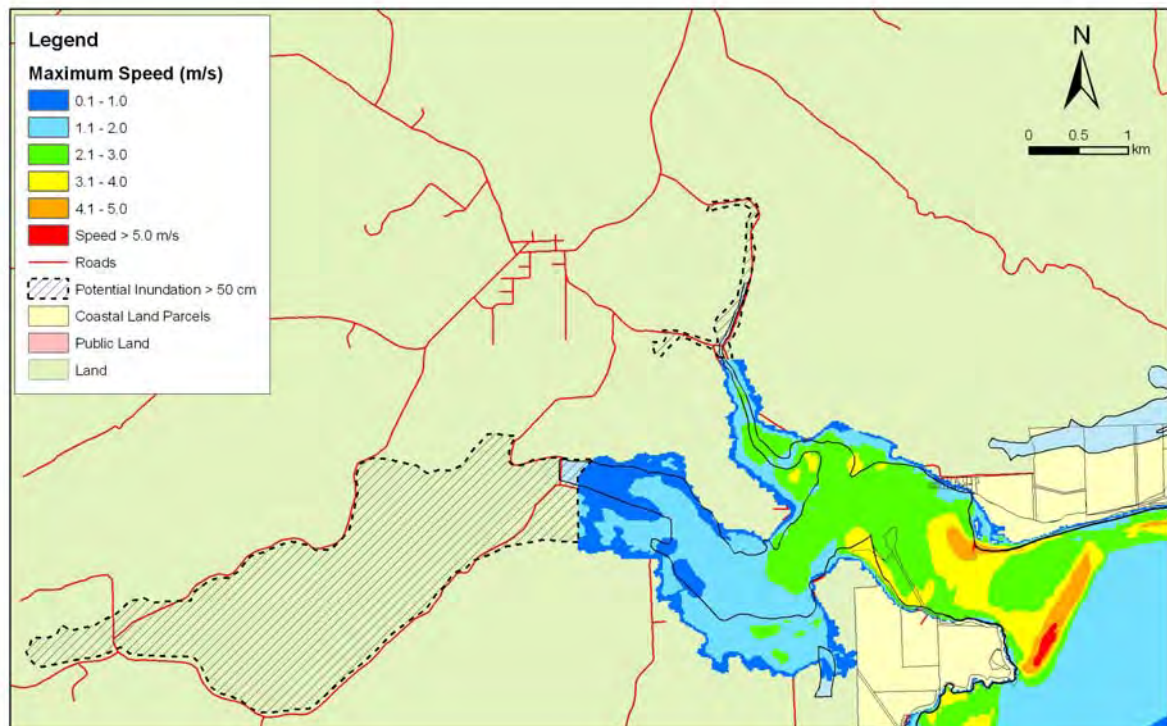
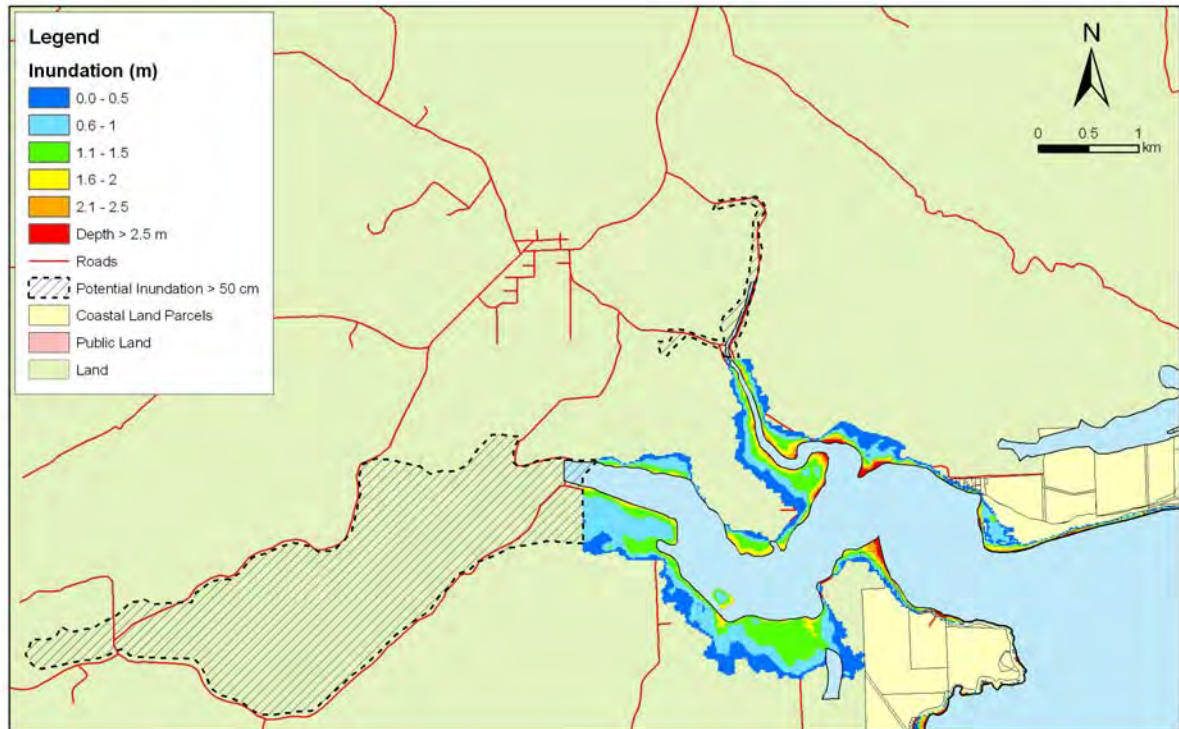


Figure 5.29: Catlins – Puysegur tsunami: Maximum water depth for inundated land (top) and maximum speed (bottom) for MHWS with a sea level rise of 30 cm.

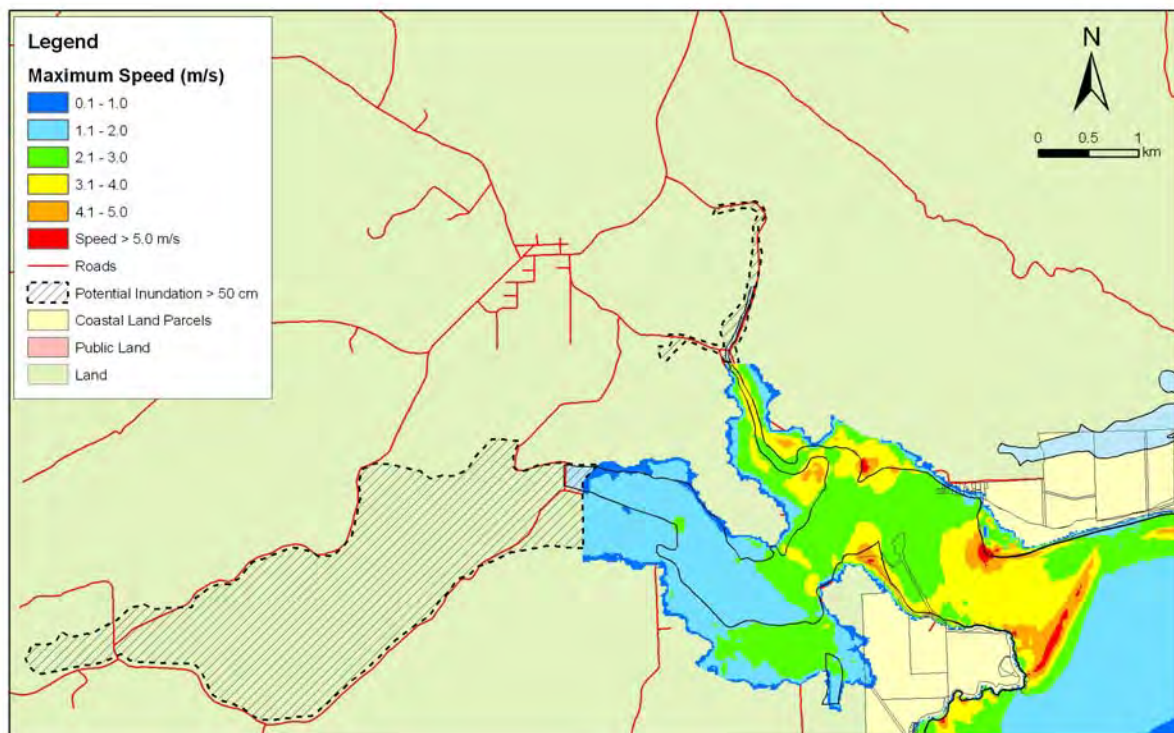
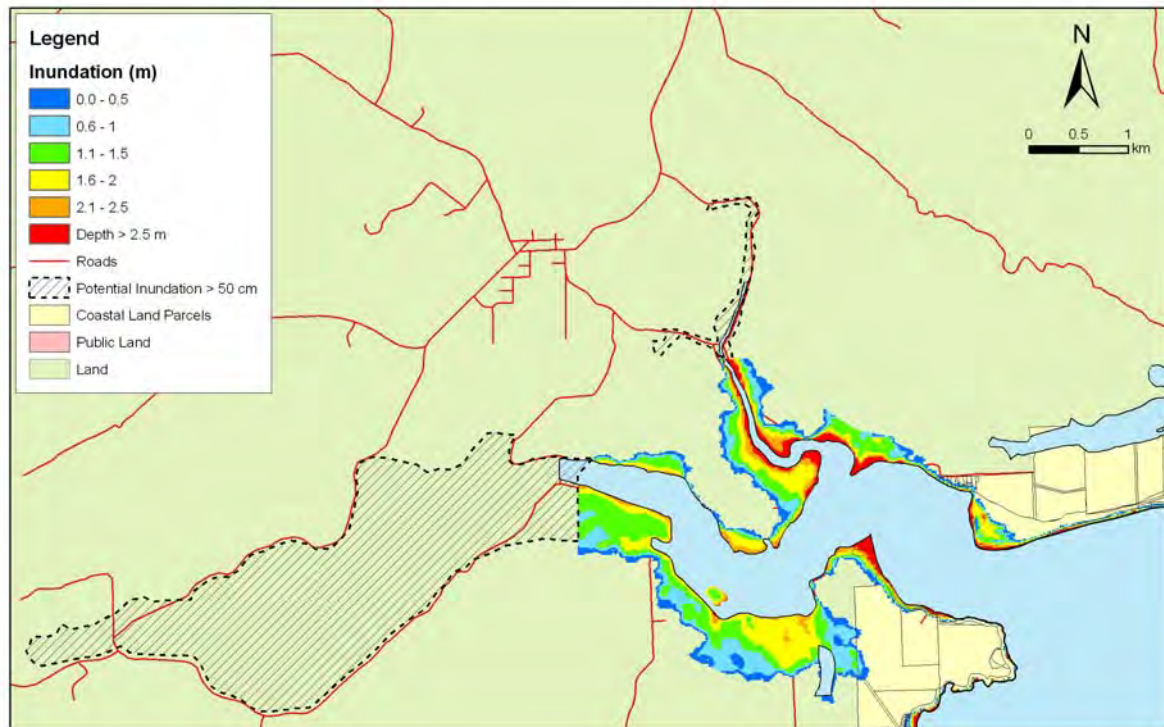


Figure 5.30: Catlins – Puysegur tsunami: Maximum water depth for inundated land (top) and maximum speed (bottom) for MHWS with a sea level rise of 50 cm.

Catlins: Far-Field

- Both remote tsunamis begin with an increase in the water level.
- Third wave is highest with amplitude 1m, total height 1.6m for the 1:100 year tsunami and amplitude 1.6m, total height 3.2m for the 1:500 year tsunami.
- Large waves for around 7 hours after first arrival followed by many smaller ones.
- Resonance period around 1.5 hours.
- Maximum runup: up to 1.9 metres for the 1:100 year tsunami and 2.2 metres for the 1:500 year tsunami.
- Pounaweia is slightly inundated by the 1:100 year tsunami and more so by the bigger tsunami and those with sea level rise also included. There is also considerable inundation along the banks of the Catlins River.
- Erosion risk along the riverbanks is less than for other settlements but the area becomes increasingly exposed as the sea level rises.

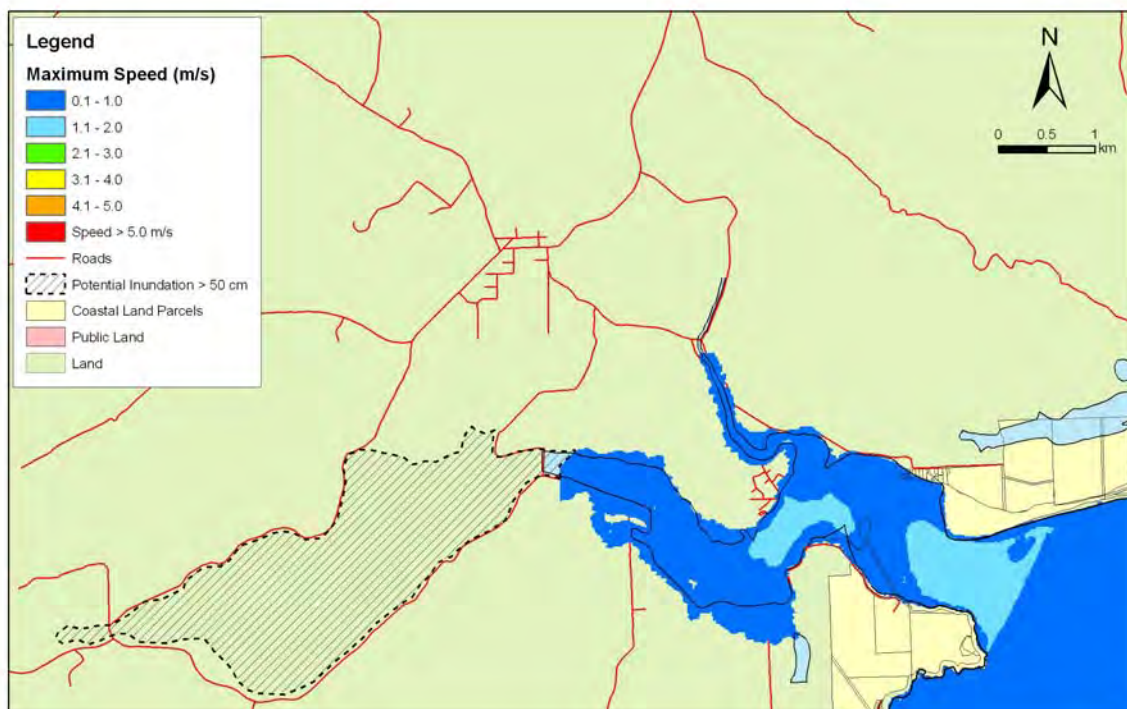


Figure 5.31: Catlins – 1:100 year remote tsunami: Maximum water depth for inundated land (top) and maximum speed (bottom) for MHWS.

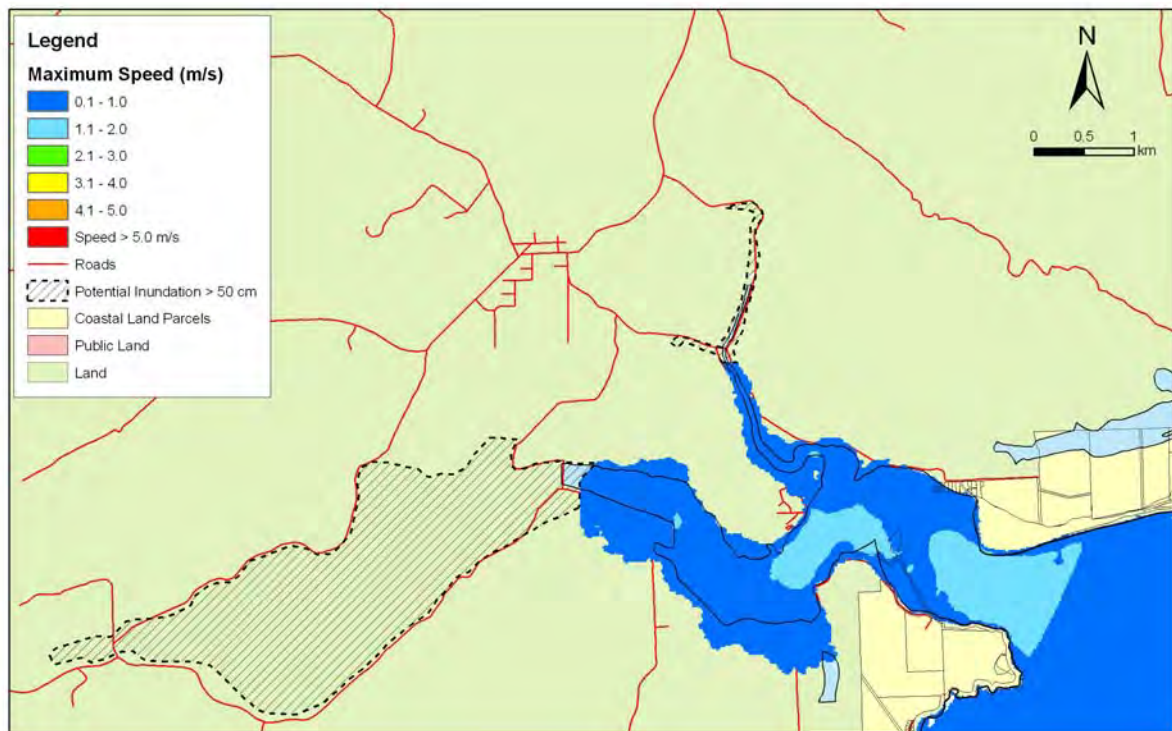
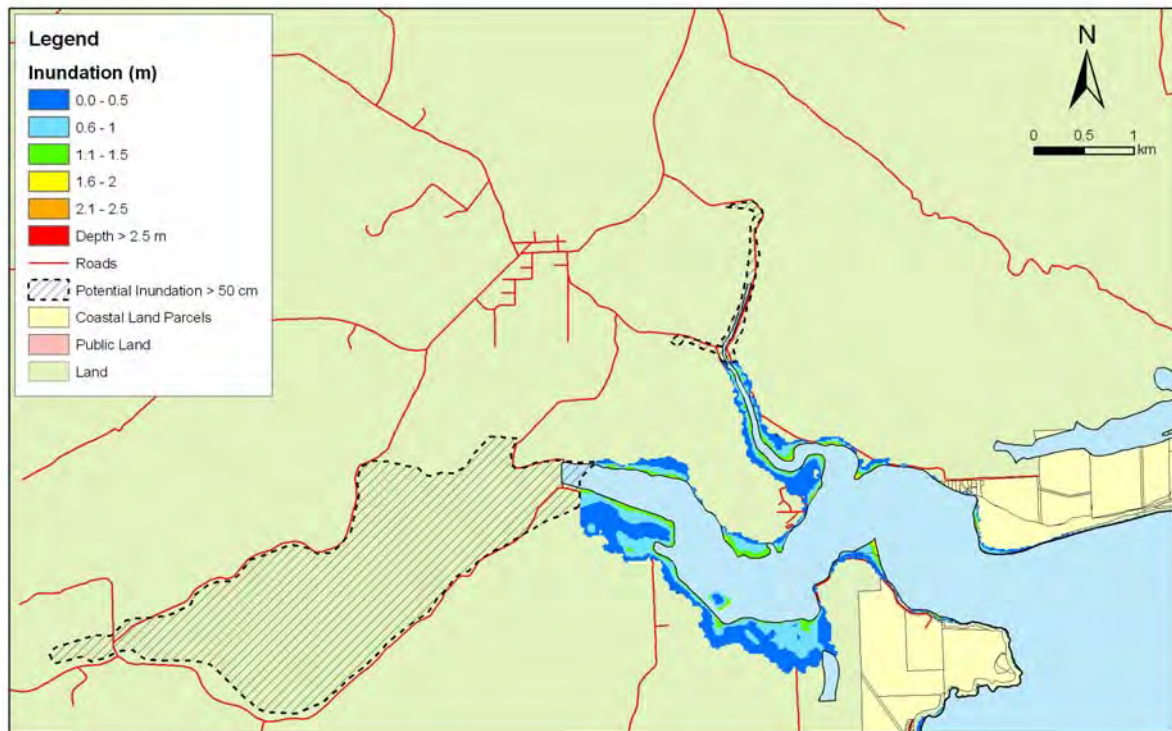


Figure 5.32: Catlins – 1:100 year remote tsunami: Maximum water depth for inundated land (top) and maximum speed (bottom) for MHWS - with a sea level rise of 30 cm.

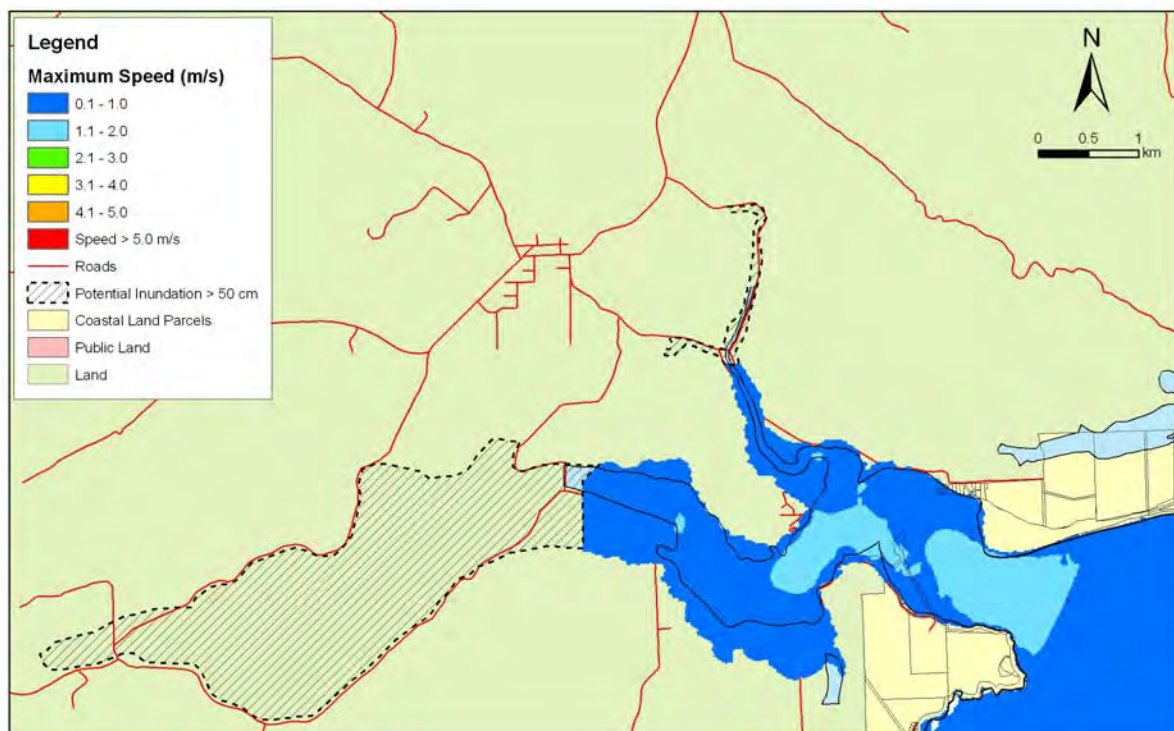
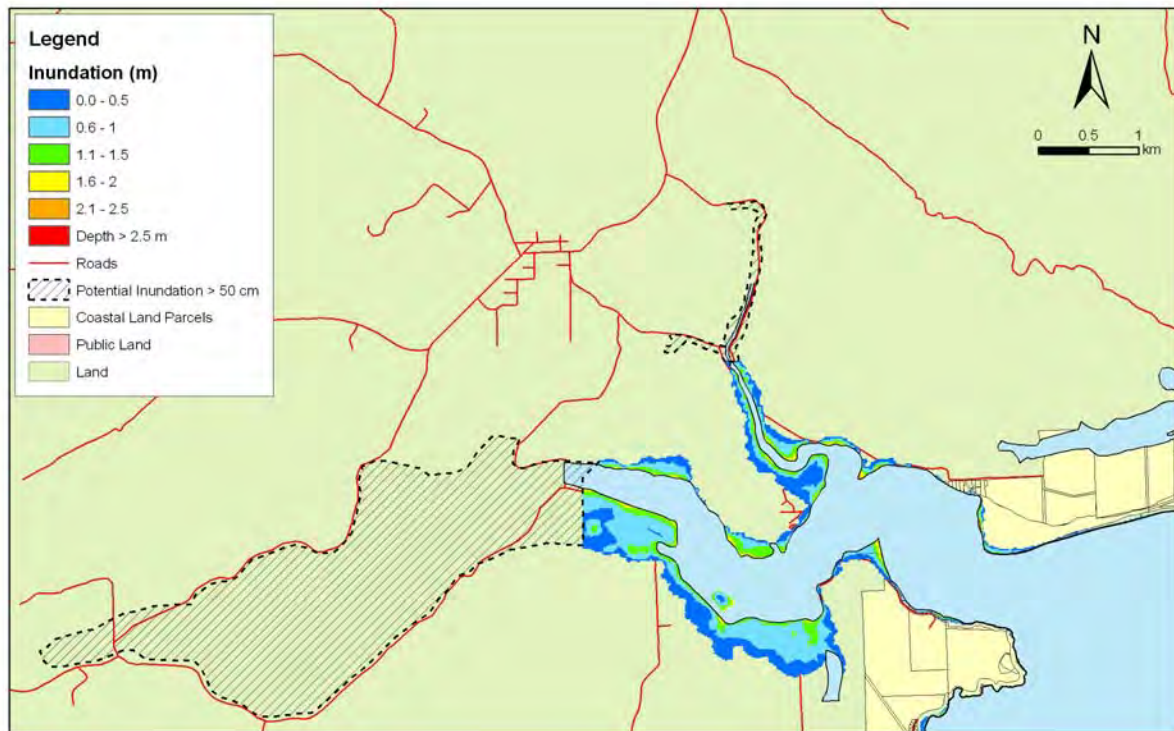


Figure 5.33: Catlins – 1:100 year remote tsunami: Maximum water depth for inundated land (top) and maximum speed (bottom) for MHWS - with a sea level rise of 50 cm.

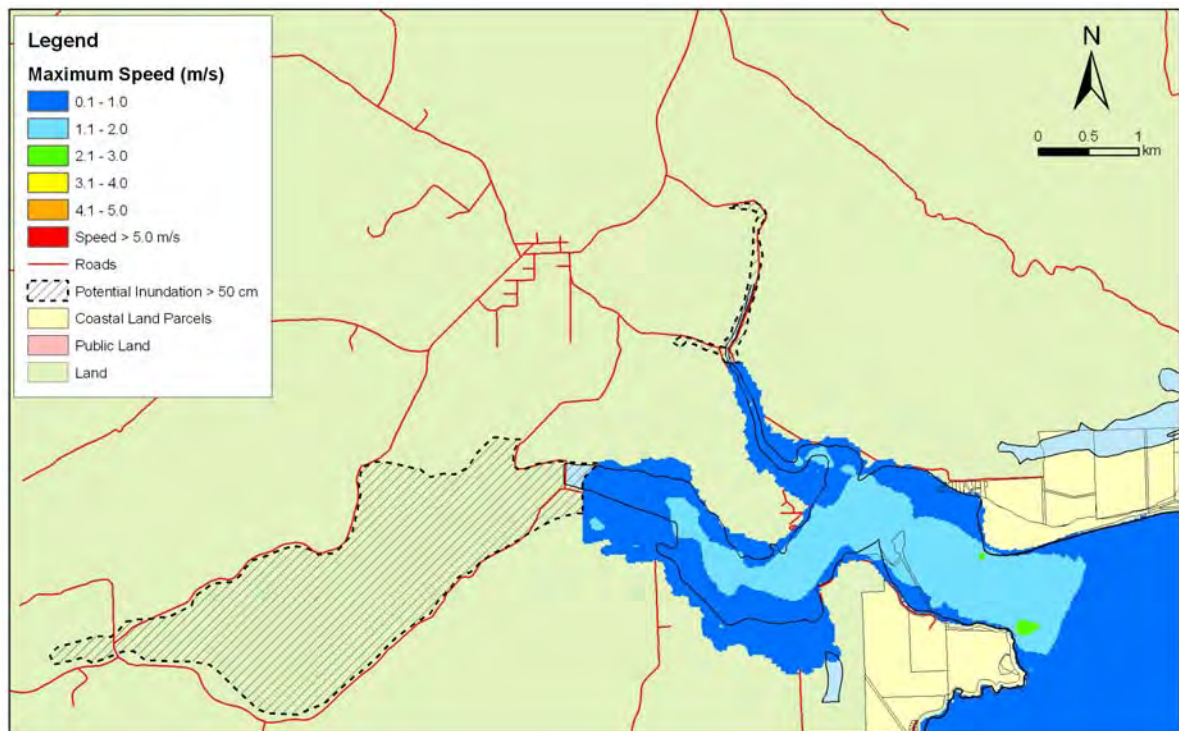
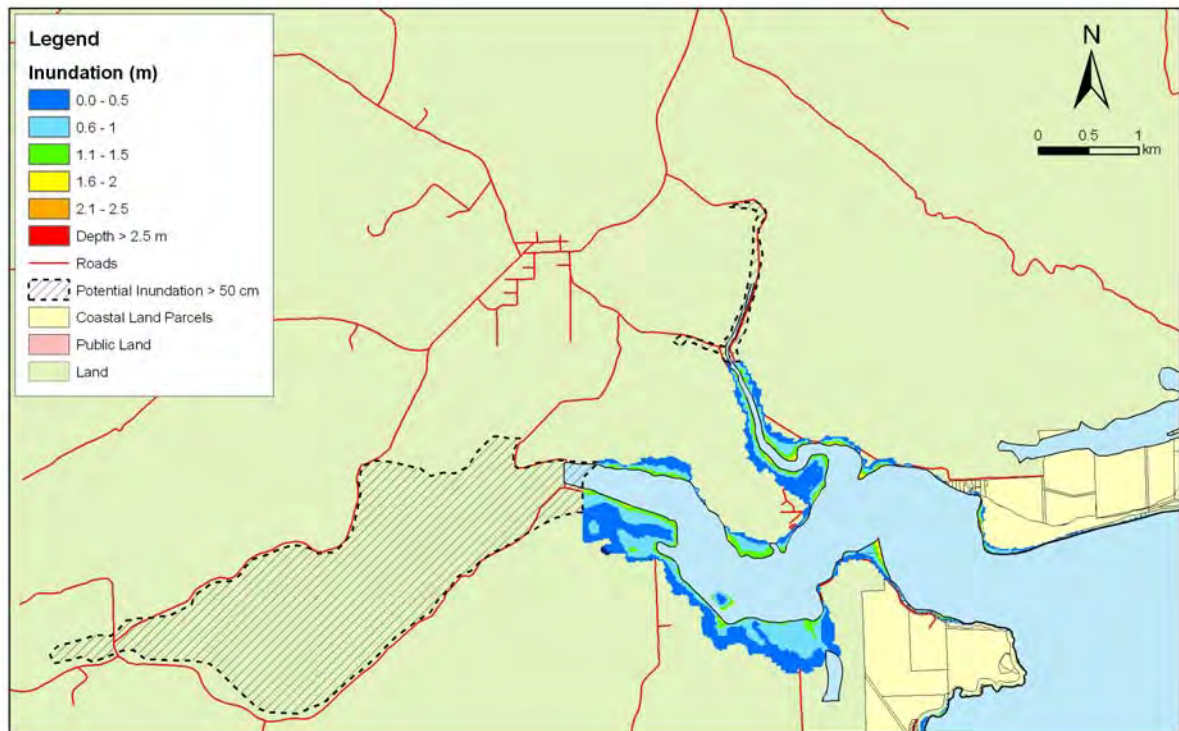


Figure 5.34: Catlins – 1:500 year remote tsunami: Maximum water depth for inundated land (top) and maximum speed (bottom) for MHWS.

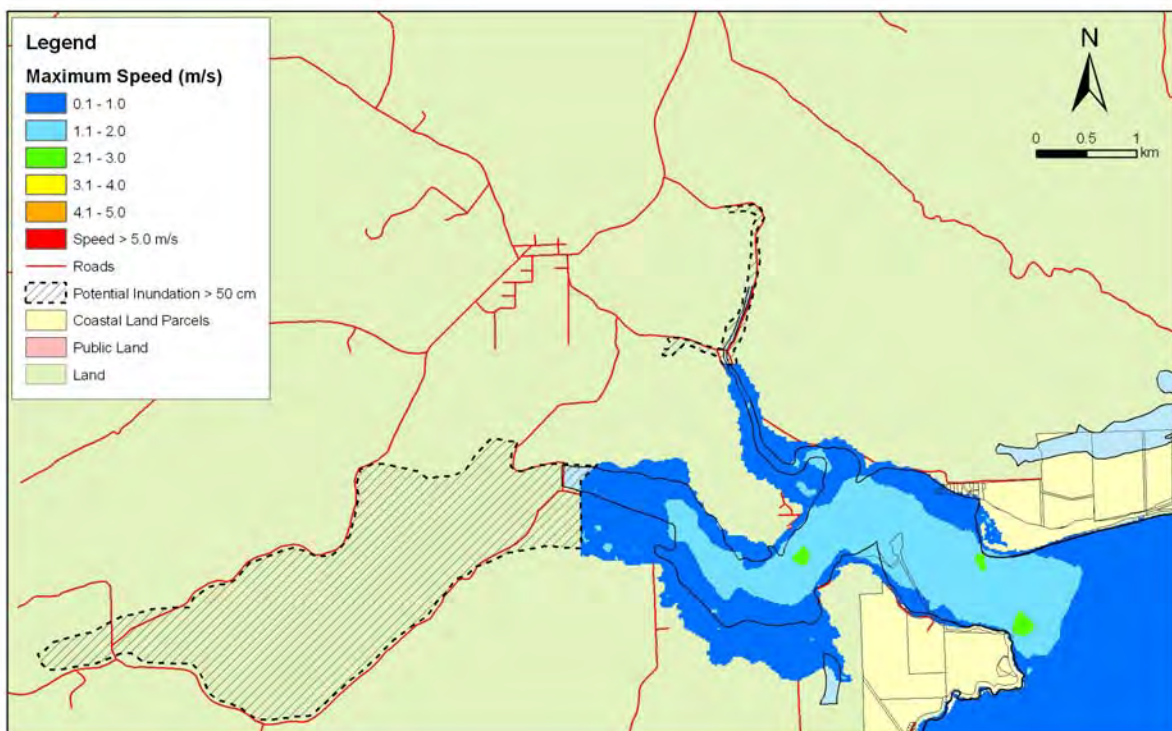
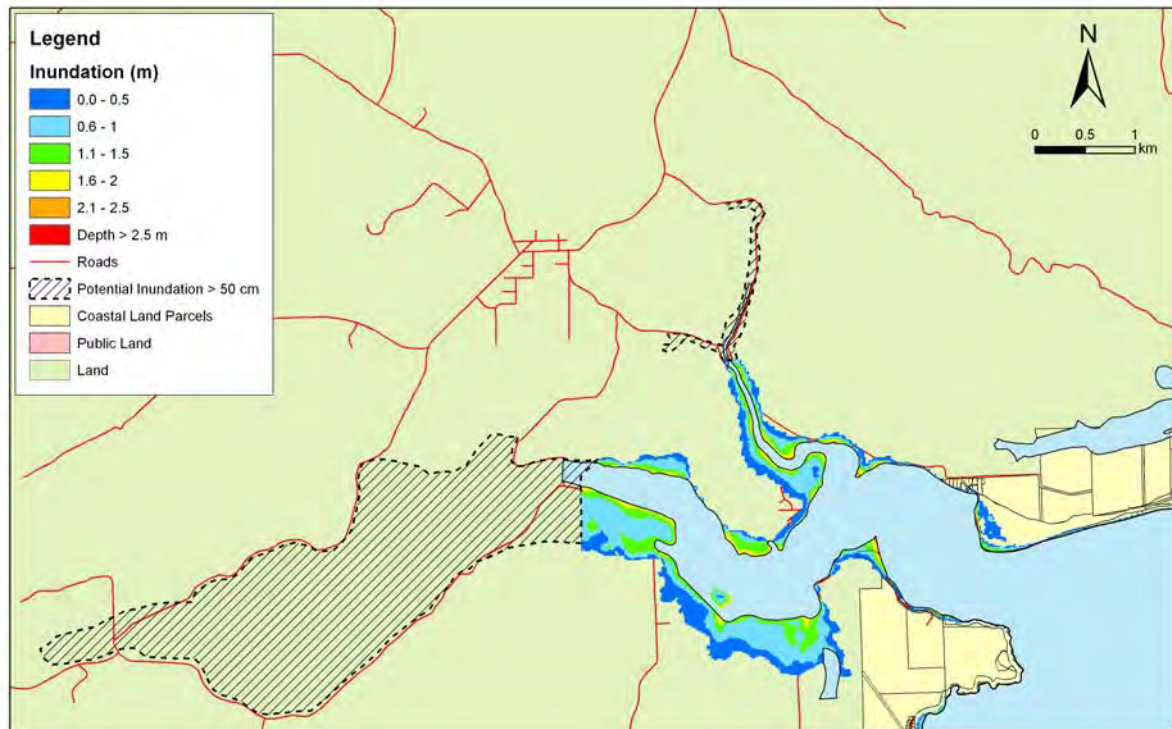


Figure 5.35: Catlins – 1:500 year remote tsunami: Maximum water depth for inundated land (top) and maximum speed (bottom) for MHWS - with a sea level rise of 30 cm.

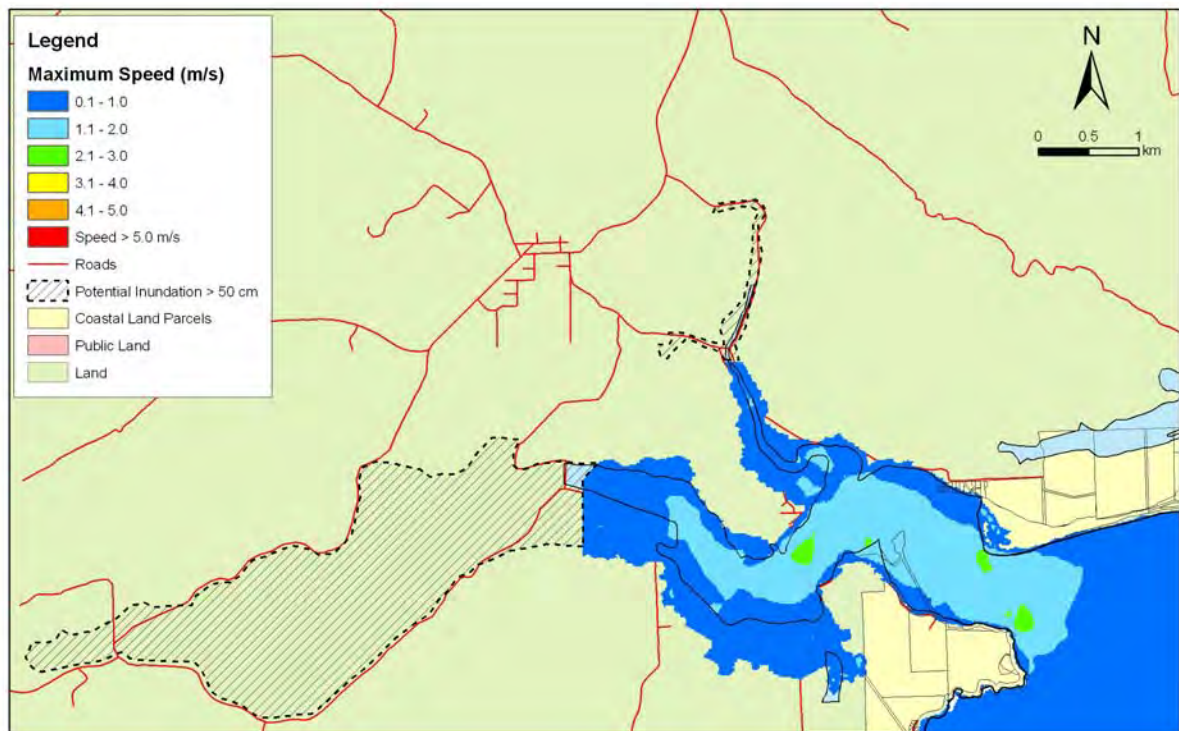
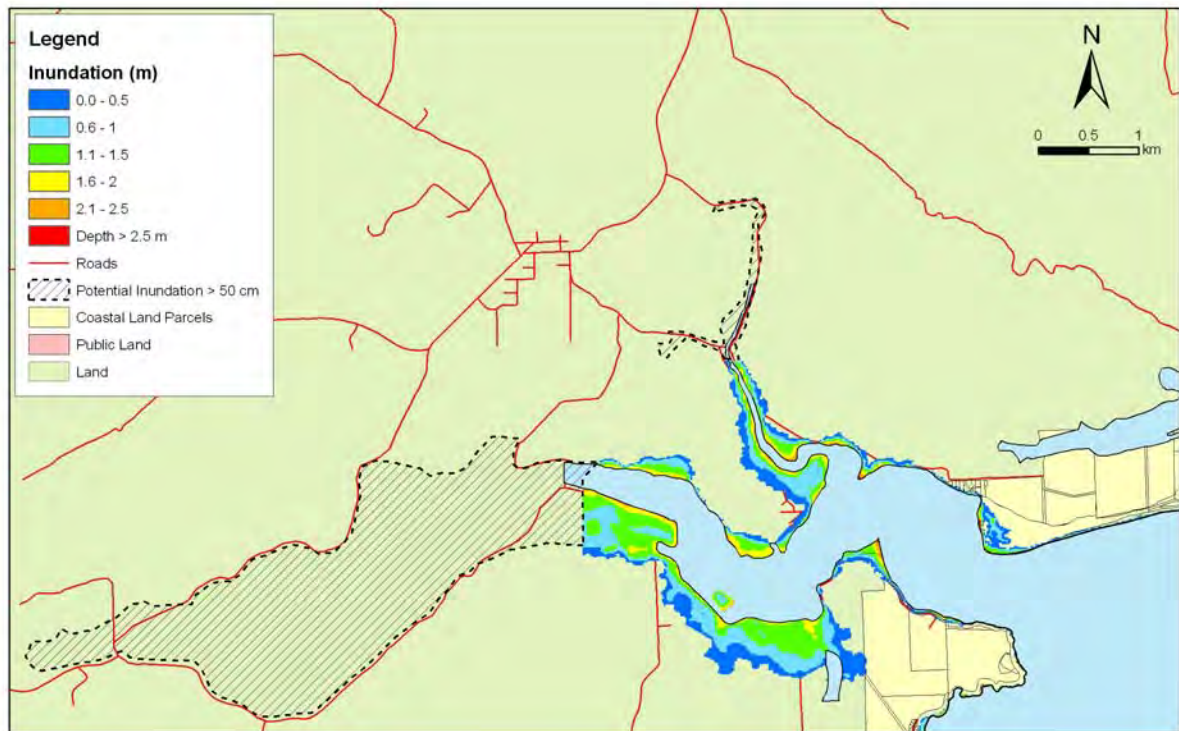


Figure 5.36 Catlins – 1:500 year remote tsunami: Maximum water depth for inundated land (top) and maximum speed (bottom) for MHWS - with a sea level rise of 50 cm.

5.3.4 Kaka Point and Clutha

Figures 5.37 – 5.39 show maximum inundation and water speed for the near-field (Puysegur) tsunami scenarios for this area. Figures 5.40-5.42 show maximum inundation and water speeds for the 1:100 year remote tsunami for Kaka Point and the Clutha Delta. Figures 5.43-5.45 show maximum inundation and water speeds for the 1:500 year remote tsunami for Kaka Point and the Clutha Delta. The model consists of a fixed-bed topographic grid, which represents the land, and any features on the land, as an impervious layer not susceptible to erosion. In reality, however, the advance and recession of waves adjacent to flood bank infrastructure may lead to bank degradation from scour, which will affect the flood banks' ability to contain the tsunami waves. It should be recognised that, although modelling indicates that inundation is contained within the flood bank infrastructure there is substantial potential that scour and subsequent breaching of the flood banks may occur during the tsunami event. Further work is now planned by the Otago Regional Council to ascertain if such scenarios are plausible and what effect breach scenarios may have on surrounding communities

Kaka Point and Clutha: Near-Field.

- For the Puysegur tsunami the wave trough arrives first, approximately 80 minutes after fault rupture. Water level decreases 75 cm over 40 minutes.
- First main wave is the biggest. Arrives around 2.3 hours after fault rupture. Amplitude 2.7 m.
- Also wave with amplitude 2.3 m arrives around 3.5 hours after fault rupture and a wave of amplitude 2.4 around 4.2 hours after fault rupture.
- Predominant period of wave arrivals: 35 minutes.
- Maximum runup: up to 4 metres at Kaka Point and up to 5 metres at the coast by the Clutha Delta.
- Considerable inundation of the coastal strip of the Clutha Delta especially south of Clutha River and for sea level rise scenarios. Most of the tsunami waves are contained by the stop banks up the rivers although there is inundation along the banks of the North branch of the Clutha River.
- Some inundation of Kaka Point Township, which is exacerbated by sea level rise.
- For a sea level rise of 50cm there is some inundation of land just north of the Puerua River.
- Velocity vector diagrams for the Puysegur tsunami showing the first large wave arriving and departing at the Clutha Delta at MHWS are shown in Appendix E.



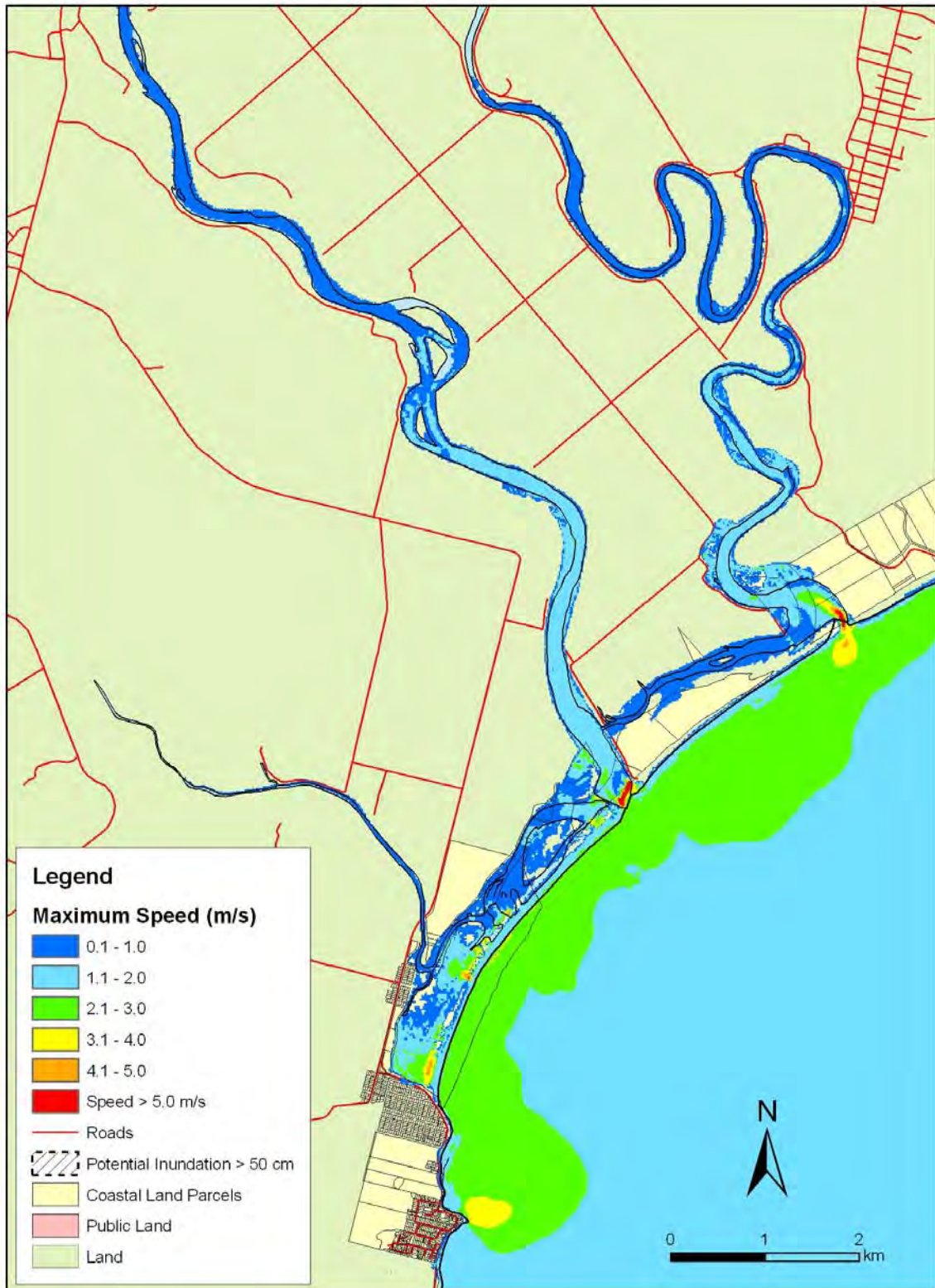
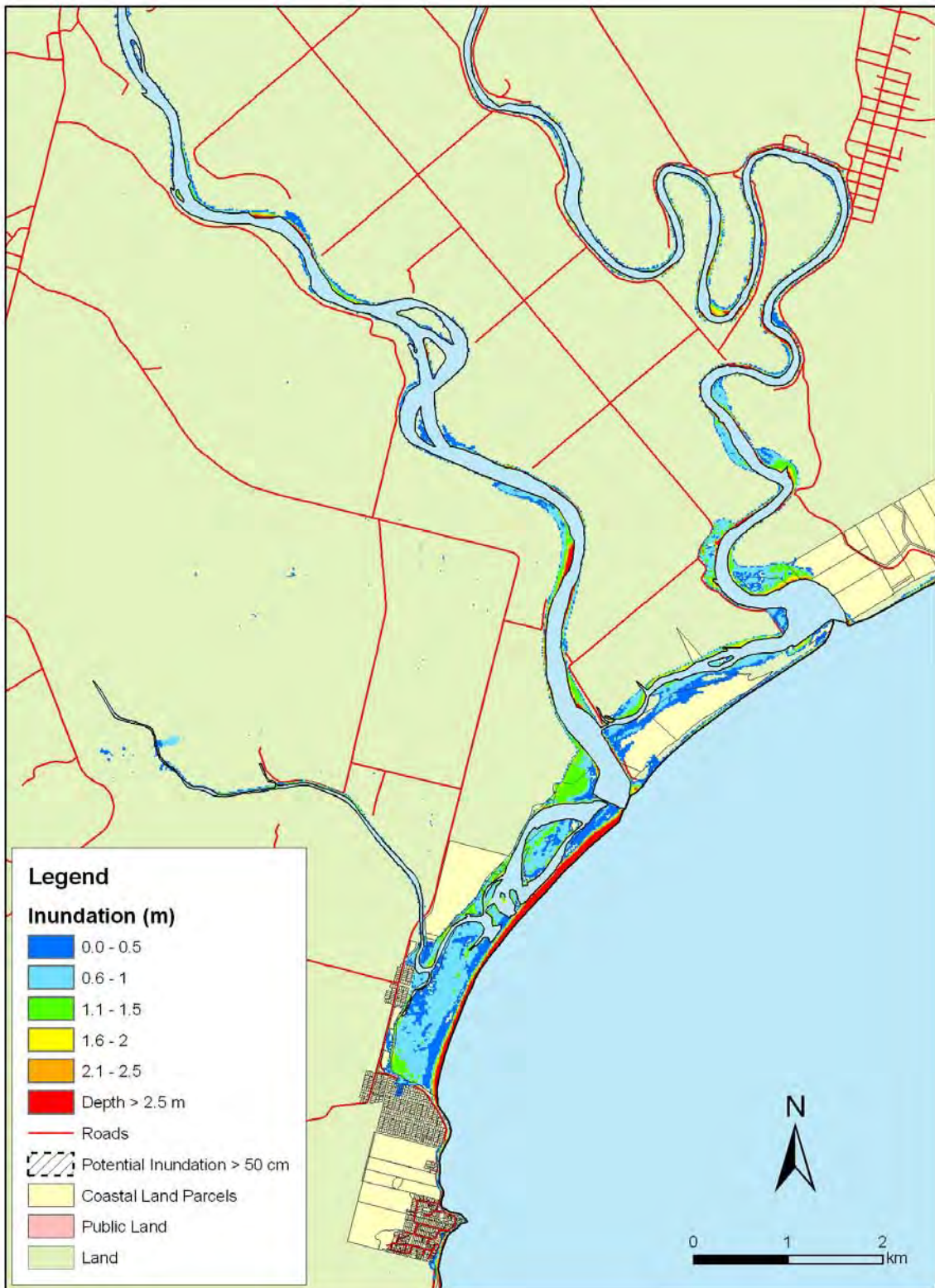


Figure 5.37: Kaka Point and Clutha – Puysegur tsunami: Maximum water depth for inundated land (previous page) and maximum speed (this page) for MHWS.



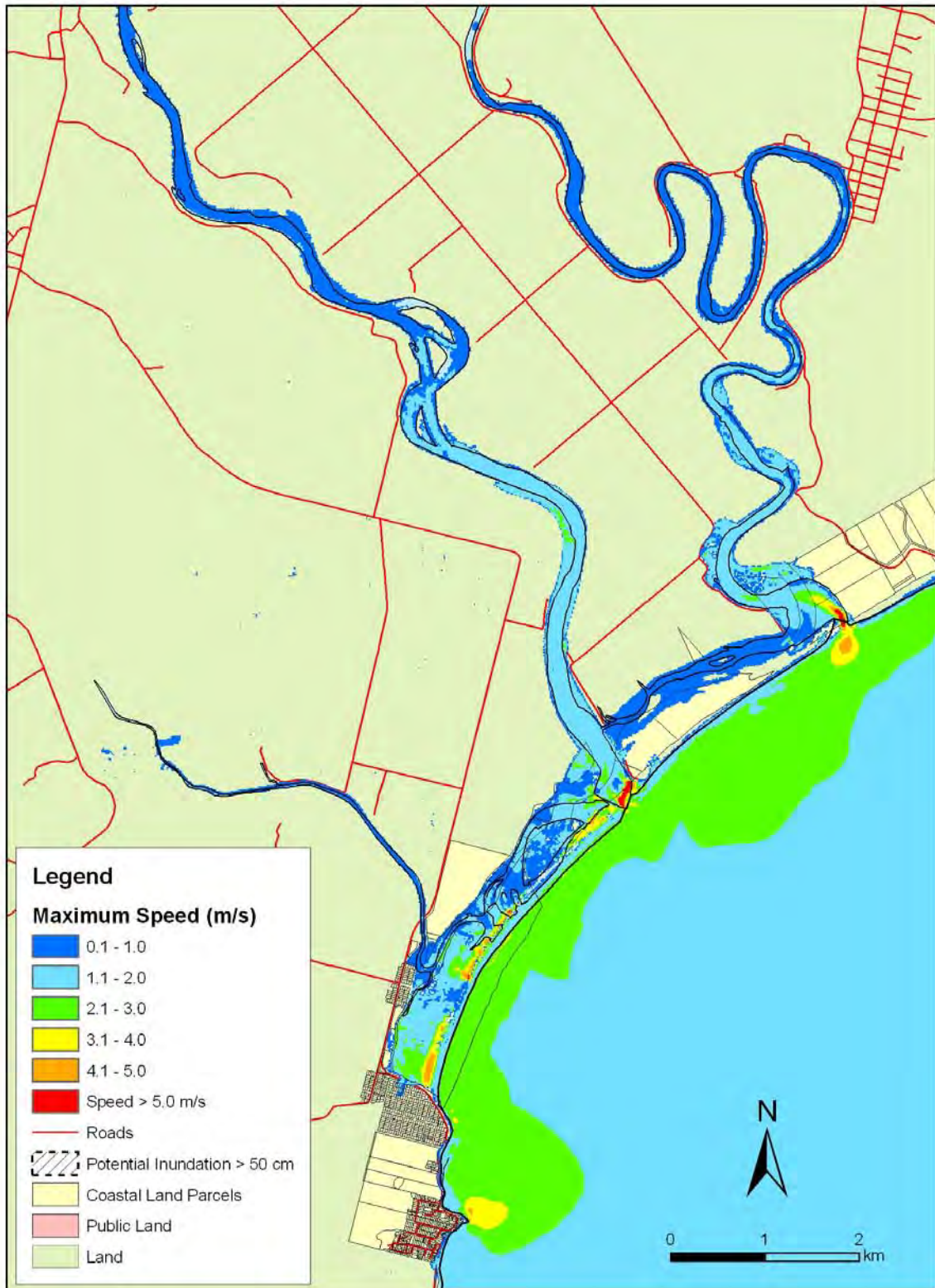


Figure 5.38: Kaka Point and Clutha – Puysegur tsunami: Maximum water depth for inundated land (previous page) and maximum speed (this page) for MHWS - with a sea level rise of 30 cm.

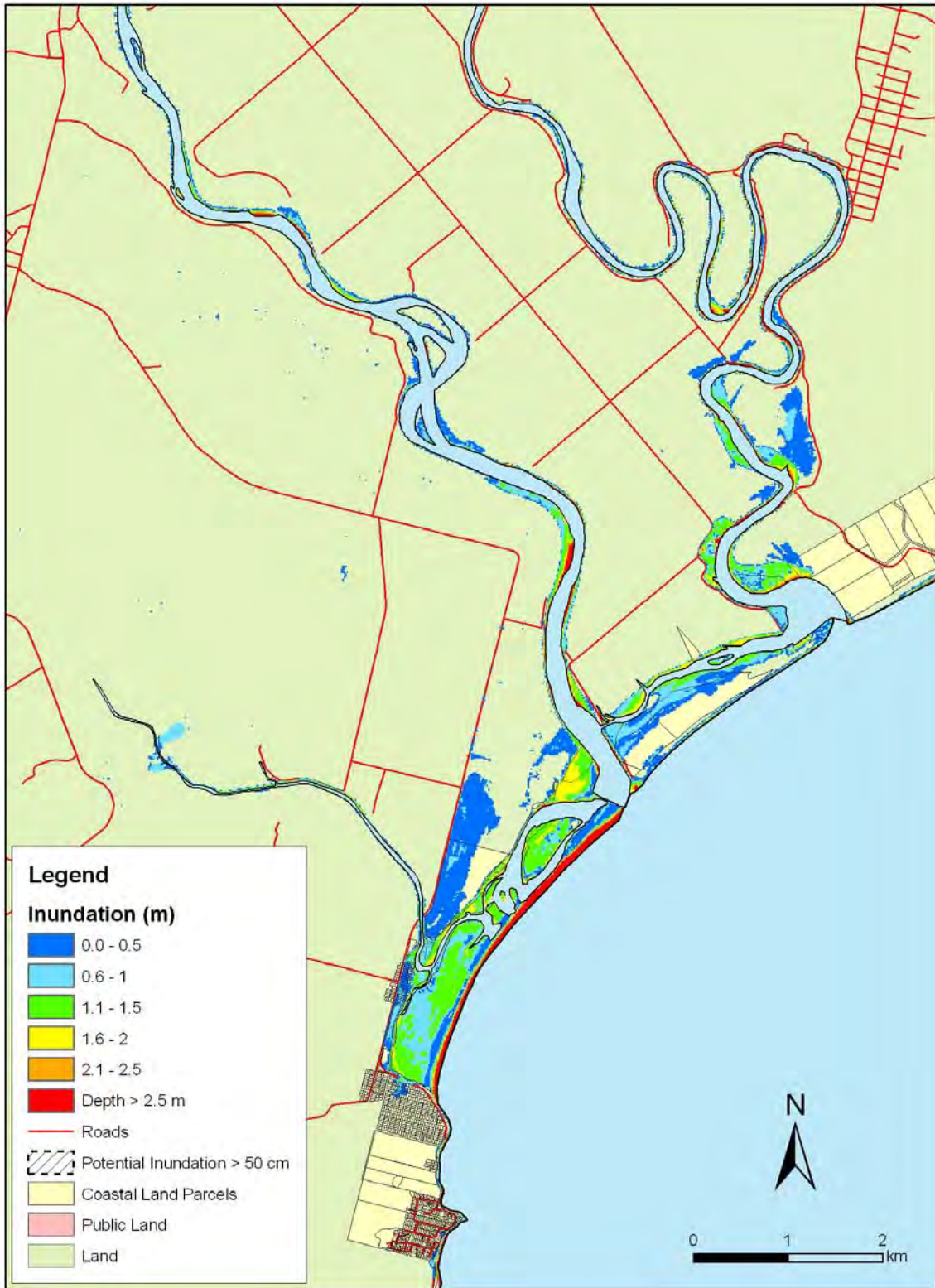
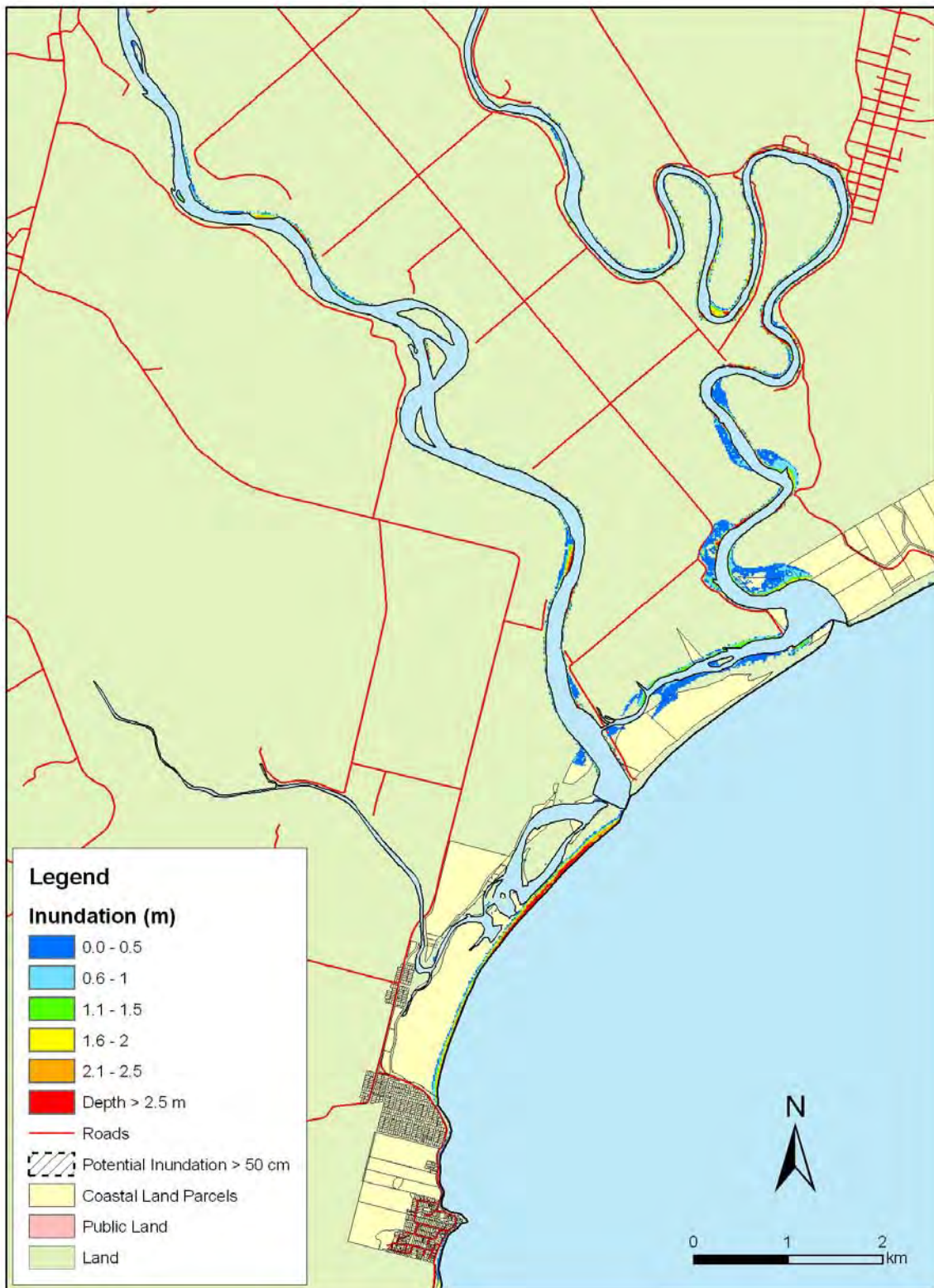




Figure 5.39: Kaka Point and Clutha – Puysegur tsunami: Maximum water depth for inundated land (previous page) and maximum speed (this page) for MHWS - with a sea level rise of 50 cm

Kaka Point and Clutha: Far-Field

- Both remote tsunamis begin with an increase in the water level.
- Second wave is highest with amplitude 1m, total height 2.2m for the 1:100 year tsunami and amplitude 1.7m, total height 3.3m for the 1:500 year tsunami.
- Big waves for around 7 hours after first arrival then many smaller ones.
- Resonance period around 1.5 hours.
- Maximum runup: up to 2.1 metres for the 1:100 year tsunami and 2.7 metres for the 1:500 year tsunami.
- Stop banks along the river channels on the Clutha Delta act to contain the tsunami waves. There is some inundation on either side of the north branch of the Clutha River. There is some inundation of the coastal strip, especially for the 1:500 year tsunami and the sea level rise scenarios.
- There are high water speeds at the Clutha River mouths. These areas have considerable risk of erosion and increased subsequent inundation.
- Maximum speeds are considerably higher under the sea level rise scenarios showing that the erosion risk is also higher. Likewise there is increased inundation especially on the north branch of the Clutha River.



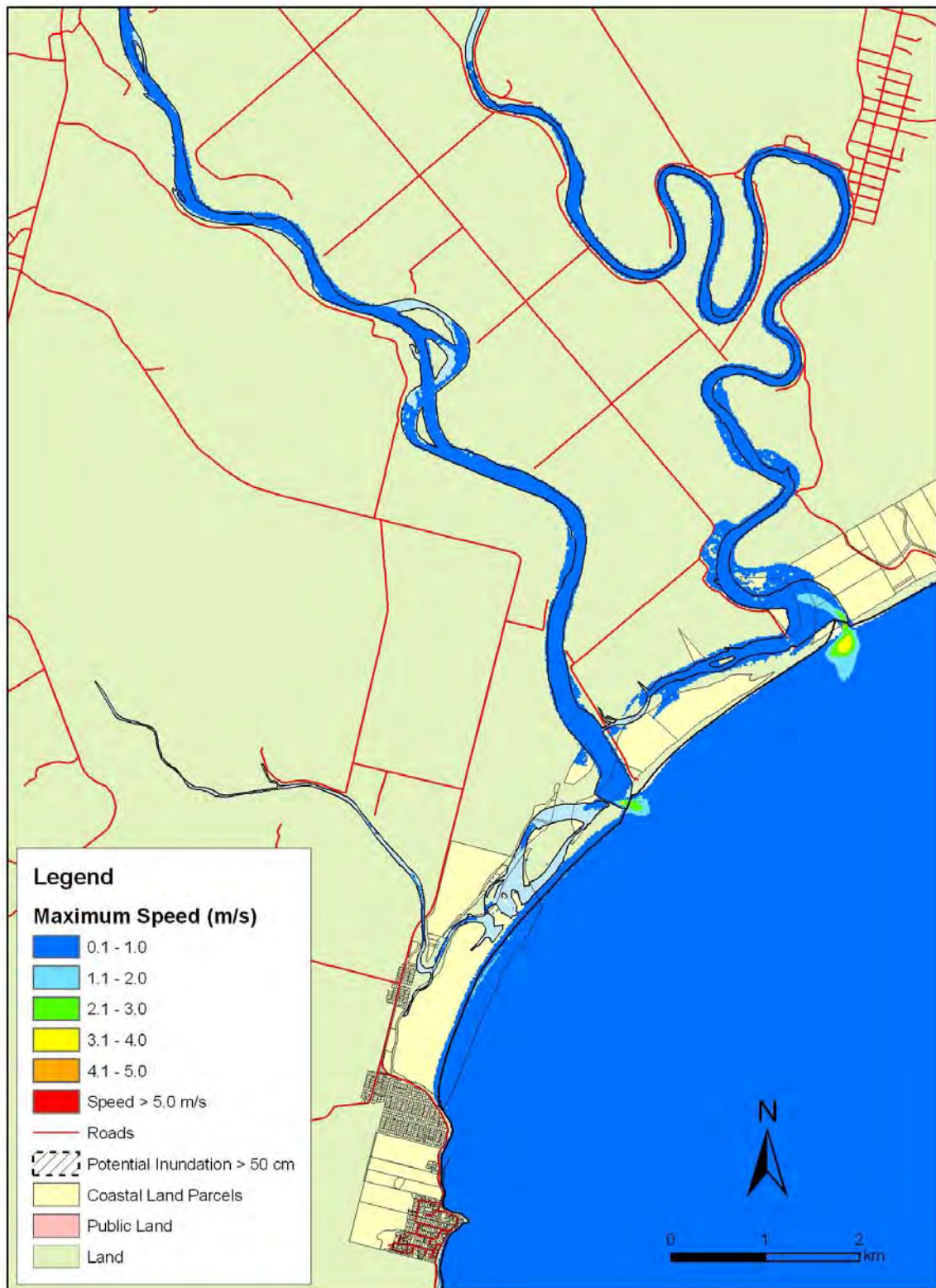


Figure 5.40: Kaka Point and Clutha – 1:100 year remote tsunami: Maximum water depth for inundated land (previous page) and maximum speed (this page) for MHWS.





Figure 5.41: Kaka Point and Clutha – 1:100 year remote tsunami: Maximum water depth for inundated land (previous page) and maximum speed (this page) for MHWS - with a sea level rise of 30 cm.



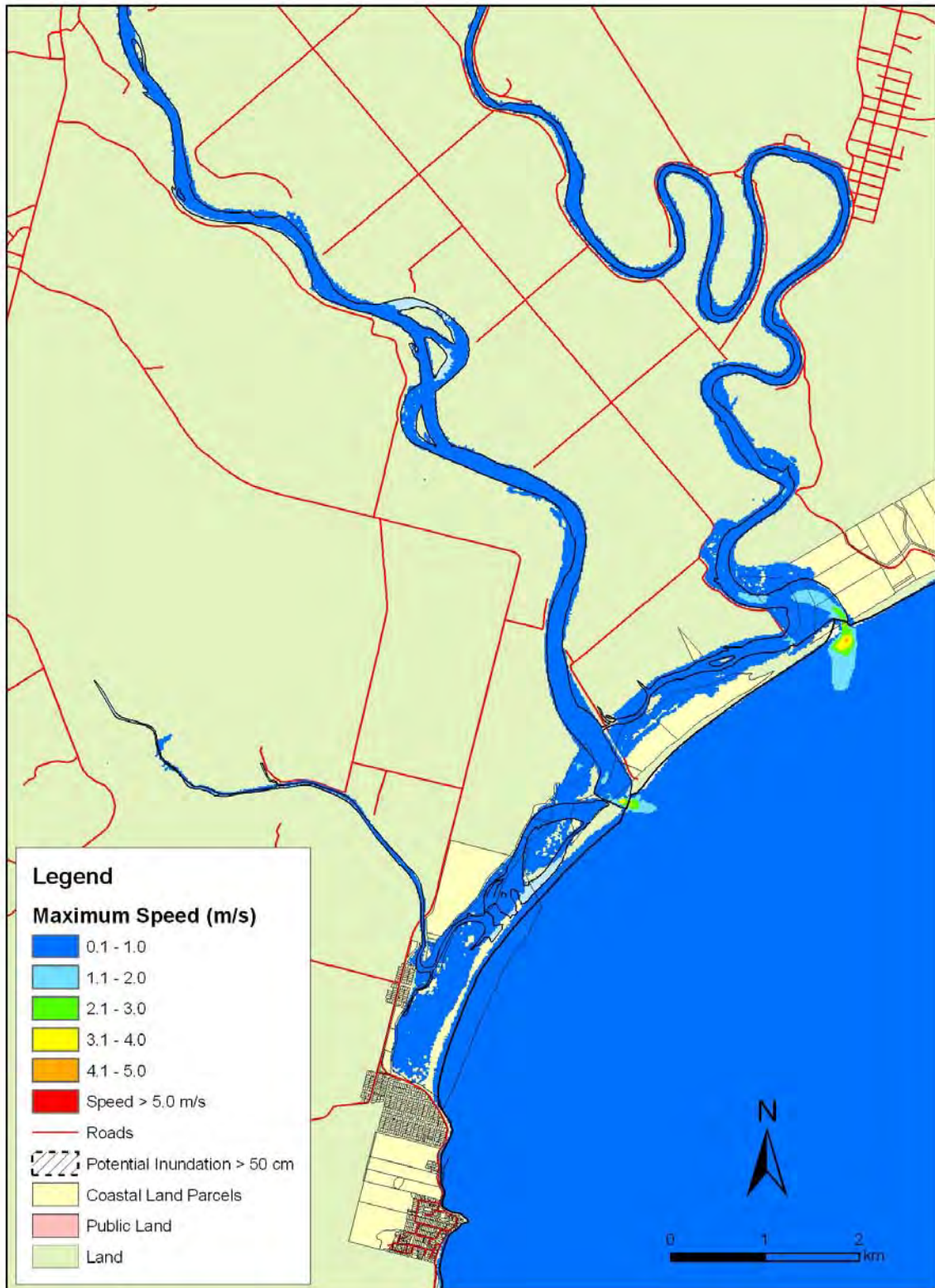
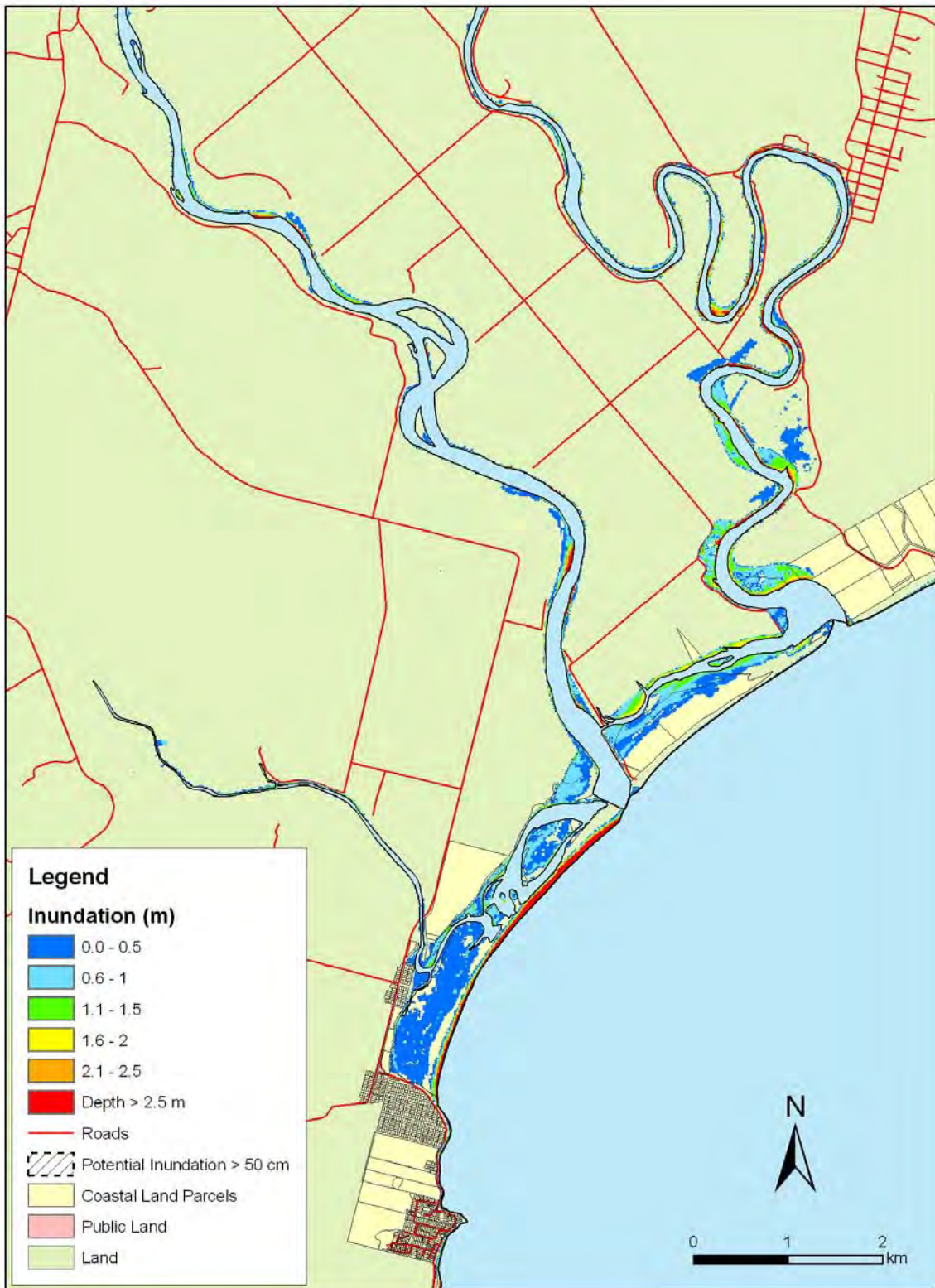


Figure 5.42: Kaka Point and Clutha – 1:100 year remote tsunami: Maximum water depth for inundated land (previous page) and maximum speed (this page) for MHWS - with a sea level rise of 50 cm.





Figure 5.43: Kaka Point and Clutha – 1:500 year remote tsunami: Maximum water depth for inundated land (previous page) and maximum speed (this page) for MHWS.



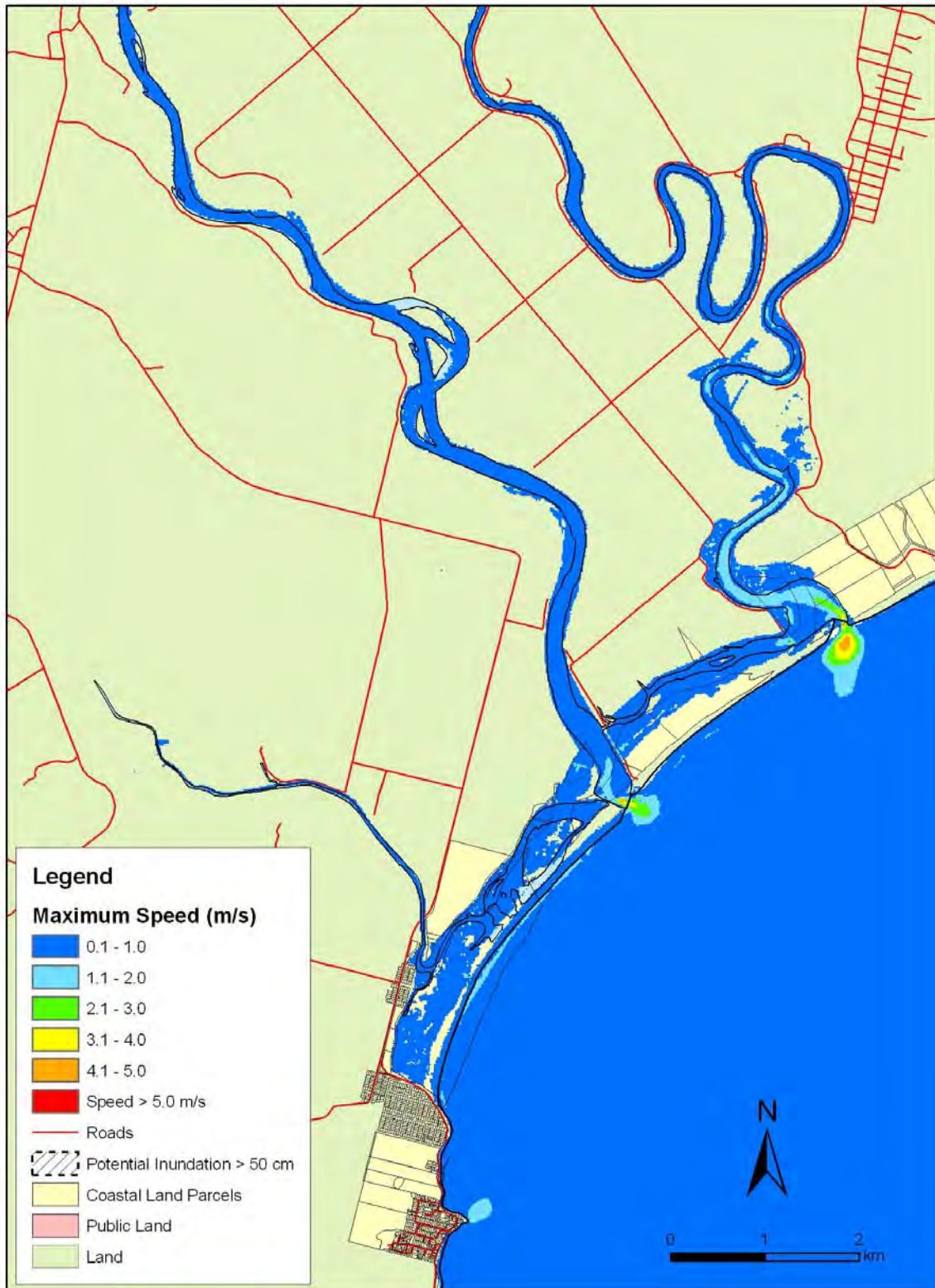


Figure 5.44: Kaka Point and Clutha – 1:500 year remote tsunami: Maximum water depth for inundated land (previous page) and maximum speed (this page) for MHWS - with a sea level rise of 30 cm.

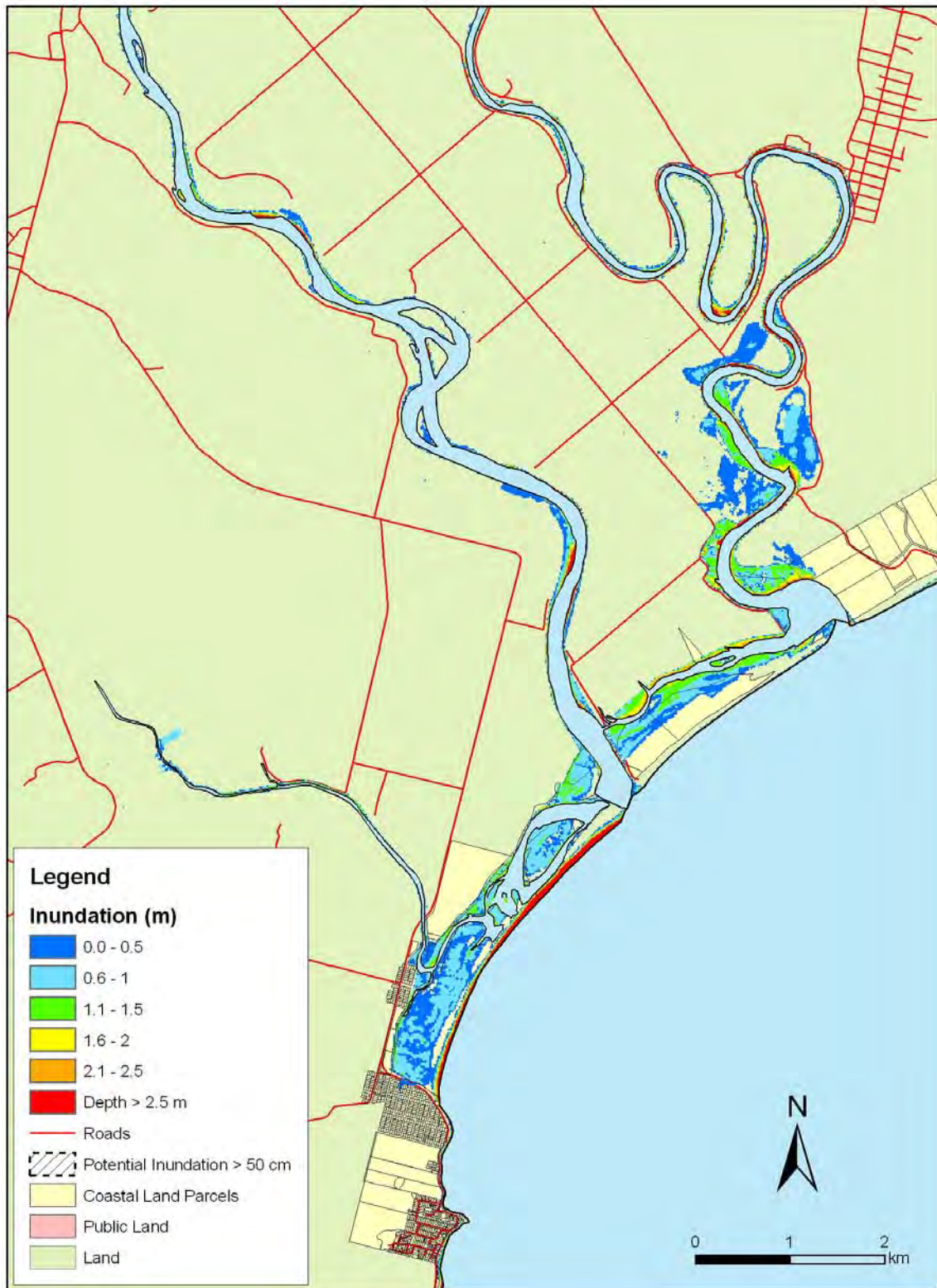




Figure 5.45: Kaka Point and Clutha – 1:500 year remote tsunami: Maximum water depth for inundated land (previous page) and maximum speed (this page) for MHWS - with a sea level rise of 50 cm.

5.3.5 Toko Mouth

Figures 5.46 – 5.48 show maximum inundation and water speed for the near-field (Puysegur) tsunami scenarios for this area. Figures 5.49-5.51 show maximum inundation and water speeds for the 1:100 year remote tsunami for Toko Mouth. Figures 5.52-5.54 show maximum inundation and water speeds for the 1:500 year remote tsunami for Toko Mouth.

Toko Mouth: Near-Field

- Trough arrives first approximately 80 minutes after fault rupture. Water level decreases 60 cm over 40 minutes.
- The first main wave is the biggest. Arrives around 2.4 hours after fault rupture. Amplitude 1.9 m.
- Also waves with amplitude 1.7 m arrive around 3.5 hours and around 5.4 hours after fault rupture.
- Predominant period of wave arrivals: 35 minutes.
- Maximum runup: up to 3.5 metres along the coast and up to 3 metres along the Tokomairiro River.
- Considerable inundation up the river to the limit of the model boundary.
- High speeds, especially over the spit at the Toko Mouth, show erosion risk and potential for increased subsequent inundation.
- Sea level rise exacerbates the inundation and also the erosion risk due to high speeds.

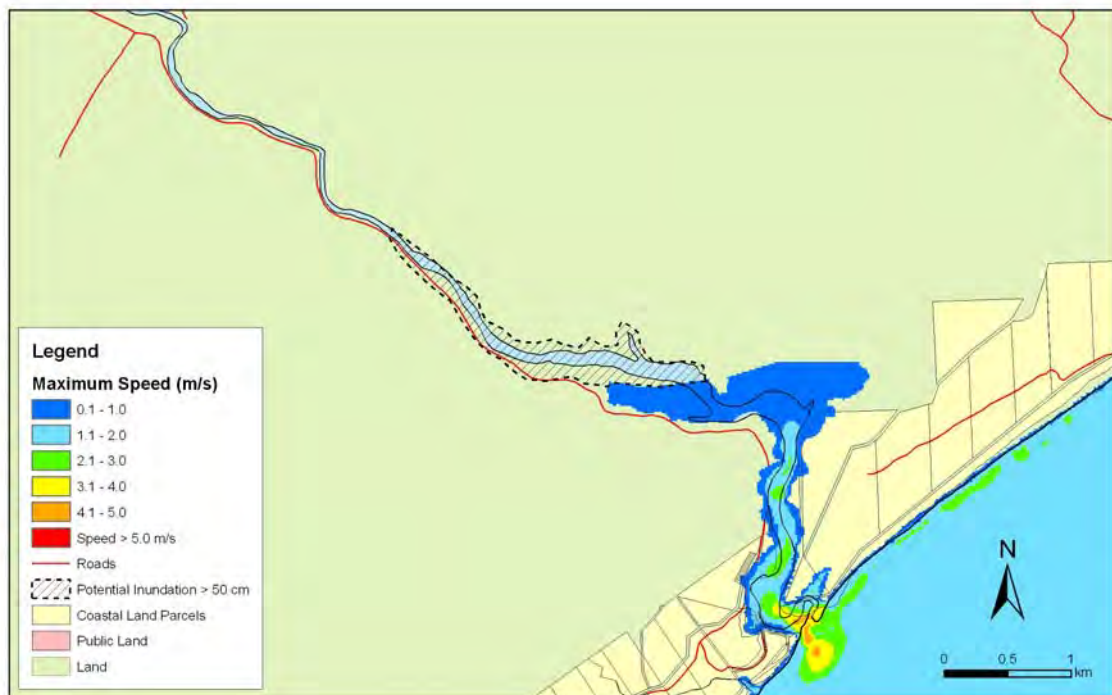


Figure 5.46: Toko Mouth – Puysegur tsunami: Maximum water depth for inundated land (top) and maximum speed (bottom) for MHWS.

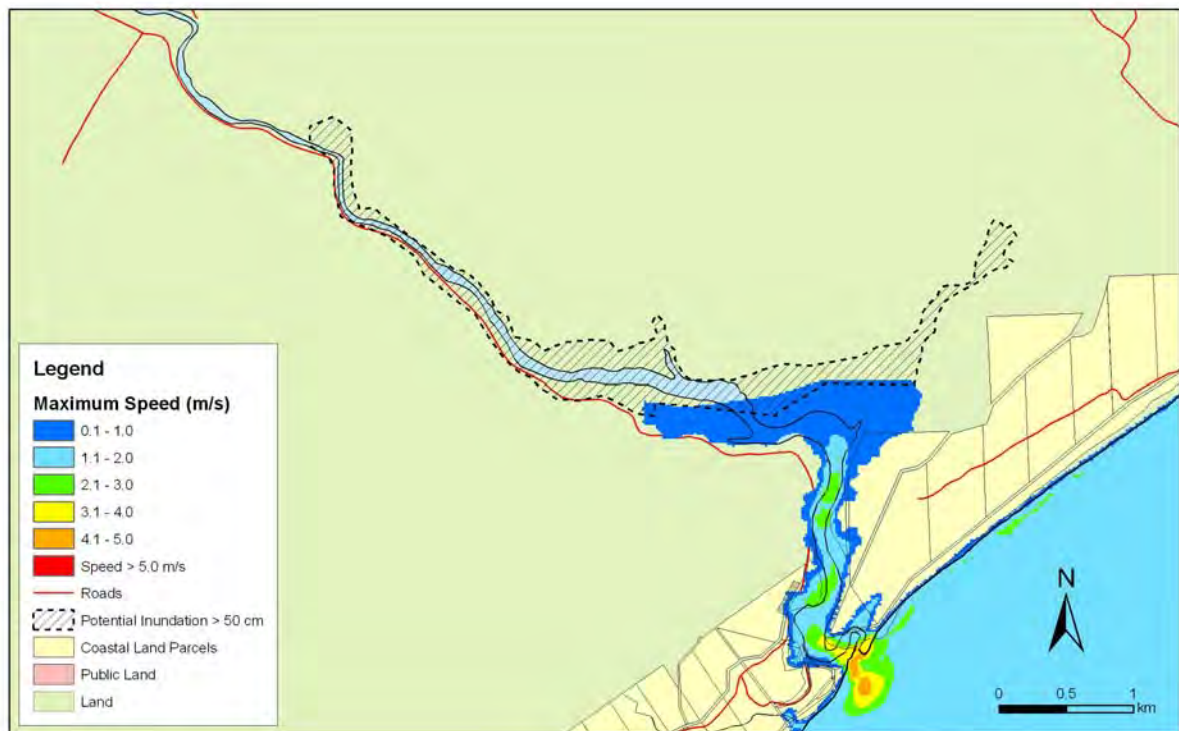


Figure 5.47: Toko Mouth – Puysegur tsunami: Maximum water depth for inundated land (top) and maximum speed (bottom) for MHWS - with a sea level rise of 30 cm.

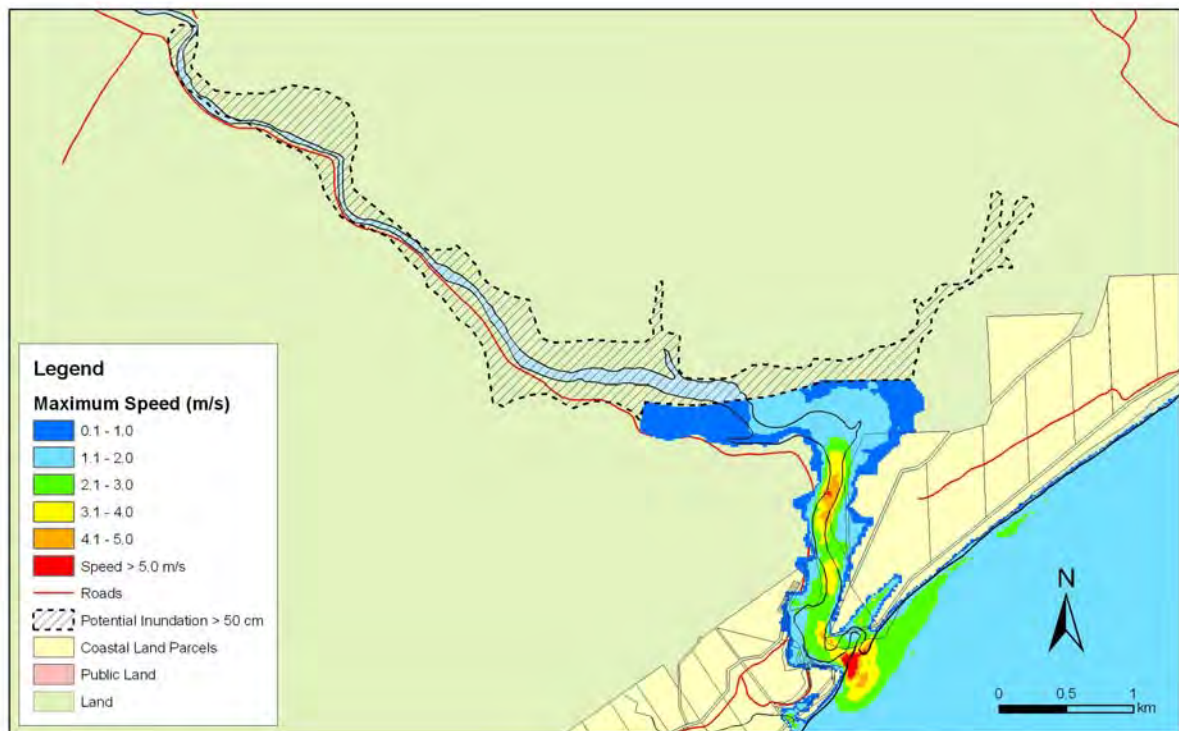
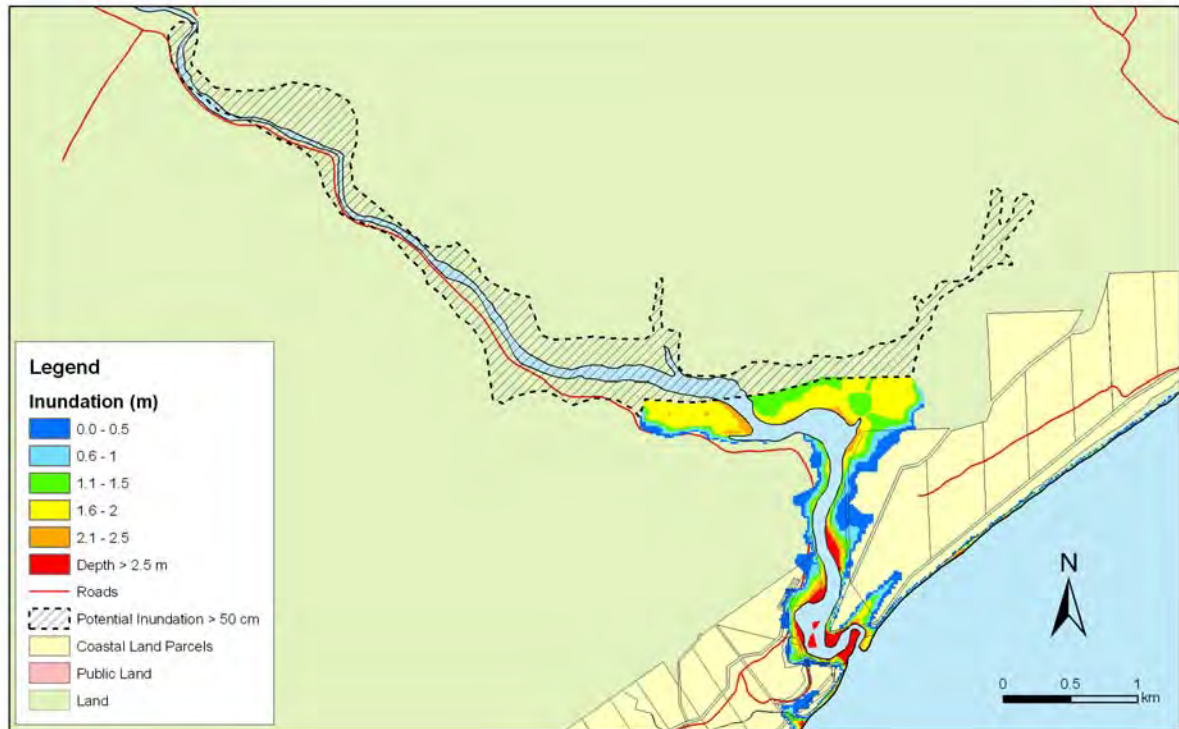


Figure 5.48: Toko Mouth– Puysegur tsunami: Maximum water depth for inundated land (top) and maximum speed (bottom) for MHWS - with a sea level rise of 50 cm.

Toko Mouth: Far-Field

- Both remote tsunamis begin with an increase in the water level.
- Third wave is highest with amplitude 1m, total height 1.8 m for 1:100 year tsunami and amplitude 1.6m, total height 3.3m for the 1:500 year tsunami.
- Big waves for around 7 hours after first arrival then lots of smaller arrivals.
- Resonance period around 1.5 hours.
- Maximum runup: up to 2.6 metres for the 1:100 year tsunami and 2.8 metres for the 1:500 year tsunami.
- All the remote scenarios inundate much of the land on either side of the Tokomairiro River.
- There is risk of the erosion of the sand bars at the mouth of the river.



Figure 5.49: Toko Mouth – 1:100 year remote tsunami: Maximum water depth for inundated land (top) and maximum speed (bottom) for MHWS



Figure 5.50: Toko Mouth– 1:100 year remote tsunami: Maximum water depth for inundated land (top) and maximum speed (bottom) for MHWS with a sea level rise of 30 cm.



Figure 5.51: Toko Mouth– 1:100 year remote tsunami: Maximum water depth for inundated land (top) and maximum speed (bottom) for MHWS with a sea level rise of 50 cm.



Figure 5.52: Toko Mouth– 1:500 year remote tsunami: Maximum water depth for inundated land (top) and maximum speed (bottom) for MHWS.

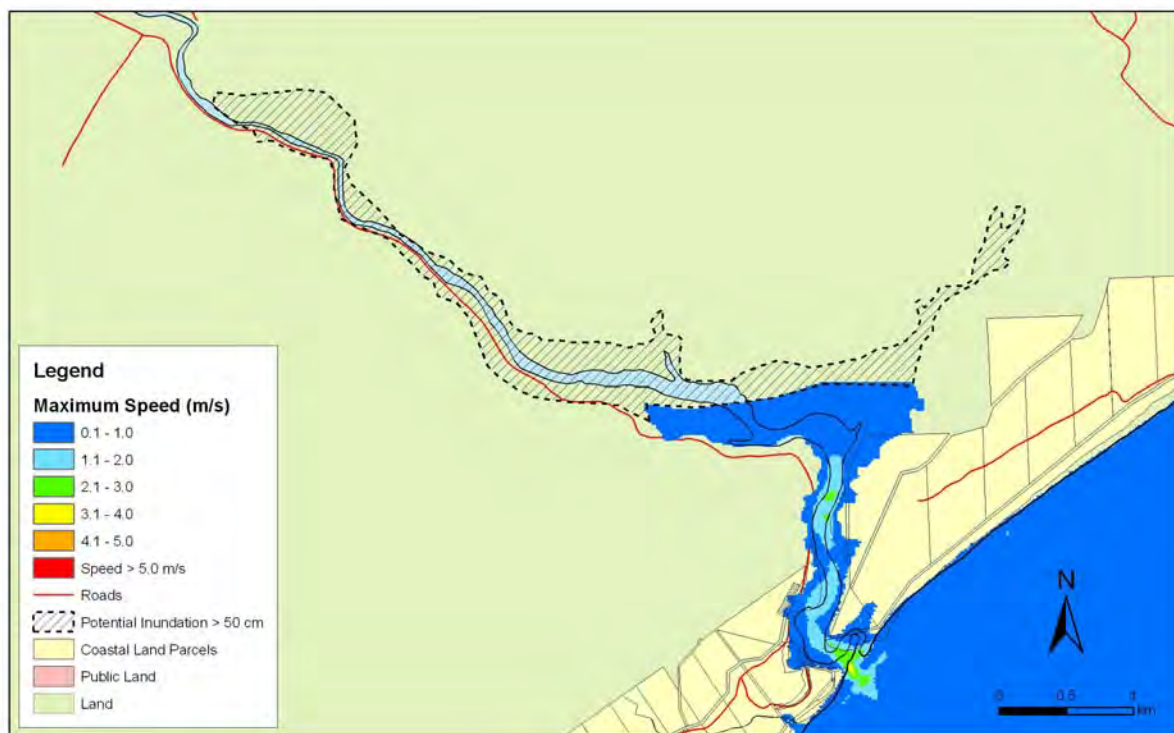
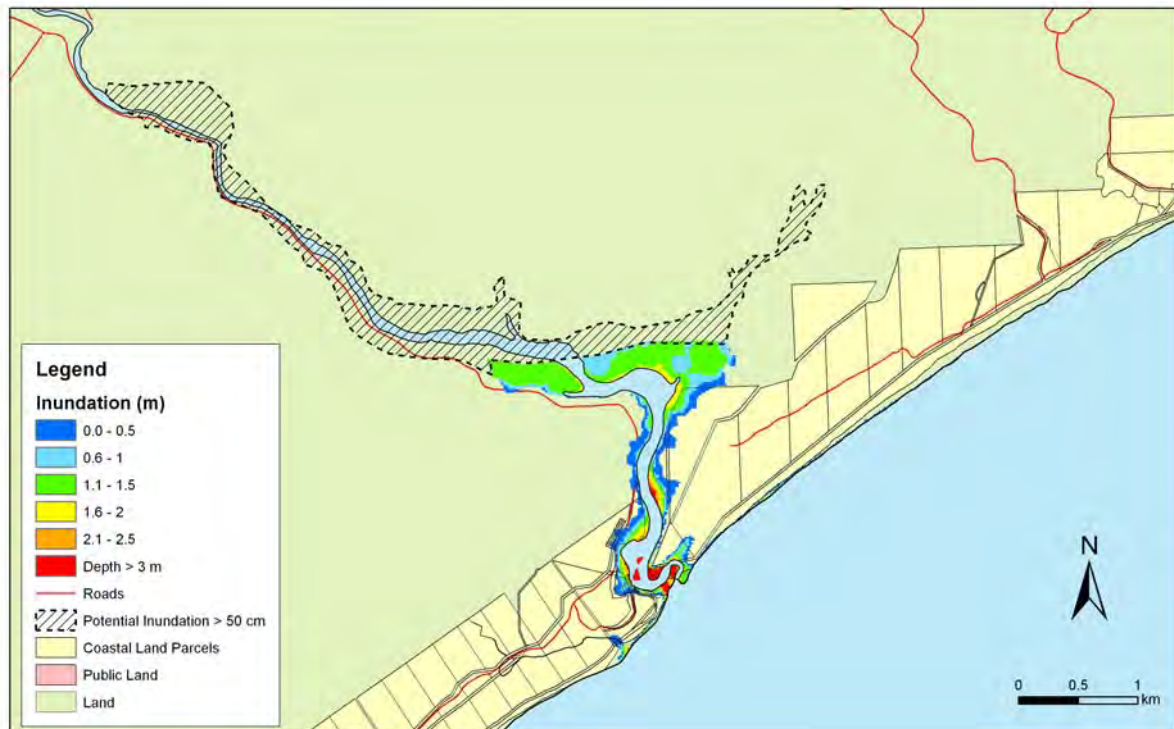


Figure 5.53: Toko Mouth– 1:500 year remote tsunami: Maximum water depth for inundated land (top) and maximum speed (bottom) for MHWS with a sea level rise of 30 cm.

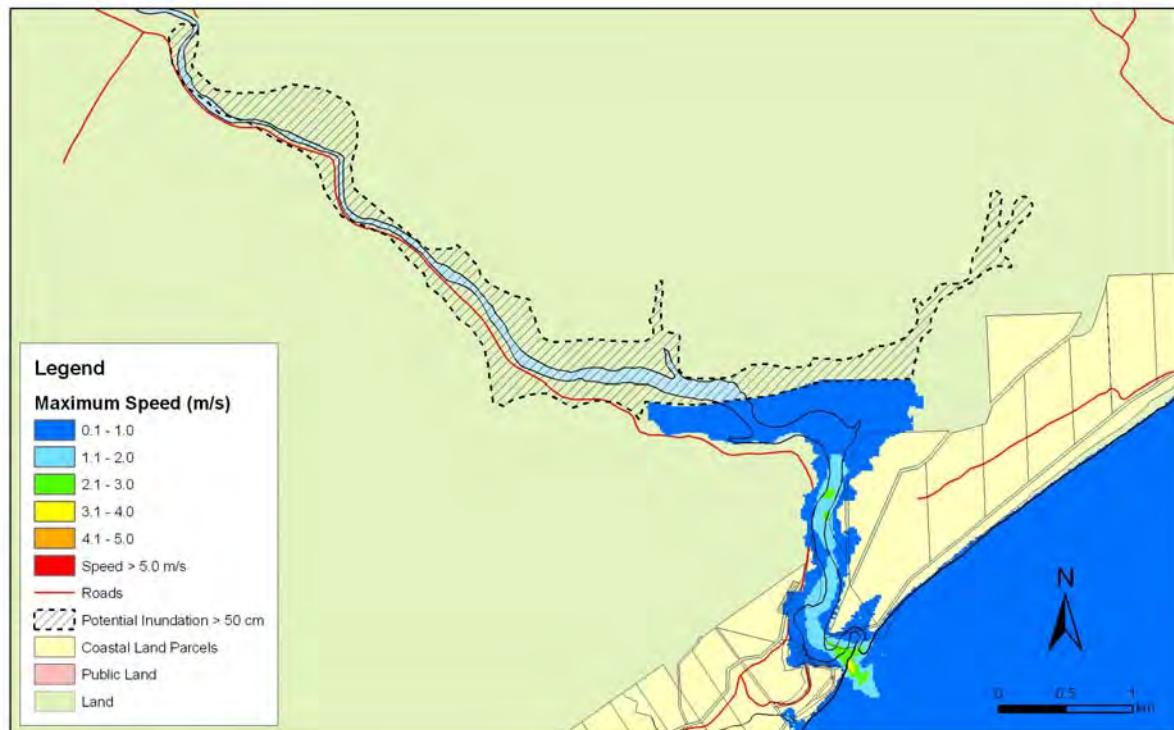
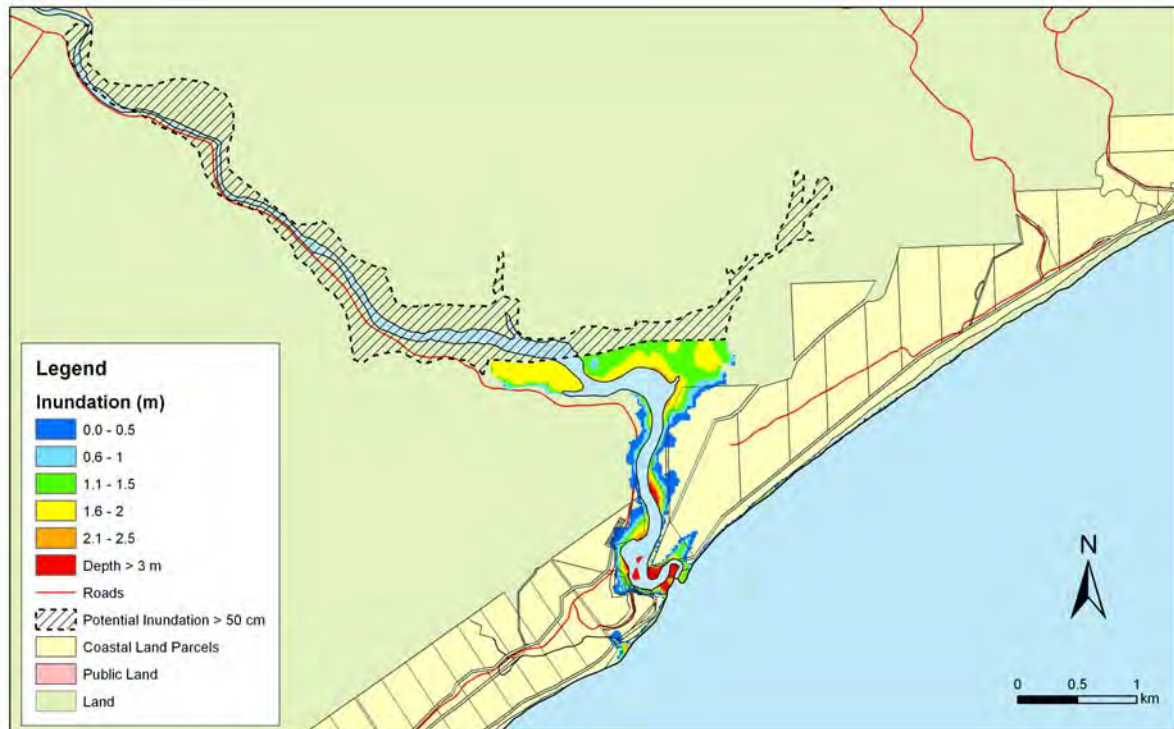


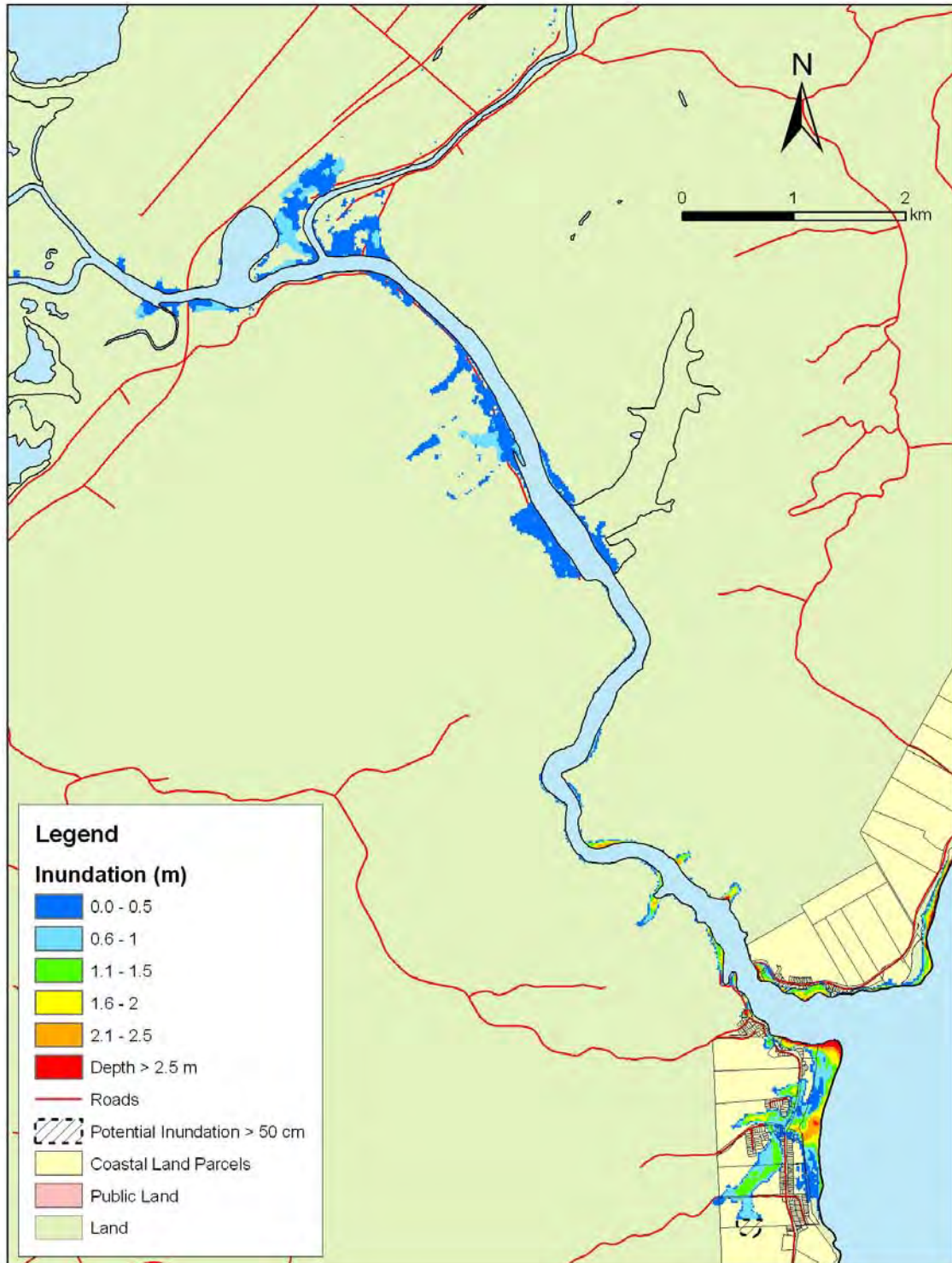
Figure 5.54: Toko Mouth– 1:500 year remote tsunami: Maximum water depth for inundated land (top) and maximum speed (bottom) for MHWS with a sea level rise of 50 cm.

5.3.6 Taieri Mouth

Figures 5.55 – 5.57 show maximum inundation and water speed for the near-field (Puysegur) tsunami scenarios for this area. Figures 5.58-5.60 show maximum inundation and water speeds for the 1:100 year remote tsunami for Taieri Mouth. Figures 5.61-5.63 show maximum inundation and water speeds for the 1:500 year remote tsunami for Taieri Mouth. Because extensive regions of the Taieri Plains lie below the baseline sea level for the modelling (MHWS) the inundation depths may be overestimated in some places. In the modelling process all areas that lie below the baseline sea level are assumed to have water up to that height in the initial conditions. In the post processing we took the maximum speed into account to remove spurious inundation. If the maximum speed is less than 5 cm/s it is assumed that the area has not been inundated. As a result of this the inundation depths may be over estimated at the edges of the inundation in areas where the surface elevation is less than the baseline sea level. Note that the black outline in the maps to the north of the Taieri River midway between the sea and the Taieri Plains shows the extent of the Takitōa Wetland.

Taieri Mouth: Near-Field

- Trough arrives first approximately 90 minutes after fault rupture. Water level decreases 60 cm over 40 minutes.
- First arrival is relatively small (amplitude around 0.5 m at around 2.3 hours after fault rupture), main wave arrives around shortly afterwards with amplitude 2.1 m.
- The second and third waves are also significant with amplitudes of 2.3 and 2.9 respectively.
- The biggest wave is the eighth wave with amplitude of 3.2 m.
- Predominant period of wave arrivals: 30 minutes.
- Maximum runup: up to 3.5 metres along coast.
- Inundation at Taieri Mouth and a small amount along the banks of the Taieri River and up to the Taieri Plains, especially for the sea level rise scenarios.
- High speeds in the river and in the land inundation show the risk of erosion – especially during the sea level rise scenarios.



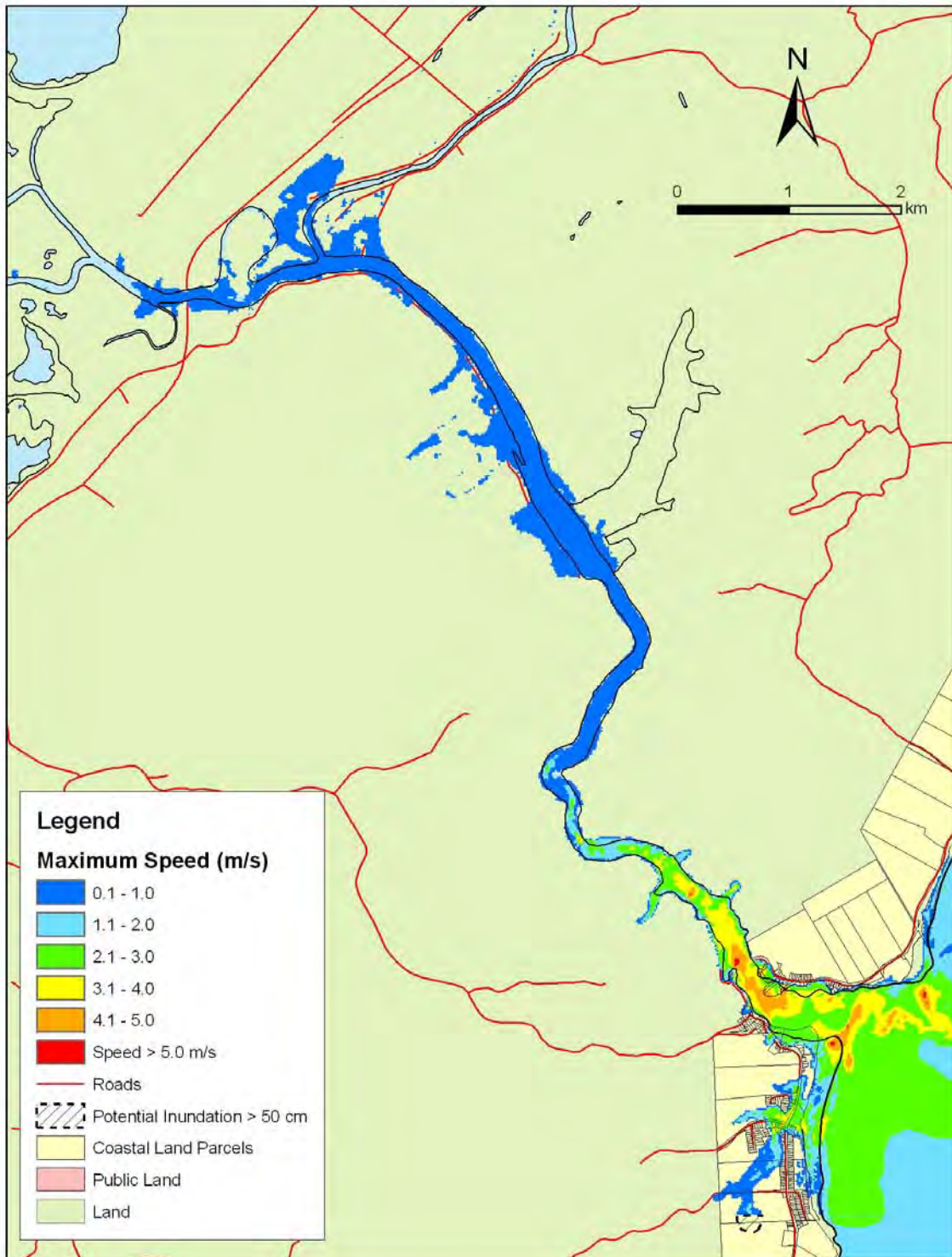
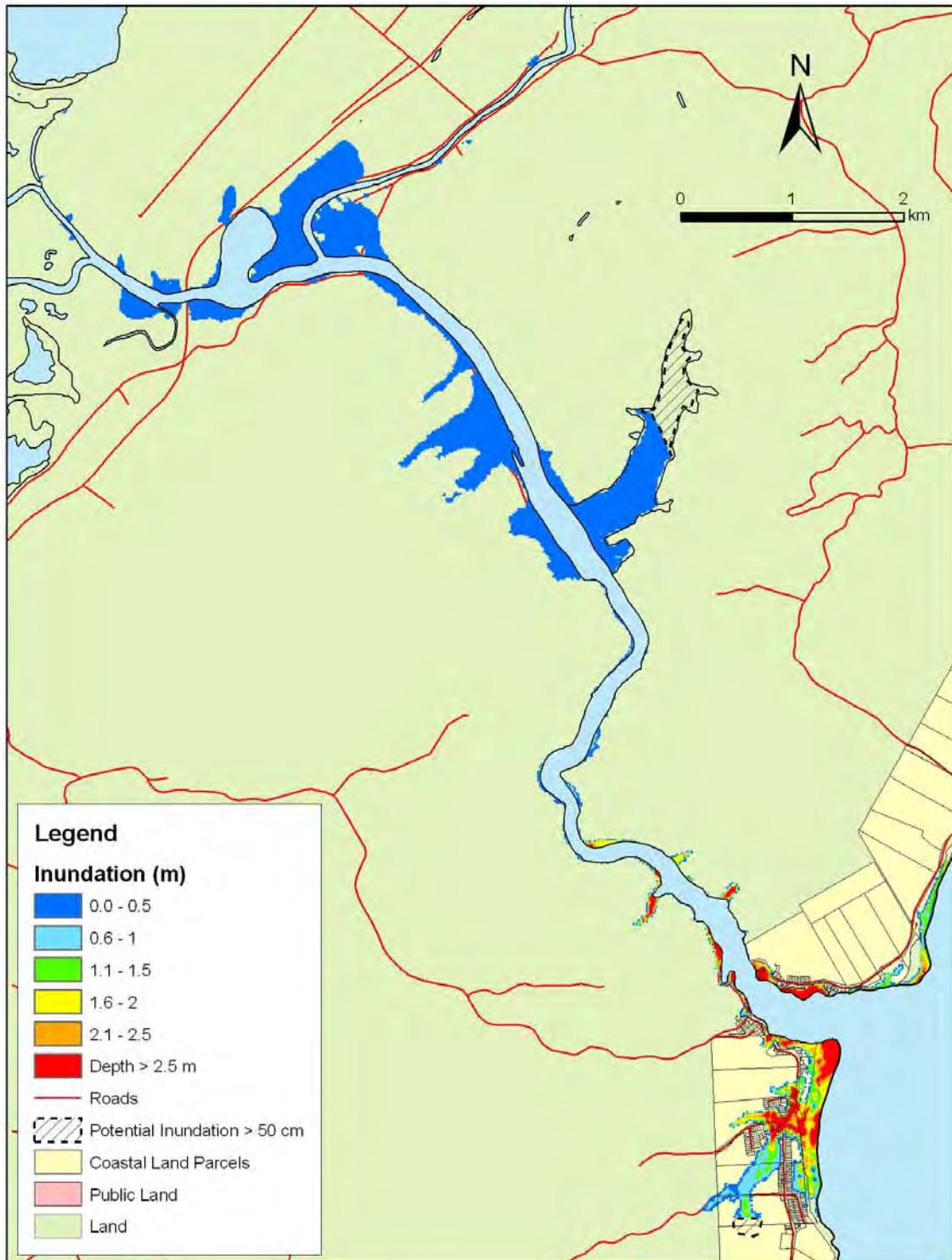


Figure 5.55: Taieri Mouth – Puysegur tsunami: Maximum water depth for inundated land (previous page) and maximum speed (this page) for MHWS.



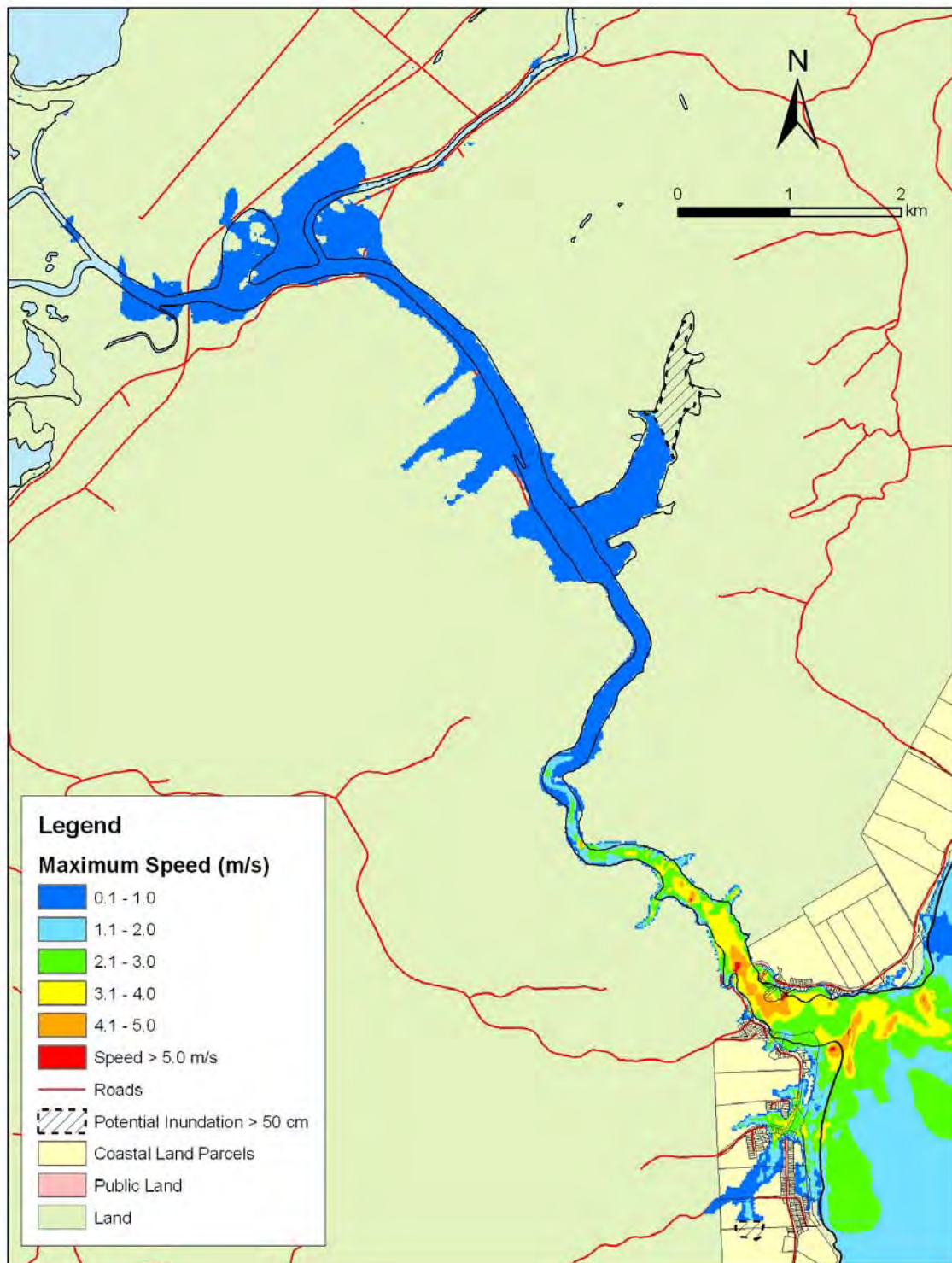
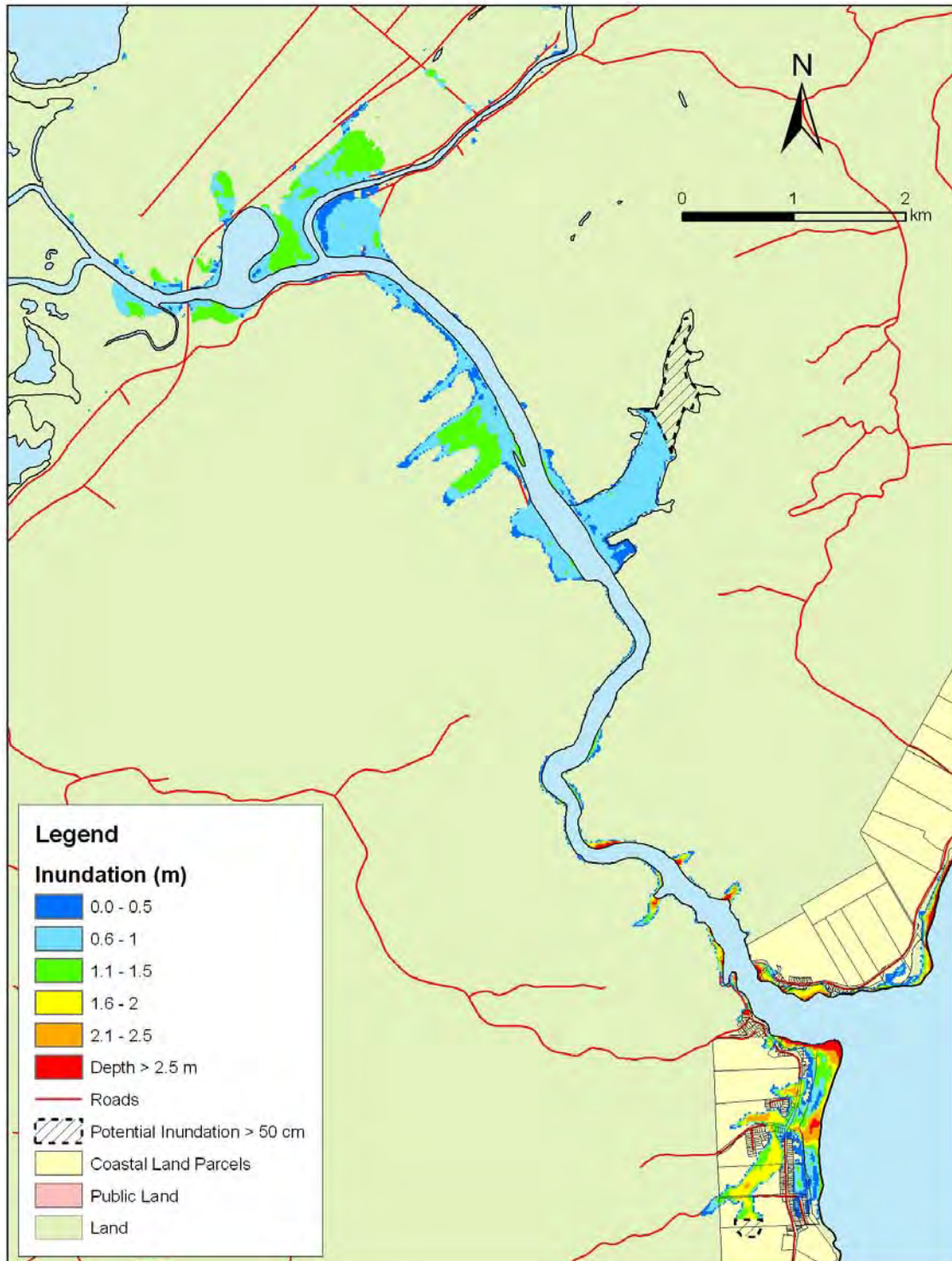


Figure 5.56: Taieri Mouth – Puysegur tsunami: Maximum water depth for inundated land (previous page) and maximum speed (this page) for MHWS with a sea level rise of 30 cm.



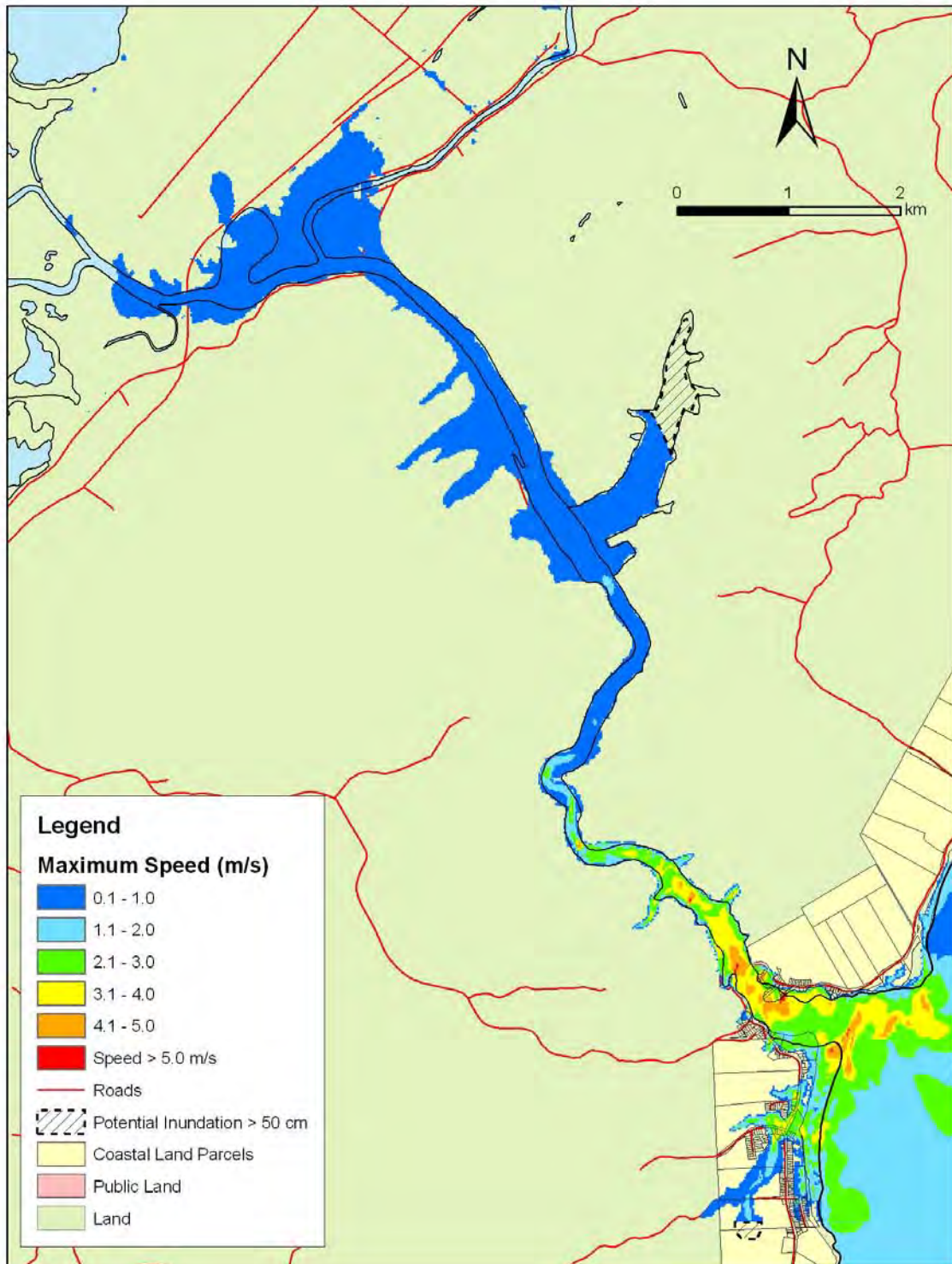
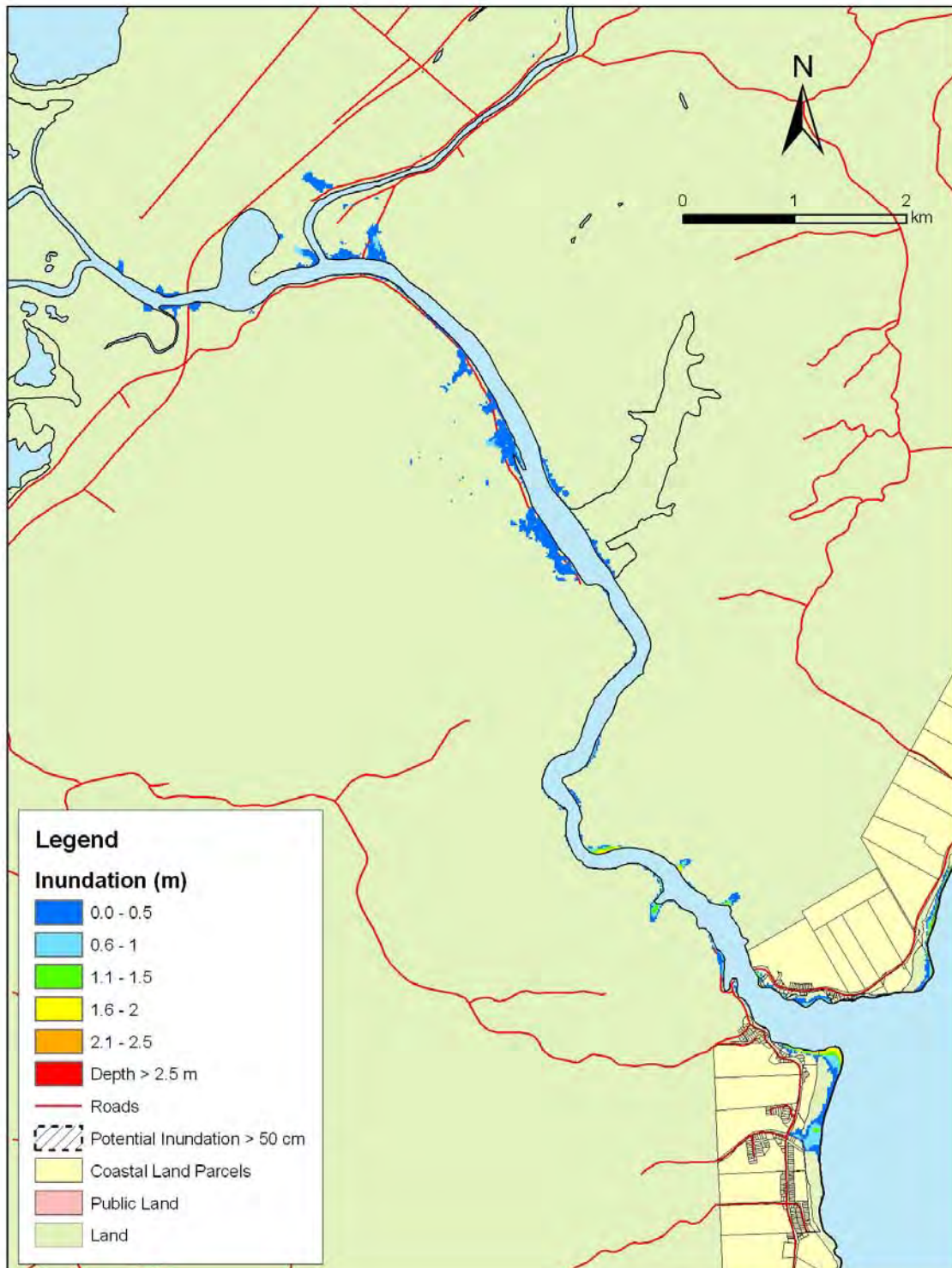


Figure 5.57: Taieri Mouth – Puysegur tsunami: Maximum water depth for inundated land (previous page) and maximum speed (this page) for MHWS with a sea level rise of 50 cm.

Taieri Mouth: Far-Field

- Both remote tsunamis begin with an increase in the water level.
- Second wave is highest with amplitude 1m, total height 2m for 1:100 year tsunami and amplitude 1.6m, total height 2.9m for 1:500 year tsunami.
- Big waves for around 7 hours after first arrival then many smaller waves.
- Resonance period around 1.5 hours, also 70 minutes.
- Maximum runup: up to 2.1 metres for the 1:100 year tsunami and 2.7 metres for the 1:500 year tsunami.
- Land along the banks of the Taieri River is partially inundated and so is the low-lying land in the township. While not as bad as the Puysegur tsunami the inundation is worse for the 1:500 year remote tsunami and the sea level rise scenarios.
- Erosion risk is not particularly high, although unconsolidated sediments will be remobilised which may impact the river channel.



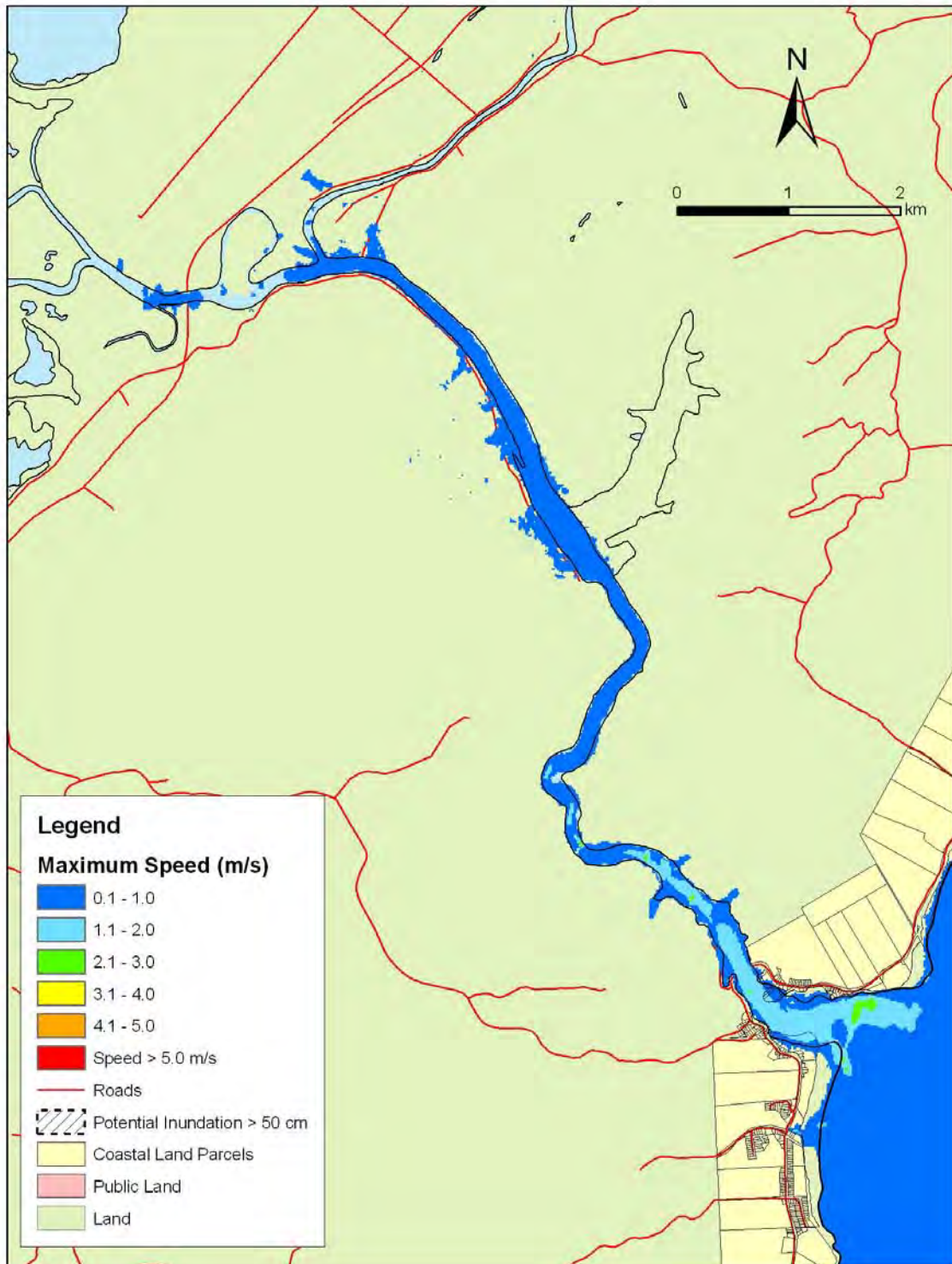
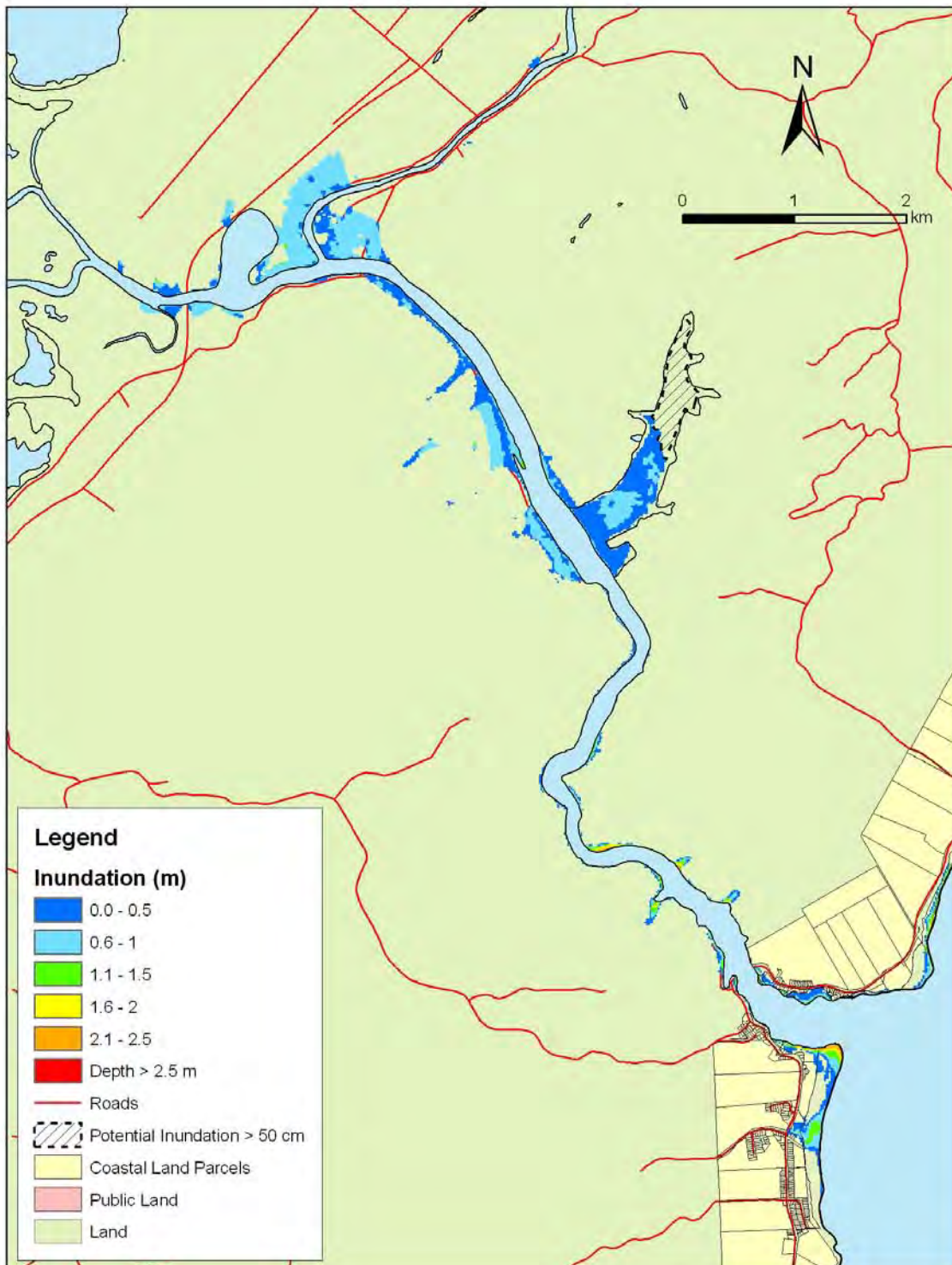


Figure 5.58: Taieri Mouth – 1:100 year remote tsunami: Maximum water depth for inundated land (previous page) and maximum speed (this page) for MHWS.



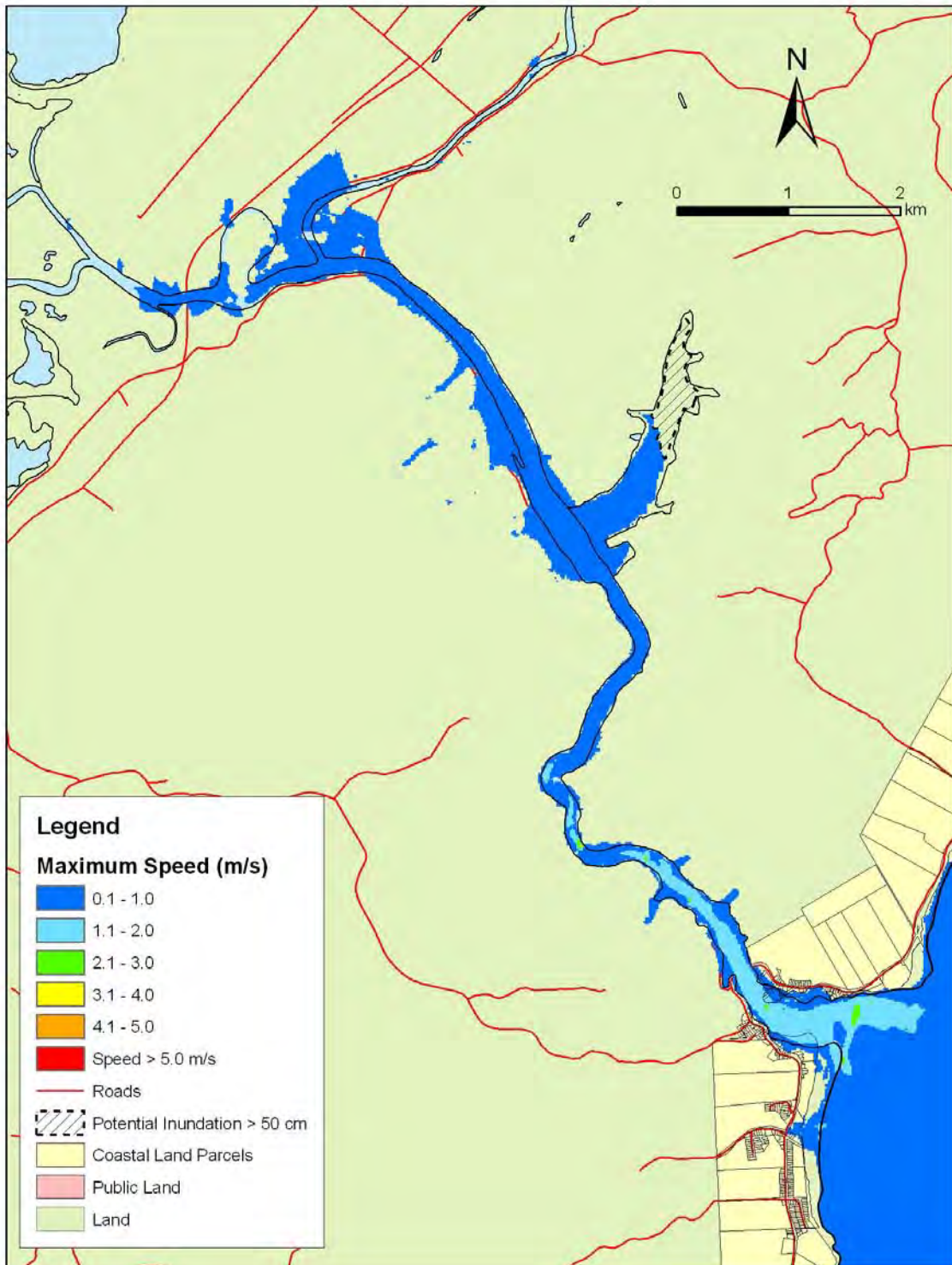
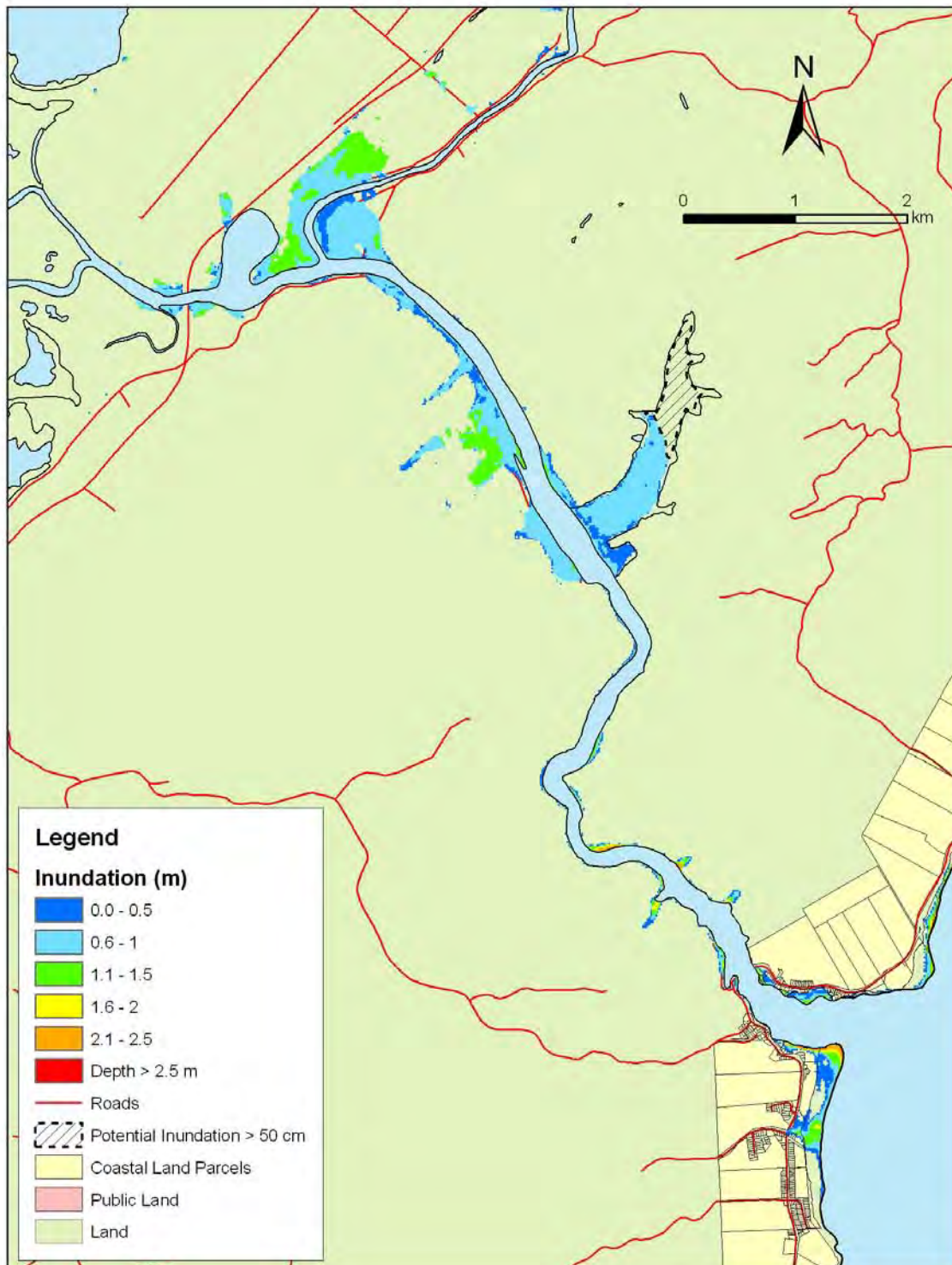


Figure 5.59: Taieri Mouth – 1:100 year remote tsunami: Maximum water depth for inundated land (previous page) and maximum speed (this page) for MHWS with a sea level rise of 30 cm.



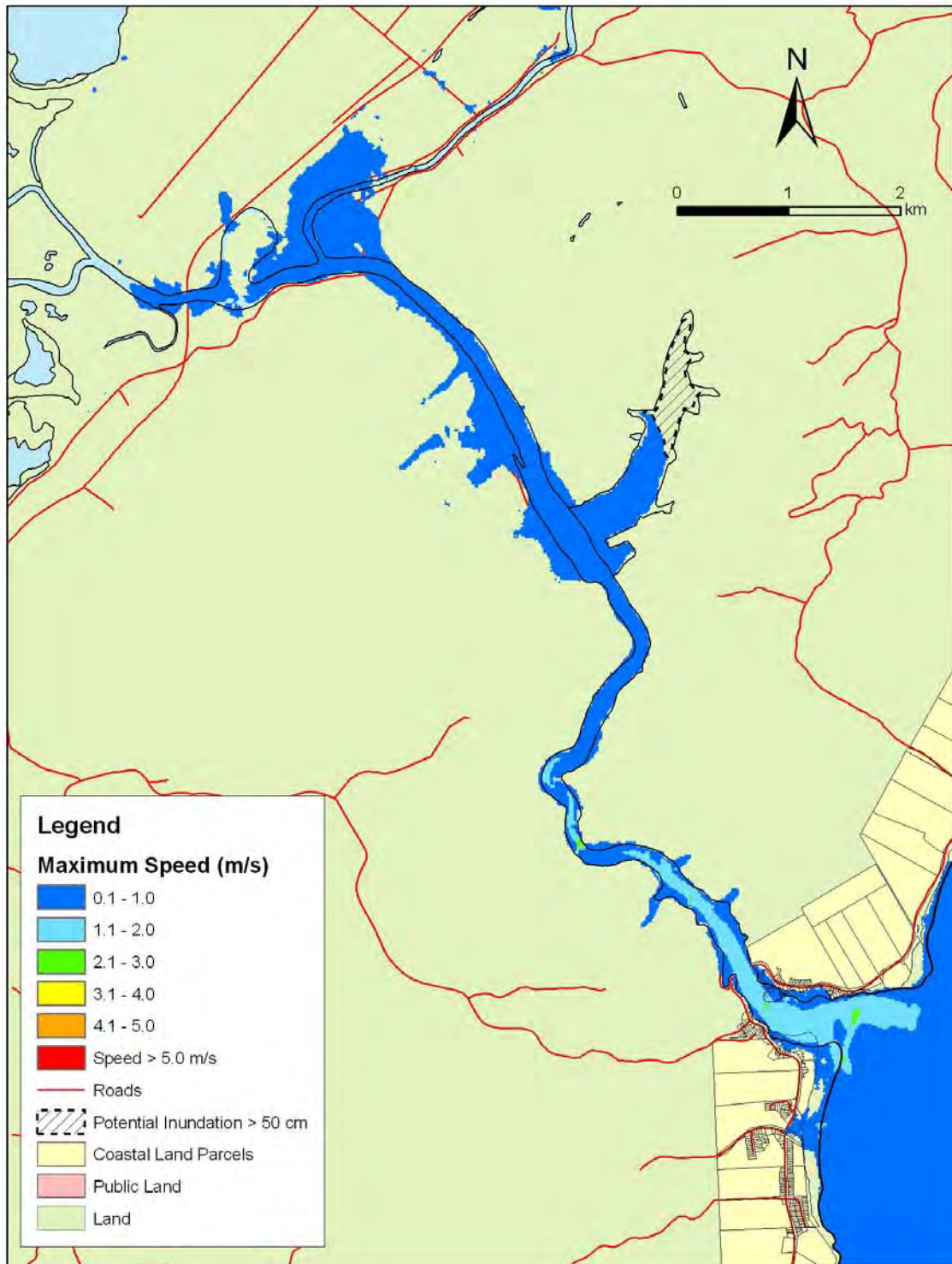
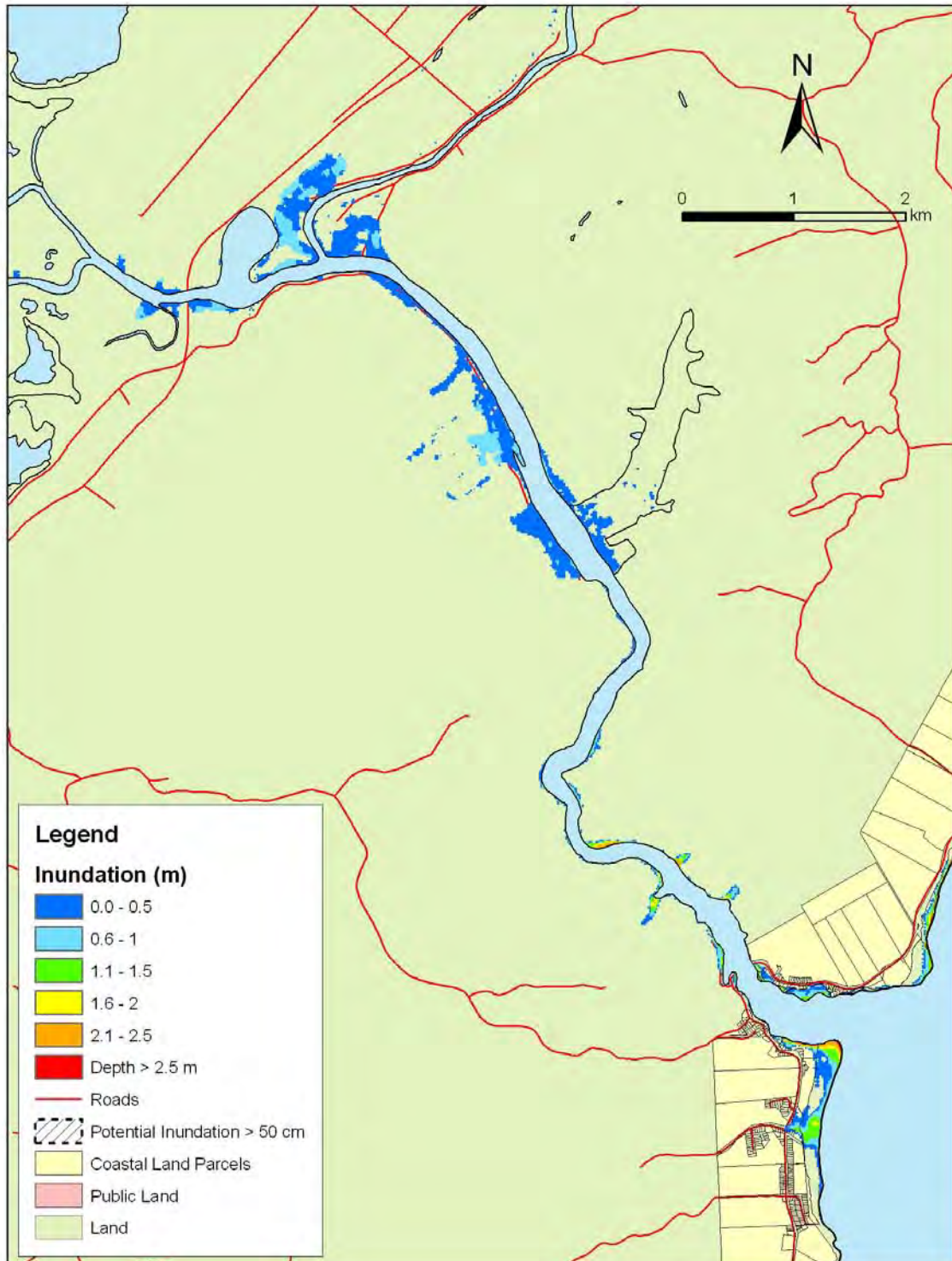


Figure 5.60: Taieri Mouth – 1:100 year remote tsunami: Maximum water depth for inundated land (previous page) and maximum speed (this page) for MHWS with a sea level rise of 50 cm.



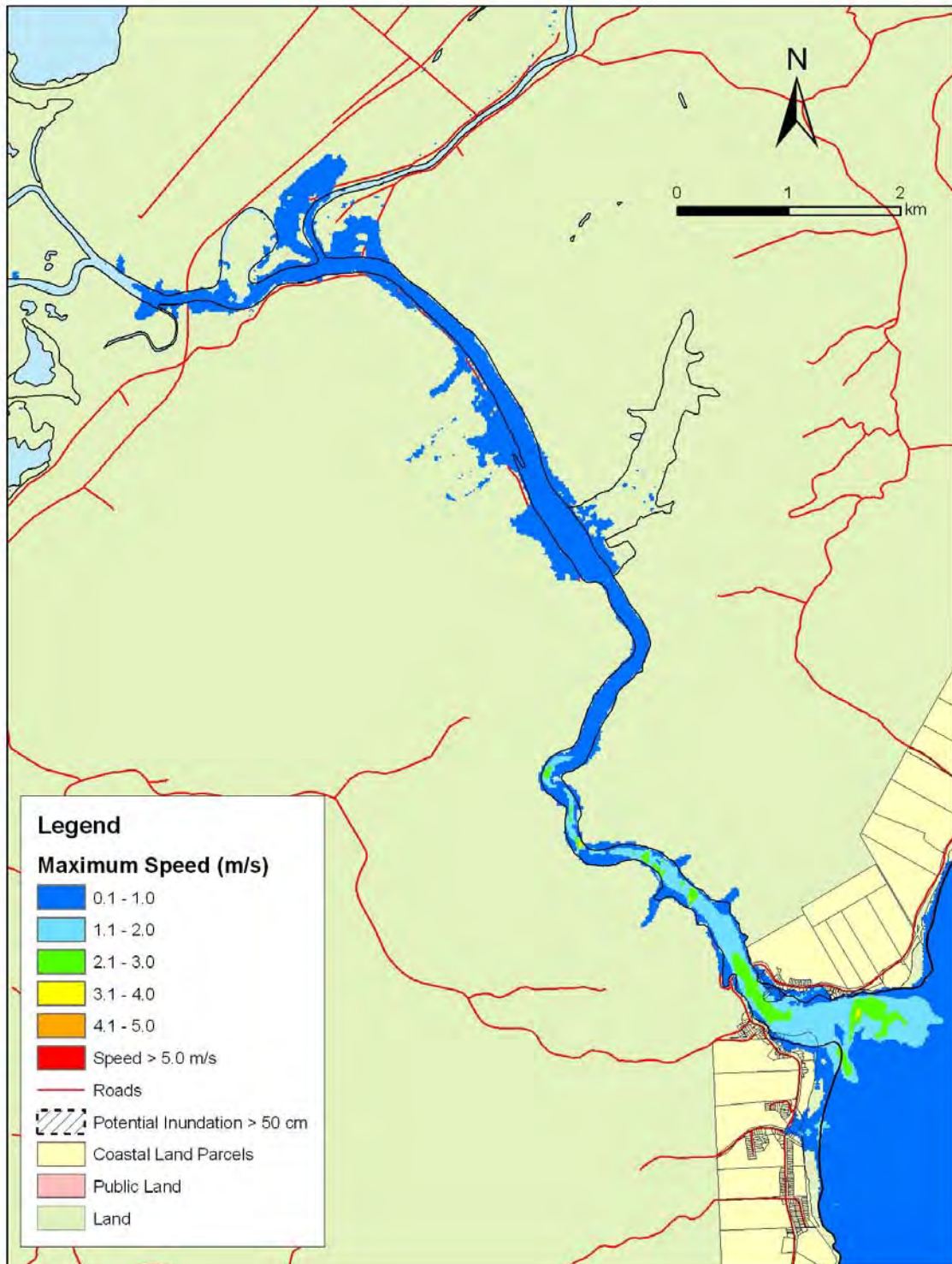
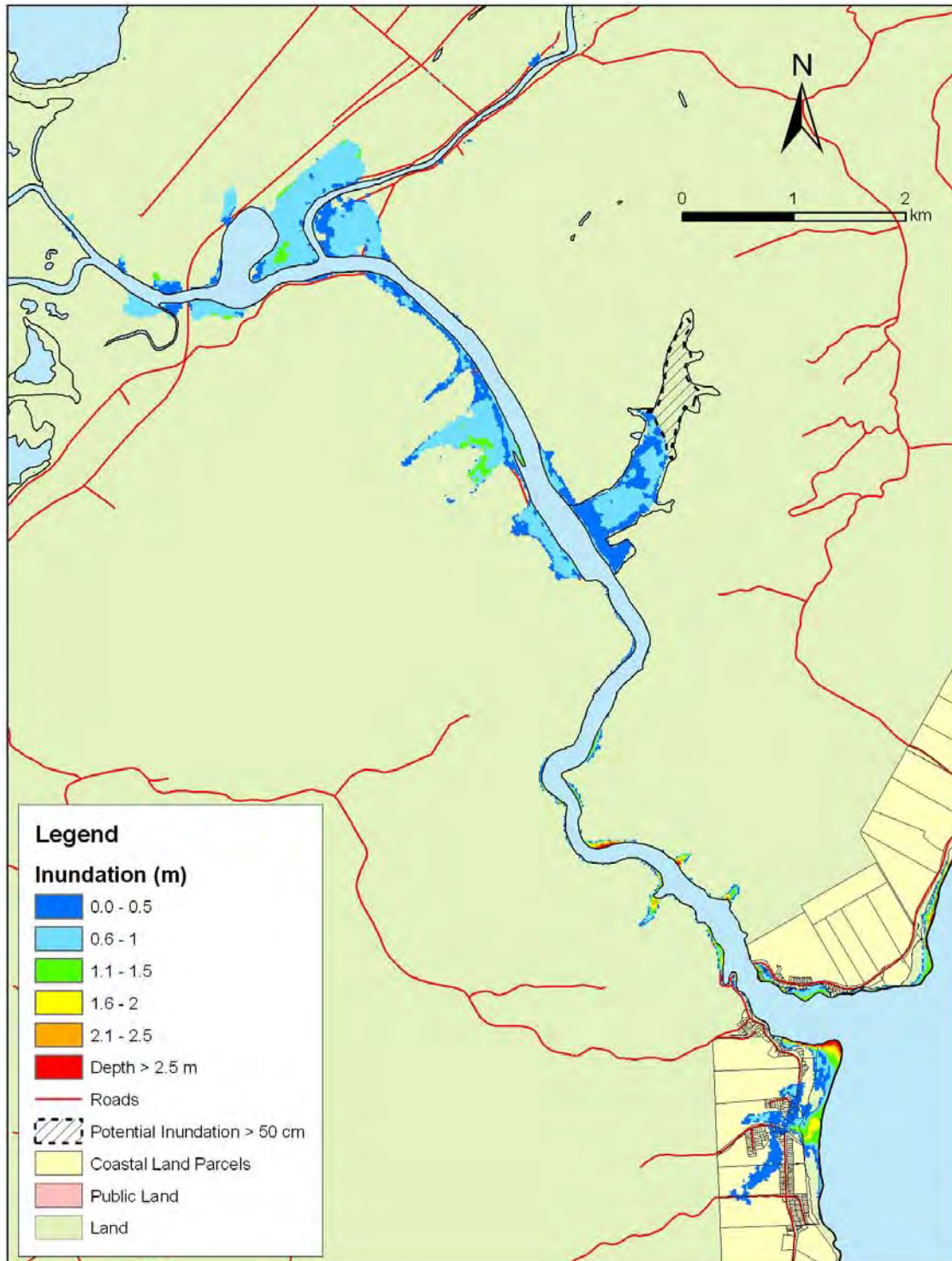


Figure 5.61: Taieri Mouth – 1:500 year remote tsunami: Maximum water depth for inundated land (previous page) and maximum speed (this page) for MHWS.



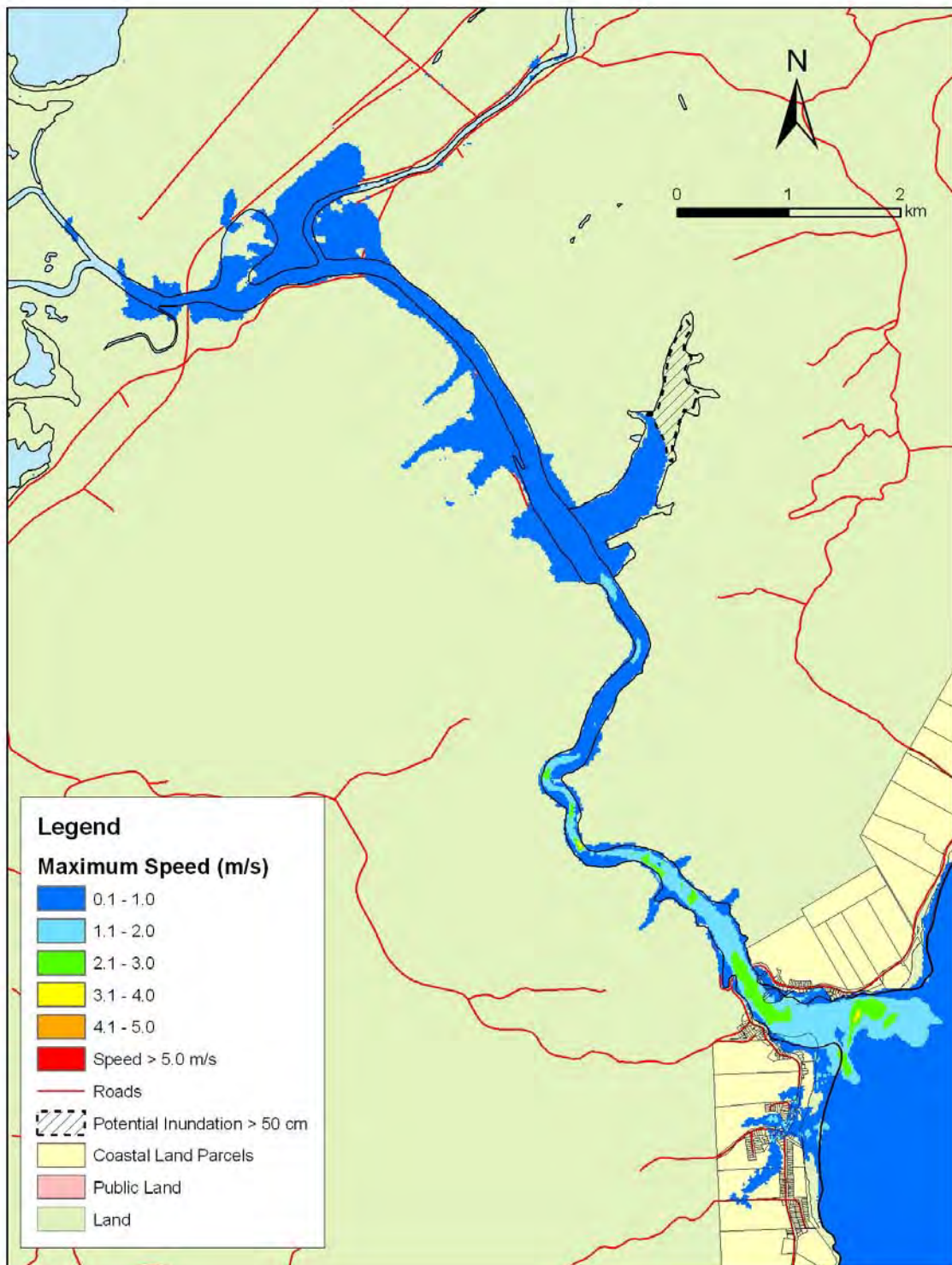
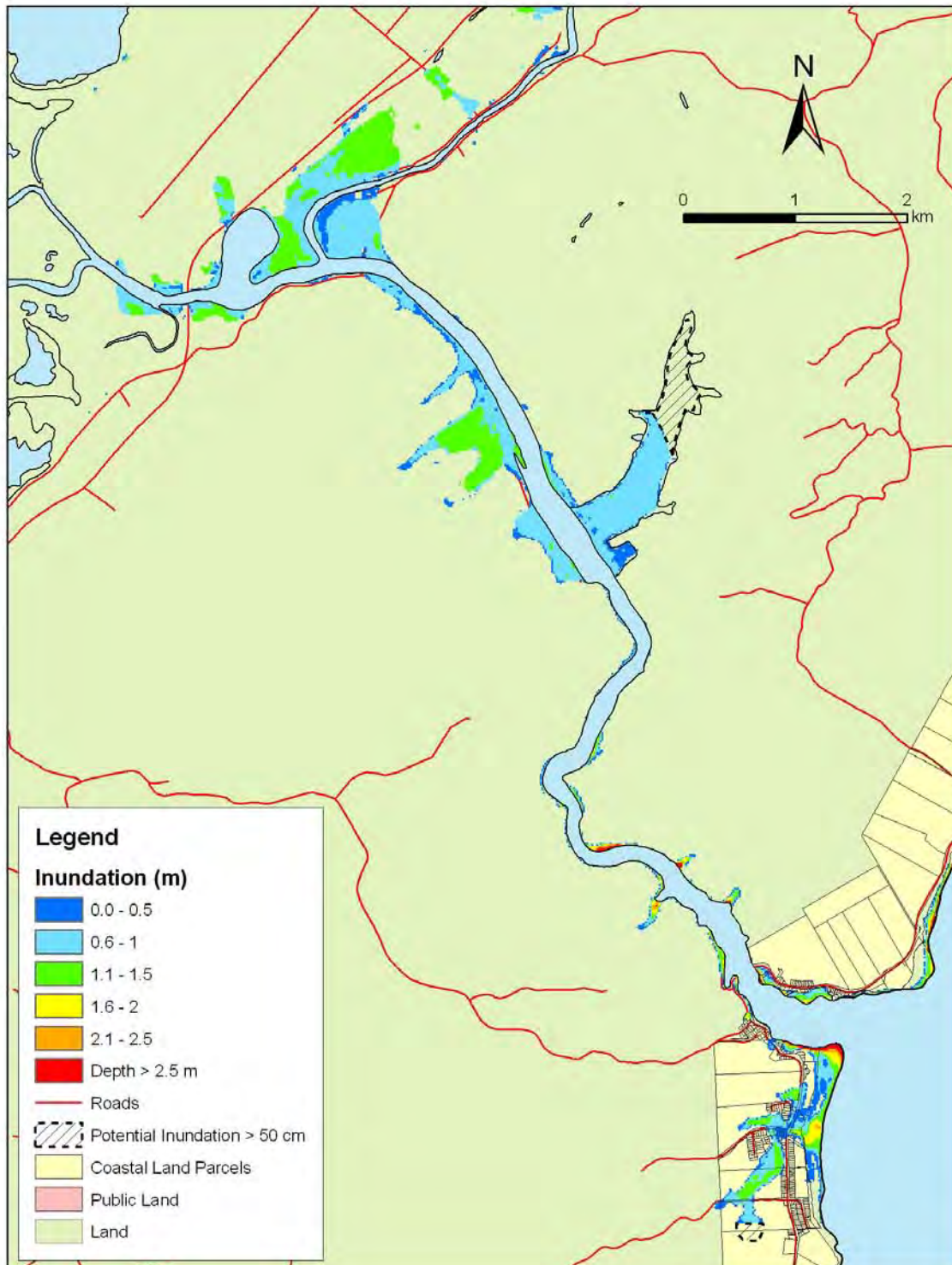


Figure 5.62: Taieri Mouth – 1:500 year remote tsunami: Maximum water depth for inundated land (previous page) and maximum speed (this page) for MHWS with a sea level rise of 30 cm.



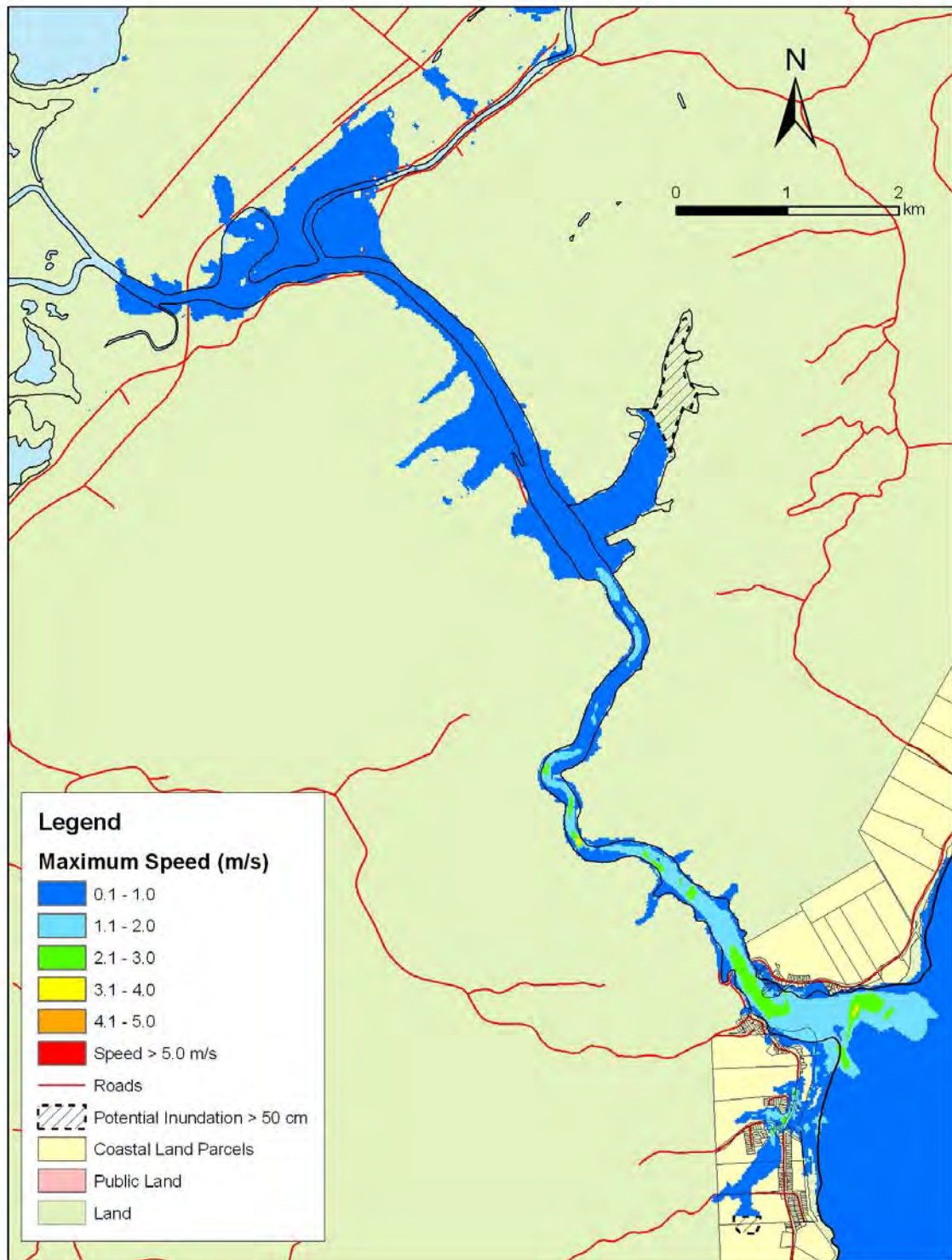


Figure 5.63: Taieri Mouth – 1:500 year remote tsunami: Maximum water depth for inundated land (previous page) and maximum speed (this page) for MHWS with a sea level rise of 50 cm.

5.3.7 Brighton

Figures 5.64 – 5.66 show maximum inundation and water speed for the near-field (Puysegur) tsunami scenarios for this area. Figures 5.67-5.69 show maximum inundation and water speeds for the 1:100 year remote tsunami for Brighton. Figures 5.70-5.72 show maximum inundation and water speeds for the 1:500 year remote tsunami for Brighton.

Brighton: Near-Field

- Trough arrives first approximately 90 minutes after fault rupture. Water level decreases 60 cm over 40 minutes.
- First arrival is small (amplitude 0.3 m about 2.3 hours after fault rupture) main wave arrives fifteen minutes later with amplitude 2 m.
- There are three other waves with amplitude over 1 m arriving at 3.1, 4.4 and 5.8 hours after fault rupture.
- Predominant period of wave arrivals: 35 minutes.
- Maximum runup: up to 3 metres
- There is some inundation, especially on the north side of Otokia creek near its mouth and along the coast.
- Increased inundation and water speeds under the sea level rise scenarios.

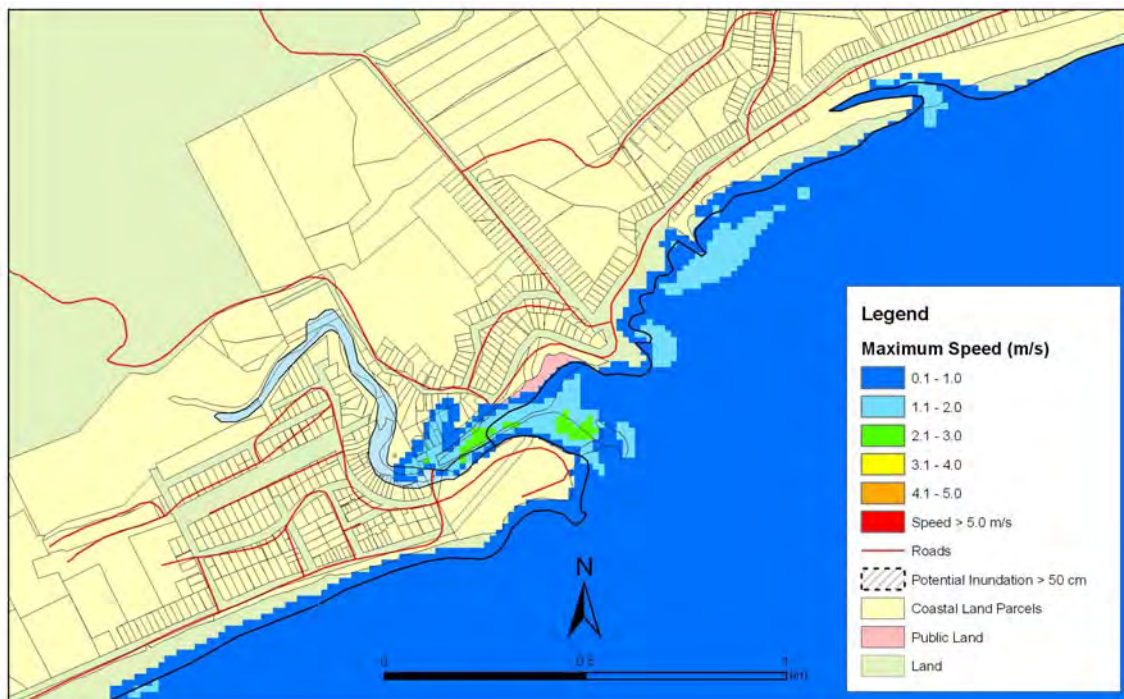
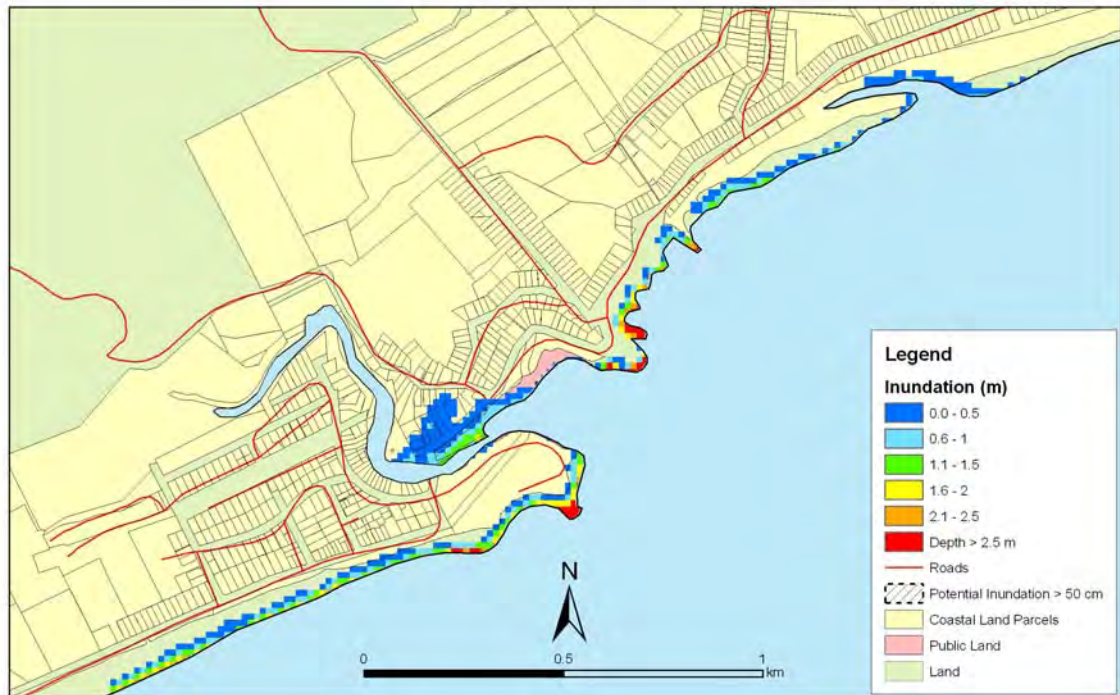


Figure 5.64: Brighton – Puysegur tsunami: Maximum water depth for inundated land (top) and maximum speed (bottom) for MHWS.

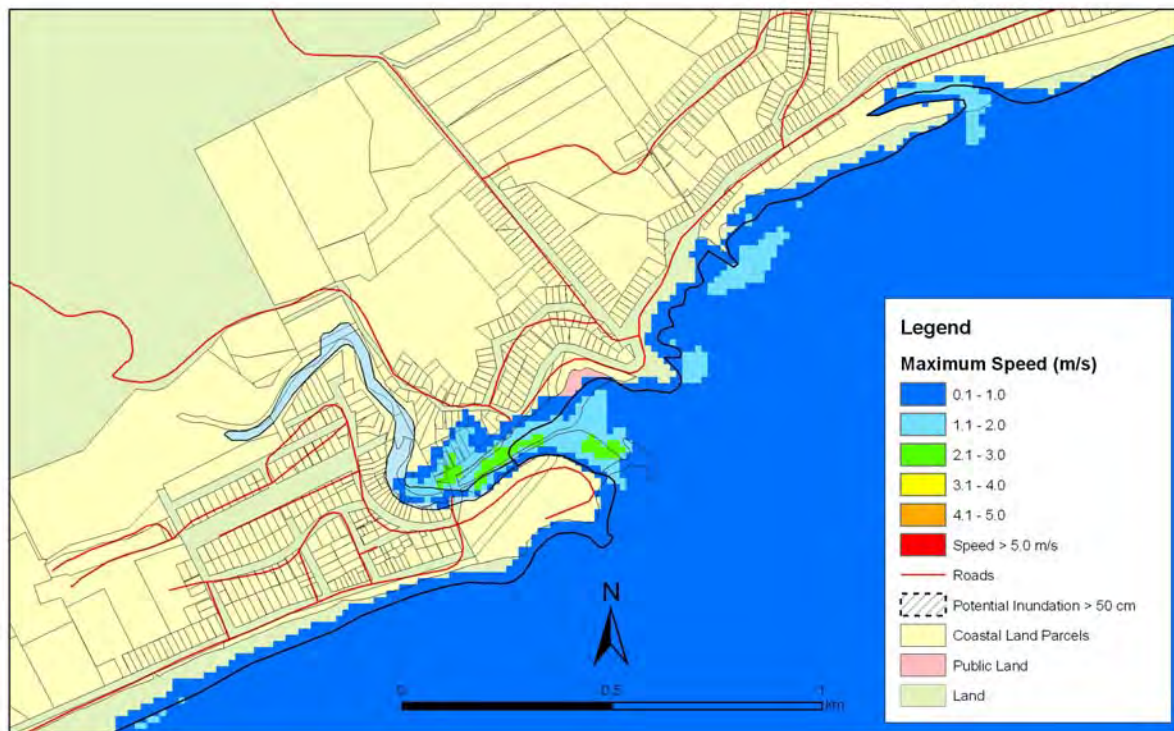
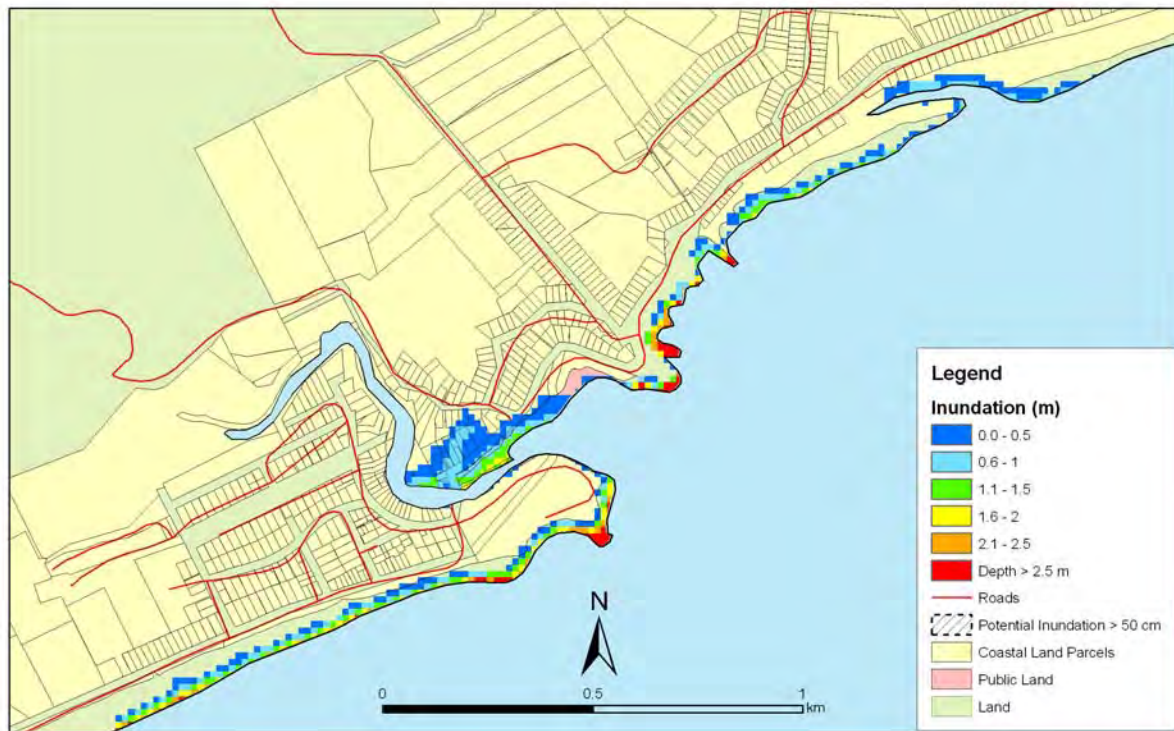


Figure 5.65: Brighton – Puysegur tsunami: Maximum water depth for inundated land (top) and maximum speed (bottom) for MHWS with a sea level rise of 30 cm.

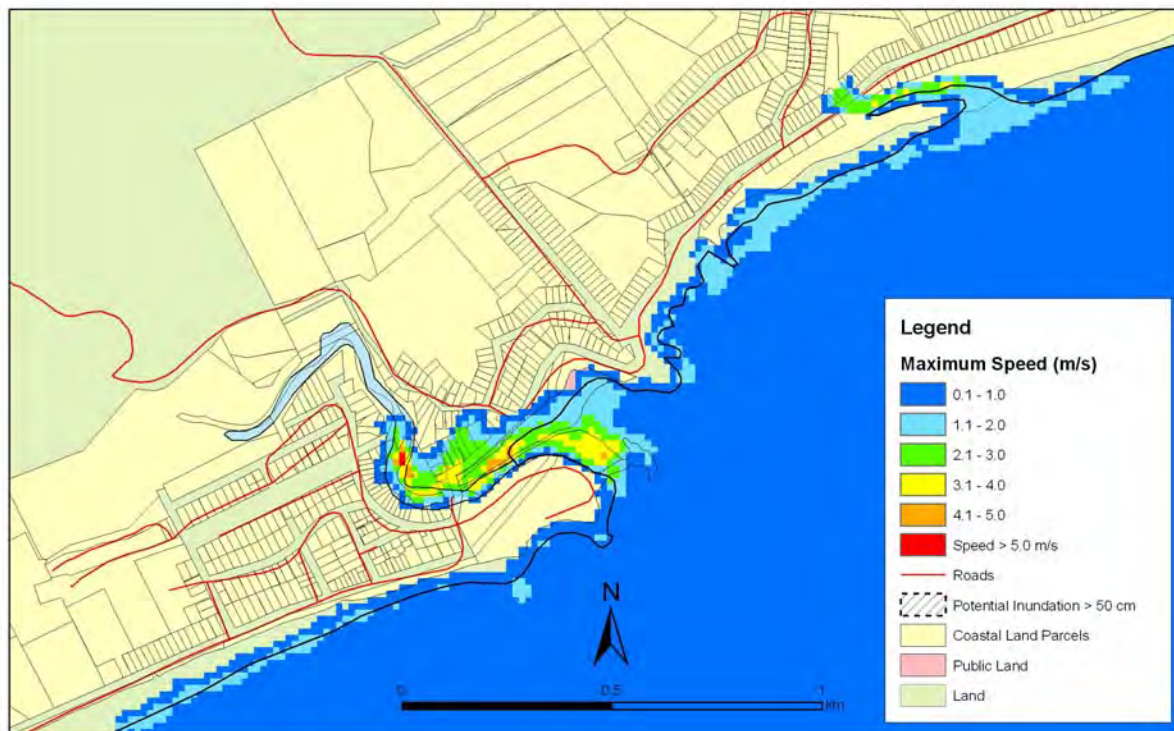
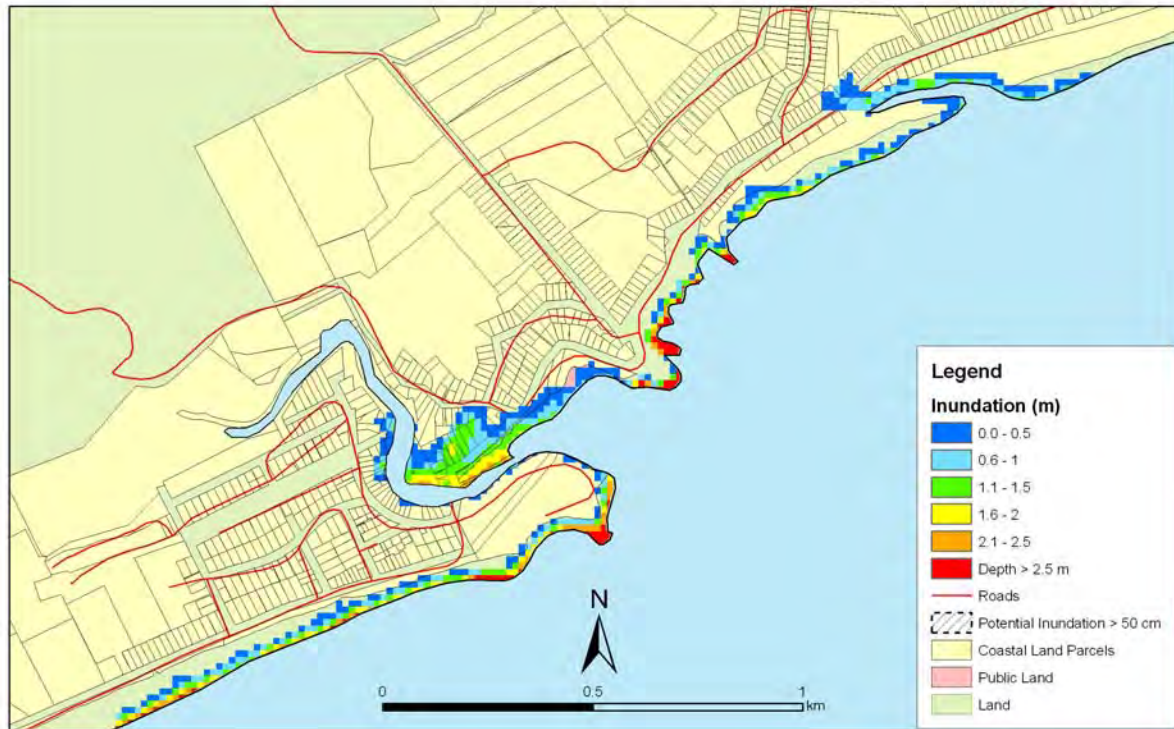


Figure 5.66: Brighton – Puysegur tsunami: Maximum water depth for inundated land (top) and maximum speed (bottom) for MHWS with a sea level rise of 50 cm.

Brighton: Far-Field

- Both remote tsunamis begin with an increase in the water level.
- Third wave is highest with amplitude 1m, total height 2.1m for the 1:100 year tsunami and amplitude 1.5m, total height 3.2m for the 1:500 year tsunami.
- Big waves for around 7 hours after first arrival then lots of smaller arrivals.
- Broad resonance period around 80-90 minutes, also 70 minutes.
- Maximum runup: Greater than 2.5 metres for the 1:100 year and 1:500 year tsunamis.

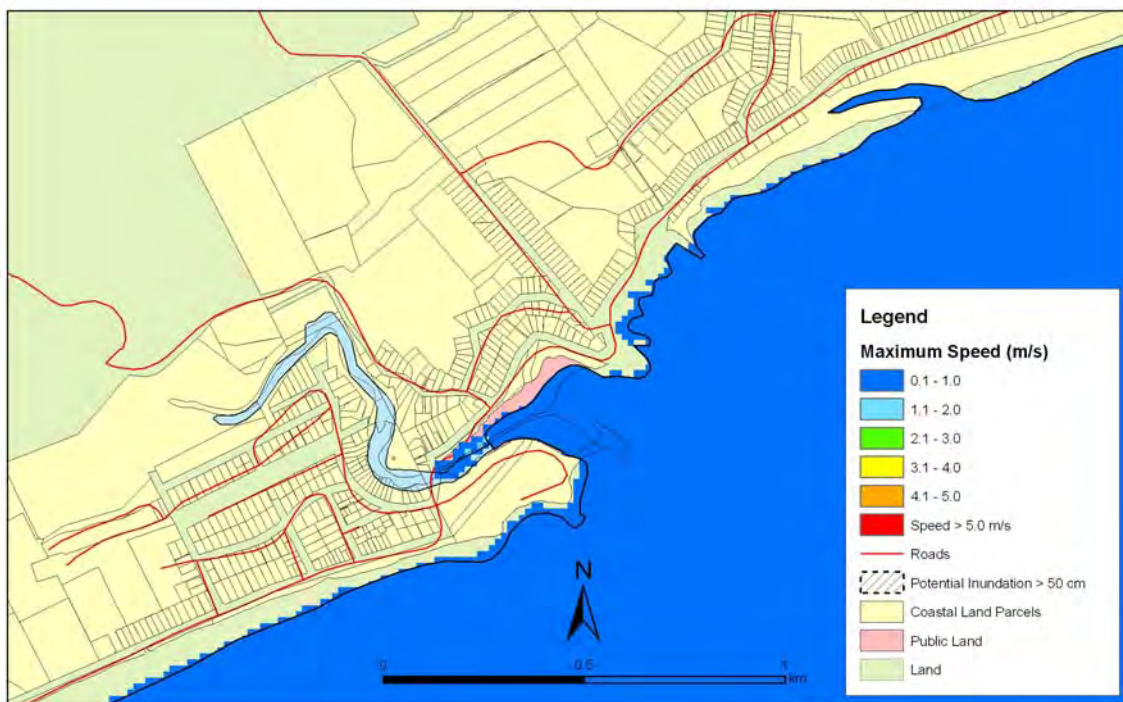
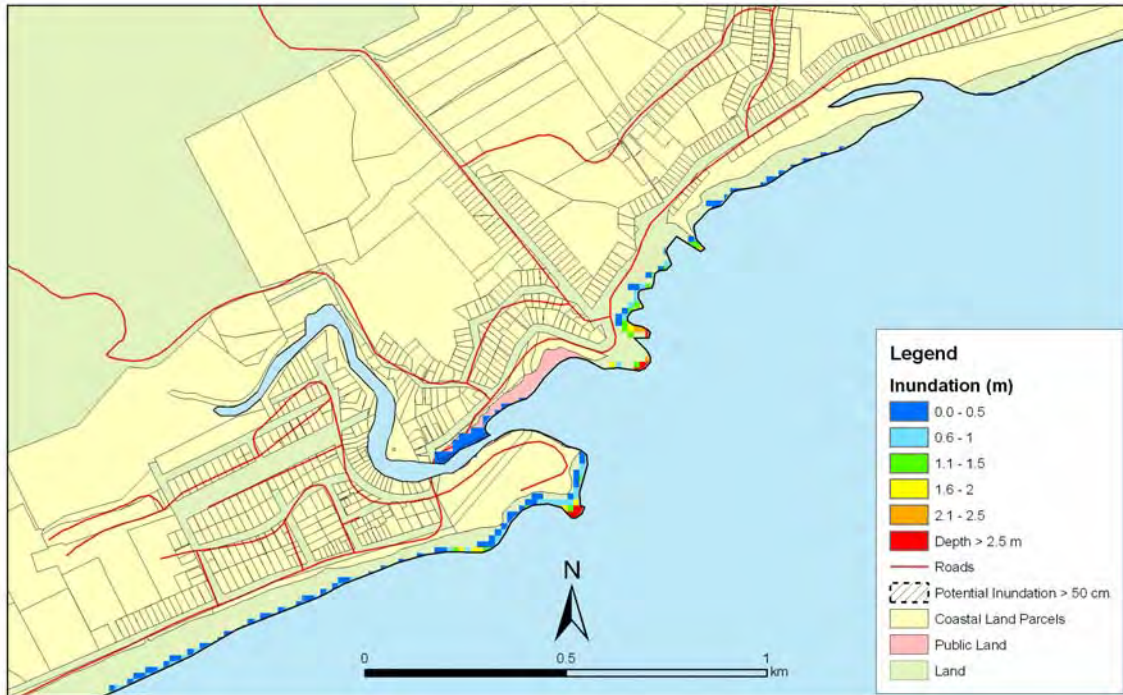


Figure 5.67: Brighton – 1:100 year remote tsunami: Maximum water depth for inundated land (top) and maximum speed (bottom) for MHWS.

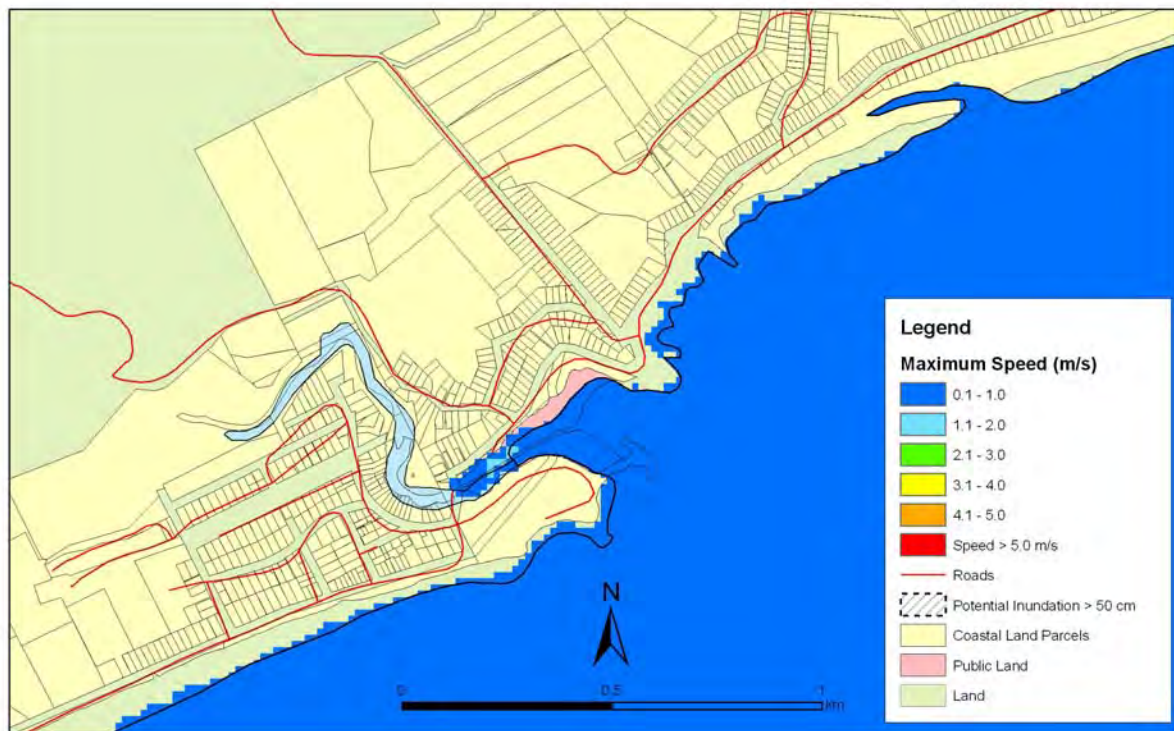
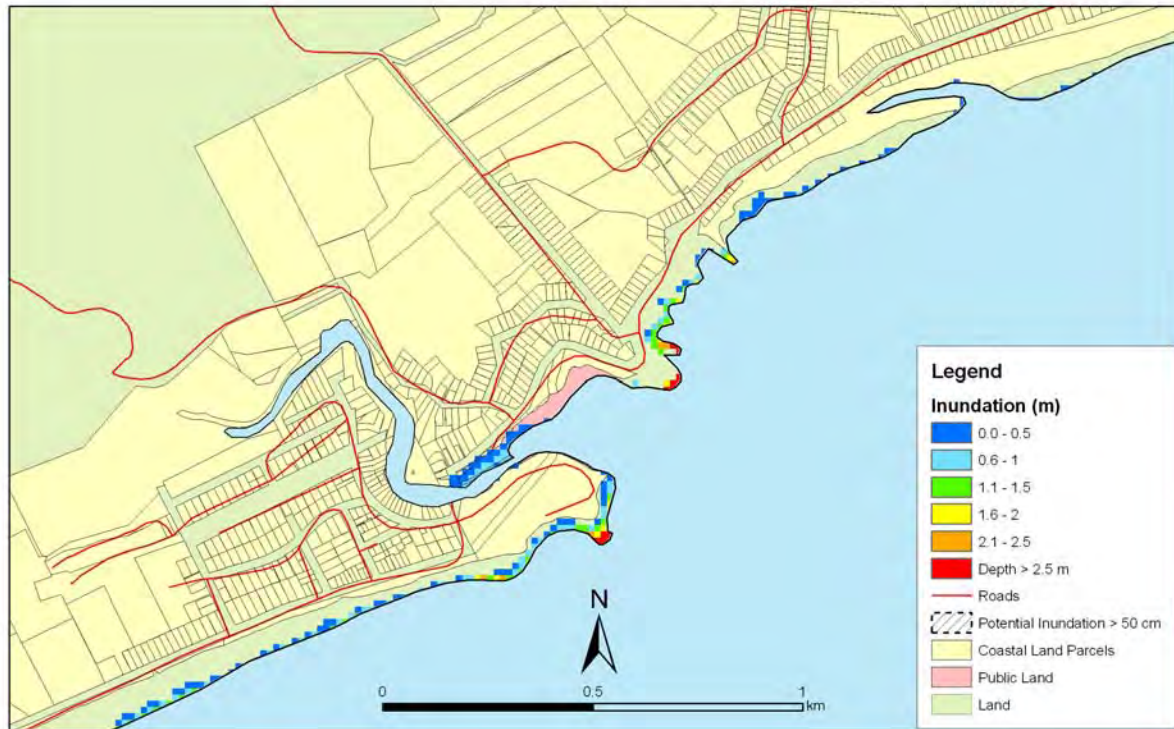


Figure 5.68: Brighton – 1:100 year remote tsunami: Maximum water depth for inundated land (top) and maximum speed (bottom) for MHWS with a sea level rise of 30 cm.

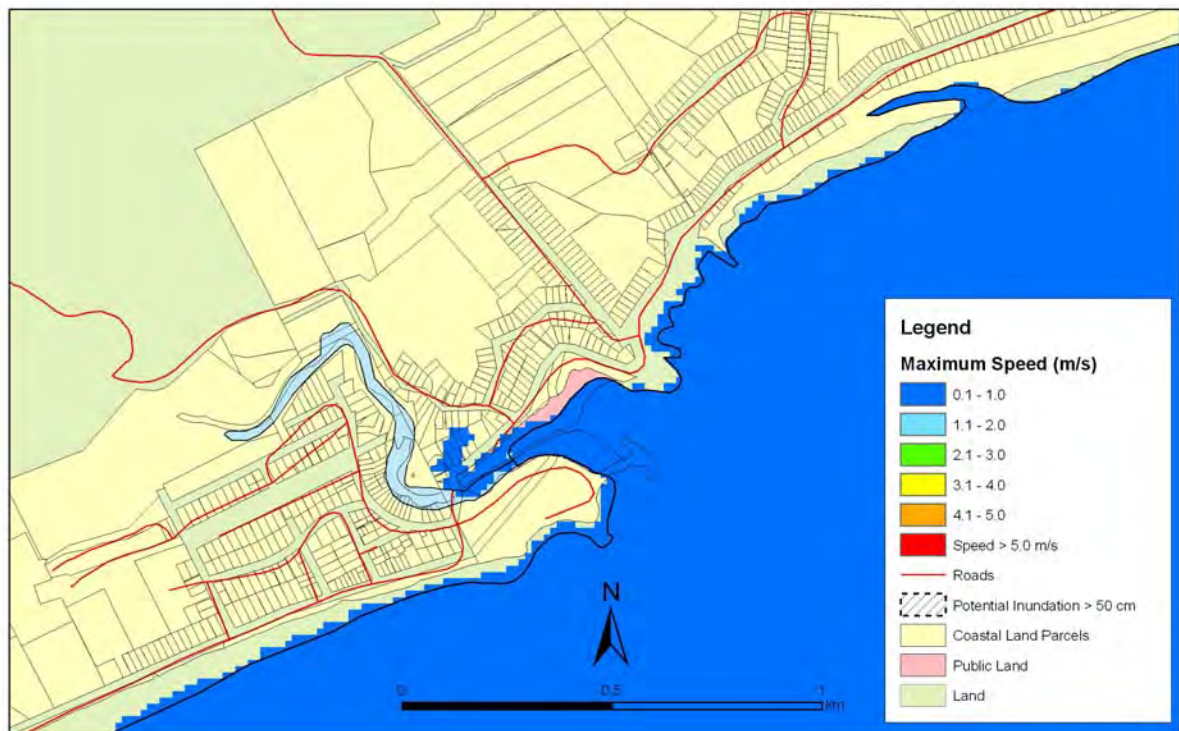
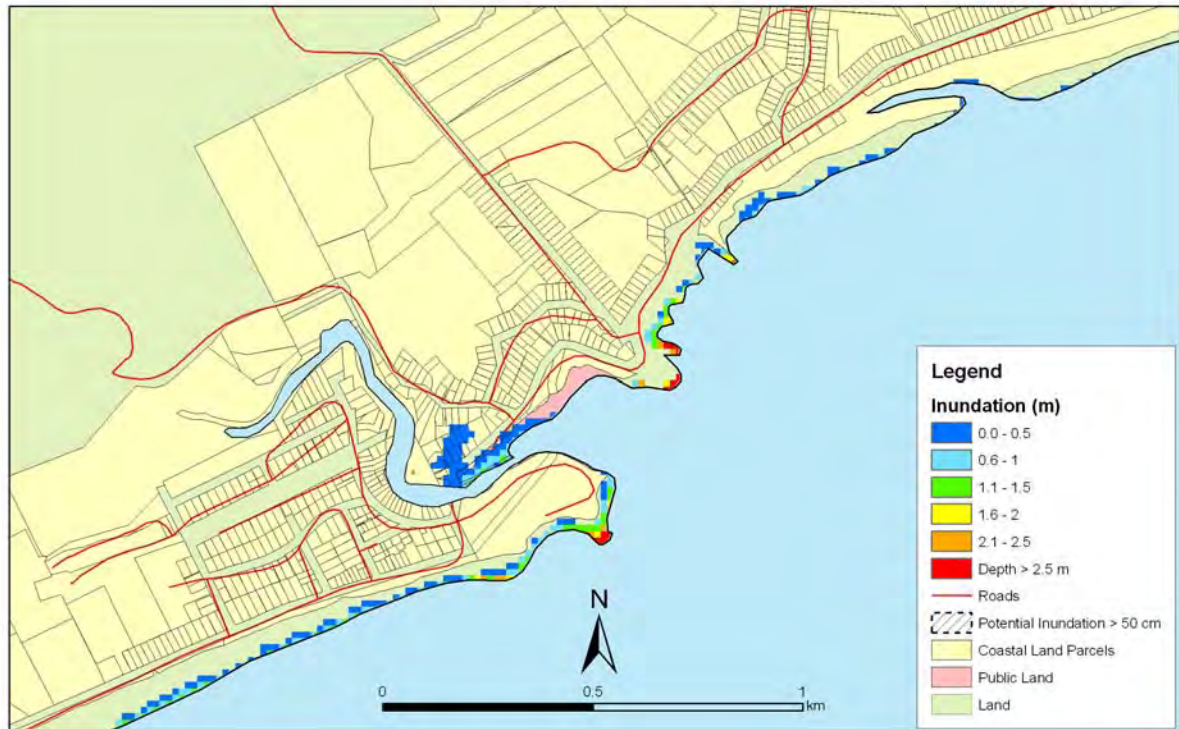


Figure 5.69: Brighton – 1:100 year remote tsunami: Maximum water depth for inundated land (top) and maximum speed (bottom) for MHWS with a sea level rise of 50 cm.

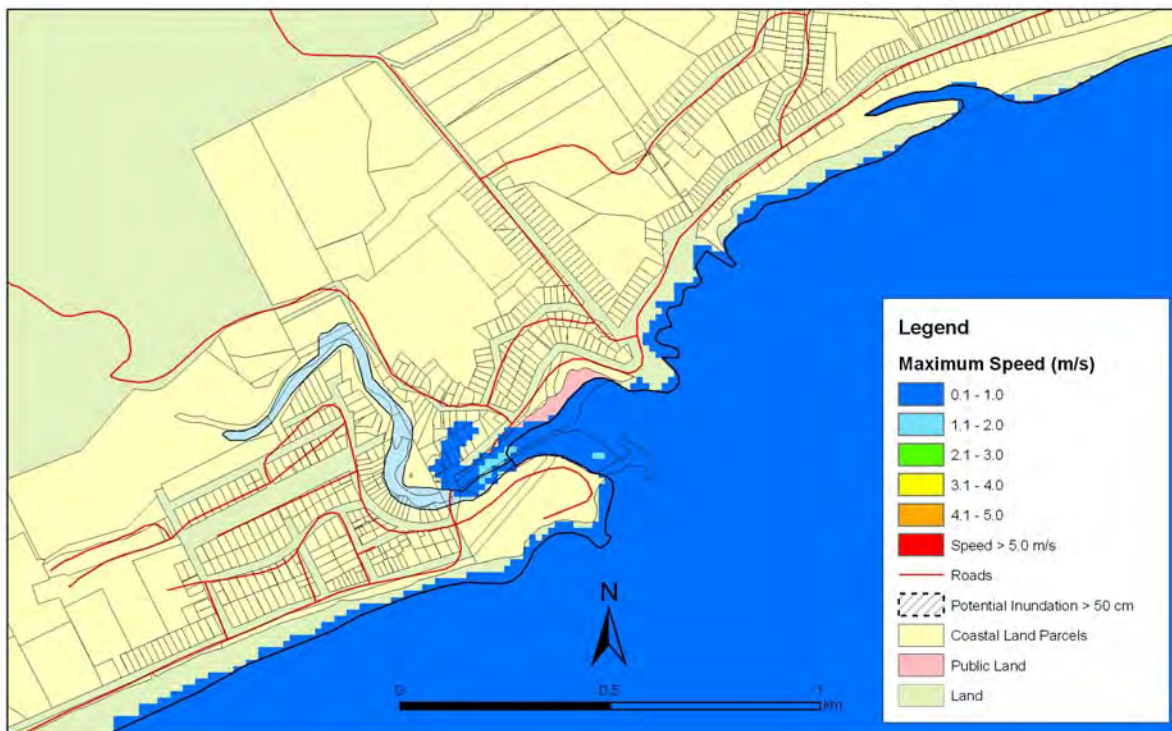
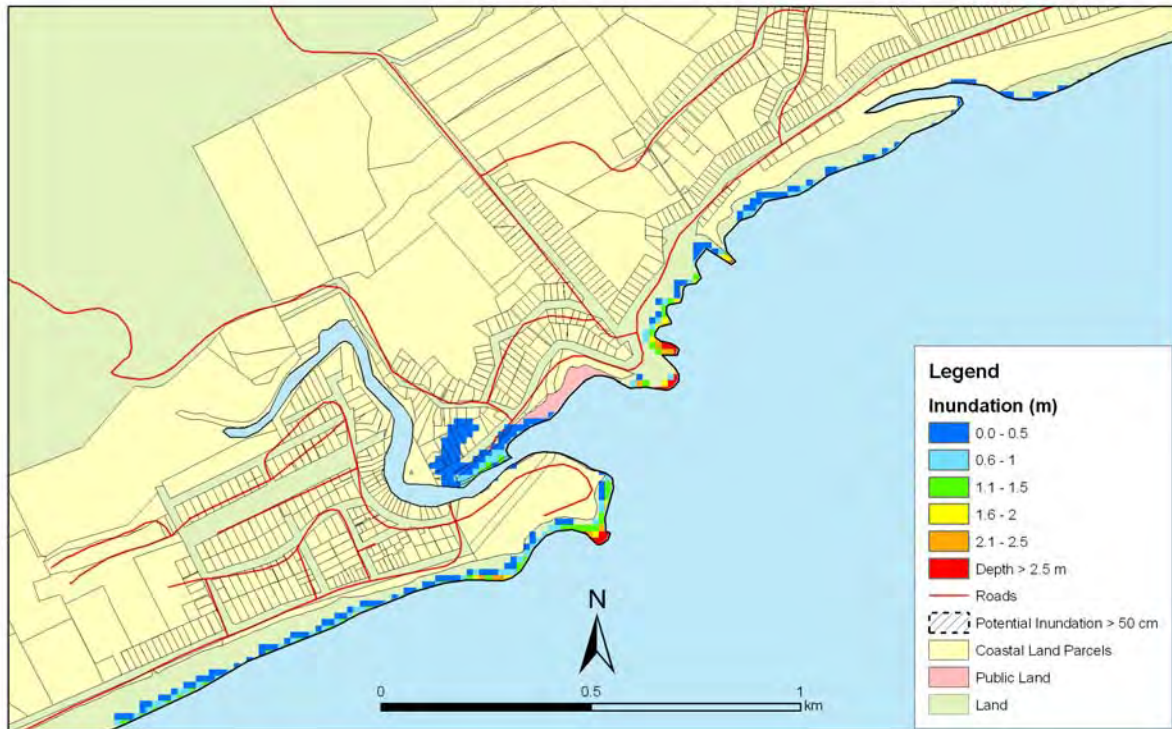


Figure 5.70: Brighton – 1:500 year remote tsunami: Maximum water depth for inundated land (top) and maximum speed (bottom) for MHWS.

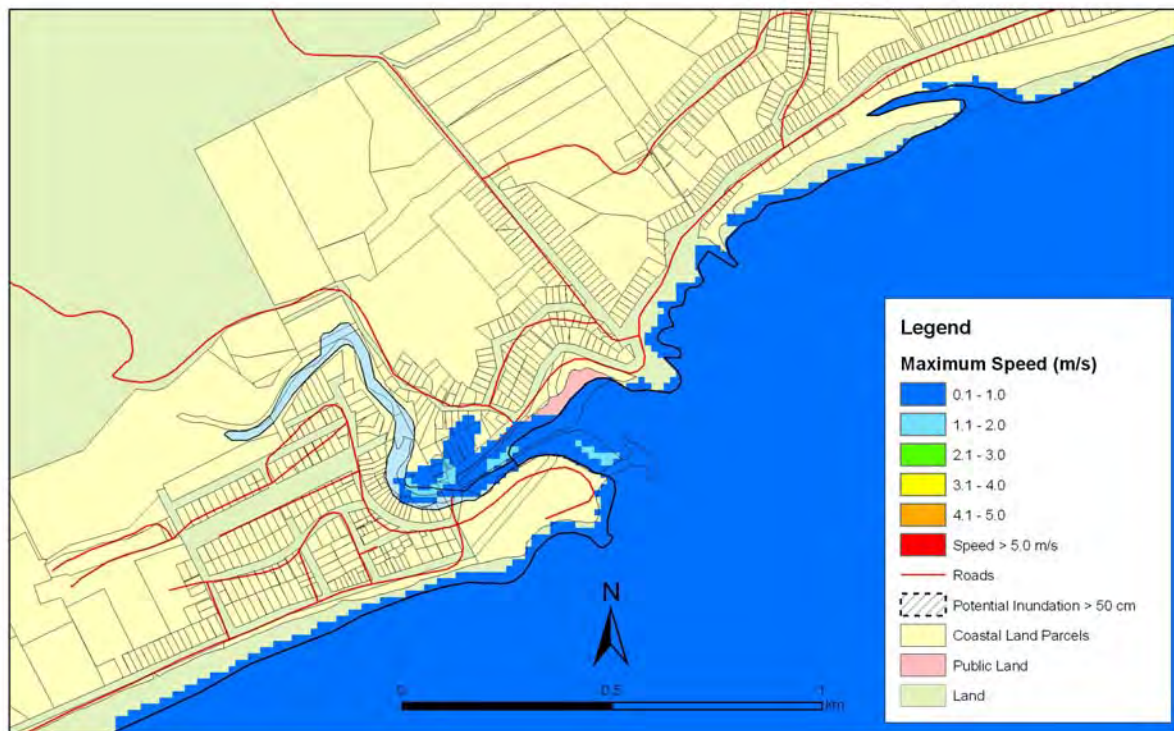
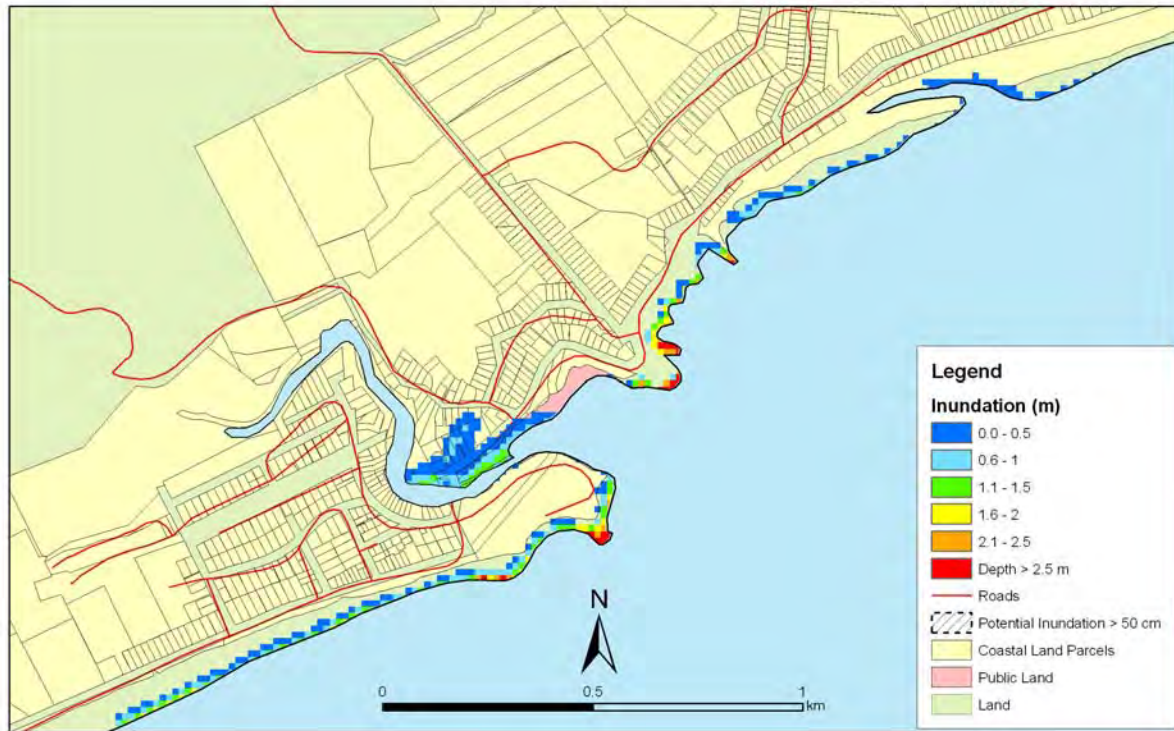


Figure 5.71: Brighton – 1:500 year remote tsunami: Maximum water depth for inundated land (top) and maximum speed (bottom) for MHWS with a sea level rise of 30 cm.

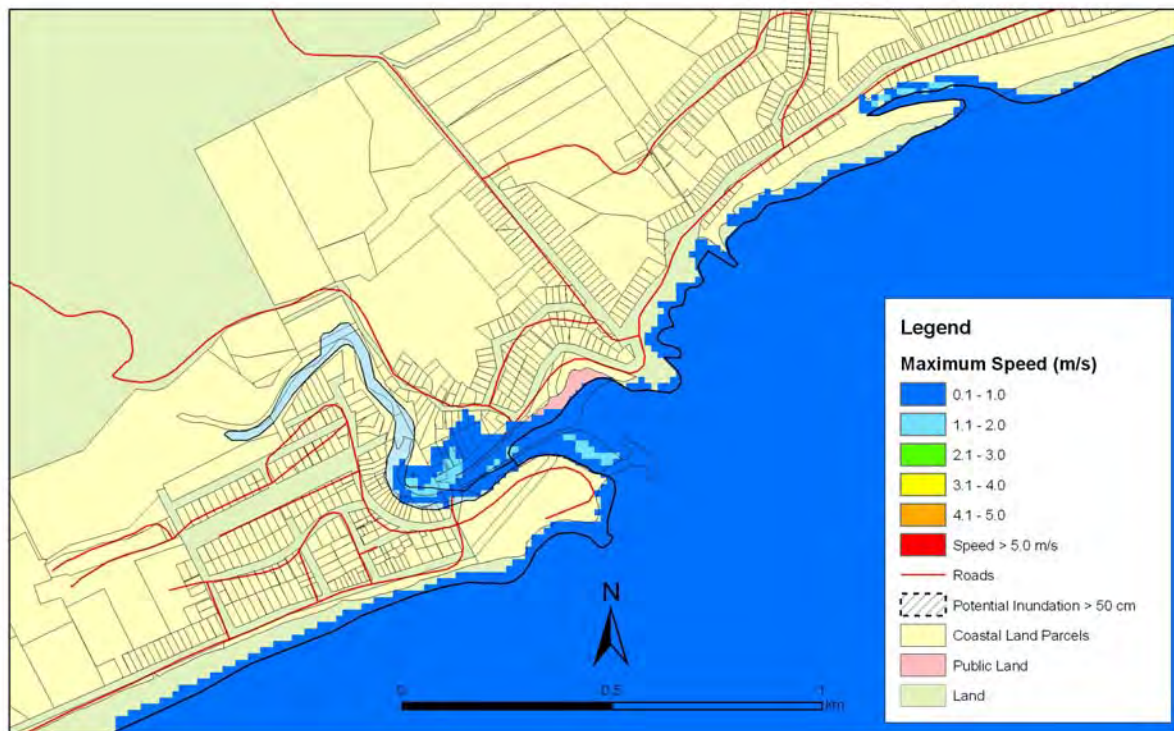
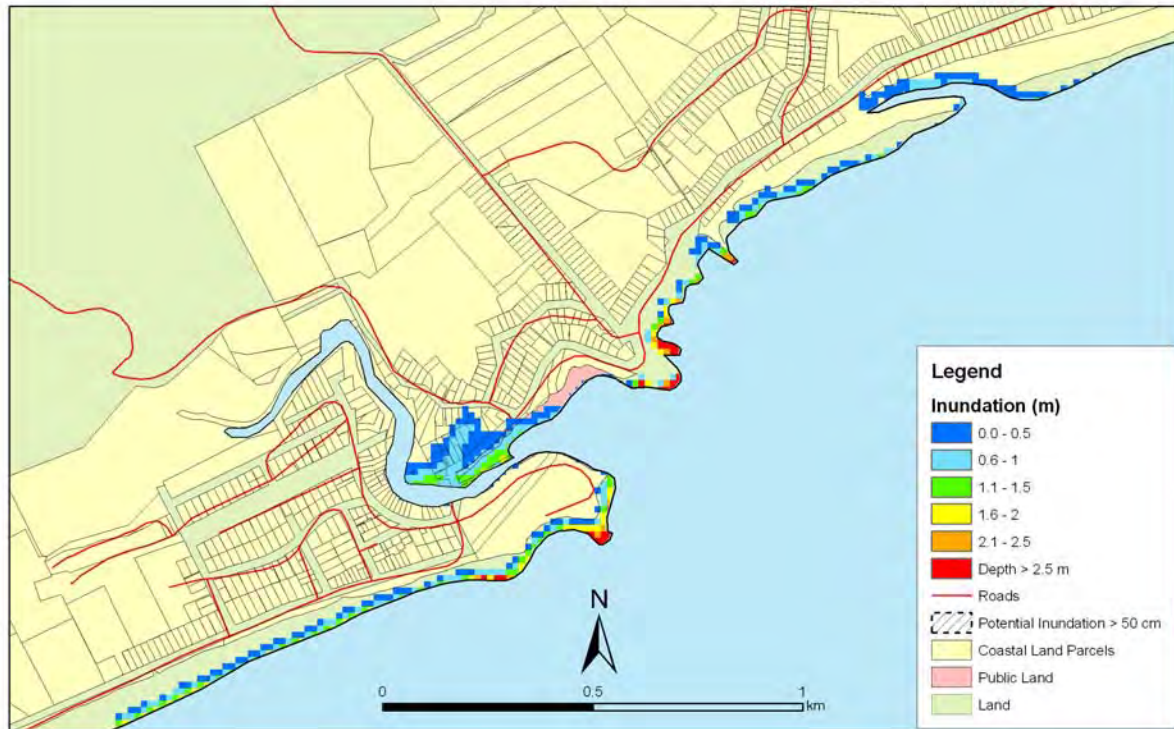


Figure 5.72: Brighton – 1:500 year remote tsunami: Maximum water depth for inundated land (top) and maximum speed (bottom) for MHWS with a sea level rise of 50 cm.

5.3.8 Kaikorai and Waldronville

Figures 5.73 – 5.75 show maximum inundation and water speed for the near-field (Puysegur) tsunami scenarios for this area. Figures 5.76-5.78 show maximum inundation and water speeds for the 1:100 year remote tsunami for Kaikorai and Waldronville. Figures 5.79-5.81 show maximum inundation and water speeds for the 1:500 year remote tsunami for Kaikorai and Waldronville.

Kaikorai and Waldronville: Near-Field

- Trough arrives first approximately 90 minutes after fault rupture. Water level decreases 50 cm over 40 minutes.
- First wave arrival is small (amplitude 0.2 m at 2.3 hours after fault rupture), first main wave arrives about 15 minutes later with amplitude 1.7 m.
- One other wave with amplitude greater than 1.1m, which arrives 5.8 hours after fault rupture.
- Predominant period of wave arrivals: 35 minutes.
- Maximum runup: up to 2.8 metres along the coast.
- There is a small amount of inundation along the coast and the sides of the Kaikorai stream.
- High speeds at the river mouth and by the bridge indicate risk of erosion especially in the sea level rise scenarios.

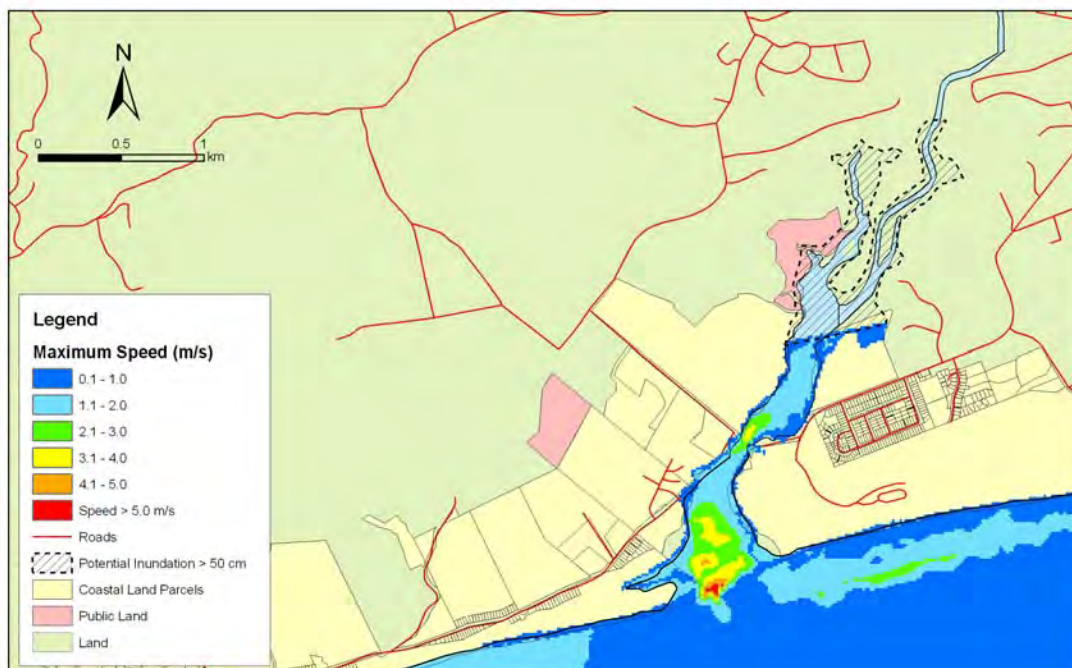
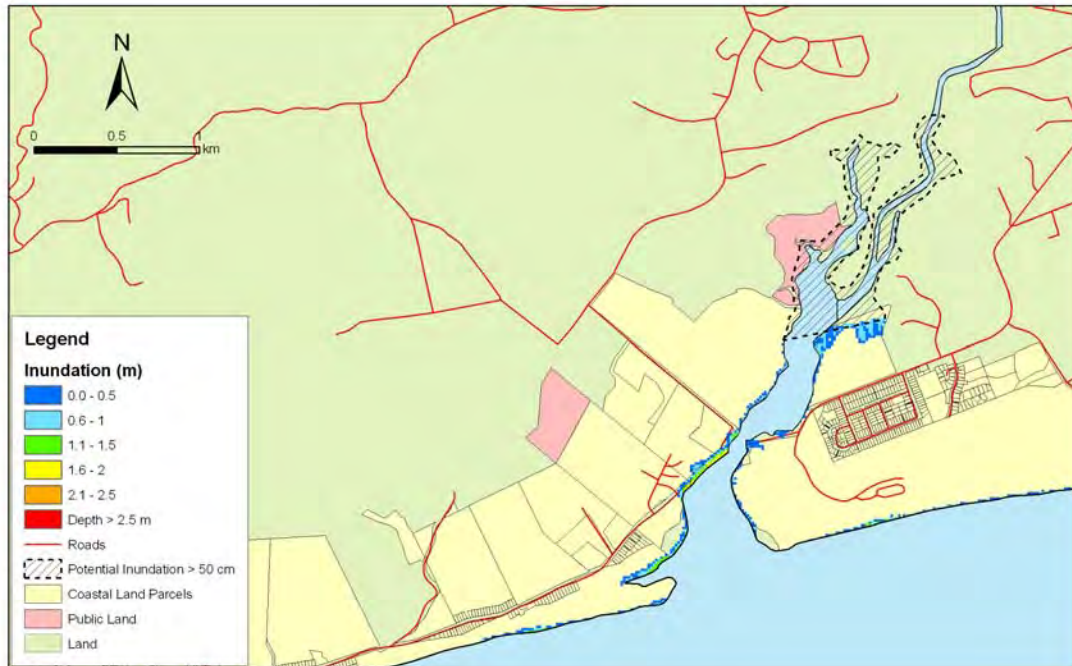


Figure 5.73: Kaikorai and Waldronville – Puysegur tsunami: Maximum water depth for inundated land (top) and maximum speed (bottom) for MHWS.

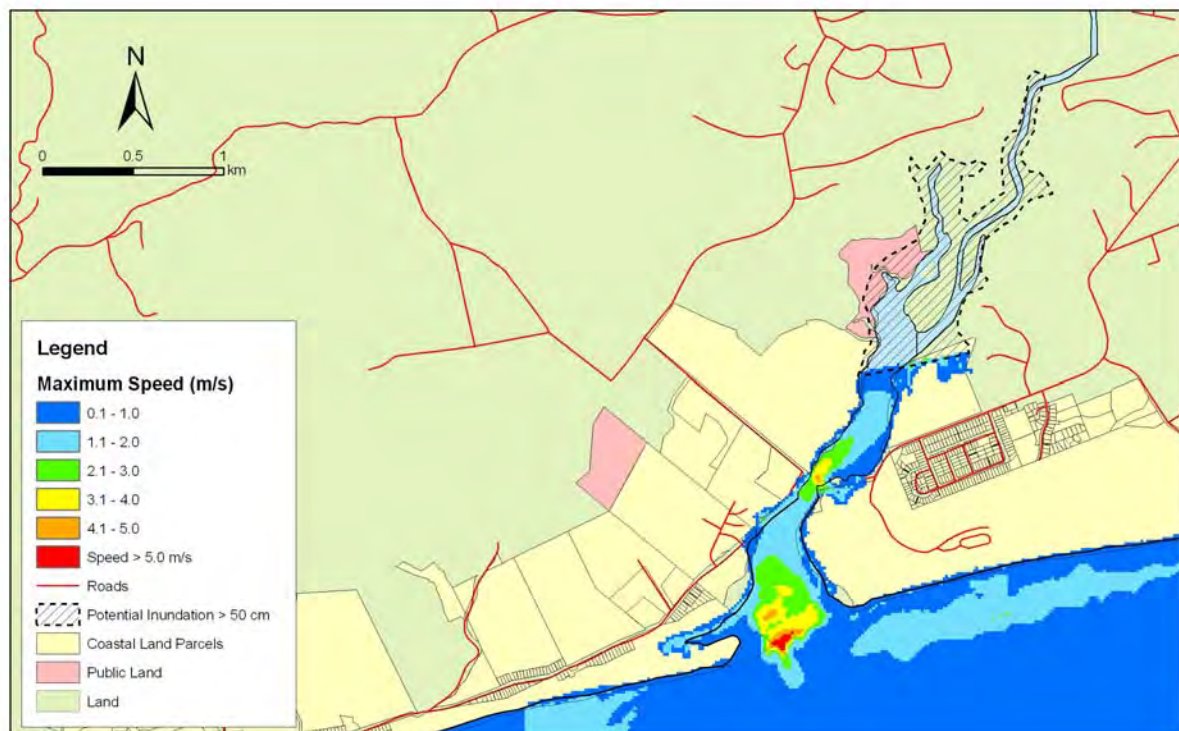
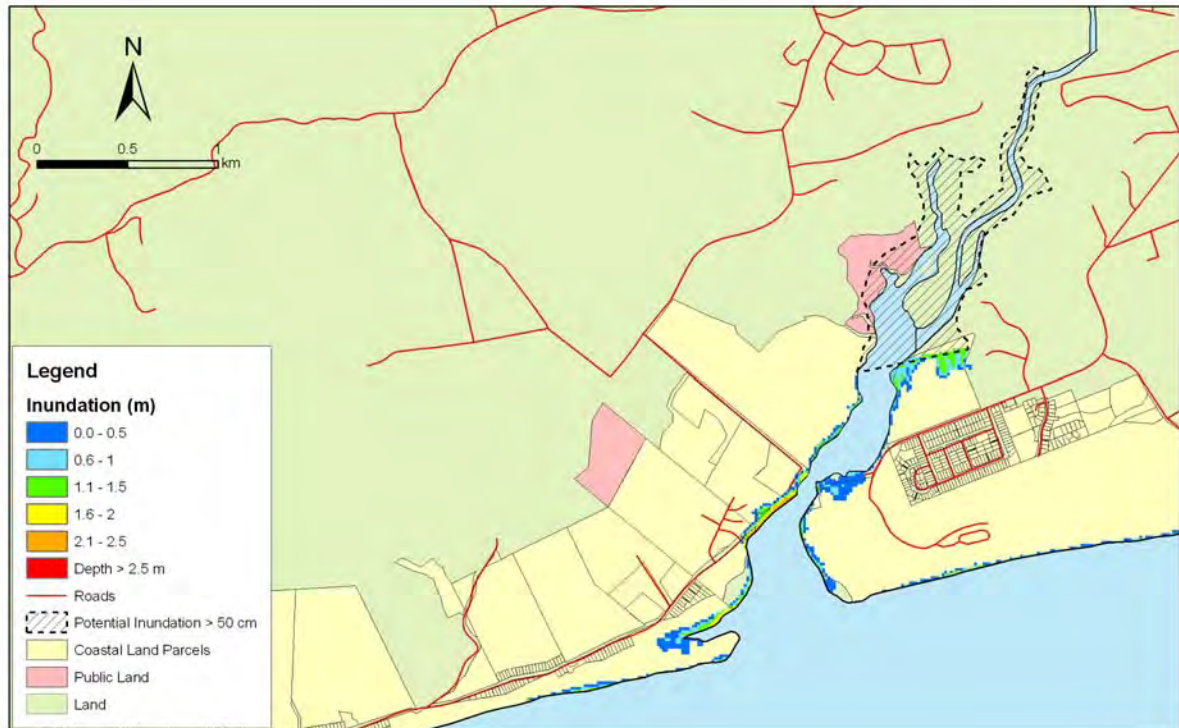


Figure 5.74: Kaikorai and Waldronville– Puysegur tsunami: Maximum water depth for inundated land (top) and maximum speed (bottom) for MHWS with a sea level rise of 30 cm.

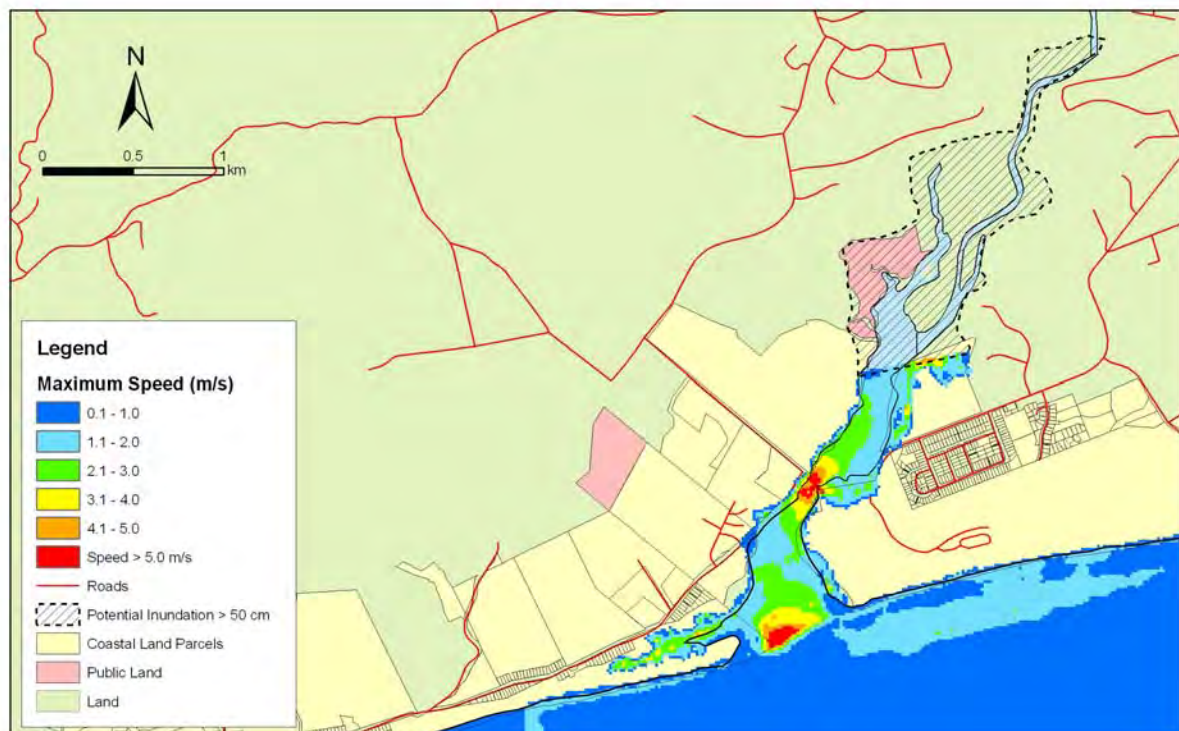
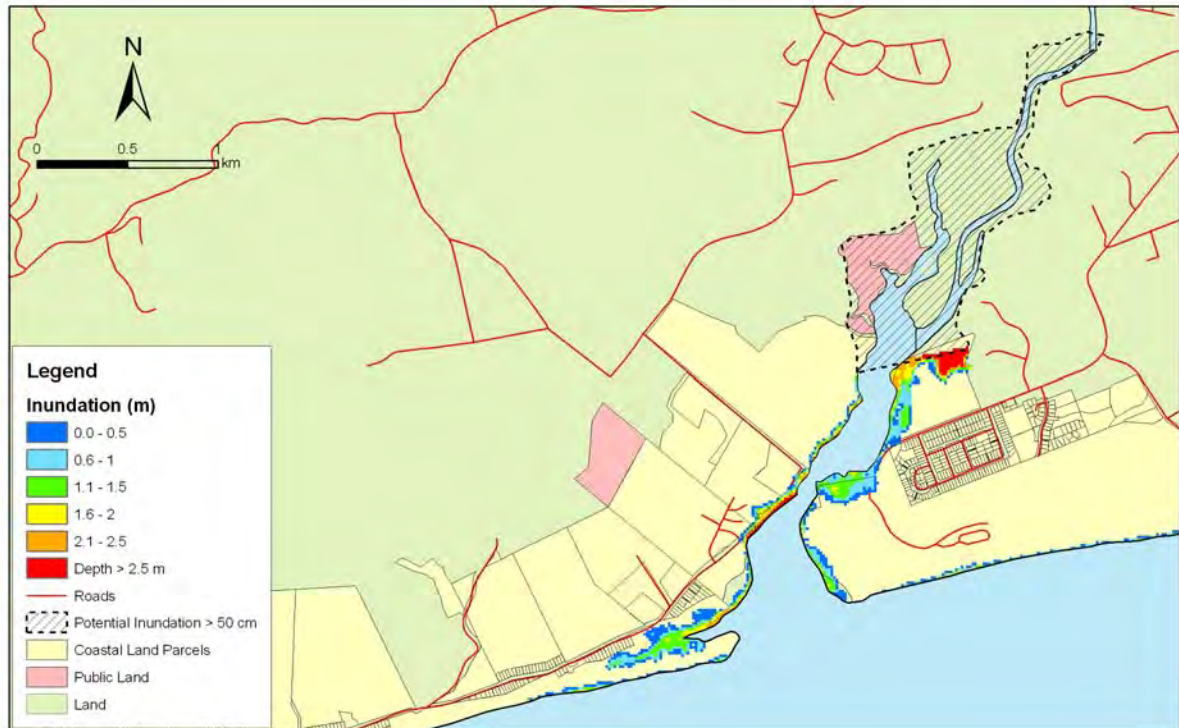


Figure 5.75: Kaikorai and Waldronville– Puysegur tsunami: Maximum water depth for inundated land (top) and maximum speed (bottom) for MHWS with a sea level rise of 50 cm.

Kaikorai and Waldronville: Far-Field

- Both remote tsunamis begin with an increase in the water level.
- Third wave is highest with amplitude 0.9m, total height 1.8m for 1:100 year tsunami and amplitude 1.6m, total height 3.1m for the 1:500 year tsunami.
- Big waves for around 7 hours after first arrival then lots of smaller arrivals.
- Broad resonance period around 80-90 minutes and also 70 minutes.
- Maximum runup: up to 2 metres for 1:100 year tsunami and 2.5 metres for 1:500 year tsunami.
- There is some inundation along the banks of the Kaikorai River and also behind Waldronville. There is some risk of erosion due to high speeds at the river mouth and where the bridge crosses the river.

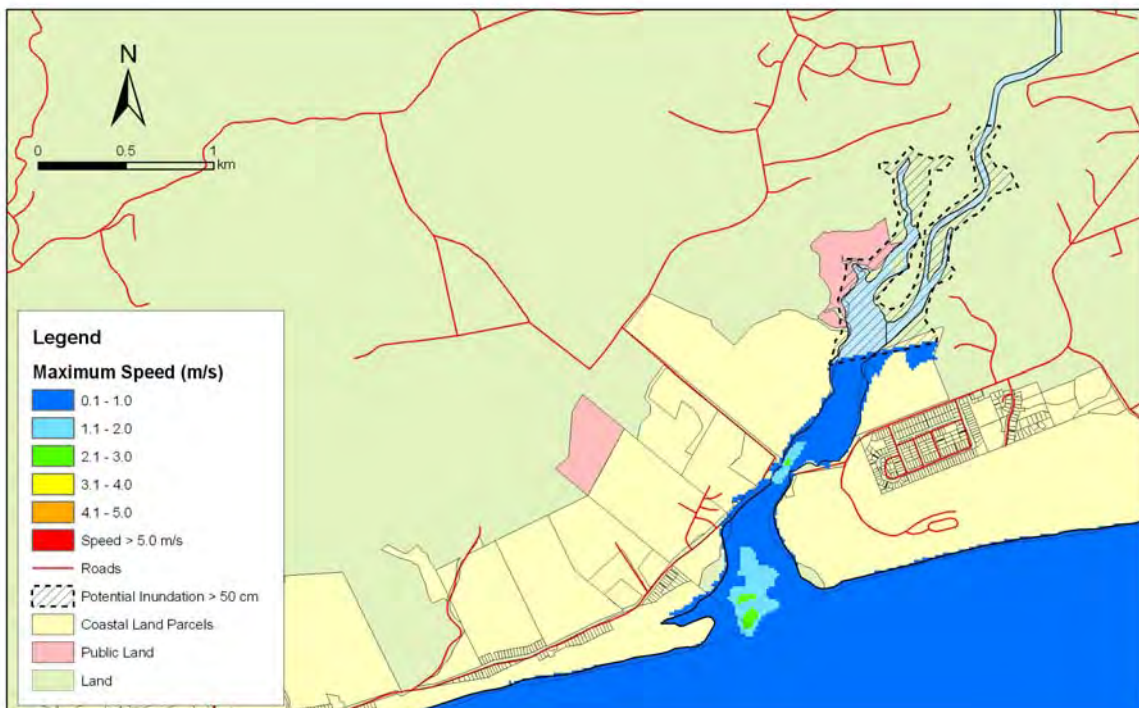
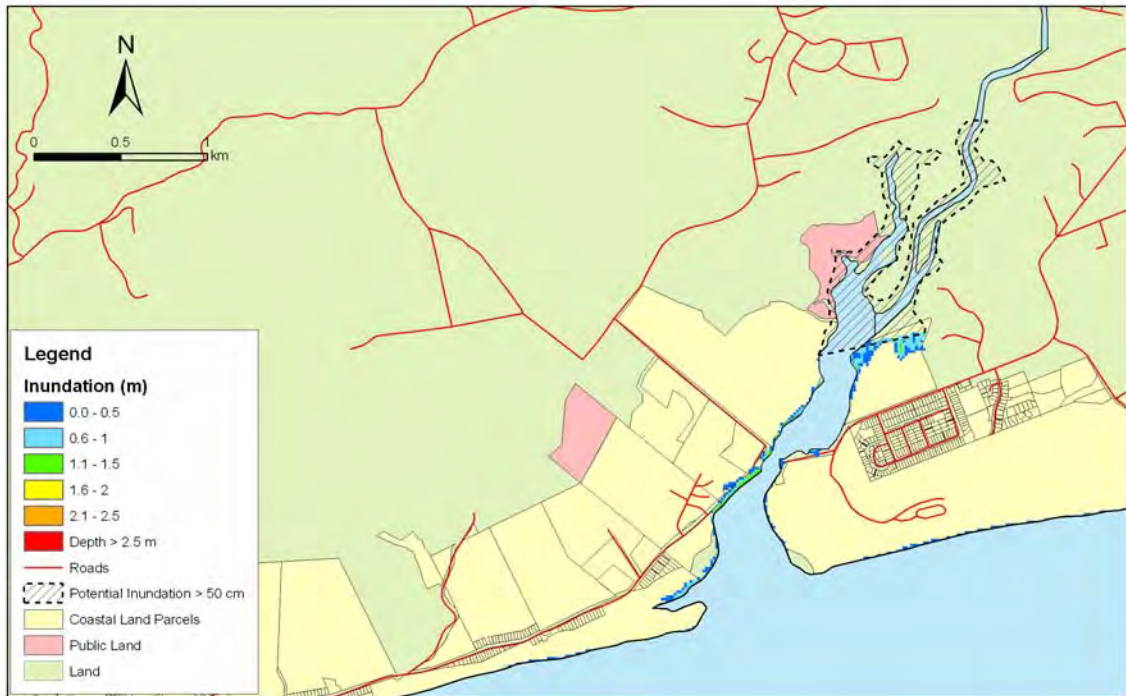


Figure 5.76: Kaikorai and Waldronville – 1:100 year remote tsunami: Maximum water depth for inundated land (top) and maximum speed (bottom) for MHWS.

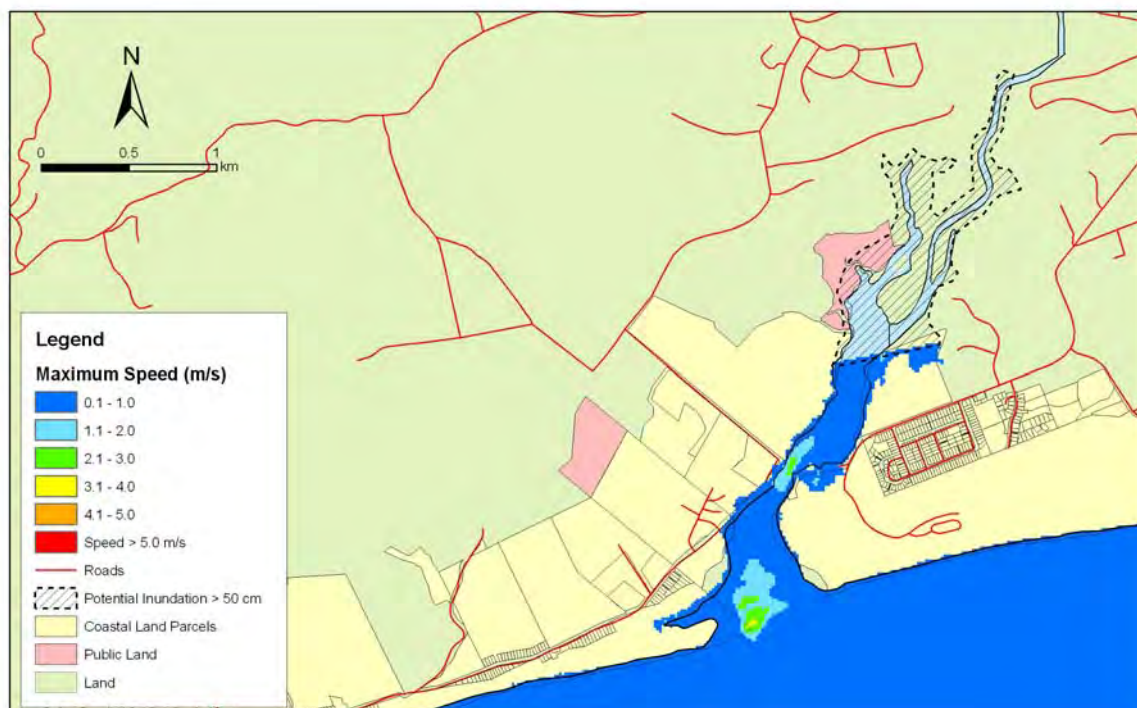


Figure 5.77: Kaikorai and Waldronville – 1:100 year remote tsunami: Maximum water depth for inundated land (top) and maximum speed (bottom) for MHWS with a sea level rise of 30 cm.

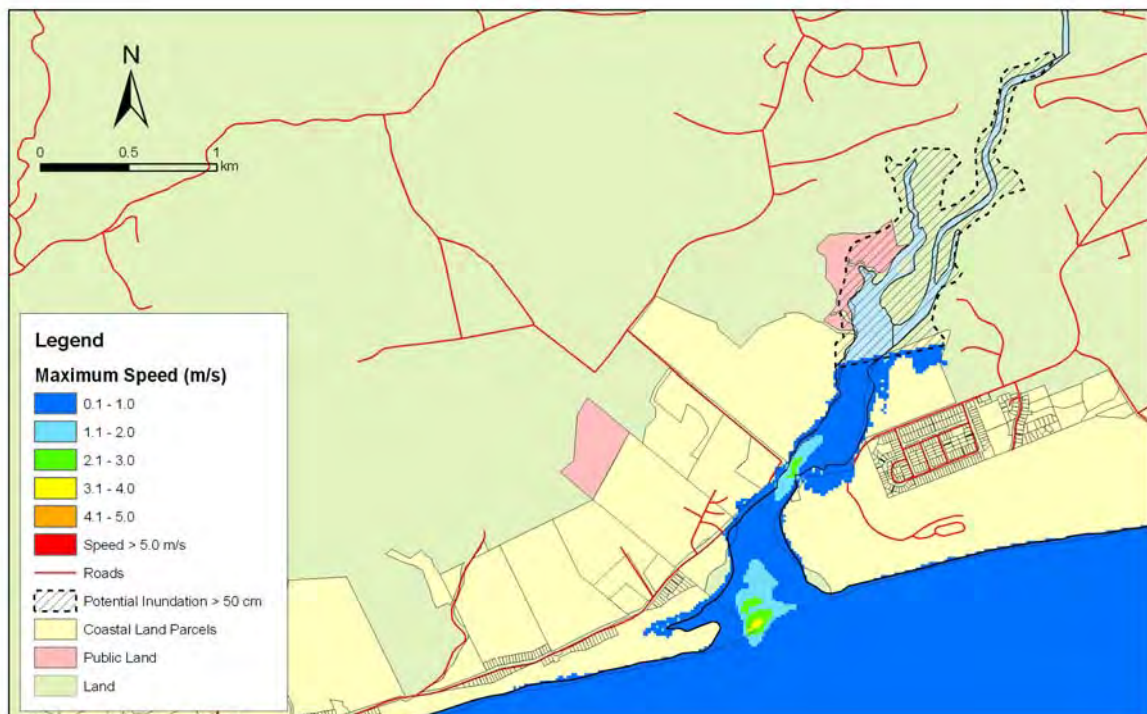
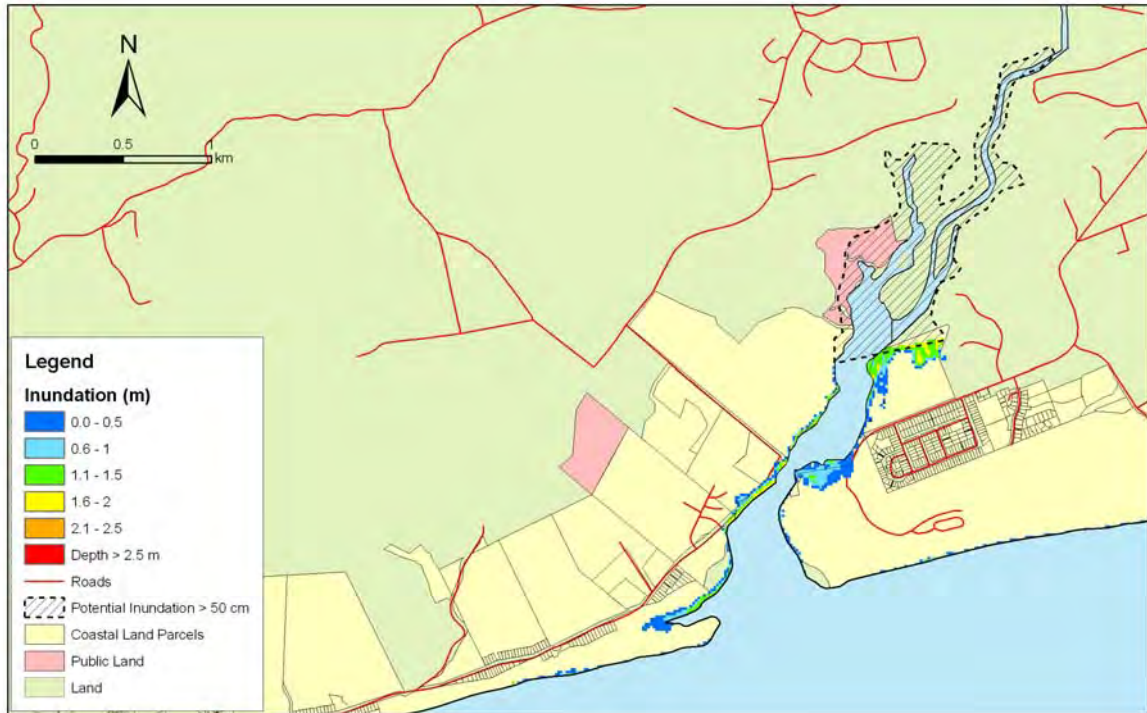


Figure 5.78: Kaikorai and Waldronville – 1:100 year remote tsunami: Maximum water depth for inundated land (top) and maximum speed (bottom) for MHWS with a sea level rise of 50 cm.

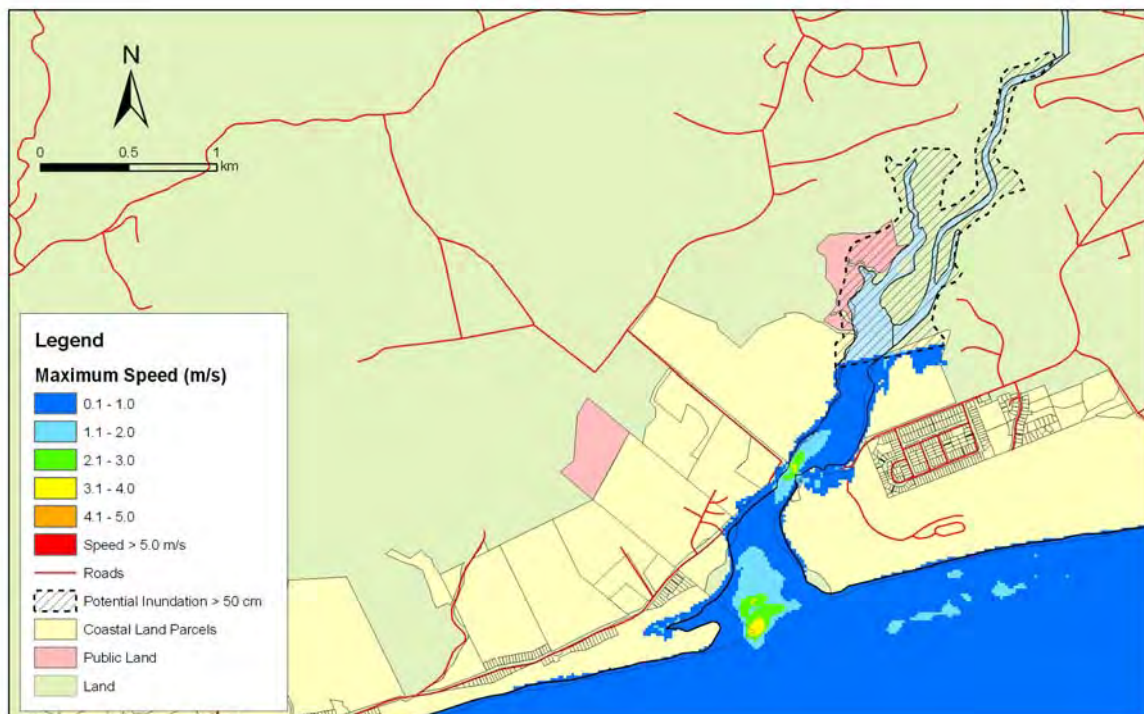
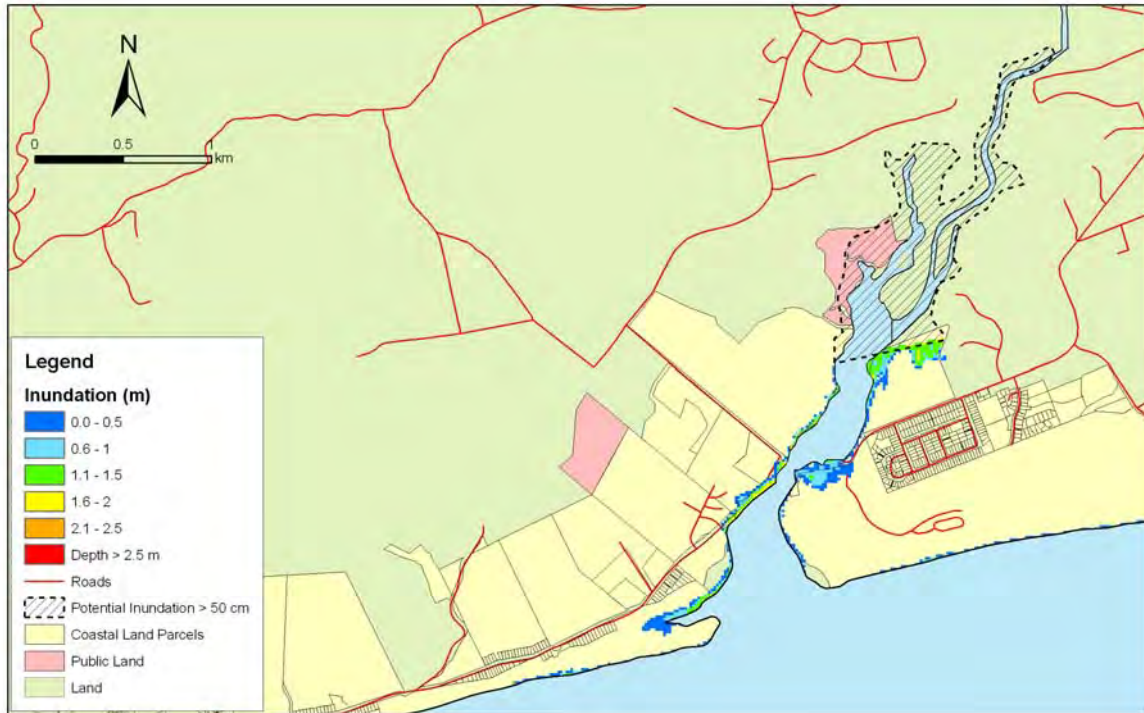


Figure 5.79: Kaikorai and Waldronville – 1:500 year remote tsunami: Maximum water depth for inundated land (top) and maximum speed (bottom) for MHWS.

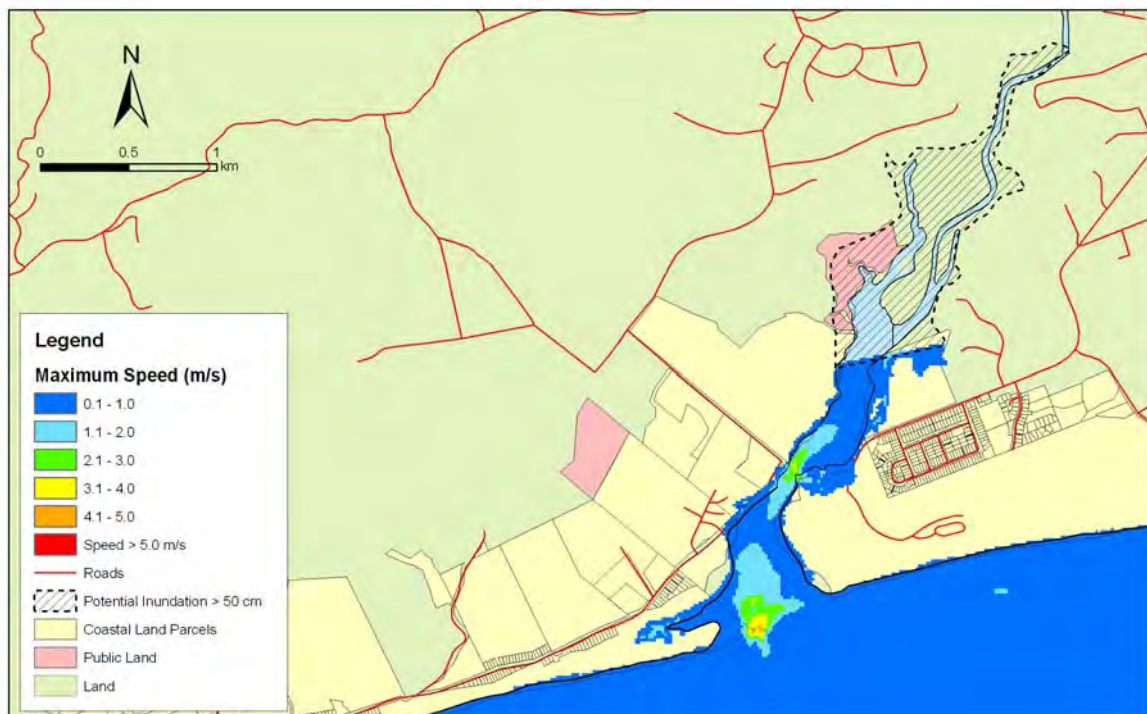
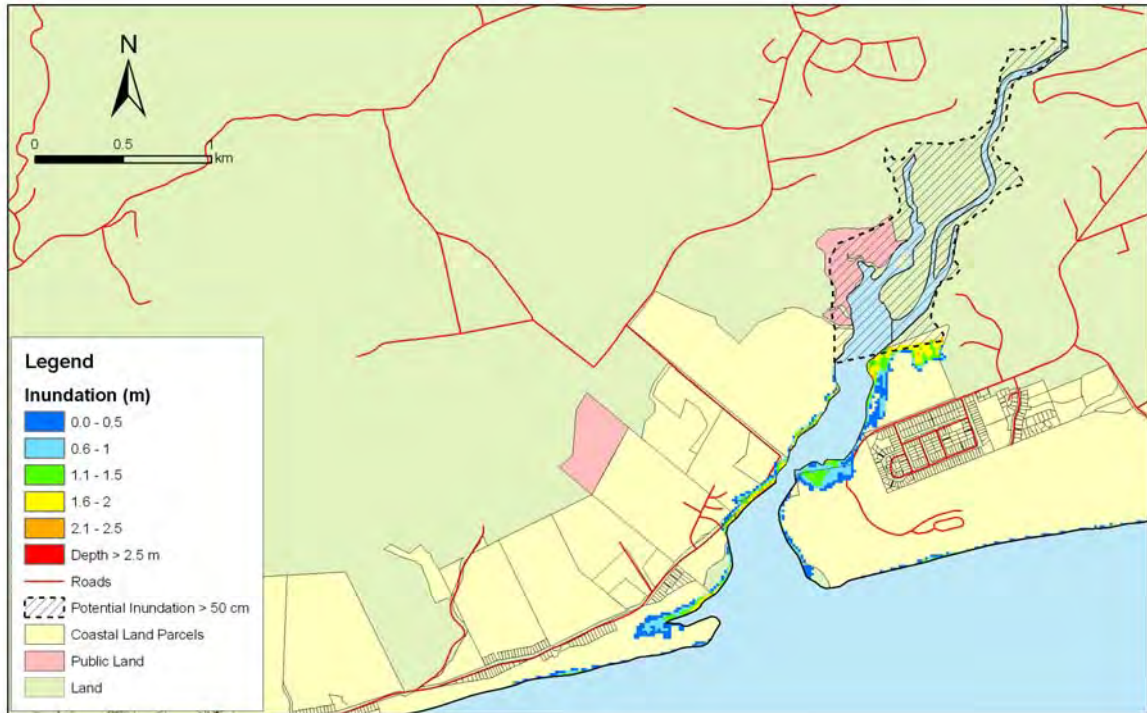


Figure 5.80: Kaikorai and Waldronville – 1:500 year remote tsunami: Maximum water depth for inundated land (top) and maximum speed (bottom) for MHWS with a sea level rise of 30 cm.

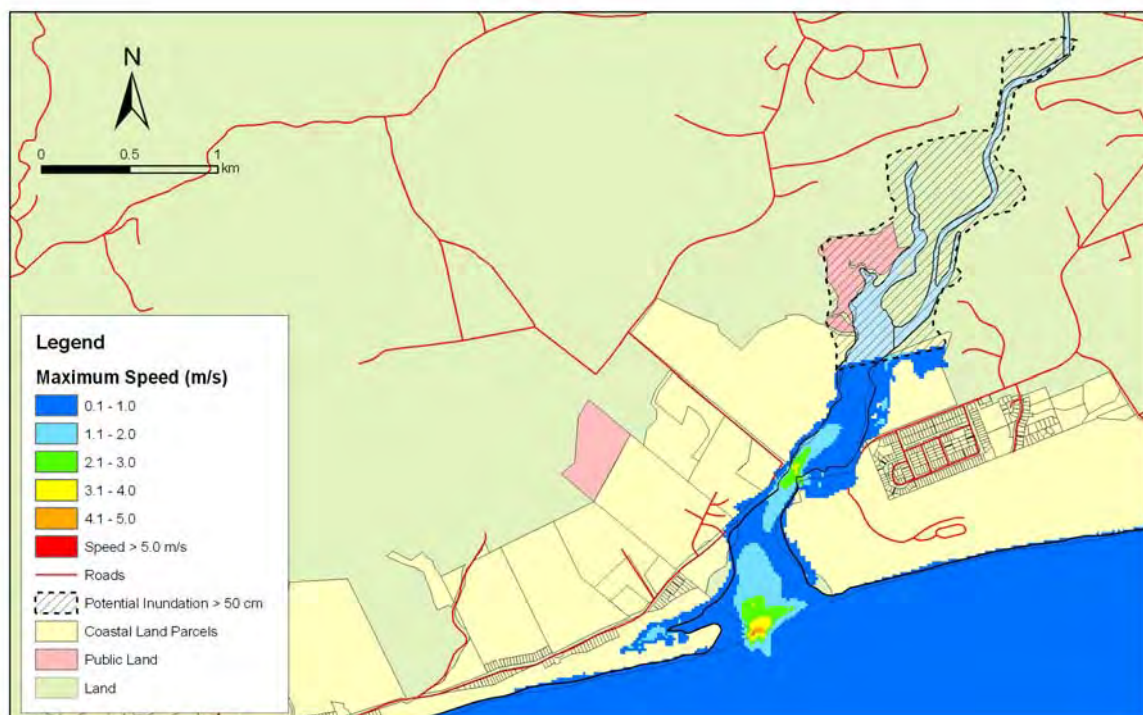
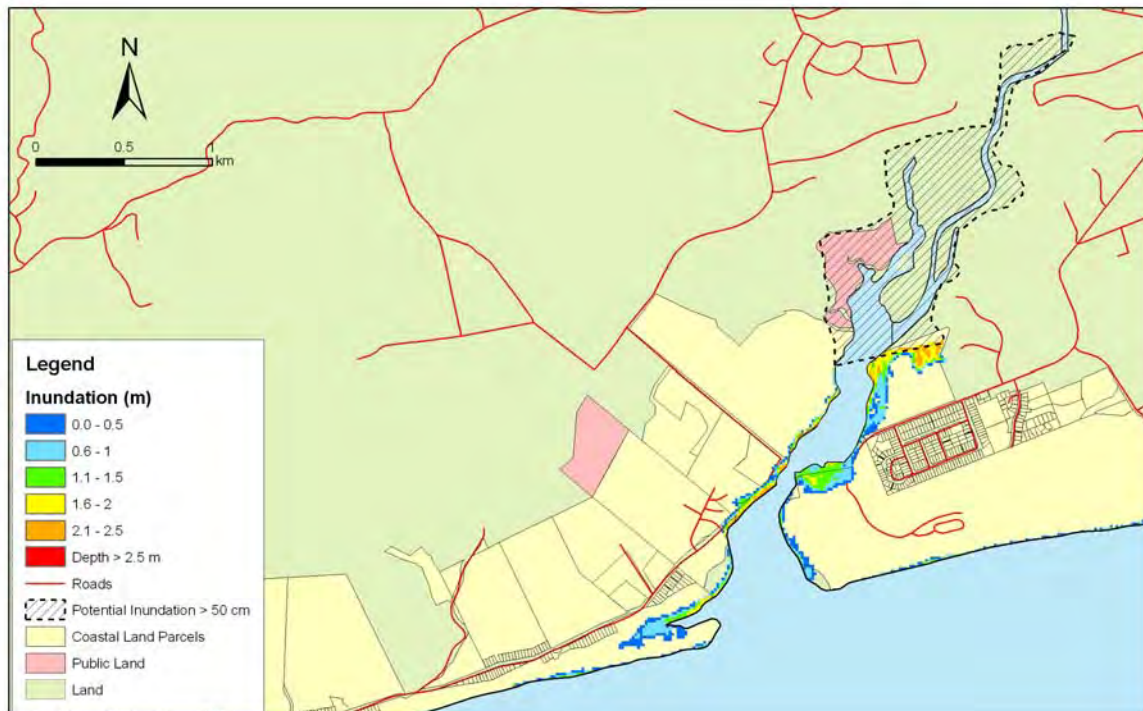


Figure 5.81: Kaikorai and Waldronville – 1:500 year remote tsunami: Maximum water depth for inundated land (top) and maximum speed (bottom) for MHWS with a sea level rise of 50 cm.

5.3.9 South Dunedin

It should be noted that the inundation scenarios for South Dunedin are based upon the 2004 LIDAR survey and therefore reflect the dune topography at that time. Dune systems such as those at South Dunedin are subject to change over time and caution should be observed in the interpretation of the inundation data.

Figures 5.82 – 5.84 show maximum inundation and water speed for the near-field (Puysegur) tsunami scenarios for this area. Figures 5.85-5.87 show maximum inundation and water speeds for the 1:100 year remote tsunami for South Dunedin. Figures 5.88-5.90 show maximum inundation and water speeds for the 1:500 year remote tsunami for South Dunedin.

South Dunedin: Near-Field

- Trough arrives first approximately 85 minutes after fault rupture. Water level decreases 45 cm over 40 minutes.
- First arrival is small (amplitude 0.4m at 2.2 hours after fault rupture), first main wave arrives about 15 minutes later with amplitude 1.7m.
- The second wave is biggest (amplitude 1.75m) and arrives 2.85 hours after fault rupture. There is one other wave with amplitude greater than 1.1m which arrives 7 hours after fault rupture.
- Predominant period of wave arrivals: 30 minutes.
- Maximum runup: up to 3 metres.
- Some inundation along the coastline.
- Maximum water speeds are relatively low indicating that the potential for serious erosion is also low.
- Sea level rise increases inundation level commensurately but does not significantly change the picture.

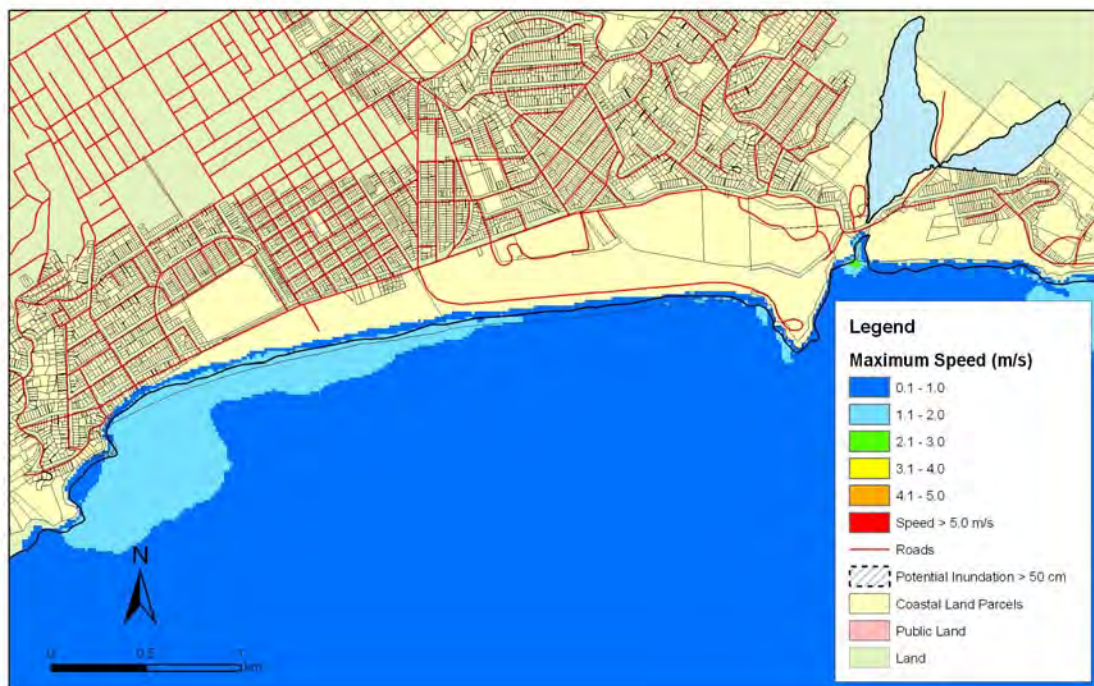


Figure 5.82: South Dunedin – Puysegur tsunami: Maximum water depth for inundated land (top) and maximum speed (bottom) for MHWS.

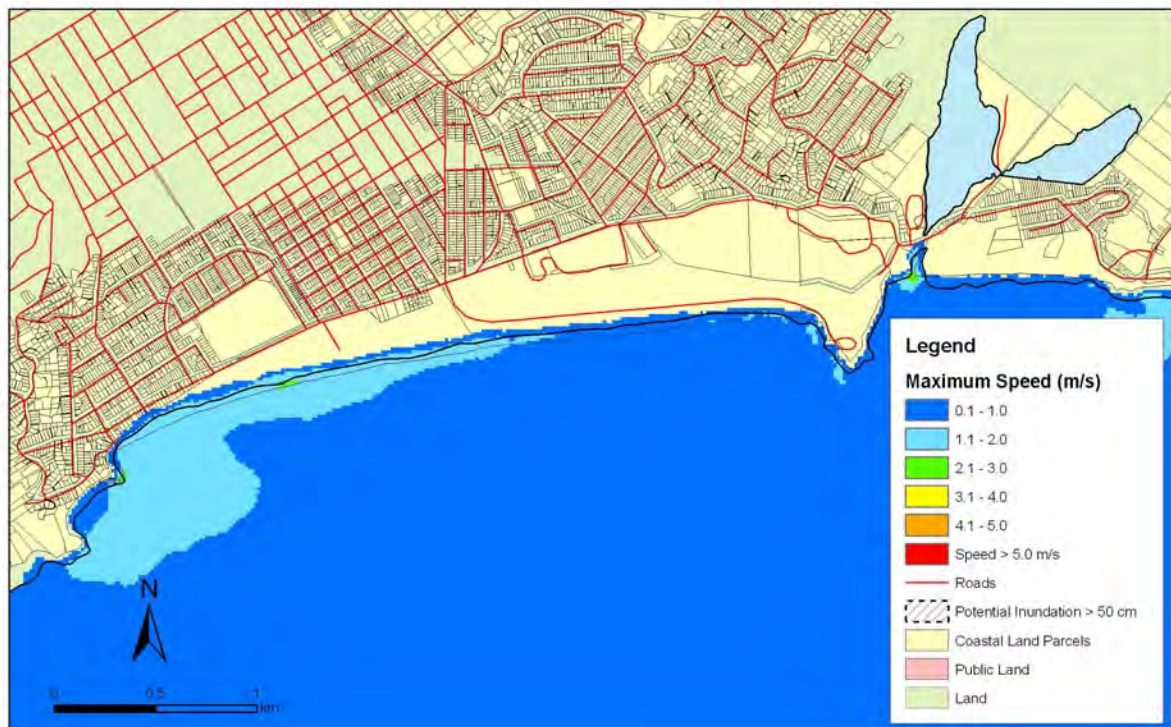
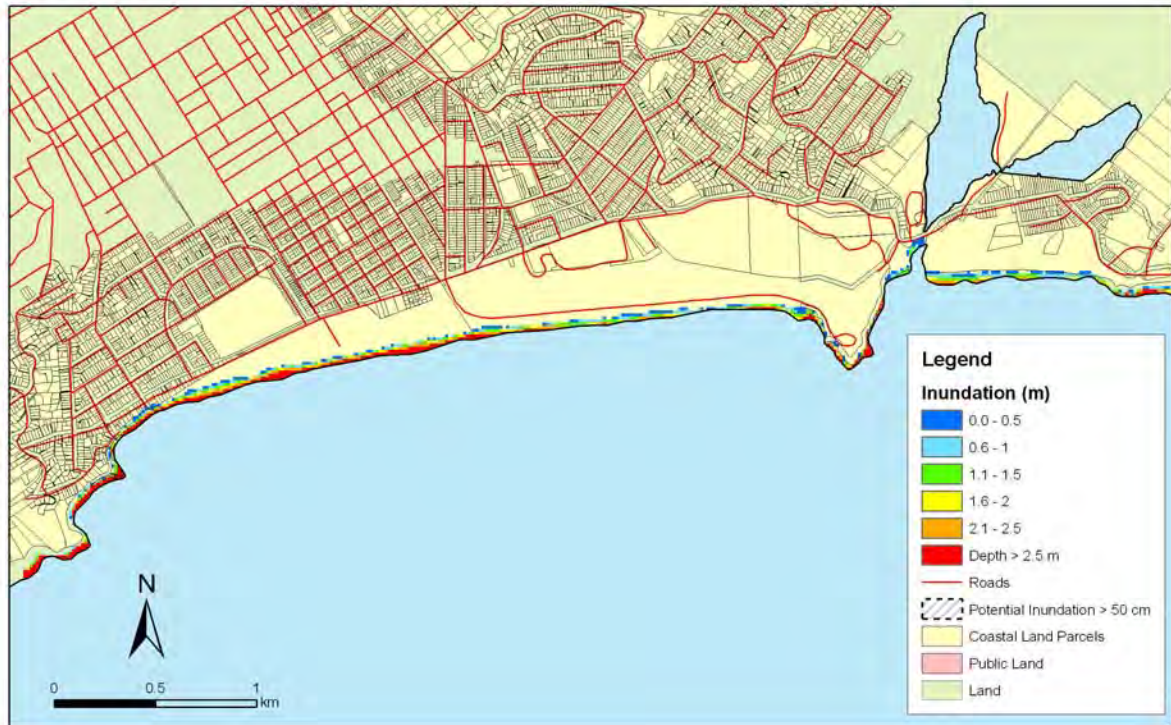


Figure 5.83: South Dunedin – Puysegur tsunami: Maximum water depth for inundated land (top) and maximum speed (bottom) for MHWS with a sea level rise of 30 cm.

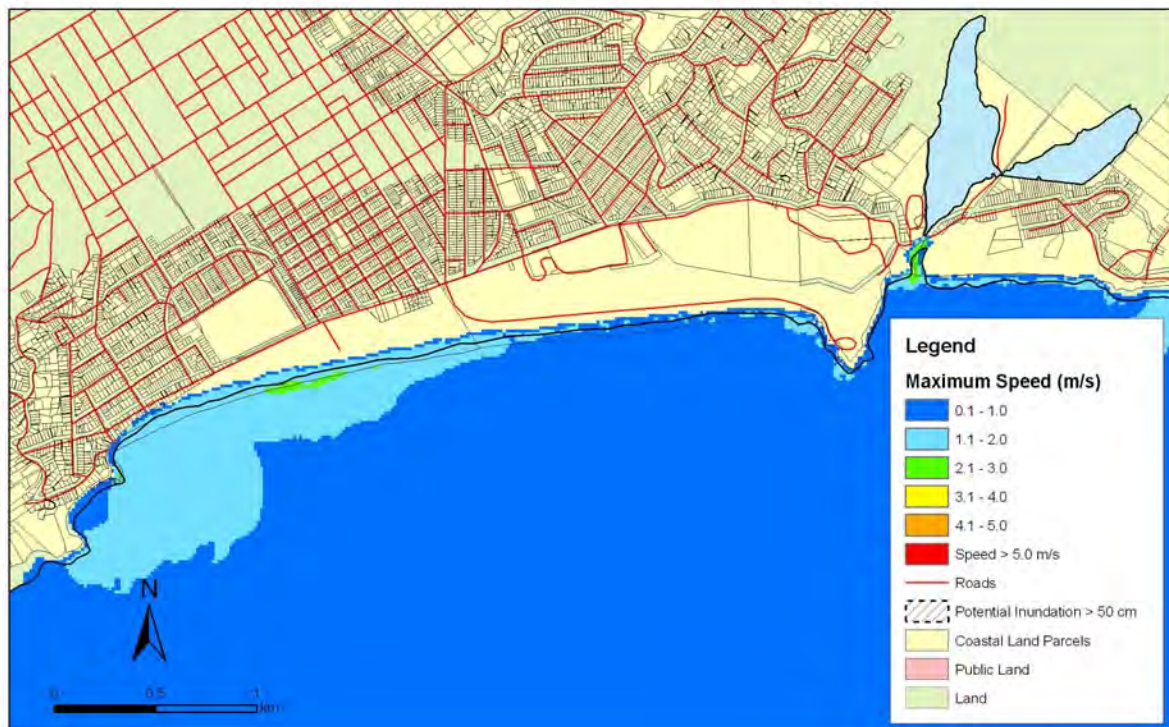


Figure 5.84: South Dunedin – Puysegur tsunami: Maximum water depth for inundated land (top) and maximum speed (bottom) for MHWS with a sea level rise of 50 cm.

South Dunedin: Far-Field

- Both remote tsunamis begin with an increase in the water level.
- Third wave is highest with amplitude 0.9m, trough to crest difference of 1.8m for the 1:100 year tsunami and amplitude 1.3m, total height 2.6m for the 1:500 year tsunami.
- Big waves for around 7 hours after first arrival then lots of smaller arrivals.
- Broad resonance period around 80-90 minutes, also 70 minutes.
- Maximum runup: up to 1.8 metres for 1:100 year tsunami and 2.3 metres for 1:500 year tsunami.
- Inundation confined to the coast.
- Maximum speeds are not high so there is not a big risk of erosion.

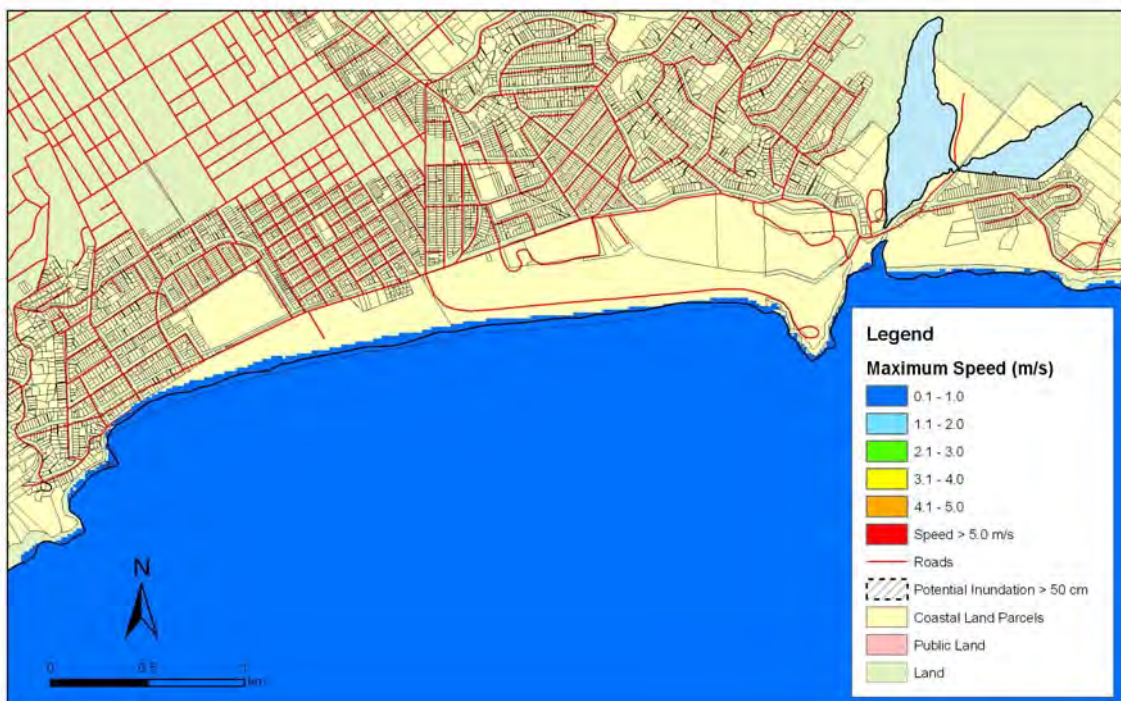
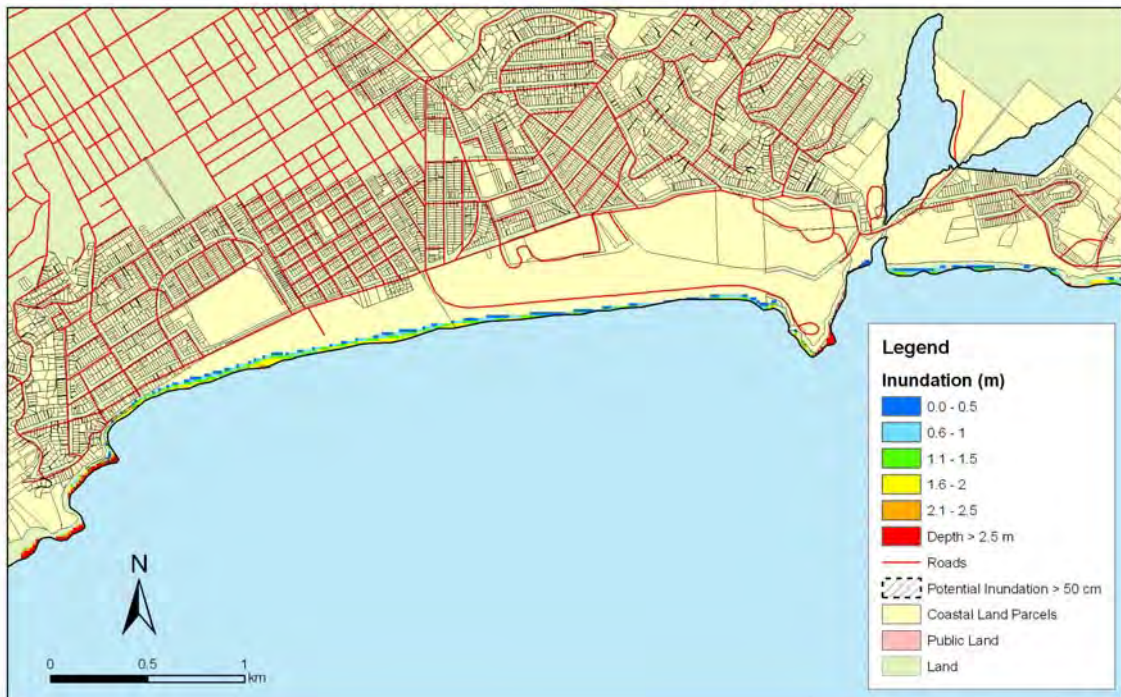


Figure 5.85: South Dunedin – 1:100 year remote tsunami: Maximum water depth for inundated land (top) and maximum speed (bottom) for MHWS.

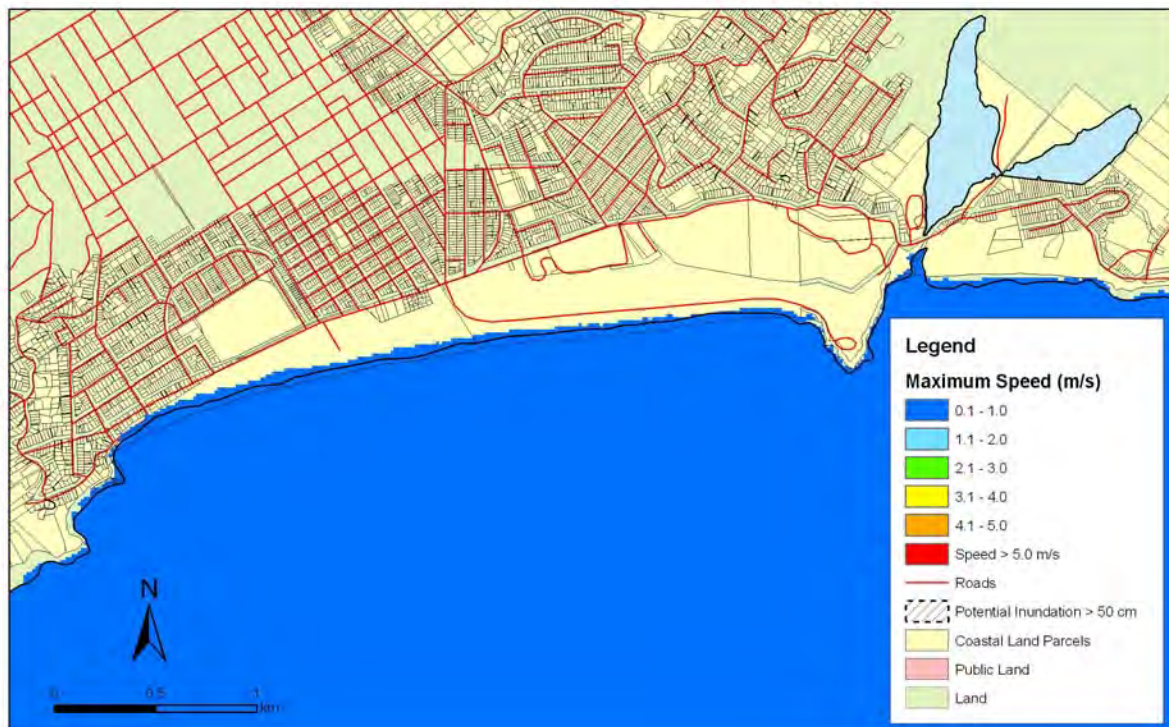


Figure 5.86: South Dunedin – 1:100 year remote tsunami: Maximum water depth for inundated land (top) and maximum speed (bottom) for MHWS with a sea level rise of 30 cm.

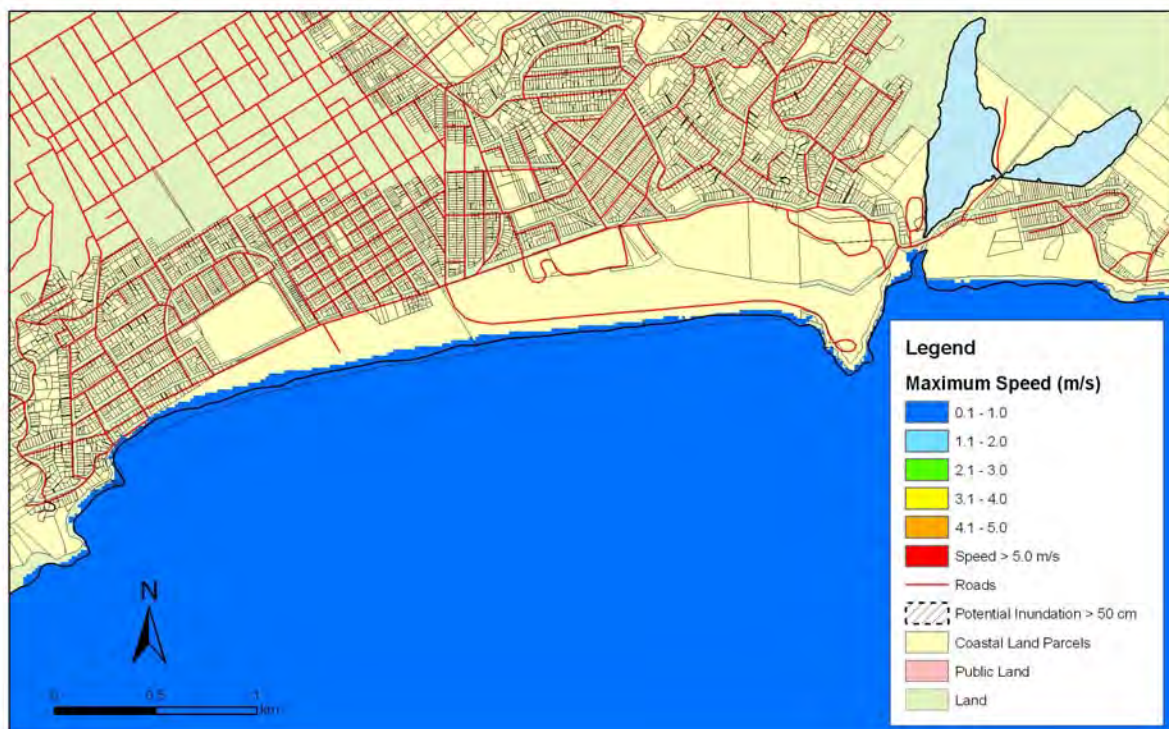


Figure 5.87: South Dunedin – 1:100 year remote tsunami: Maximum water depth for inundated land (top) and maximum speed (bottom) for MHWS with a sea level rise of 50 cm.

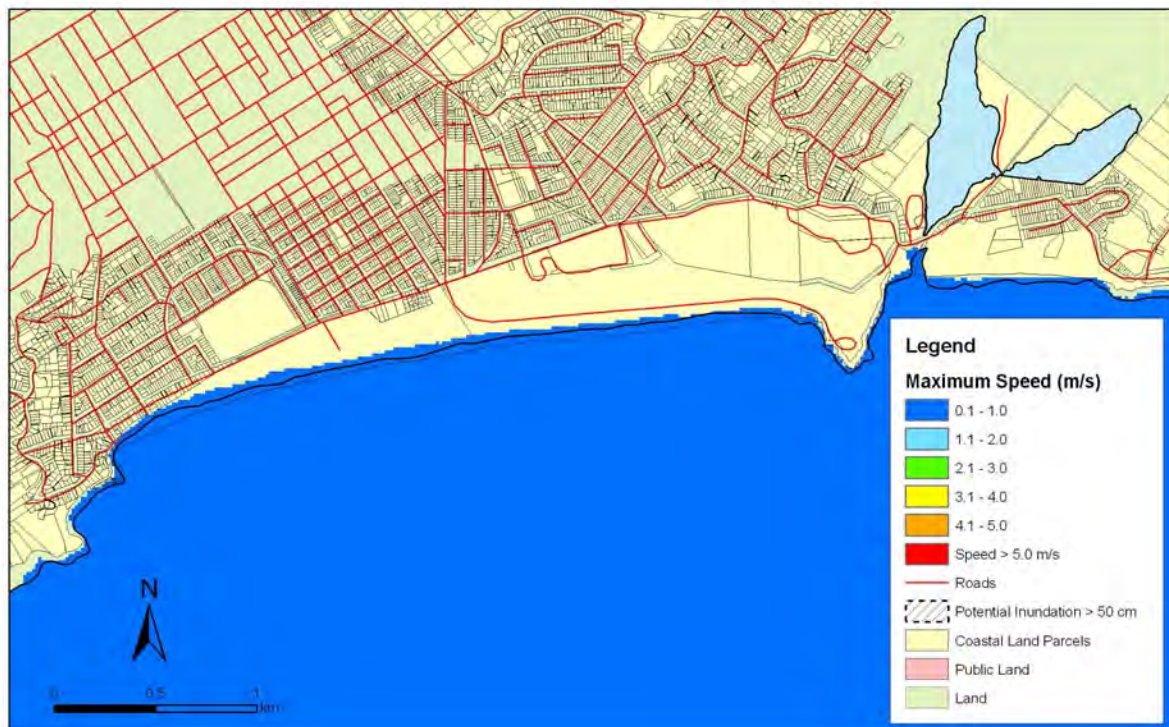


Figure 5.88: South Dunedin – 1:500 year remote tsunami: Maximum water depth for inundated land (top) and maximum speed (bottom) for MHWS.

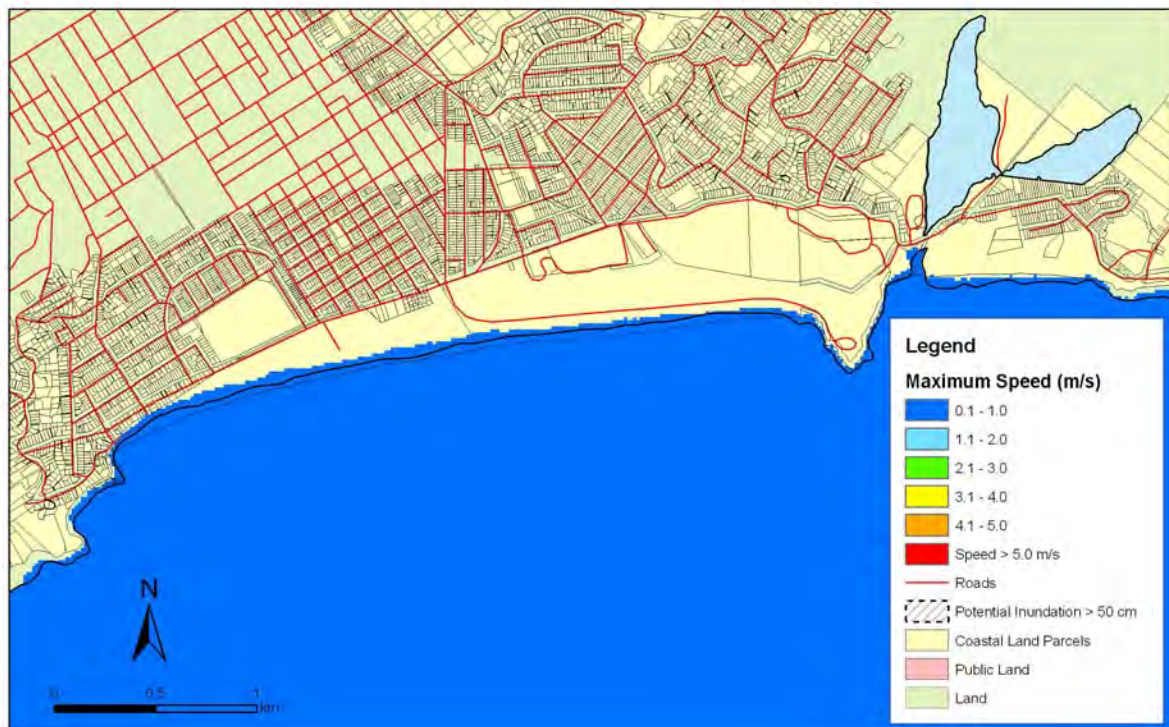


Figure 5.89: South Dunedin – 1:500 year remote tsunami: Maximum water depth for inundated land (top) and maximum speed (bottom) for MHWS with a sea level rise of 30 cm.

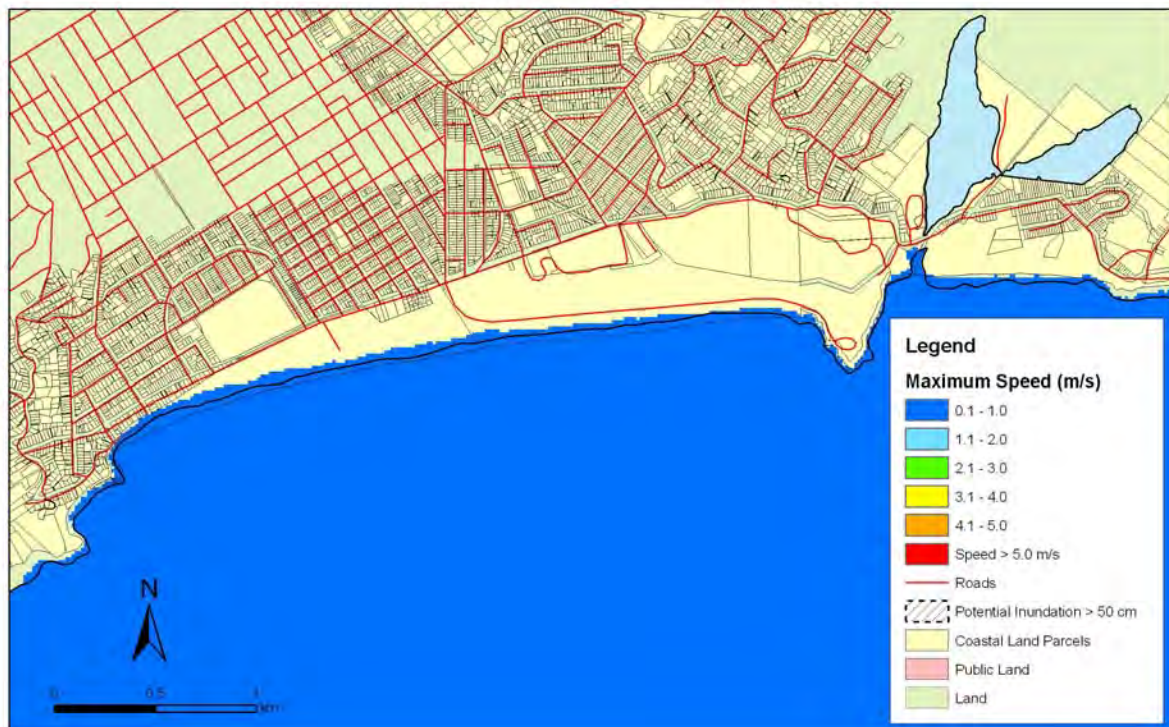
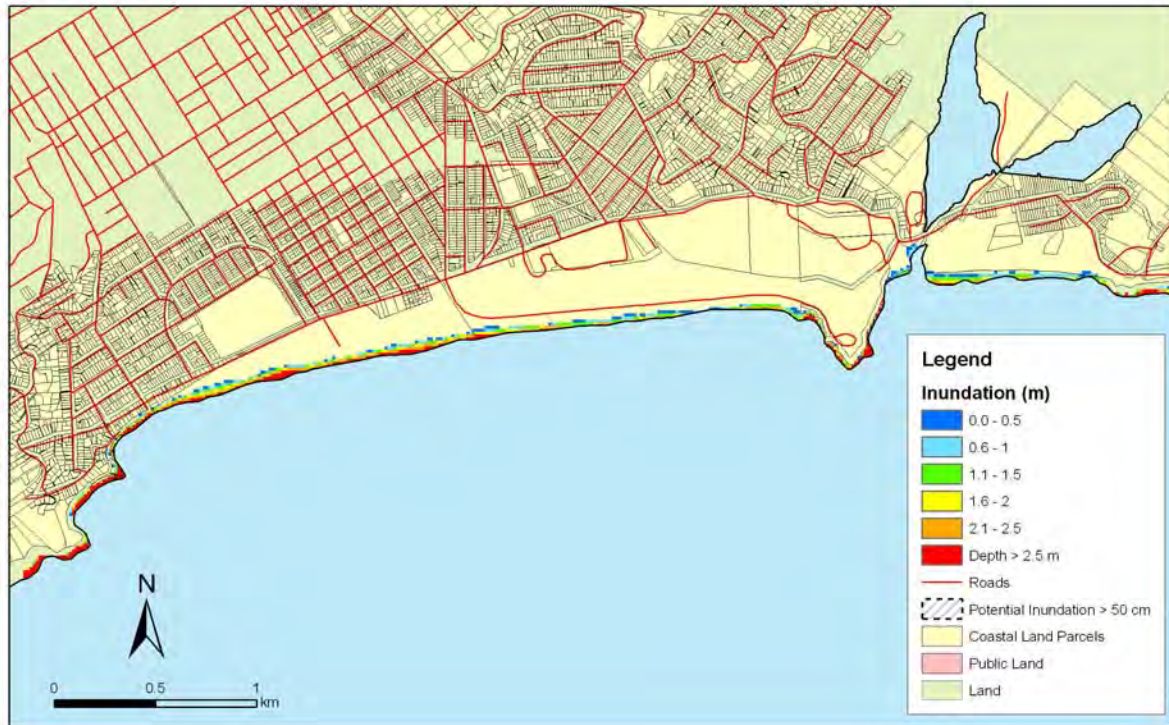


Figure 5.90: South Dunedin – 1:500 year remote tsunami: Maximum water depth for inundated land (top) and maximum speed (bottom) for MHWS with a sea level rise of 50 cm.

5.3.10 Dunedin Harbour

Based upon historical data (e.g. De Lange and Healy, 1986) and the geomorphological and bathymetric setting of the harbour, inundation here will be minimal.

Figures 5.91 – 5.93 show maximum inundation and water speed for the near-field (Puysegur) tsunami scenarios for this area. Figures 5.94-5.96 show maximum inundation and water speeds for the 1:100 year remote tsunami for Dunedin Harbour. Figures 5.97-5.99 show maximum inundation and water speeds for the 1:500 year remote tsunami for Dunedin Harbour.

Dunedin Harbour: Near-Field

- Trough arrives first approximately 2.6 hours after fault rupture. Water level decreases over one hour.
- Total disturbance is less than +/- 15 cm. Predominant period of wave arrivals: 1.5 hours.
- The effects of the tsunami in upper Dunedin harbour will be less than can occur due to normal tidal and atmospheric forcing. This is also true in the case of a rise in sea level.

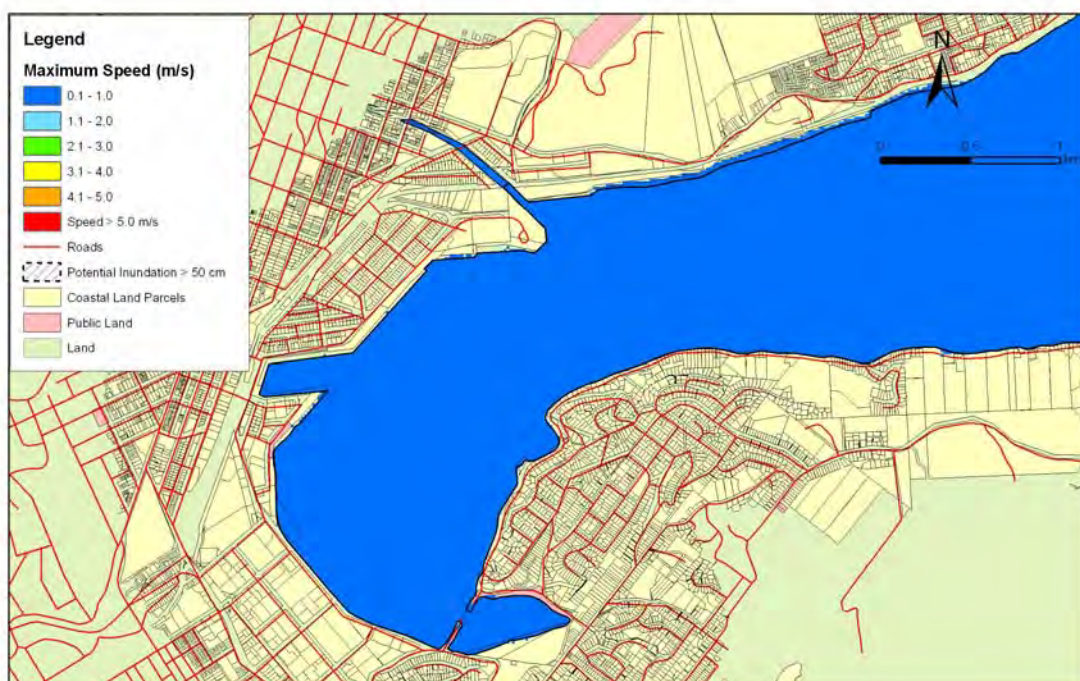
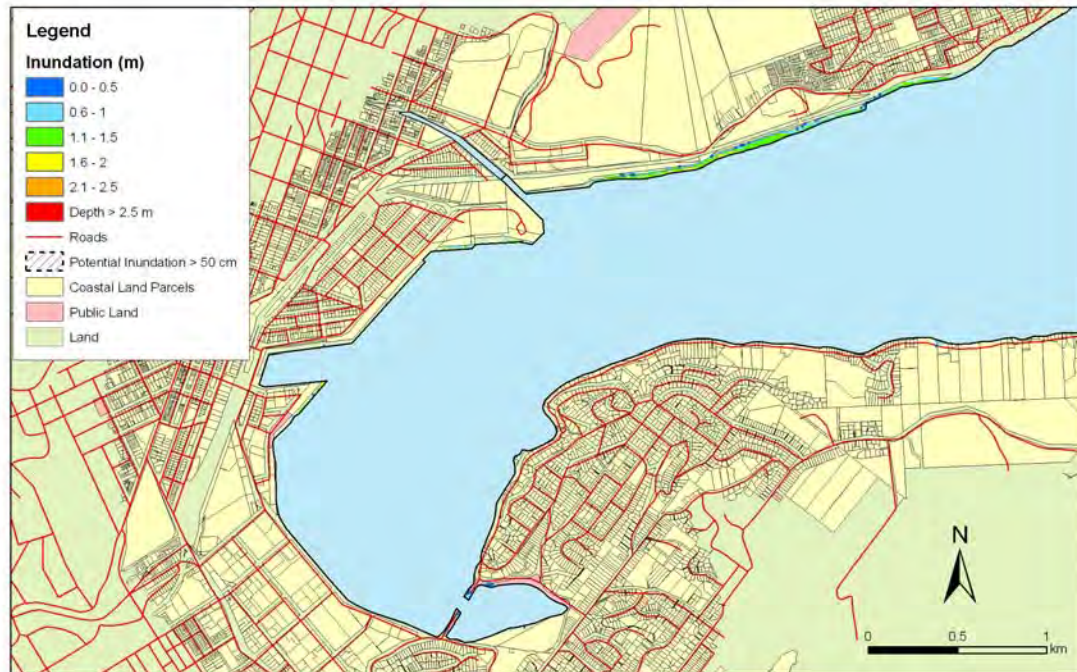


Figure 5.91: Dunedin Harbour – Puysegur tsunami: Maximum water depth for inundated land (top) and maximum speed (bottom) for MHWS.

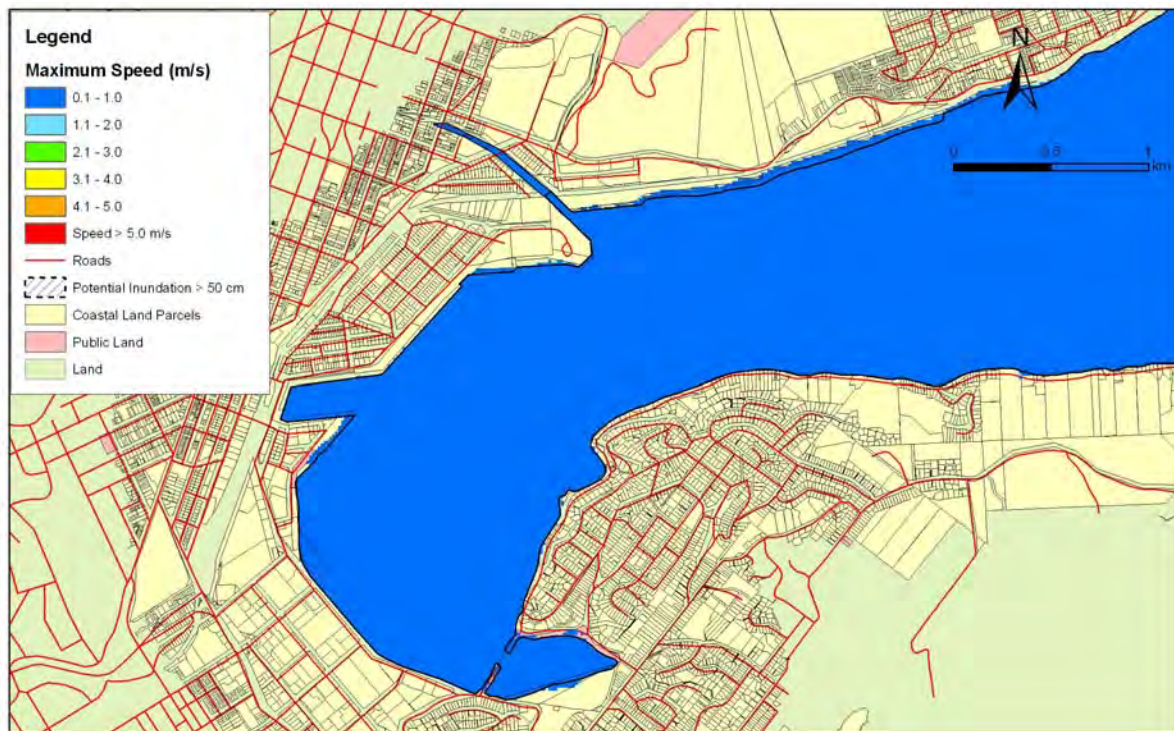
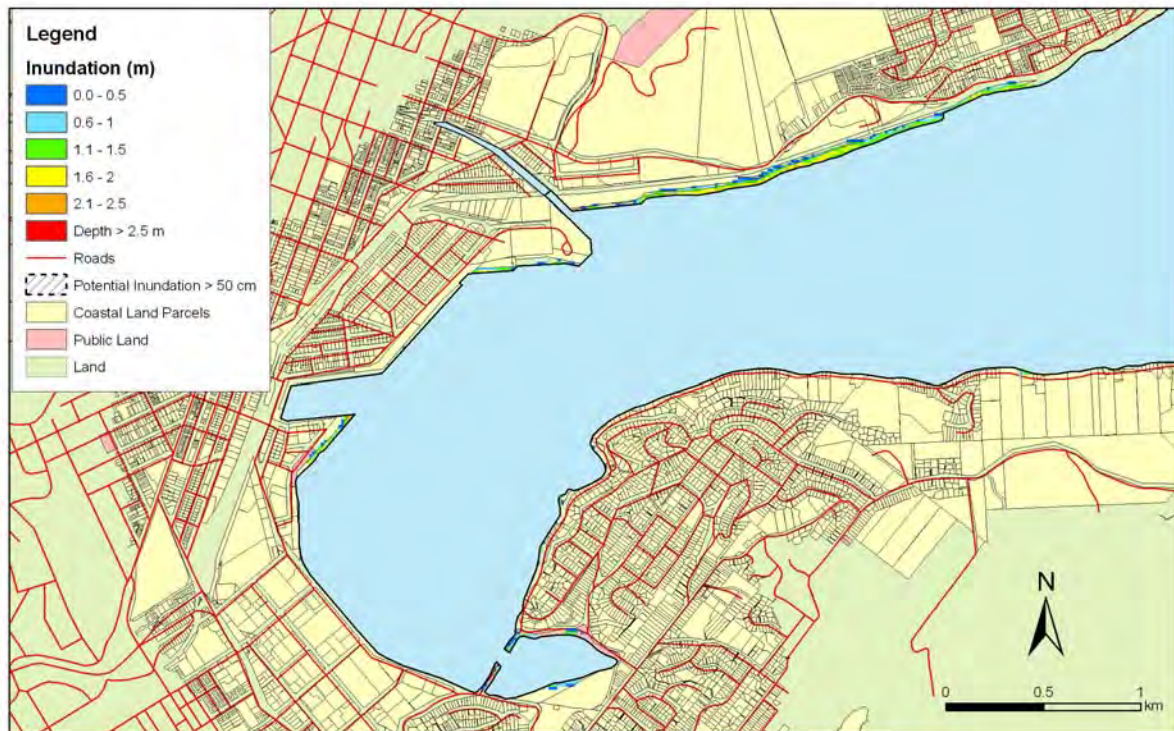


Figure 5.92: Dunedin Harbour – Puysegur tsunami: Maximum water depth for inundated land (top) and maximum speed (bottom) for MHWS with a sea level rise of 30 cm.

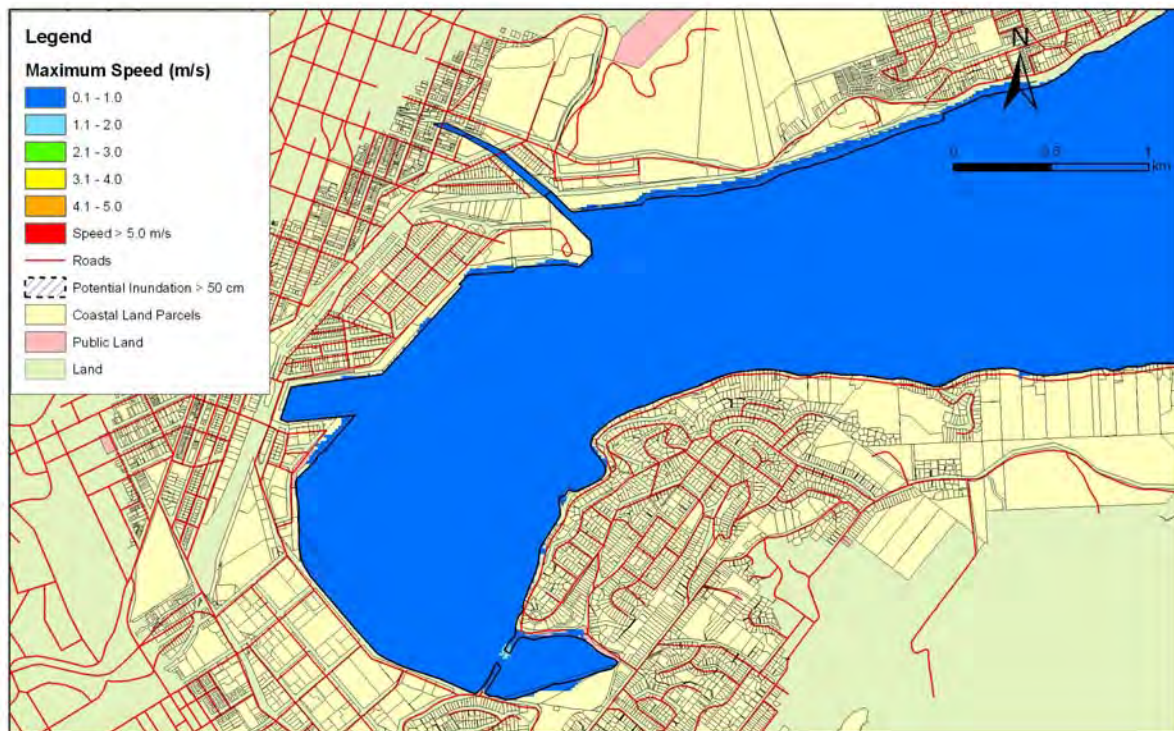
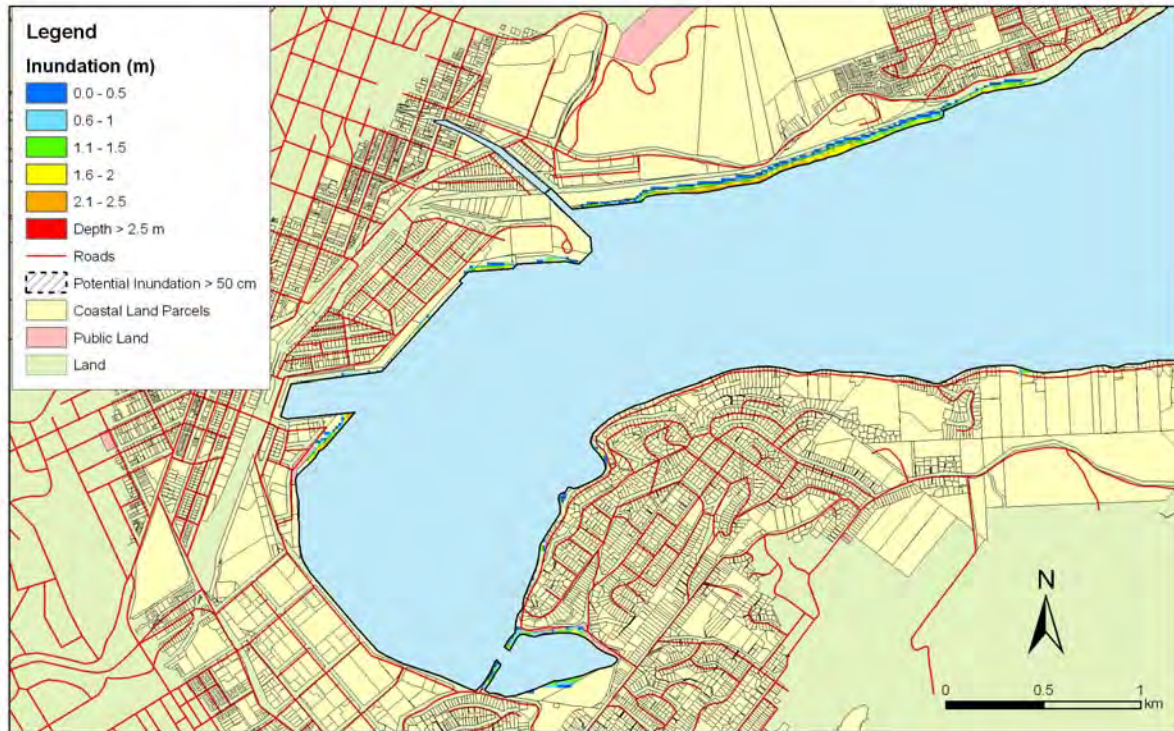


Figure 5.93: Dunedin Harbour – Puysegur tsunami: Maximum water depth for inundated land (top) and maximum speed (bottom) for MHWS with a sea level rise of 50 cm.

Dunedin Harbour: Far-Field

- First arrival in upper Dunedin harbour about 40 minutes after arrivals at exposed coast.
- Only small disturbances, maximum amplitude 30 cm (50 cm for 1:500 year tsunami). There is not expected to be any significant runup or inundation above what occurs regularly as normal water level fluctuations due to tidal and atmospheric forcing.
- Resonance period around 105 minutes.

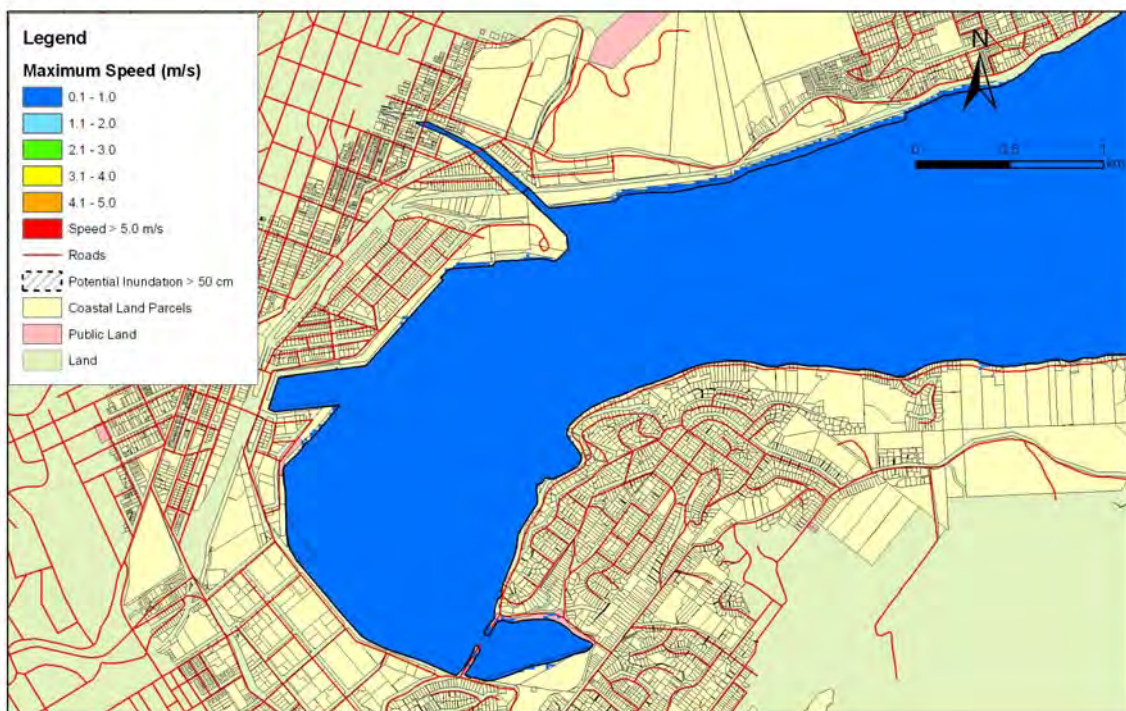
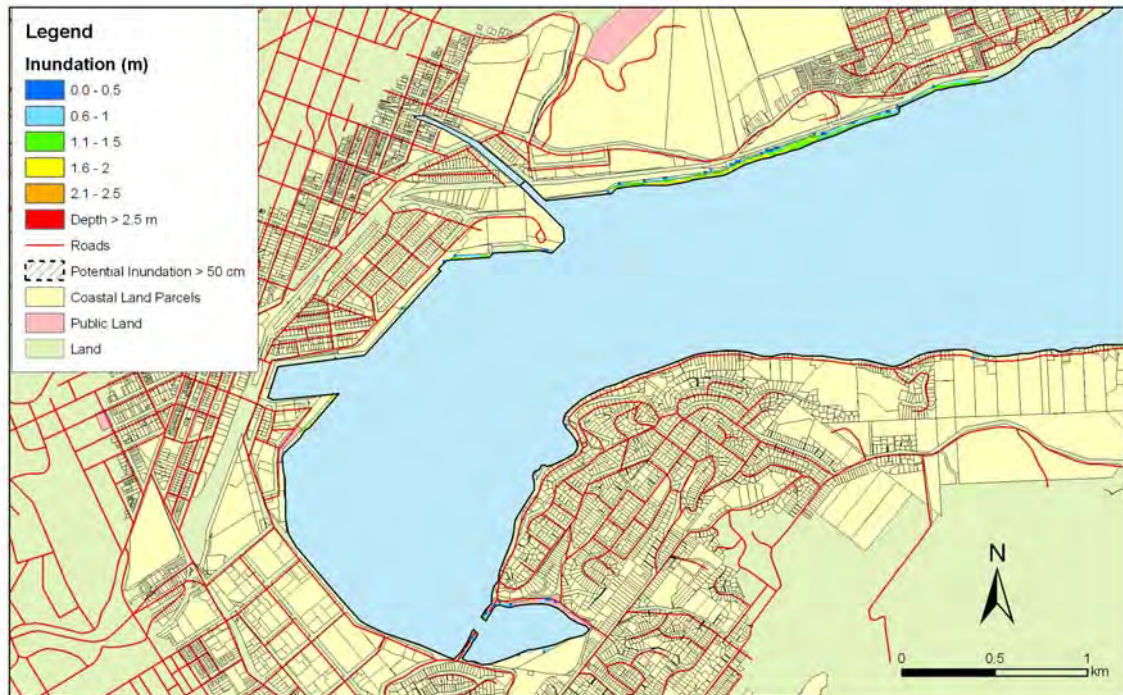


Figure 5.94: Dunedin Harbour – 1:100 year remote tsunami: Maximum water depth for inundated land (top) and maximum speed (bottom) for MHWS.

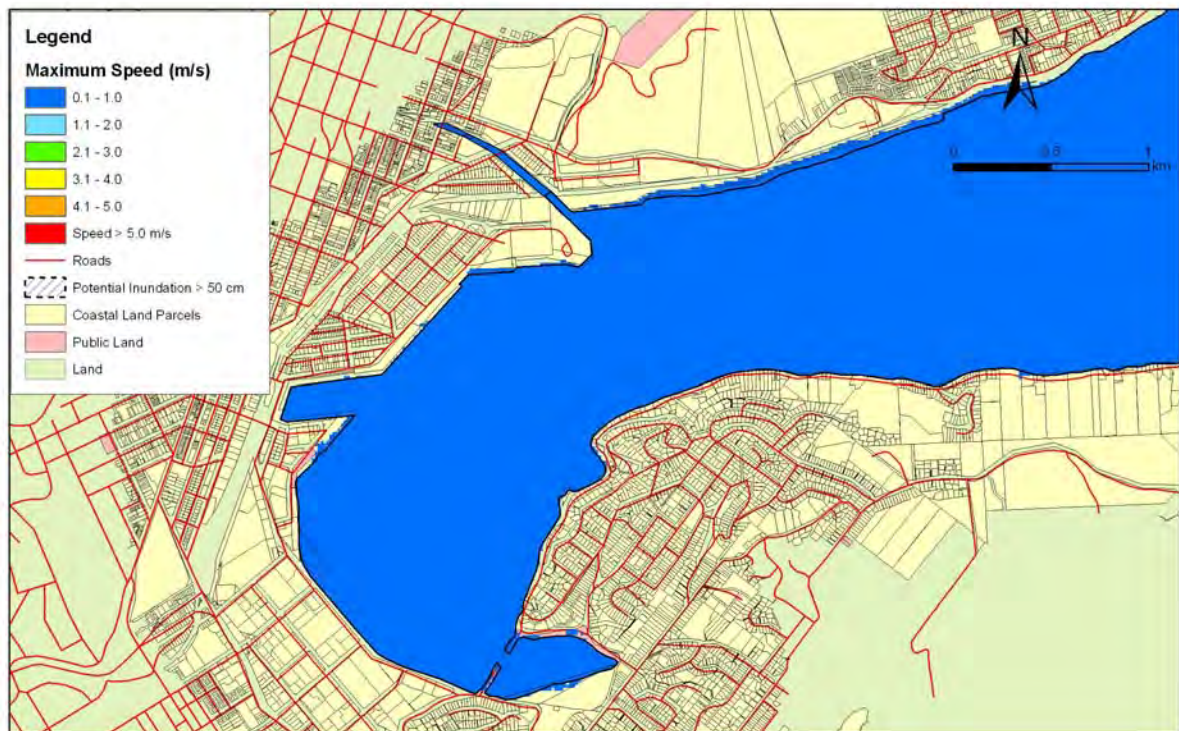
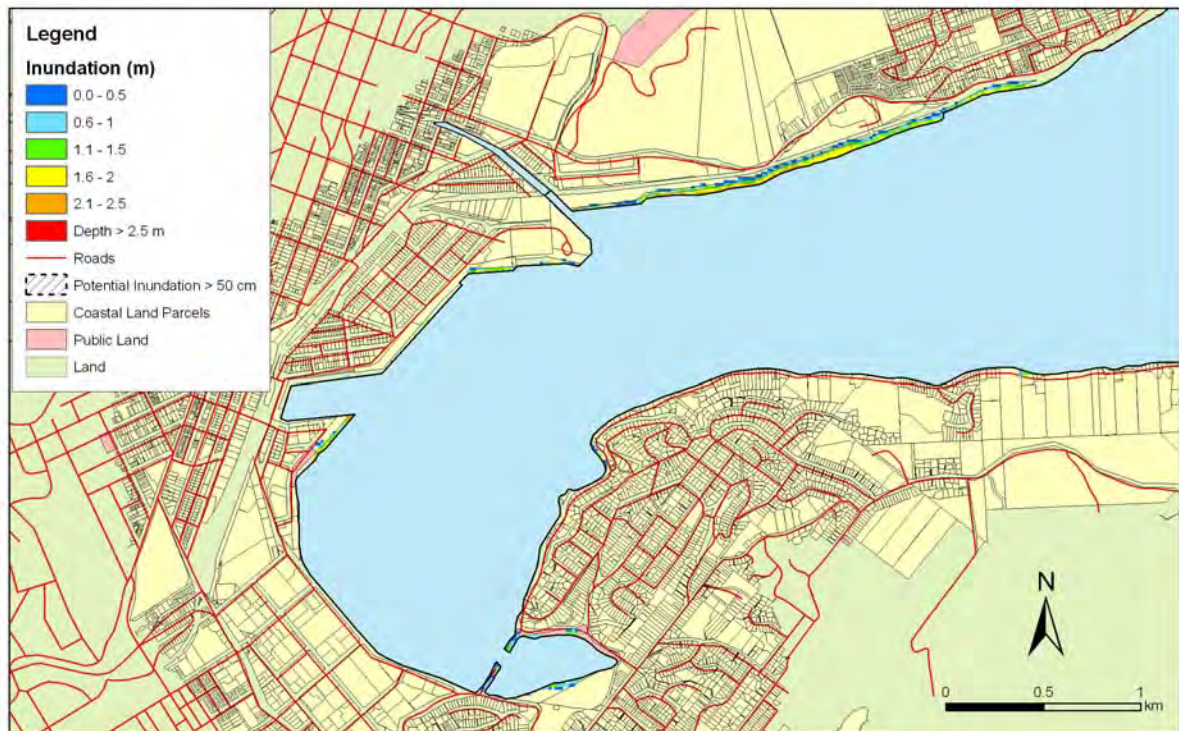


Figure 5.95: Dunedin Harbour – 1:100 year remote tsunami: Maximum water depth for inundated land (top) and maximum speed (bottom) for MHWS with a sea level rise of 30 cm.

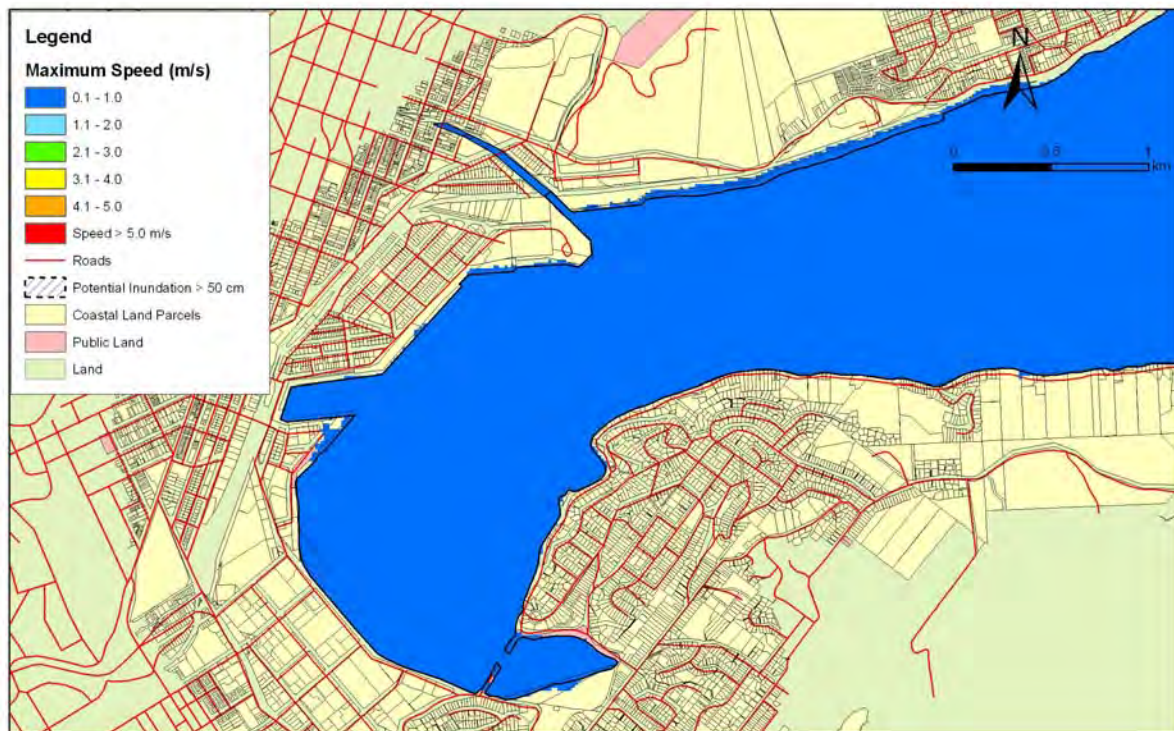
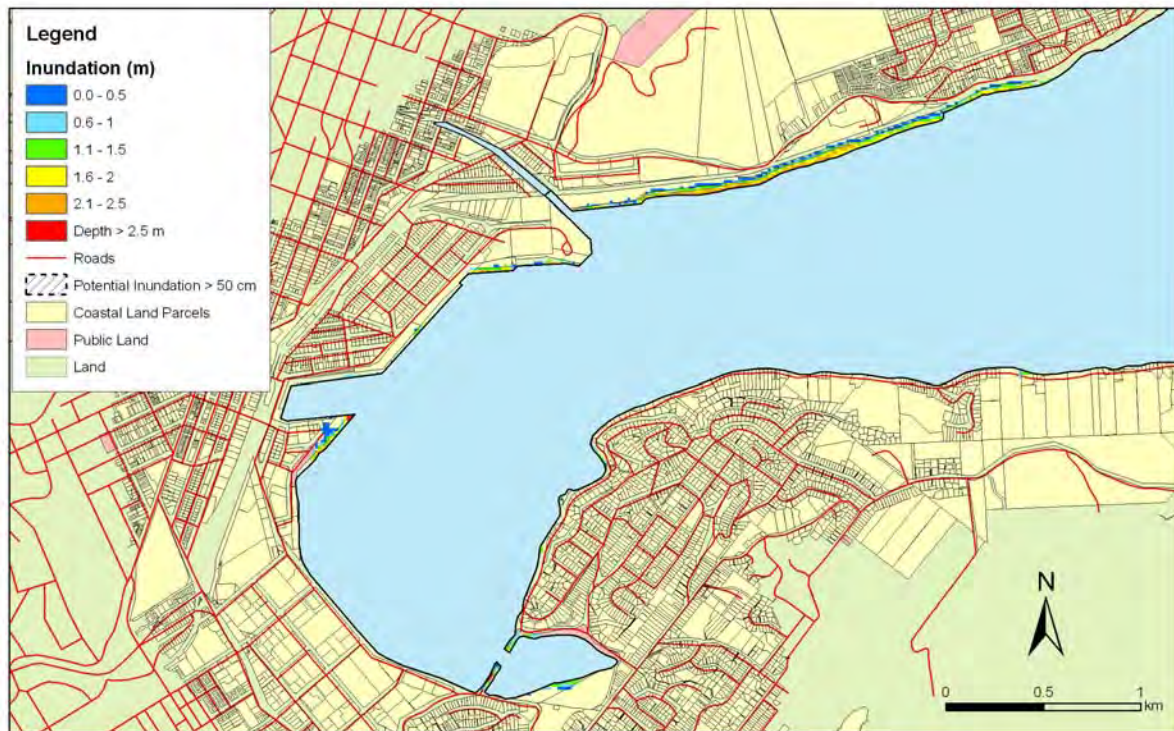


Figure 5.96: Dunedin Harbour – 1:100 year remote tsunami: Maximum water depth for inundated land (top) and maximum speed (bottom) for MHWS with a sea level rise of 50 cm.

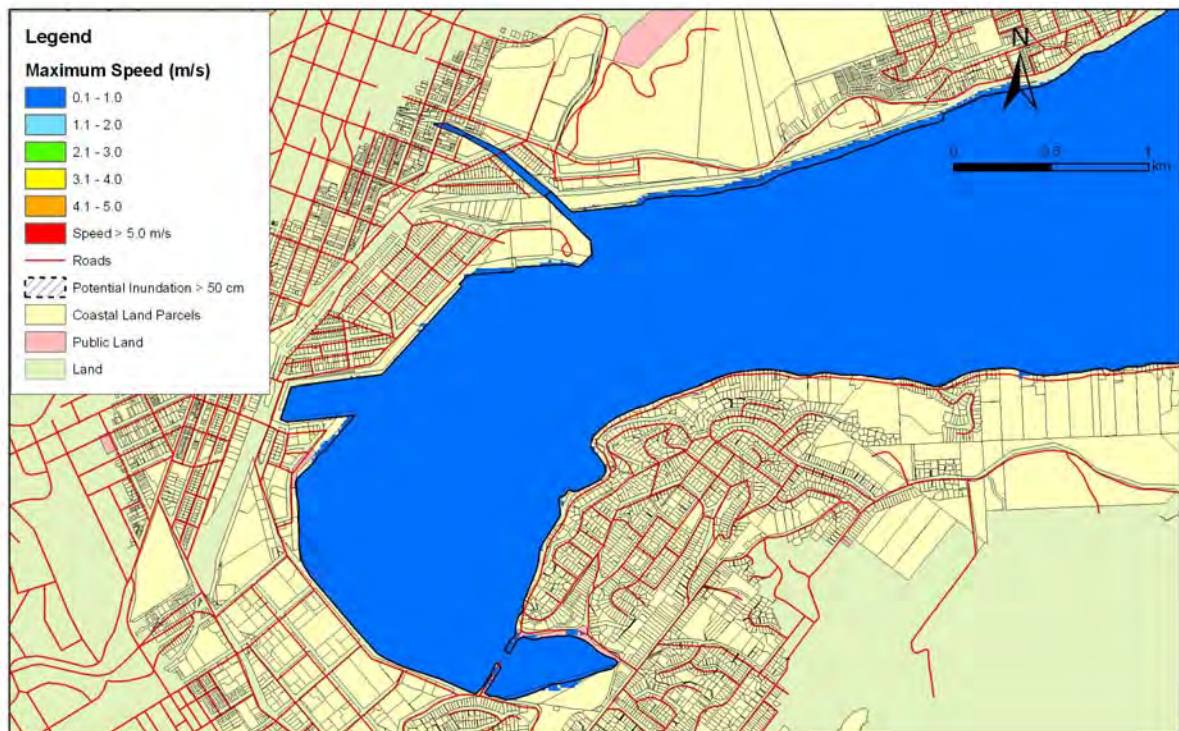
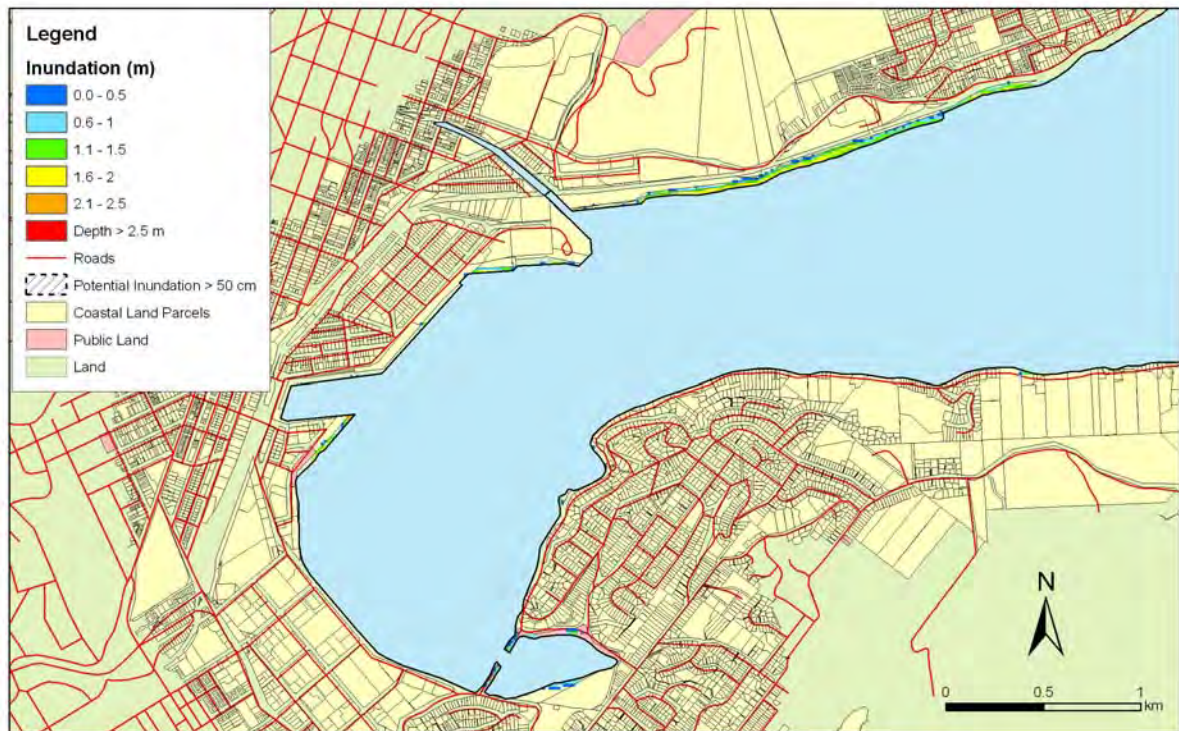


Figure 5.97: Dunedin Harbour – 1:500 year remote tsunami: Maximum water depth for inundated land (top) and maximum speed (bottom) for MHWS.

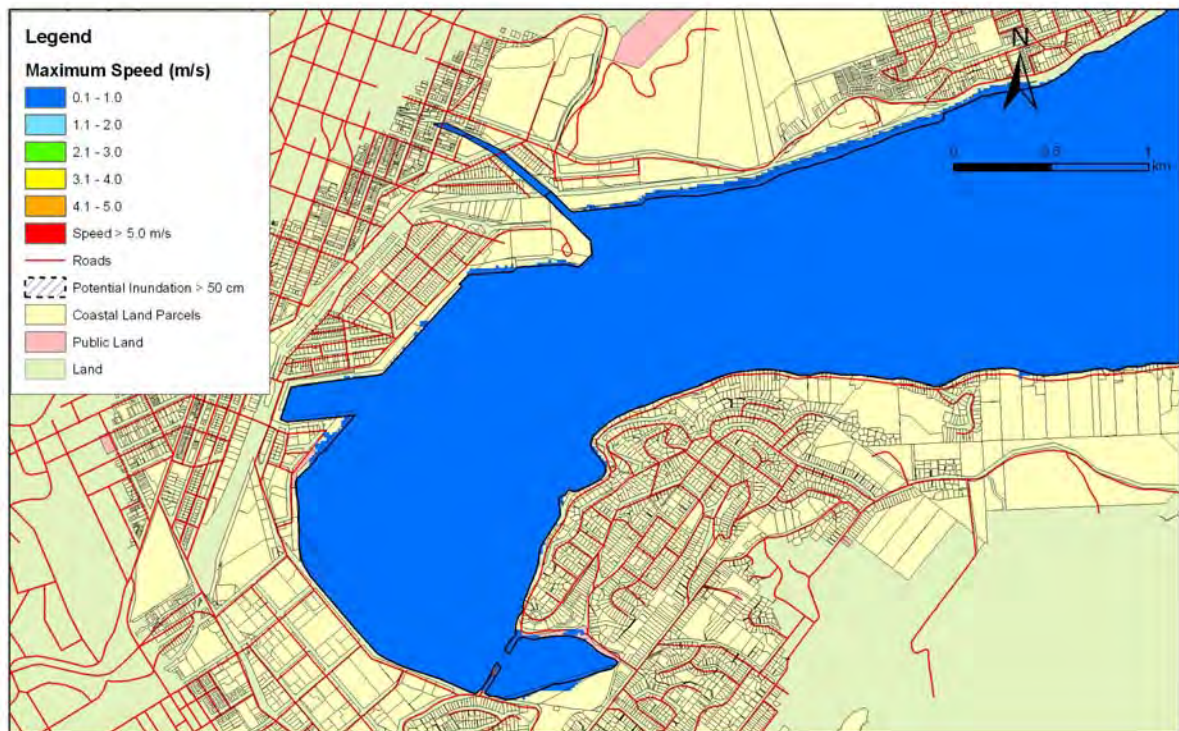
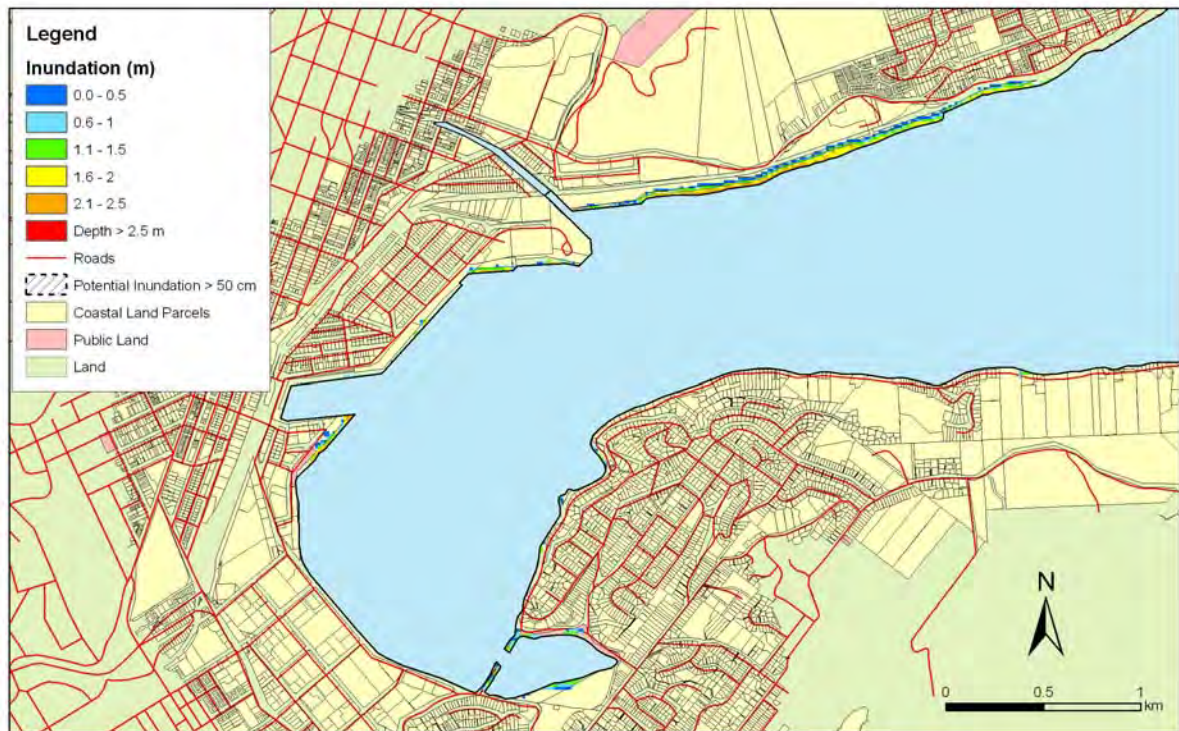


Figure 5.98: Dunedin Harbour – 1:500 year remote tsunami: Maximum water depth for inundated land (top) and maximum speed (bottom) for MHWS with a sea level rise of 30 cm.

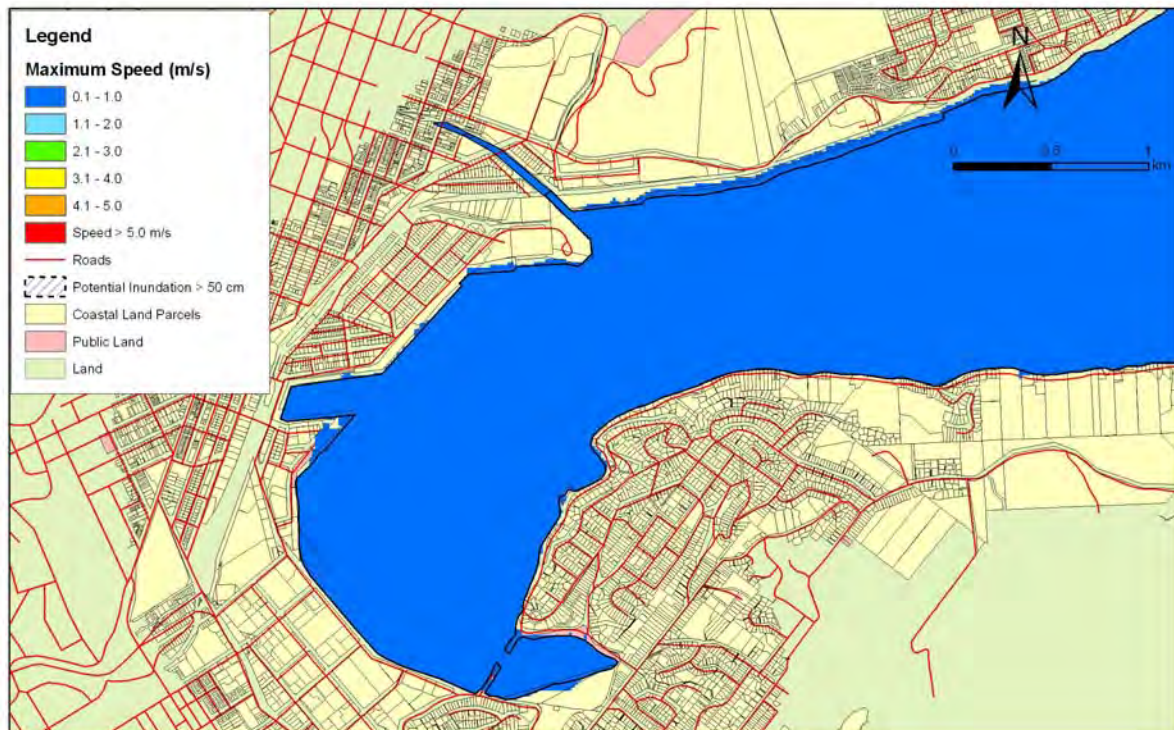
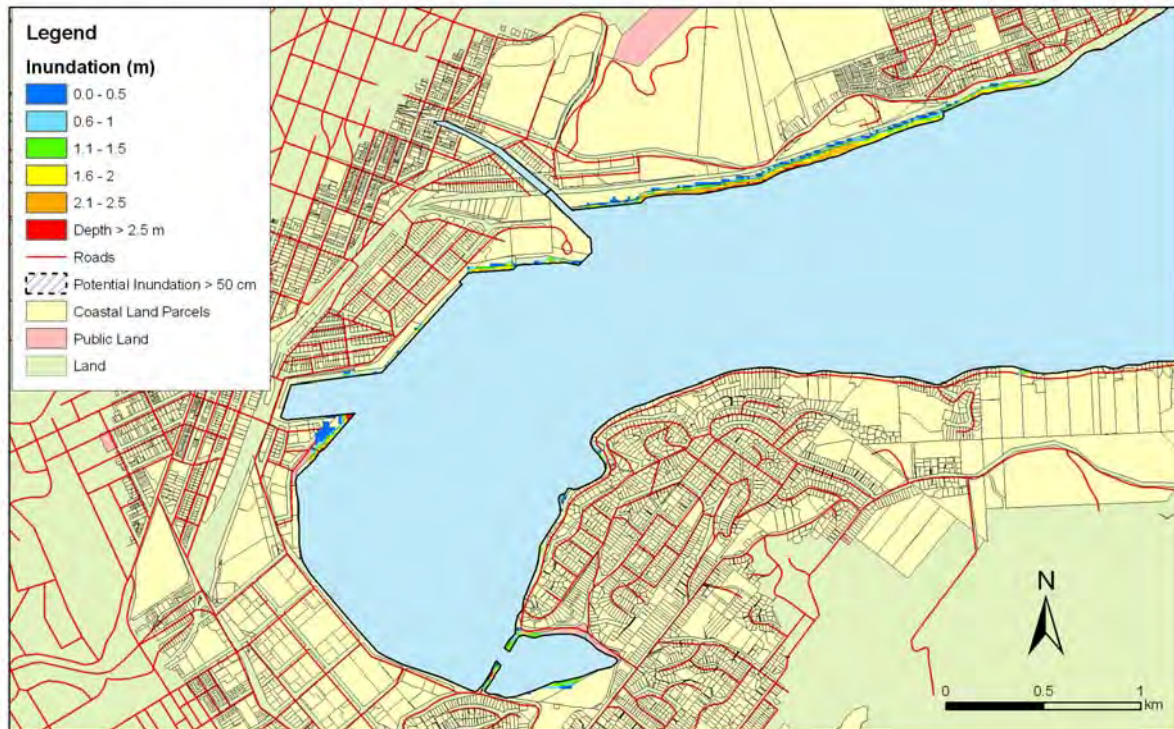


Figure 5.99: Dunedin Harbour – 1:500 year remote tsunami: Maximum water depth for inundated land (top) and maximum speed (bottom) for MHWS with a sea level rise of 50 cm.

5.3.11 Long Beach and Purakanui

Figures 5.100 – 5.102 show maximum inundation and water speed for the near-field (Puysegur) tsunami scenarios for this area. Figures 5.103-5.105 show maximum inundation and water speeds for the 1:100 year remote tsunami for Long Beach and Purakanui. Figures 5.106-5.108 show maximum inundation and water speeds for the 1:500 year remote tsunami for Long Beach and Purakanui.

Long Beach and Purakanui: Near-Field

- There is considerable difference between the wave arrivals at Long Beach and Purakanui, Purakanui being more similar to Warrington and Blueskin Bay.
- Trough arrives first approximately 85-95 minutes after fault rupture. Water level decreases 35 cm over 40 minutes.
- There is a small first arrival (amplitude 45 cm) at Long Beach but this is subsumed in the first main wave arrival at Purakanui. The first main wave has amplitude 1.05 m at Long Beach (2.6 hours after fault rupture) and 1.3 m at Purakanui (2.8 hours after fault rupture).
- There is one other wave with amplitude over 1 m which arrives at Long Beach 3.8 hours after fault rupture and 4 hours after fault rupture at Purakanui.
- Predominant period of wave arrivals: Long Beach 20 and 85 minutes. Purakanui 30 and 40 minutes.
- Maximum runup: up to 2 metres on Long Beach and mouth to Purakanui inlet. slightly higher towards Mapoutahi.
- Some inundation at the south end of Long Beach and in Purakanui inlet, especially on the north side for current sea level.
- There is considerably more inundation of Long Beach given the sea level rise scenarios. The area to the north of Purakanui inlet also get far more inundation in these scenarios.
- With sea level rise the maximum velocities are also considerably higher indicating increased erosion risk.

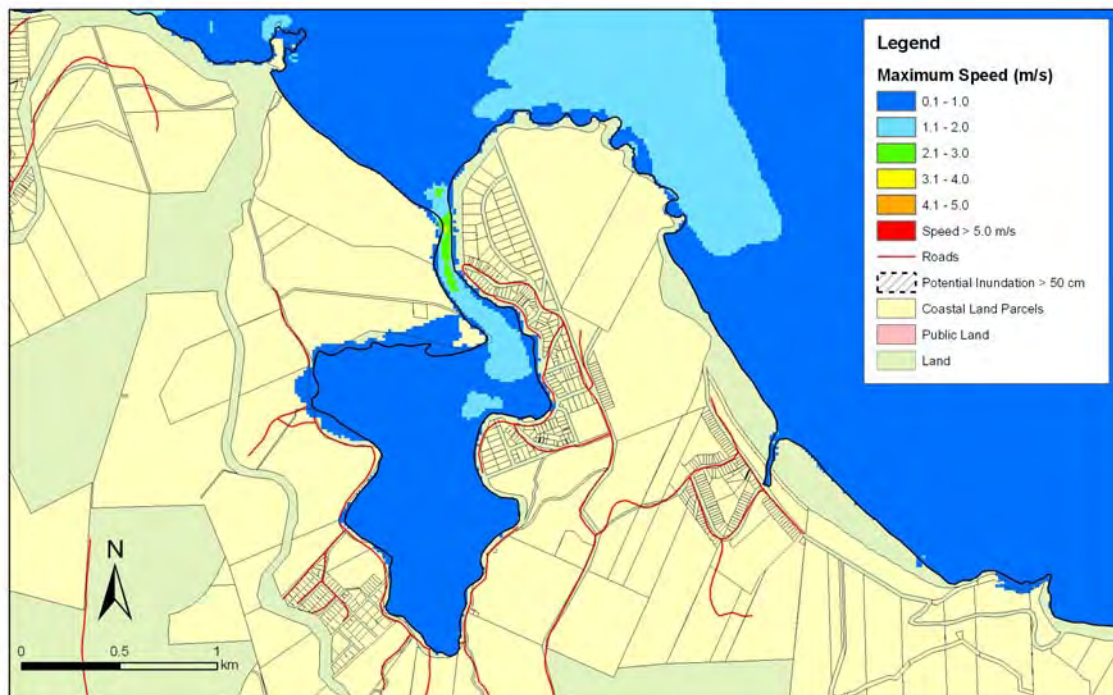
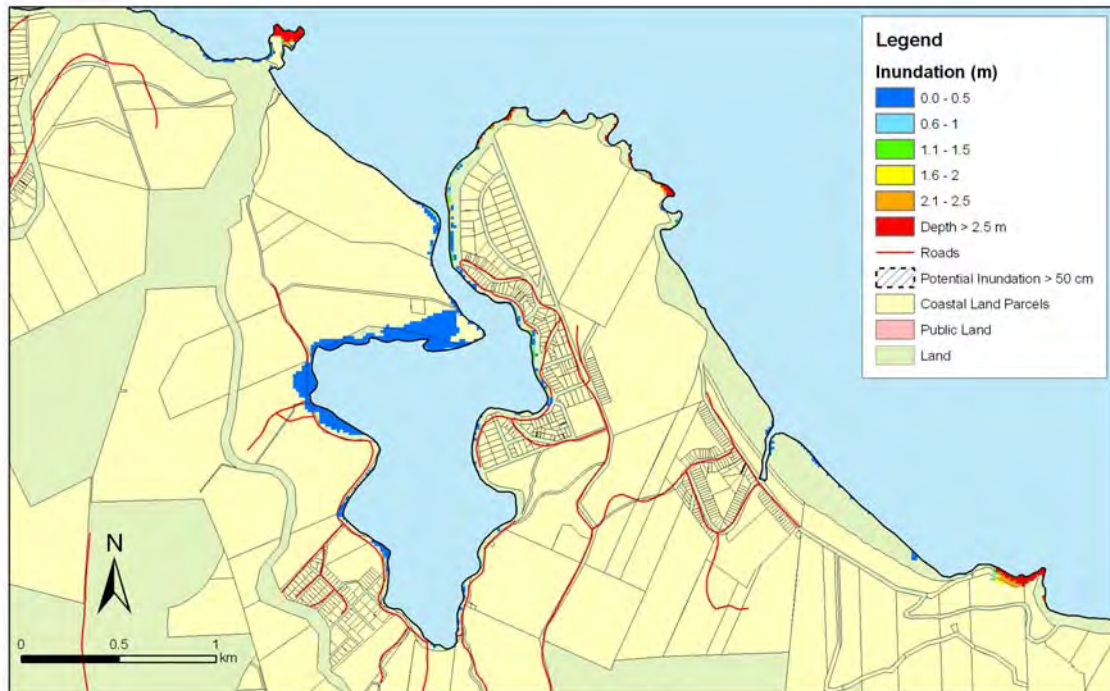


Figure 5.100 Long Beach and Purakanui – Puysegur tsunami: Maximum water depth for inundated land (top) and maximum speed (bottom) for MHWS.

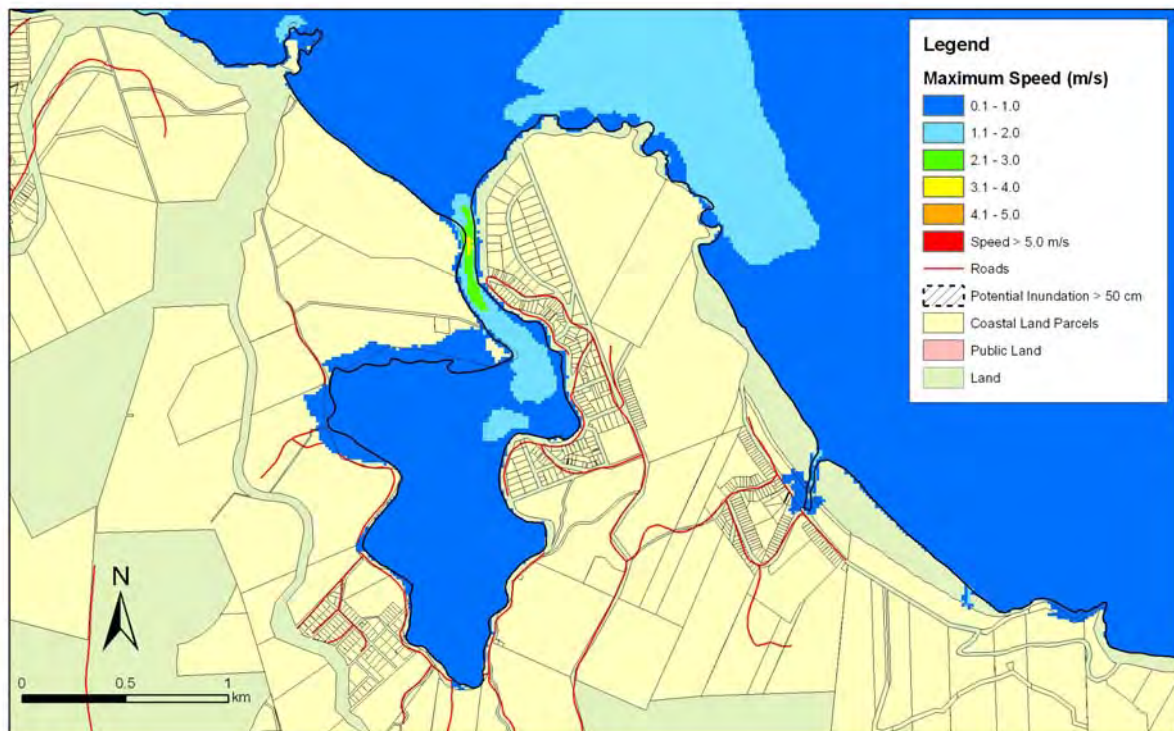
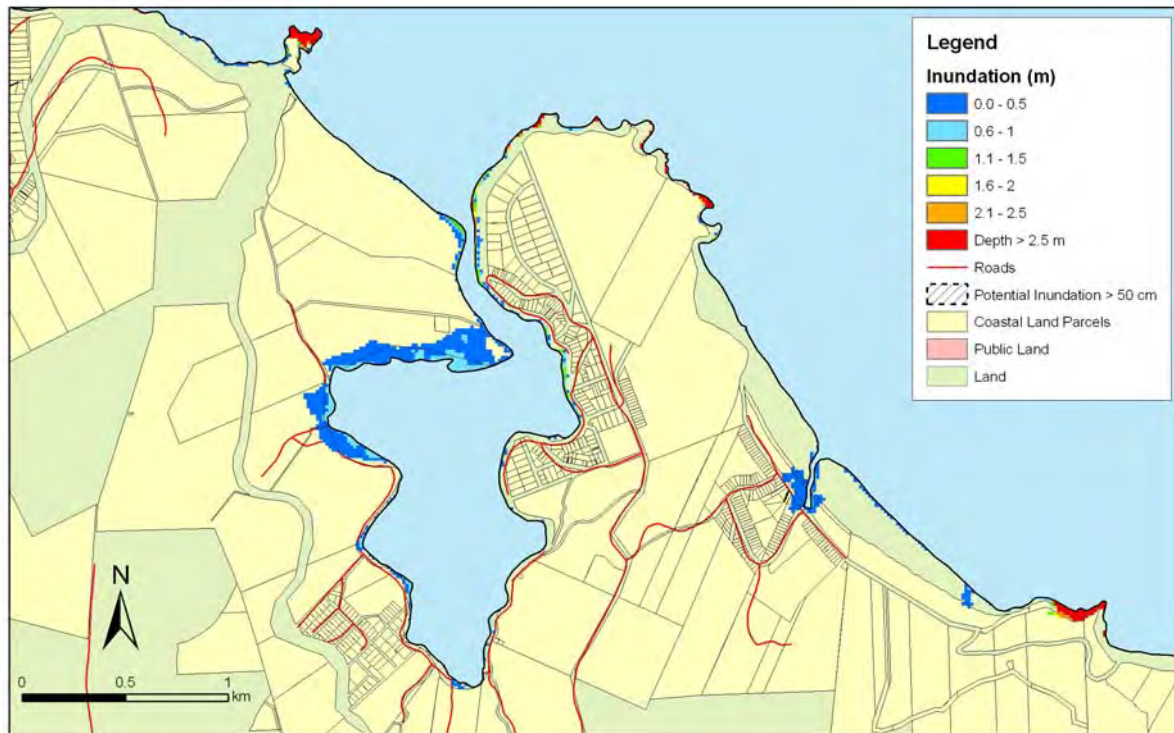


Figure 5.101: Long Beach and Purakanui – Puysegur tsunami: Maximum water depth for inundated land (top) and maximum speed (bottom) for MHWS with a sea level rise of 30 cm.

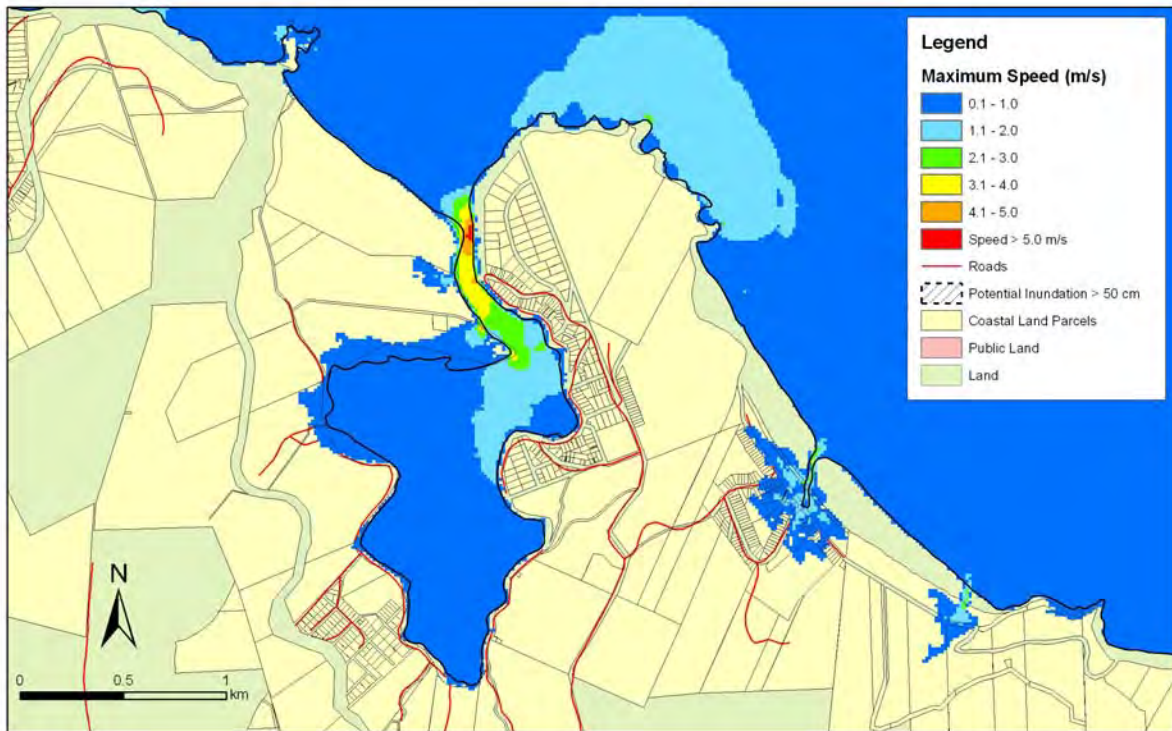
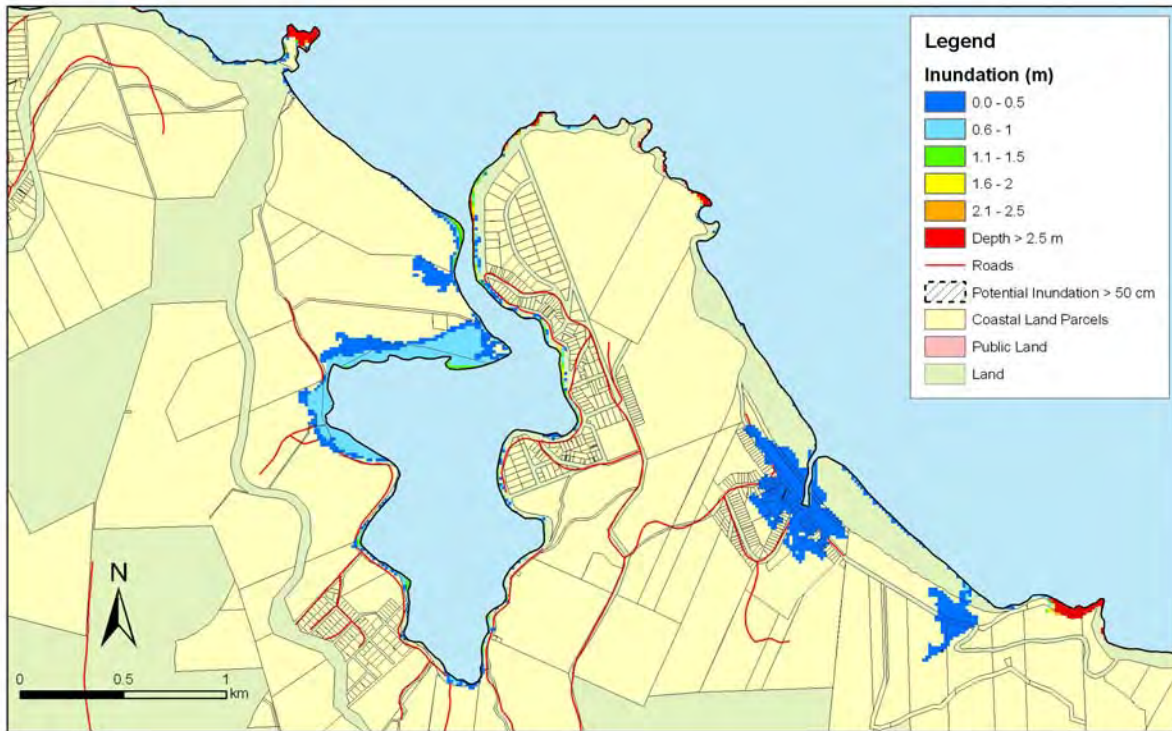


Figure 5.102: Long Beach and Purakanui – Puysegur tsunami: Maximum water depth for inundated land (top) and maximum speed (bottom) for MHWS with a sea level rise of 50 cm.

Long Beach and Purakanui: Far-Field

- Both remote tsunamis begin with an increase in the water level.
- Third wave is highest with amplitude 80 cm, total height 1.6m for the 1:100 year tsunami and amplitude 1.3m, total height 2.2m for the 1:500 year tsunami.
- Big waves noticeable for around 7 hours after first arrival then many smaller waves following later.
- Resonance period around 105 minutes and 80 minutes.
- Maximum runup: up to 1.8 metres for 1:100 year tsunami and 2.2 metres for 1:500 year tsunami.
- There is a little inundation in the Purakanui inlet for the 1:100 year tsunami but nowhere else. However for the sea level rise scenarios and for the 1:500 year tsunami there is also inundation in Long Beach. For the 1:500 year remote tsunami with the sea level rise Long Beach is inundated at two points.
- The erosion risk and inundation becomes significantly more of a concern as sea level rises.

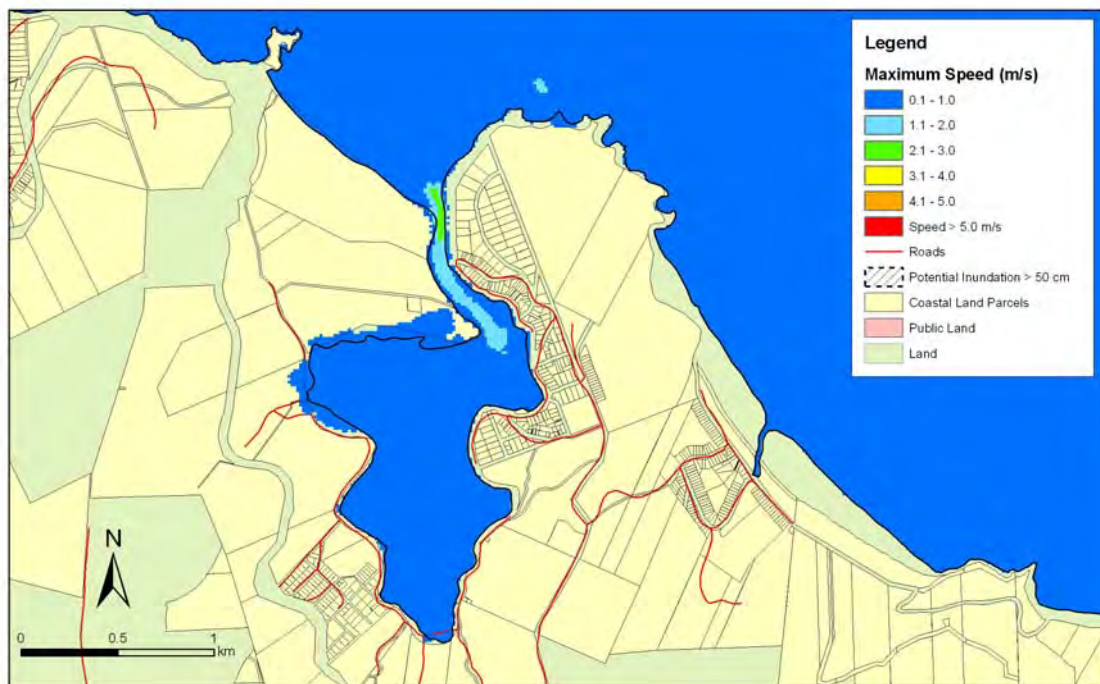
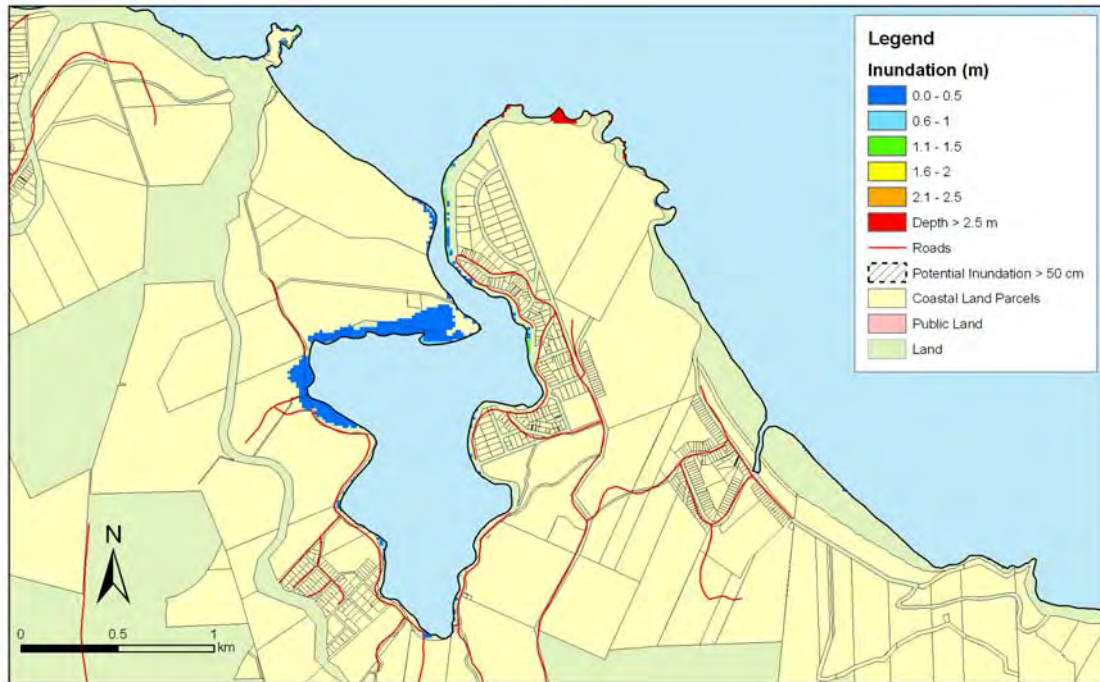


Figure 5.103: Long Beach and Purakanui – 1:100 year remote tsunami: Maximum water depth for inundated land (top) and maximum speed (bottom) for MHWS.

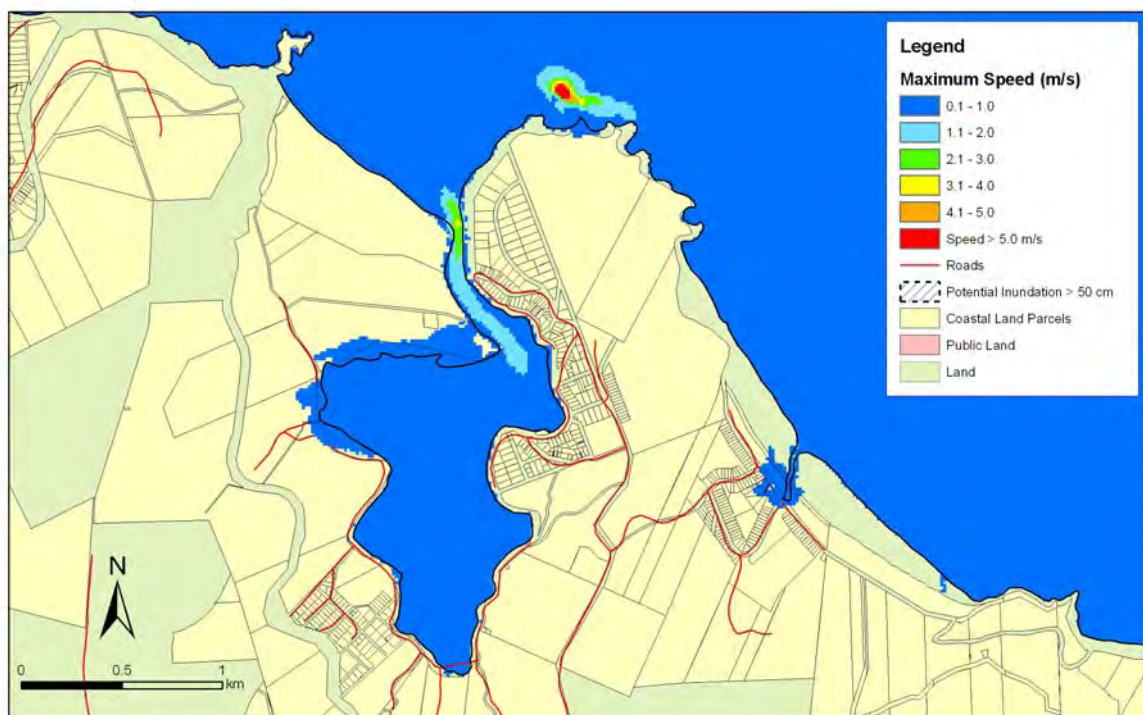
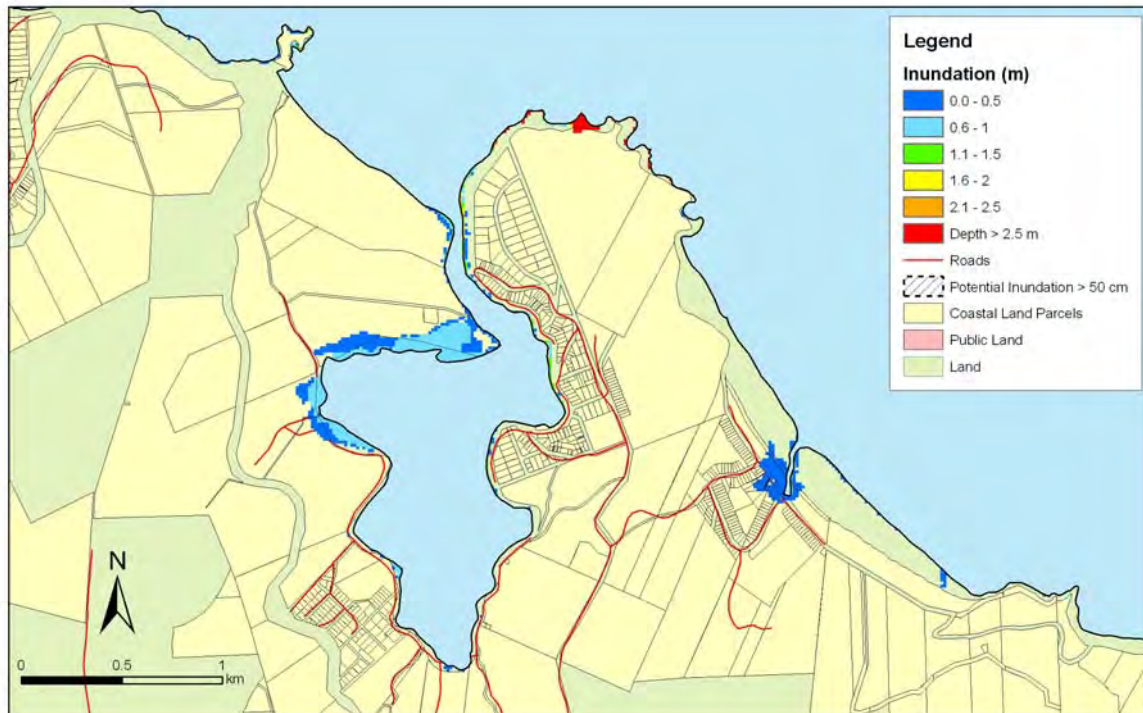


Figure 5.104: Long Beach and Purakanui – 1:100 year remote tsunami: Maximum water depth for inundated land (top) and maximum speed (bottom) for MHWS with a sea level rise of 30 cm.

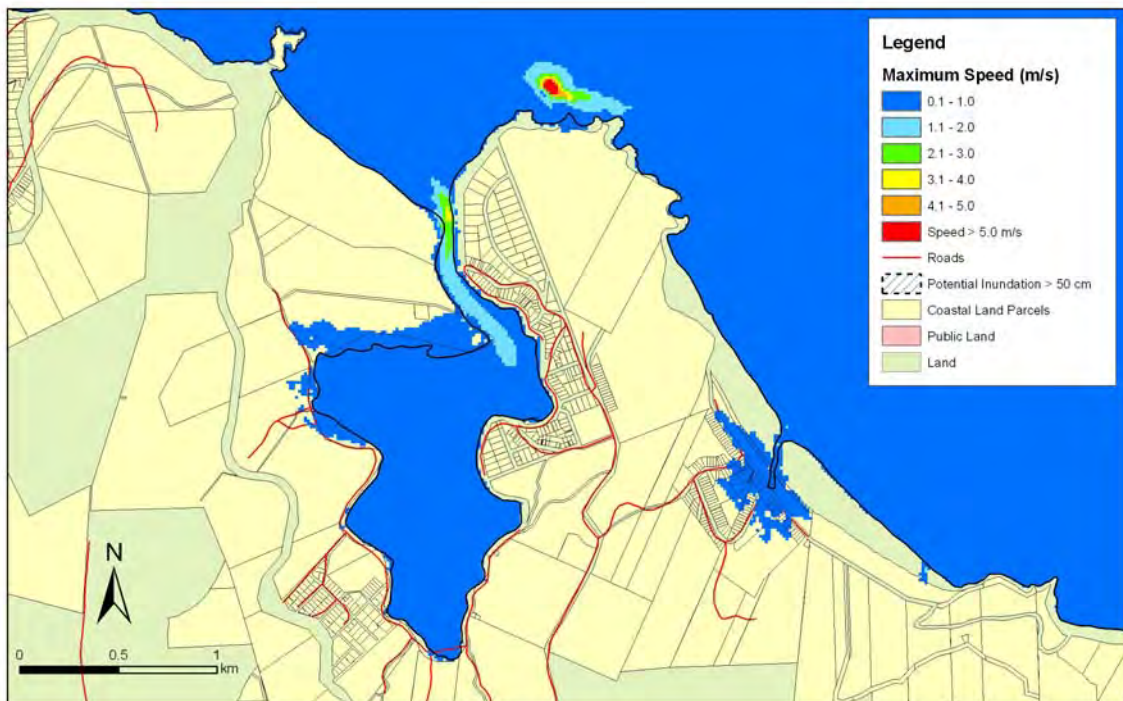
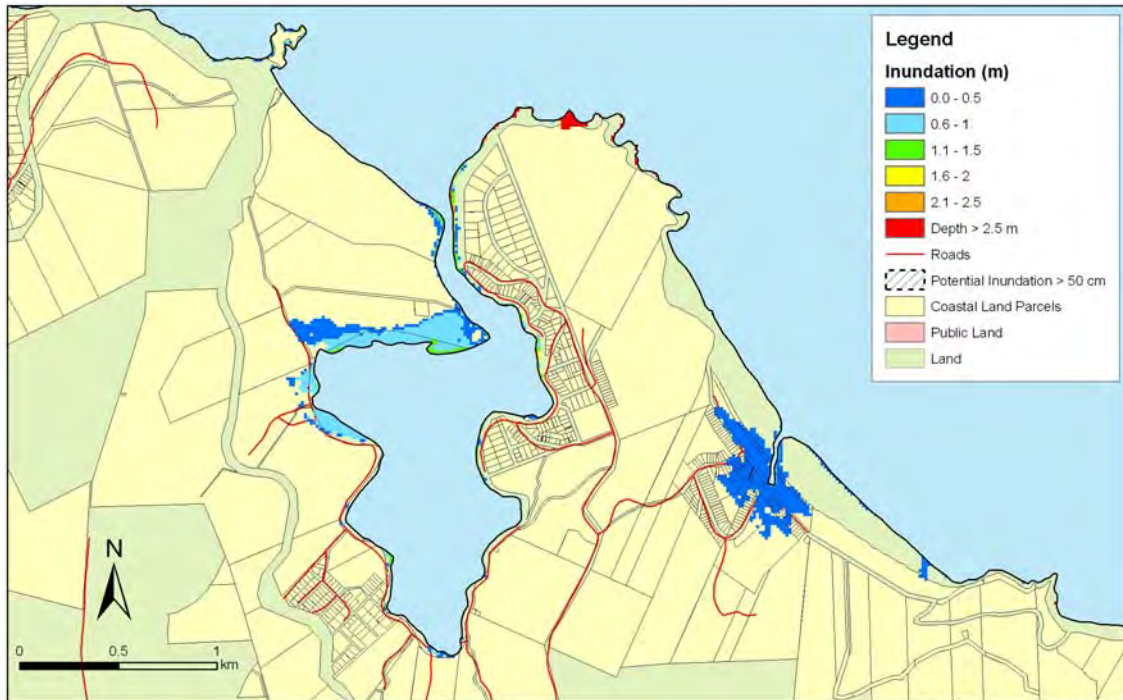


Figure 5.105: Long Beach and Purakanui – 1:100 year remote tsunami: Maximum water depth for inundated land (top) and maximum speed (bottom) for MHWS with a sea level rise of 50 cm.

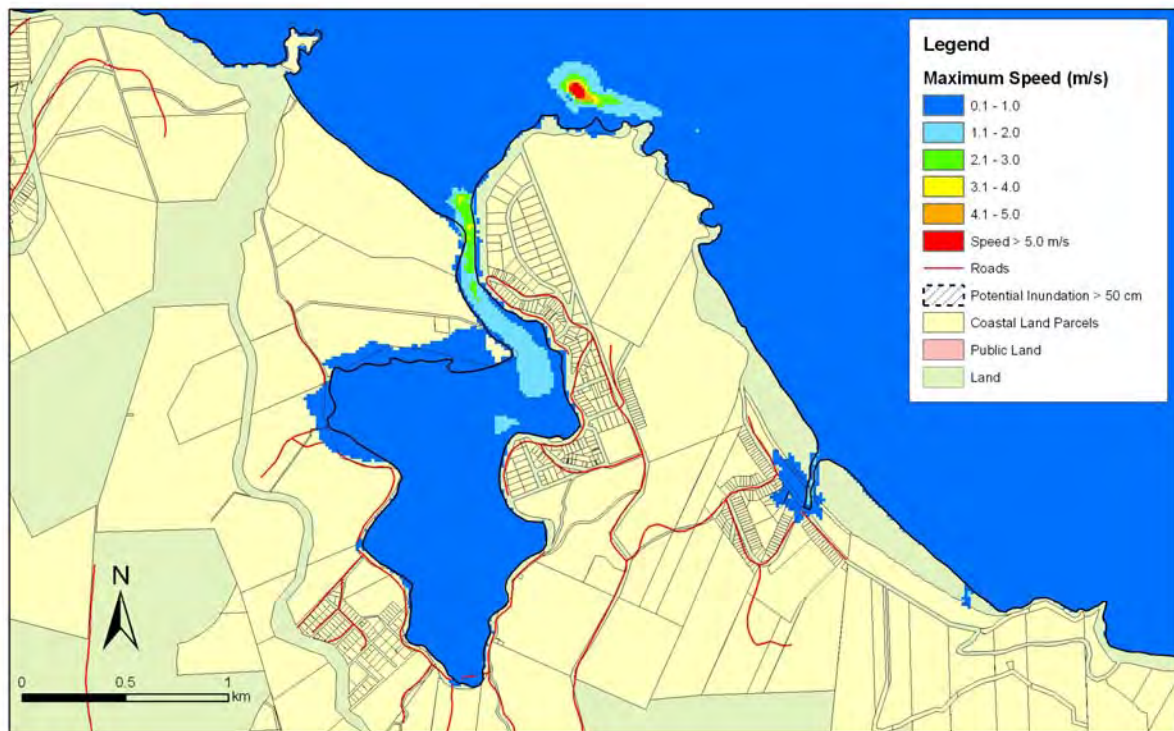
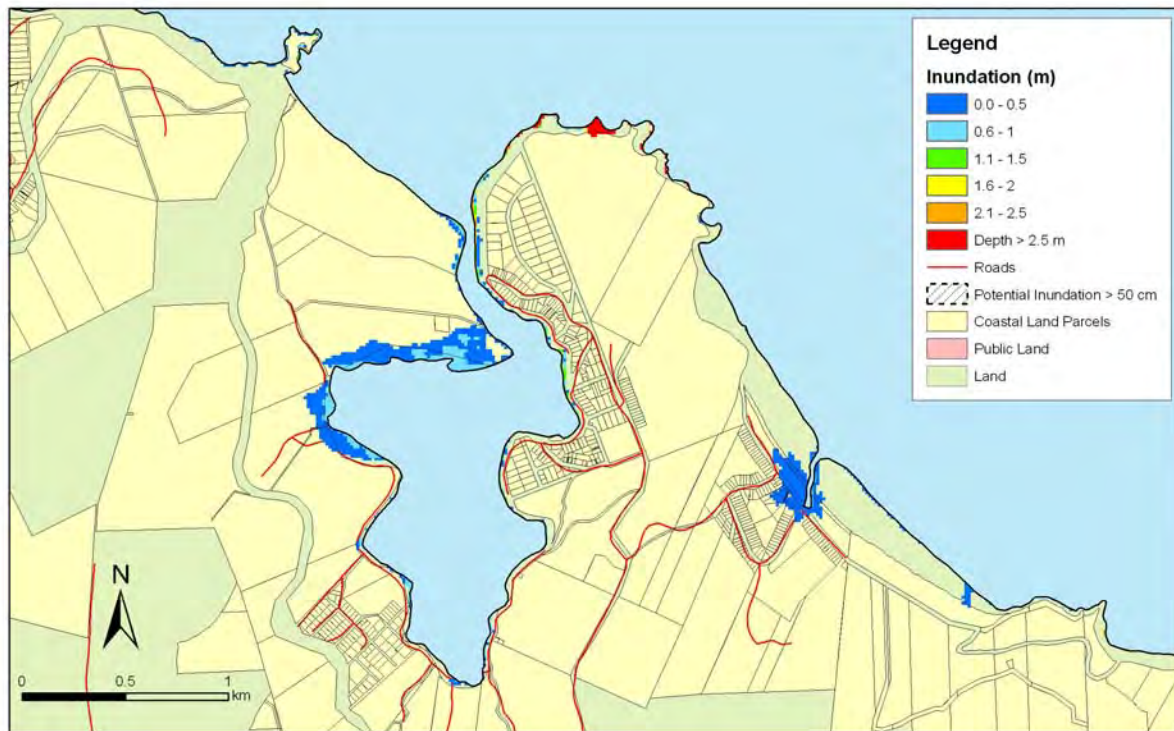


Figure 5.106: Long Beach and Purakanui – 1:500 year remote tsunami: Maximum water depth for inundated land (top) and maximum speed (bottom) for MHWS.

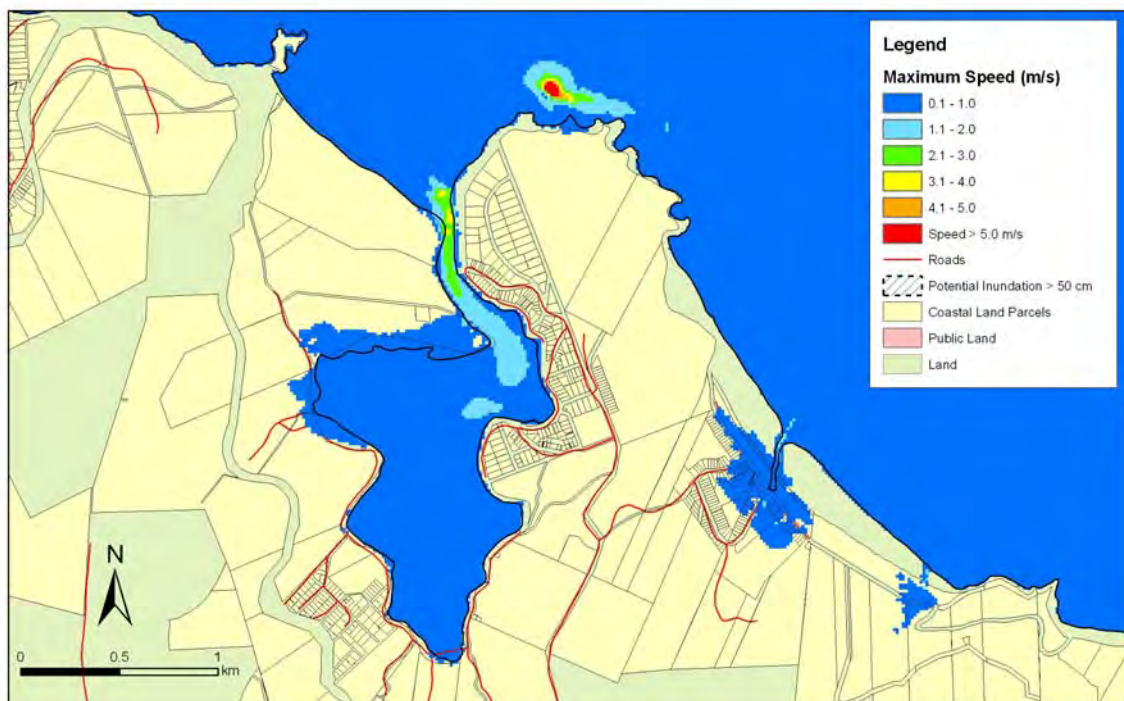
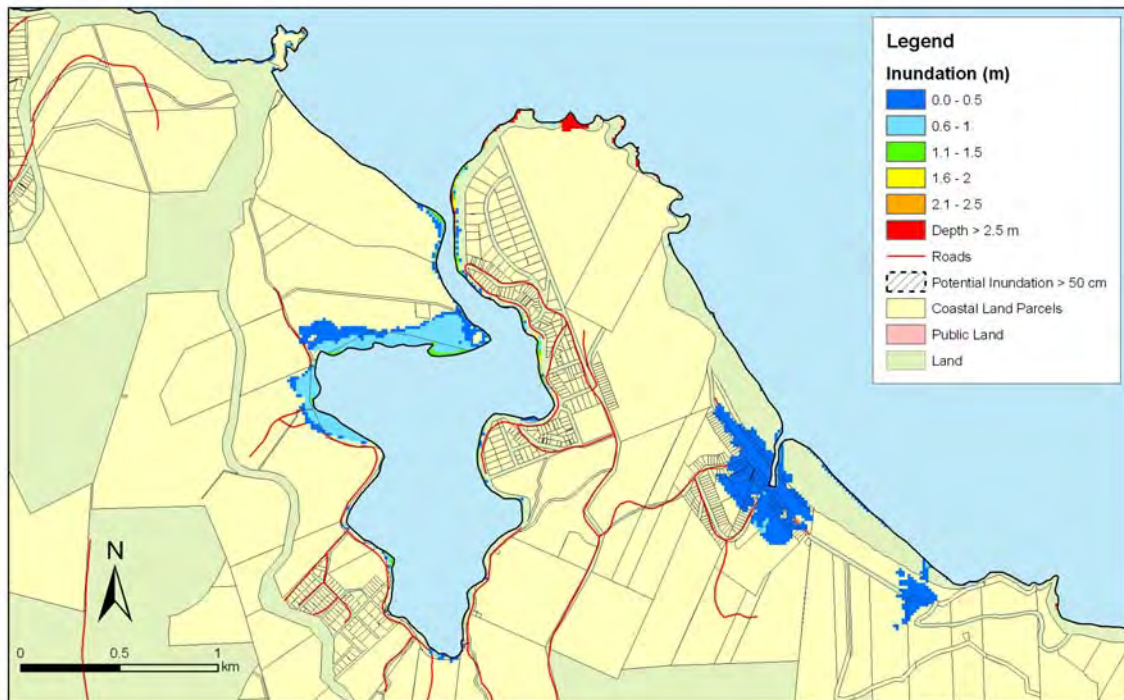


Figure 5.107: Long Beach and Purakanui – 1:500 year remote tsunami: Maximum water depth for inundated land (top) and maximum speed (bottom) for MHWS with a sea level rise of 30 cm.

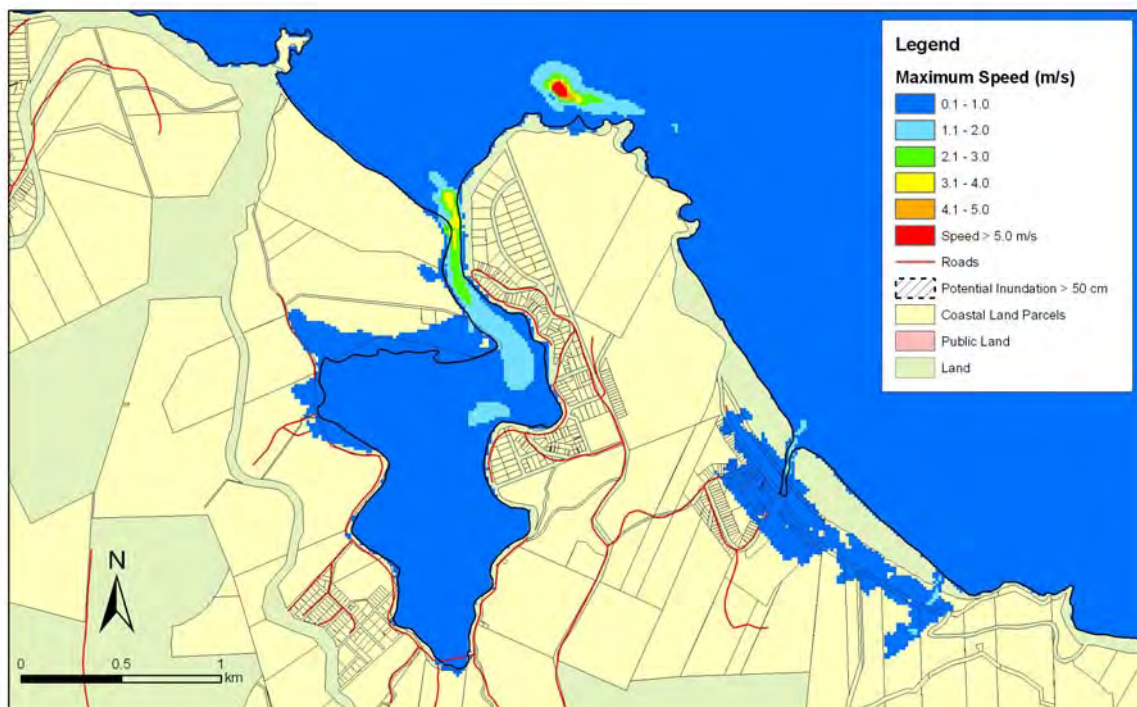
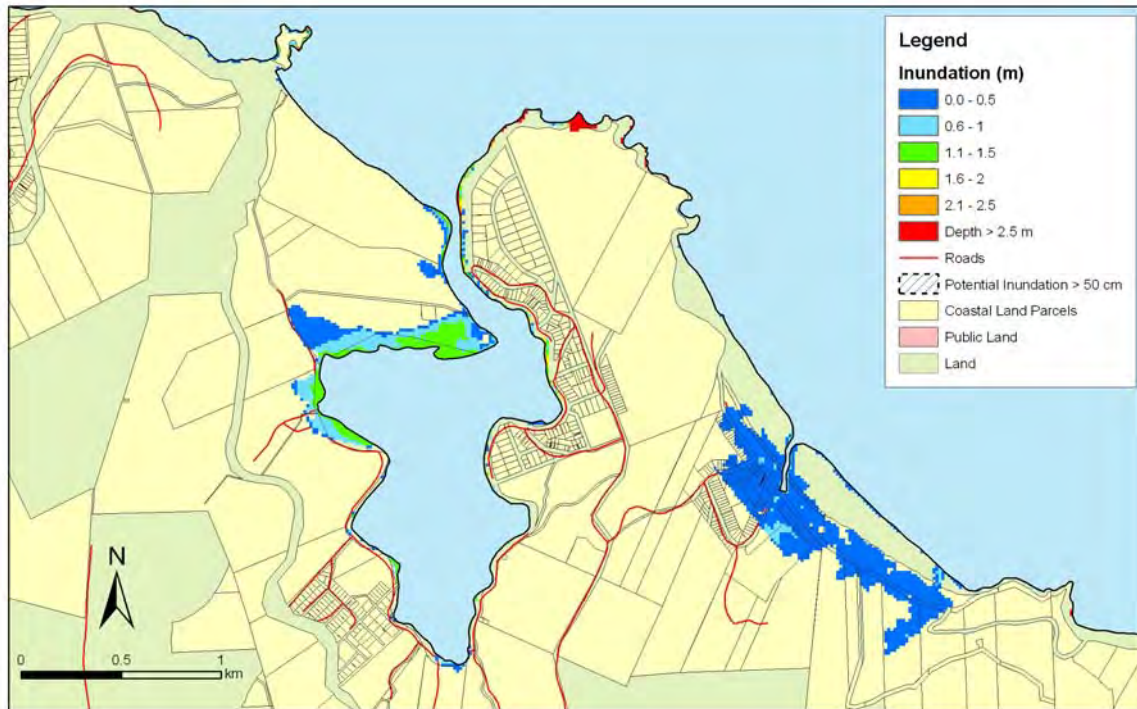


Figure 5.108: Long Beach and Purakanui – 1:500 year remote tsunami: Maximum water depth for inundated land (top) and maximum speed (bottom) for MHWS with a sea level rise of 50 cm.

5.3.12 Warrington and Blueskin Bay

Figures 5.109 – 5.111 show maximum inundation and water speed for the near-field (Puysegur) tsunami scenarios for this area. Figures 5.112-5.114 show maximum inundation and water speeds for the 1:100 year remote tsunami for Warrington and Blueskin Bay. Figures 5.115-5.117 show maximum inundation and water speeds for the 1:500 year remote tsunami for Warrington and Blueskin Bay.

- Trough arrives first approximately 95 minutes after fault rupture. Water level decreases 45 cm over 40 minutes.
- There is a small first arrival and then the first main has amplitude 1.7 m and arrives 2.8 hours after fault rupture.
- There is one other wave with amplitude over 1 m (1.5 m), which arrives 4 hours after fault rupture.
- Predominant period of wave arrivals: 25, 30 and 40 minutes.
- Maximum runup: up to 2.8 metres along the coast and up to 2 metres in the bay.
- Waves overtop the sandspit inundating land there. There is also a little inundation around the edges of Blueskin Bay, especially near Evansdale.
- There is a risk of erosion where the waves overtop the sandspit.
- In the sea level rise scenarios there is increased inundation in the areas already mentioned and Waitati also sees more inundation. The erosion risk is also significantly increased.

Warrington and Blueskin Bay: Near-Field

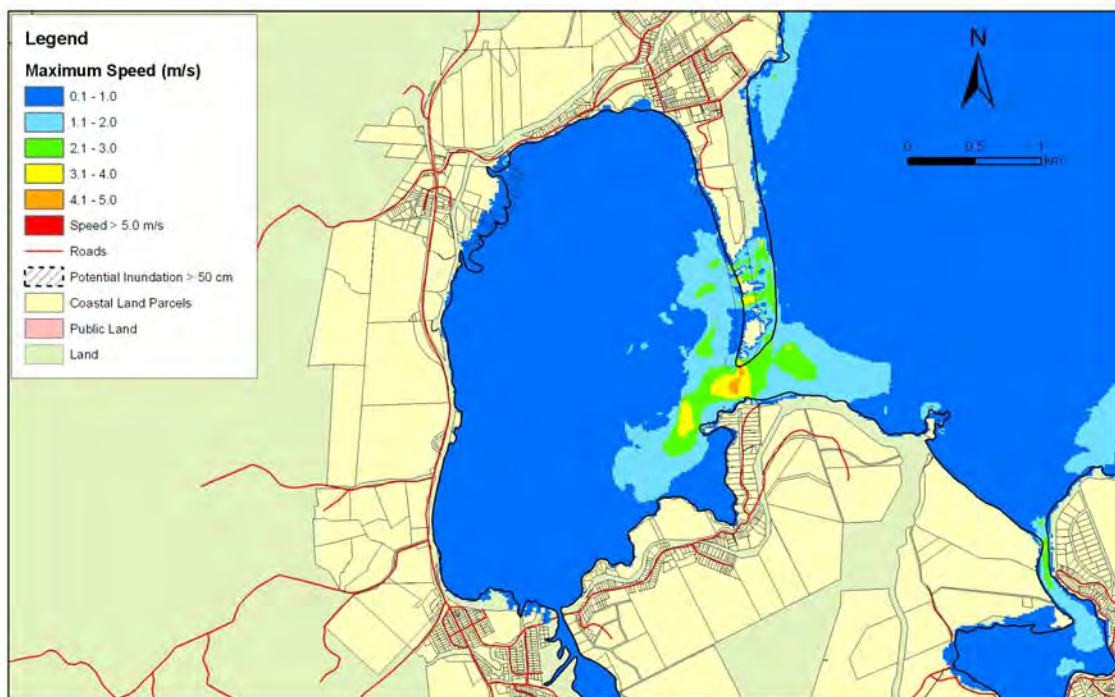


Figure 5.109: Warrington and Blueskin Bay – Puysegur tsunami: Maximum water depth for inundated land (top) and maximum speed (bottom) for MHWS.

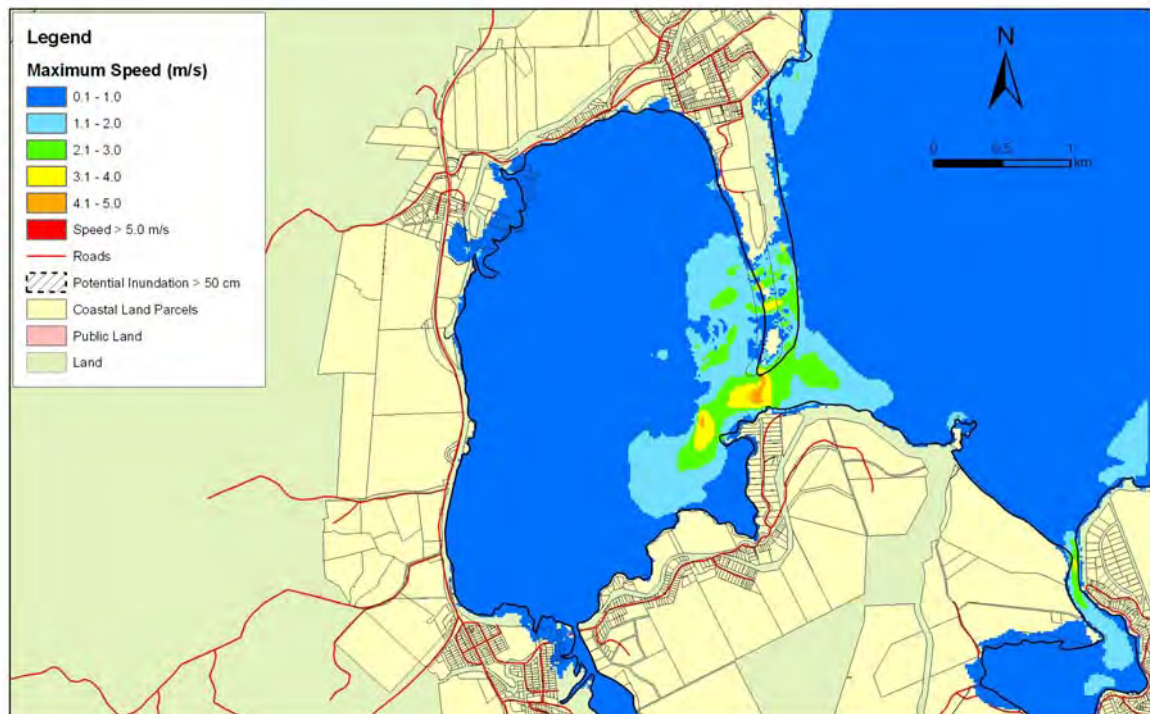


Figure 5.110: Warrington and Blueskin Bay – Puysegur tsunami: Maximum water depth for inundated land (top) and maximum speed (bottom) for MHWS with a sea level rise of 30 cm.

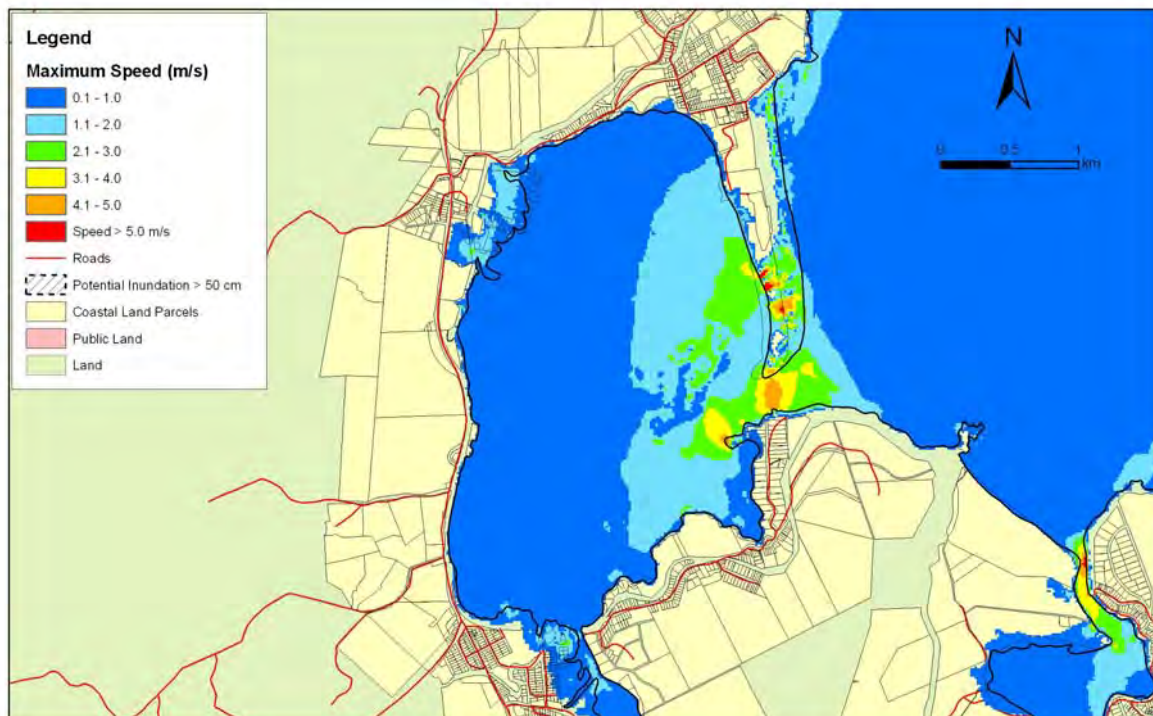
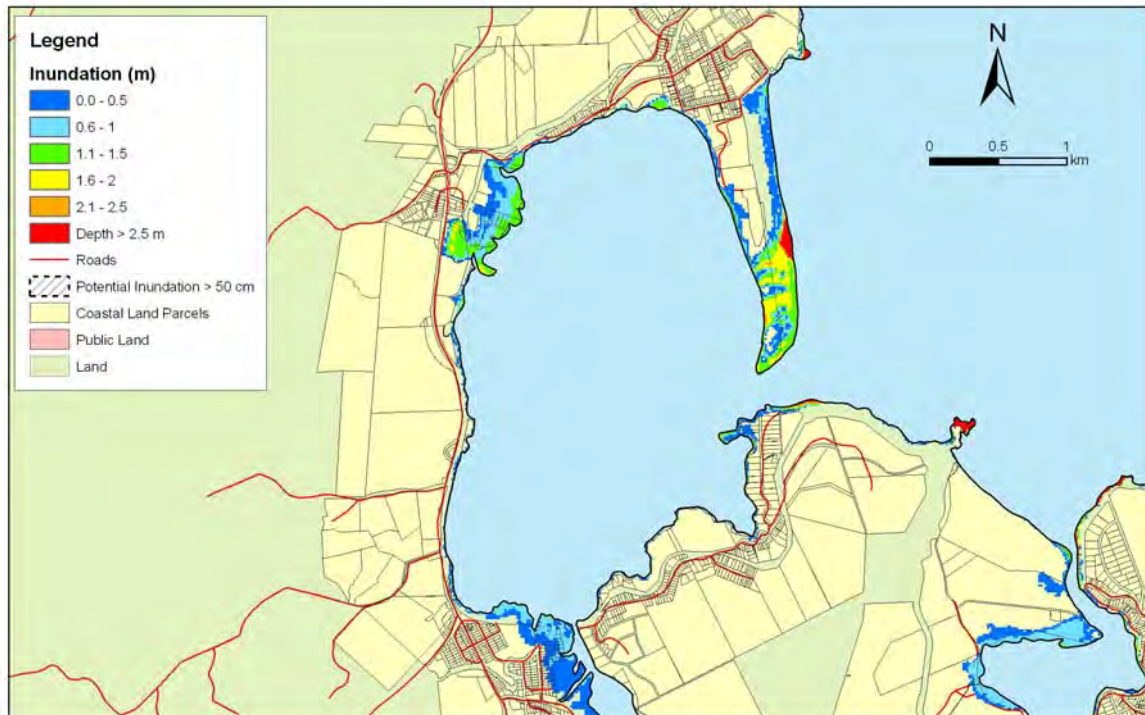


Figure 5.111: Warrington and Blueskin Bay – Puysegur tsunami: Maximum water depth for inundated land (top) and maximum speed (bottom) for MHWS with a sea level rise of 50 cm.

Warrington and Blueskin Bay: Far-Field

- Both remote tsunamis begin with an increase in the water level.
- Third wave is highest with amplitude 80 cm, total height 1.6m for the 1:100 year tsunami and amplitude 1.3m, total height 2.4m for the 1:500 year tsunami.
- Big waves for around 7 hours after first arrival then lots of smaller arrivals.
- Resonance period around 105 minutes and also 80 minutes.
- Maximum runup: up to 1.8 metres for 1:100 year tsunami and 2.3 m for 1:500 year tsunami.
- The sand spit is overtopped in all scenarios and parts of Evansdale and Waitati are inundated. For sea level rises and the 1:500 year scenario this is more pronounced.
- Erosion risk is not as high as the Puysegur scenarios but still could occur especially on the sand spit where overtopping has occurred.



Figure 5.112: Warrington and Blueskin Bay – 1:100 year remote tsunami: Maximum water depth for inundated land (top) and maximum speed (bottom) for MHWS.



Figure 5.113: Warrington and Blueskin Bay – 1:100 year remote tsunami: Maximum water depth for inundated land (top) and maximum speed (bottom) for MHWS with a sea level rise of 30 cm.



Figure 5.114: Warrington and Blueskin Bay – 1:100 year remote tsunami: Maximum water depth for inundated land (top) and maximum speed (bottom) for MHWS with a sea level rise of 50 cm..



Figure 5.115: Warrington and Blueskin Bay – 1:500 year remote tsunami: Maximum water depth for inundated land (top) and maximum speed (bottom) for MHWS.

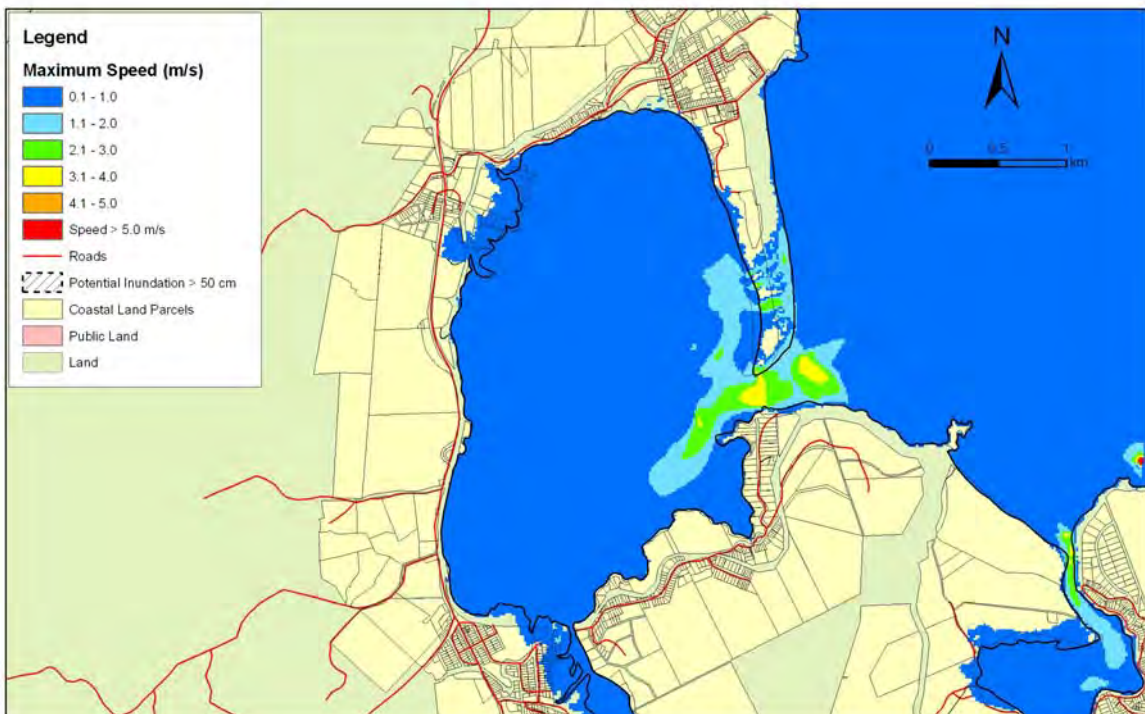


Figure 5.116: Warrington and Blueskin Bay – 1:500 year remote tsunami: Maximum water depth for inundated land (top) and maximum speed (bottom) for MHWS with a sea level rise of 30 cm.

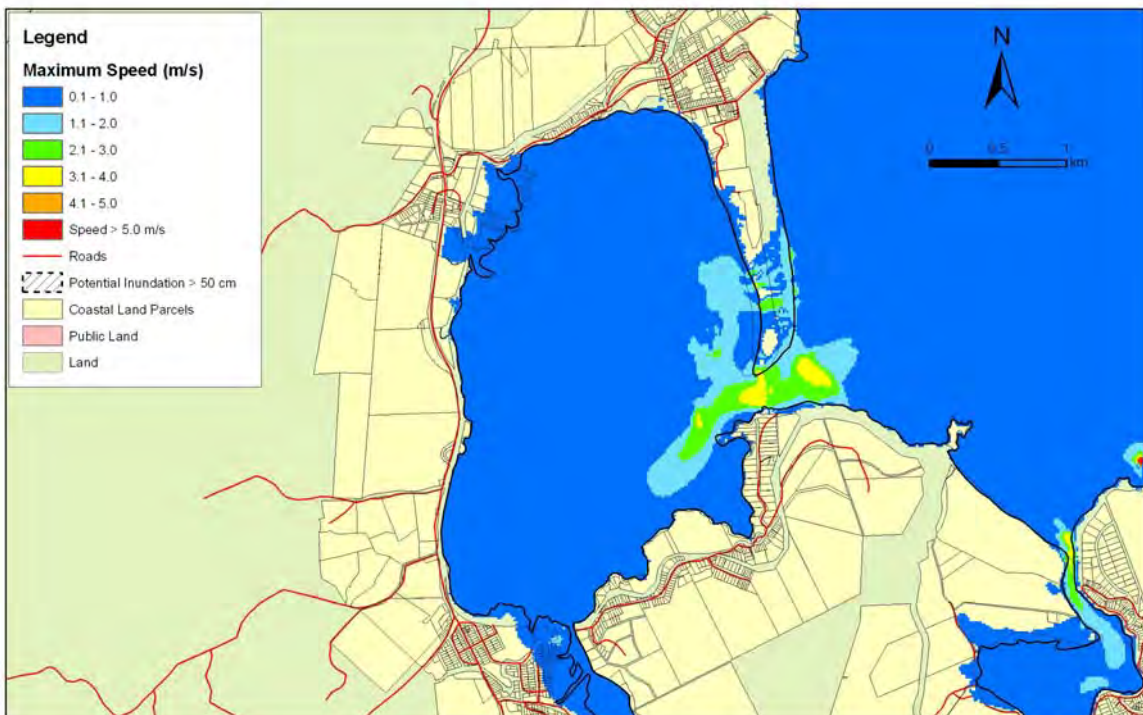
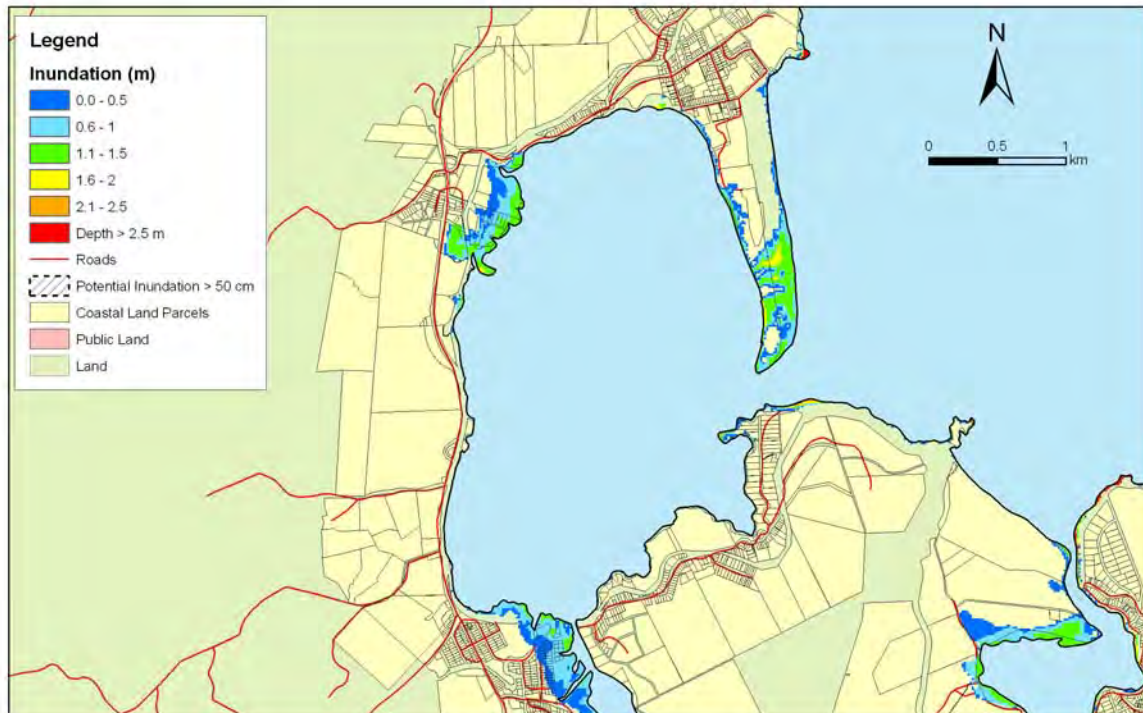


Figure 5.117: Warrington and Blueskin Bay – 1:500 year remote tsunami: Maximum water depth for inundated land (top) and maximum speed (bottom) for MHWS with a sea level rise of 50 cm.

5.3.13 Karitane

Figures 5.118 – 5.120 show maximum inundation and water speed for the near-field (Puysegur) tsunami scenarios for this area. Figures 5.121-5.123 show maximum inundation and water speeds for the 1:100 year remote tsunami for Karitane. Figures 5.124-5.126 show maximum inundation and water speeds for the 1:500 year remote tsunami for Karitane.

Karitane: Near-Field

- Trough arrives first approximately 90 minutes after fault rupture. Water level decreases 40 cm over 50 minutes.
- There is a small first arrival (2.45 hours after fault rupture) and then the first main has amplitude 1.55 m and arrives 2.8 hours after fault rupture.
- There is one other wave with amplitude 1 m (1.5 m), which arrives 5 hours after fault rupture. All other waves are smaller than this.
- Predominant period of wave arrivals: 25 minutes.
- Maximum runup: up to 2.7 metres.
- There is considerable inundation of Karitane and further up the Waikouaiti River on both sides. Some of Karitane is inundated from behind by water that has gone up the Waikouaiti River. There is also some inundation near the entrance to the Hawksbury Lagoon.
- With sea level rises some land on the south side of Hawksbury Lagoon is also inundated and even more of Karitane is inundated.
- The risk of erosion is also increased due to sea level rise.



Figure 5.118: Karitane – Puysegur tsunami: Maximum water depth for inundated land (top) and maximum speed (bottom) for MHWS.



Figure 5.119: Karitane – Puysegur tsunami: Maximum water depth for inundated land (top) and maximum speed (bottom) for MHWS with a sea level rise of 30 cm.

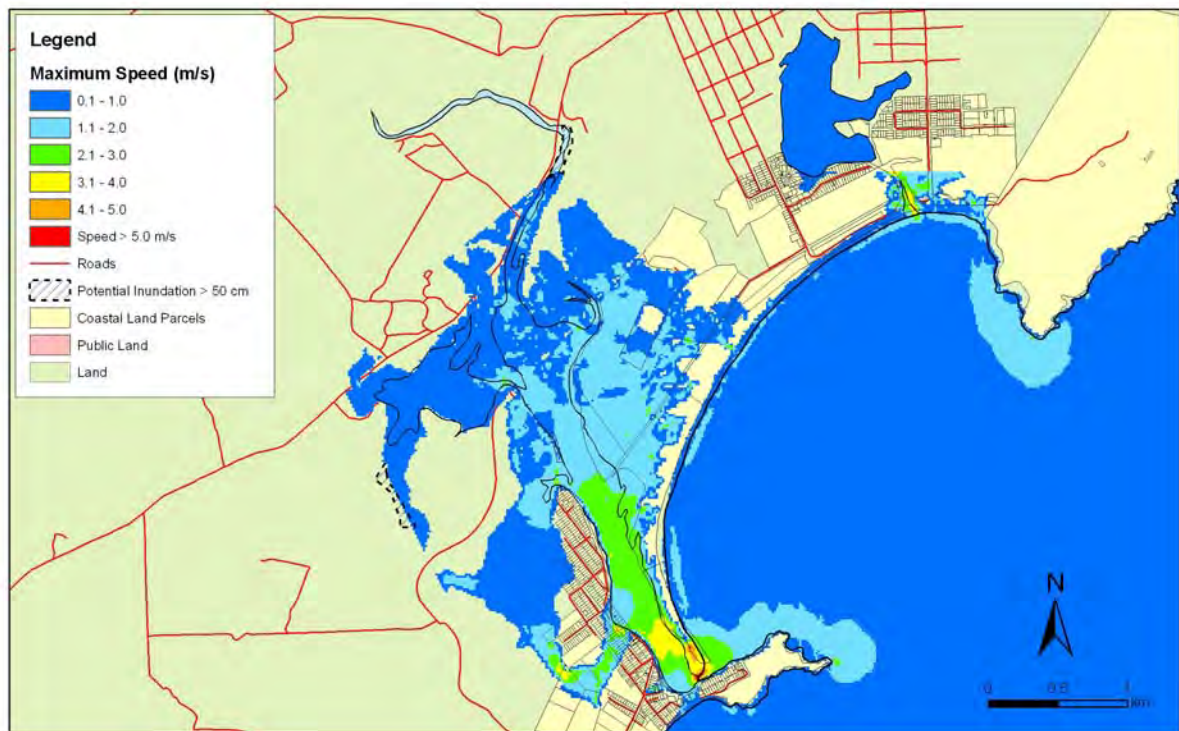
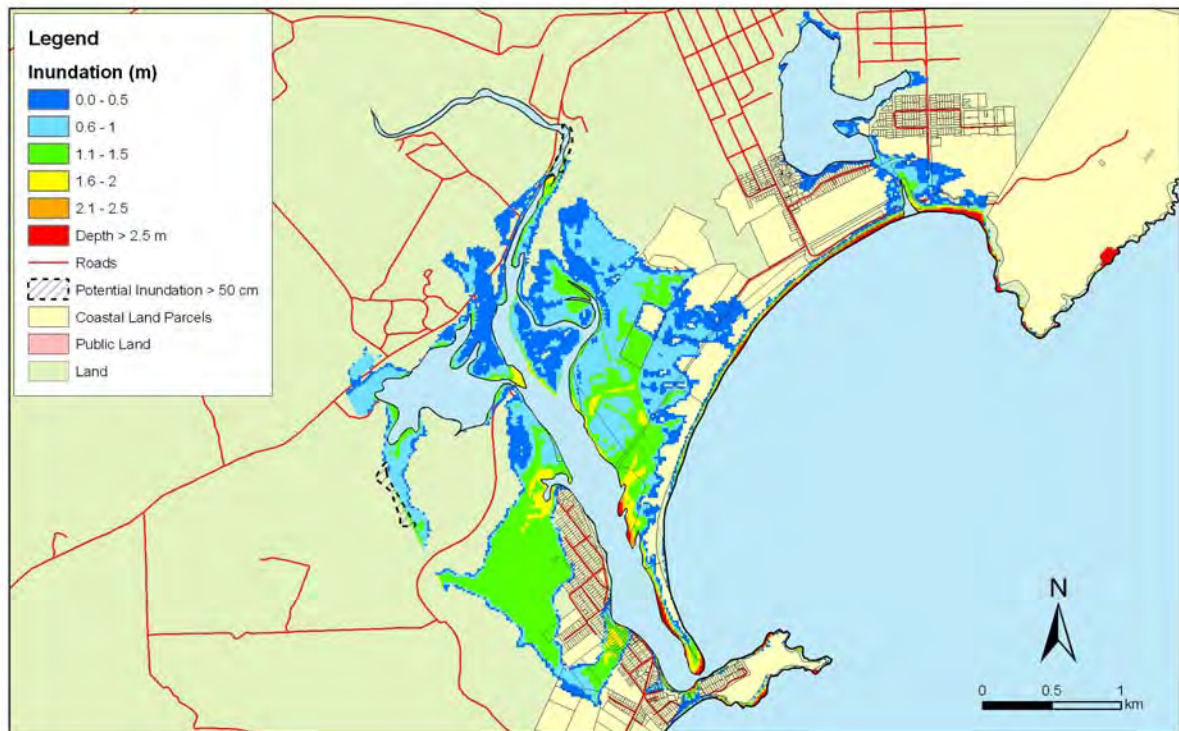


Figure 5.120: Karitane – Puysegur tsunami: Maximum water depth for inundated land (top) and maximum speed (bottom) for MHWS with a sea level rise of 50 cm.

Karitane: Far-Field

- Both remote tsunamis begin with an increase in the water level.
- Third wave is highest with amplitude 70 cm, total height 1.3 m for the 1:100 year tsunami. Second wave has larger total height 1.4 m but only has amplitude 55 cm for the 1:100 year tsunami. For the 1:500 year tsunami the third wave has amplitude 1.2m and total height 2.2m.
- Big waves for around 7 hours after first arrival then lots of smaller arrivals.
- Resonance period around 105 minutes and 80 minutes.
- Maximum runup: up to 1.7 for 1:100 year tsunami and 2.1 metres for 1:500 year tsunami.
- Inundation for 1:100 year tsunami is less than Puysegur but still covers significant areas, whilst inundation for the 1:500 year tsunami is similar to that of the Puysegur.
- Erosion risk is relatively low although the tip of the spit at the mouth of the Waikouaiti River is overtopped.

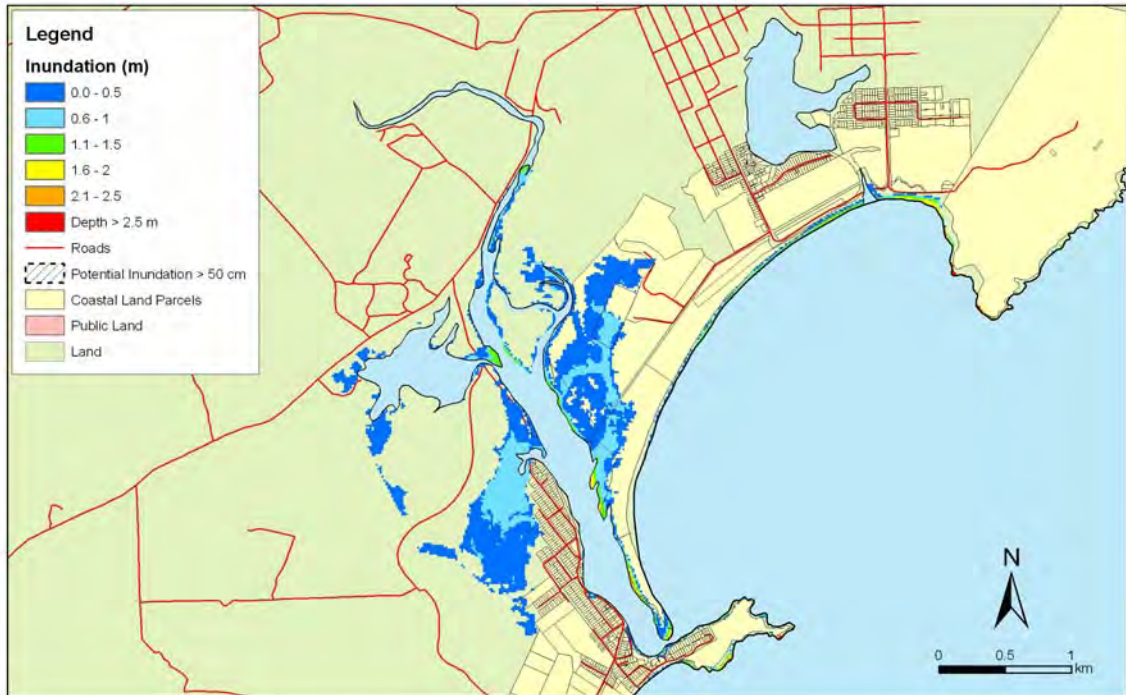


Figure 5.121: Karitane – 1:100 year remote tsunami: Maximum water depth for inundated land (top) and maximum speed (bottom) for MHWS.



Figure 5.122: Karitane – 1:100 year remote tsunami: Maximum water depth for inundated land (top) and maximum speed (bottom) for MHWS with a sea level rise of 30 cm.

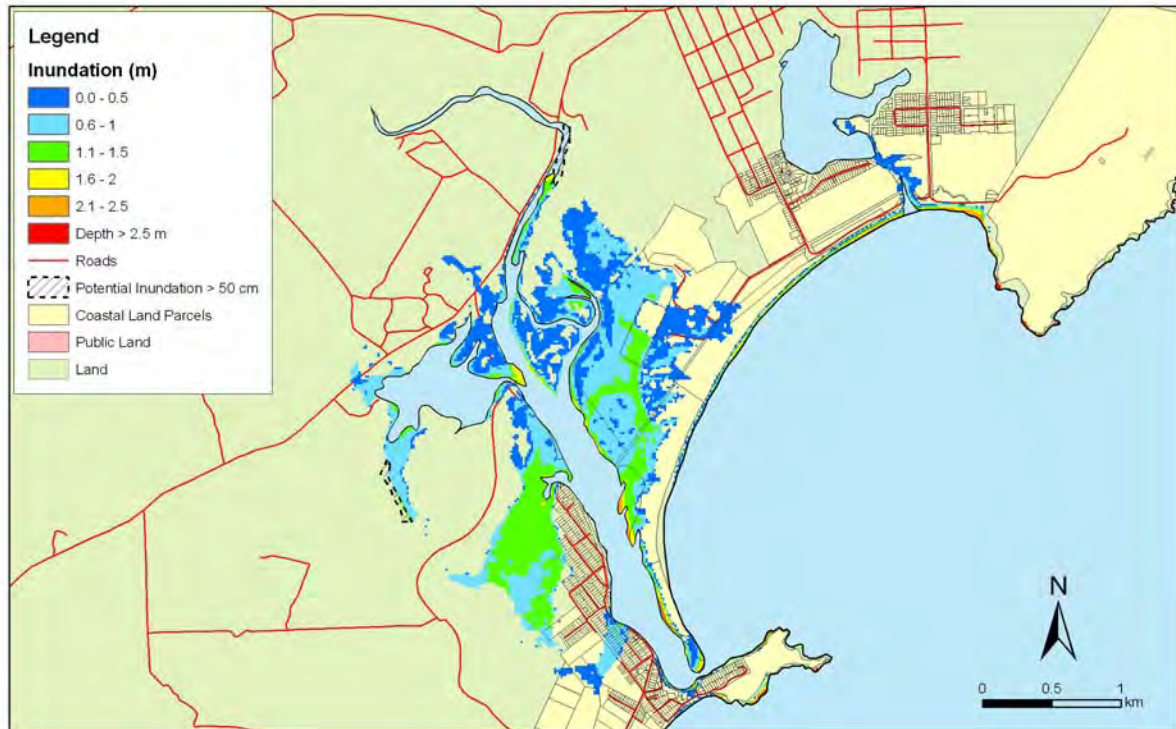


Figure 5.123: Karitane – 1:100 year remote tsunami: Maximum water depth for inundated land (top) and maximum speed (bottom) for MHWS with a sea level rise of 50 cm.



Figure 5.124: Karitane – 1:500 year remote tsunami: Maximum water depth for inundated land (top) and maximum speed (bottom) for MHWS.

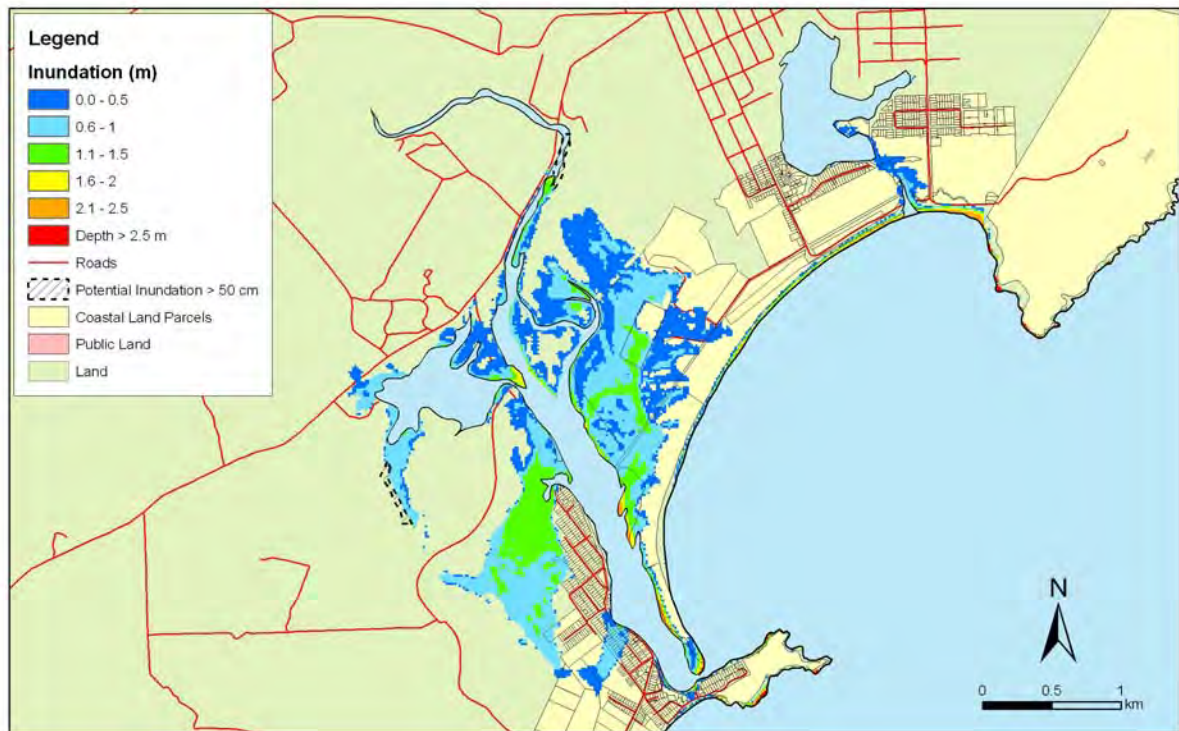


Figure 5.125: Karitane – 1:500 year remote tsunami: Maximum water depth for inundated land (top) and maximum speed (bottom) for MHWS with a sea level rise of 30 cm.



Figure 5.126: Karitane – 1:500 year remote tsunami: Maximum water depth for inundated land (top) and maximum speed (bottom) for MHWS with a sea level rise of 50 cm.

5.3.14 Moeraki

Figures 5.127 – 5.129 show maximum inundation and water speed for the near-field (Puysegur) tsunami scenarios for this area. Figures 5.130-5.132 show maximum inundation and water speeds for the 1:100 year remote tsunami for Moeraki. Figures 5.133-5.135 show maximum inundation and water speeds for the 1:500 year remote tsunami for Moeraki.

Moeraki: Near-Field

- Trough arrives first approximately 95 minutes after fault rupture. Water level decreases 40 cm over 50 minutes.
- There is a small first arrival and then the first main arrival is the biggest with amplitude 90 cm and arriving 2.85 hours after fault rupture.
- The second largest wave has amplitude 85 cm and arrives 5 hours after fault rupture. All other waves are smaller than this although there is a very large trough (1.5 m below undisturbed level of the sea), which arrives 4 hours after fault rupture.
- Predominant period of wave arrivals: 40 and 100 minutes.
- Maximum runup: up to 2.7 metres
- Water speeds are not significant.
- Inundation depths rise commensurate with the two sea level rises but otherwise there are not qualitative differences.



Figure 5.127: Moeraki – Puysegur tsunami: Maximum water depth for inundated land (top) and maximum speed (bottom) for MHWS.



Figure 5.128: Moeraki – Puysegur tsunami: Maximum water depth for inundated land (top) and maximum speed (bottom) for MHWS with a sea level rise of 30 cm.



Figure 5.129: Moeraki – Puysegur tsunami: Maximum water depth for inundated land (top) and maximum speed (bottom) for MHWS with a sea level rise of 50 cm.

Moeraki: Far-Field

- Both remote tsunamis begin with an increase in the water level.
- Second wave is highest with amplitude 1.2m, trough to crest difference of 2.2m for 1:100 year tsunami and amplitude 1.7m, total height 3.3m for the 1:500 year tsunami.
- Big waves well after the main arrivals – up to 12 hours – with smaller waves after that.
- Resonance period around 105 minutes and also 80 minutes.
- Maximum runup: up to 2.1 metres for 1:100 year tsunami and 2.7 metres for 1:500 year tsunami.
- Land right on the coast may be inundated, especially for the larger scenarios. Inundation confined to the coastline however and does not reach significantly inland.



Figure 5.130: Moeraki – 1:100 year remote tsunami: Maximum water depth for inundated land (top) and maximum speed (bottom) for MHWS.



Figure 5.131: Moeraki – 1:100 year remote tsunami: Maximum water depth for inundated land (top) and maximum speed (bottom) for MHWS with a sea level rise of 30 cm.



Figure 5.132: Moeraki – 1:100 year remote tsunami: Maximum water depth for inundated land (top) and maximum speed (bottom) for MHWS with a sea level rise of 50 cm.



Figure 5.133: Moeraki – 1:500 year remote tsunami: Maximum water depth for inundated land (top) and maximum speed (bottom) for MHWS.



Figure 5.134: Moeraki – 1:500 year remote tsunami: Maximum water depth for inundated land (top) and maximum speed (bottom) for MHWS with a sea level rise of 30 cm.



Figure 5.135: Moeraki – 1:500 year remote tsunami: Maximum water depth for inundated land (top) and maximum speed (bottom) for MHWS with a sea level rise of 50 cm.

5.3.15 Hampden

Figures 5.136 – 5.138 show maximum inundation and water speed for the near-field (Puysegur) tsunami scenarios for this area. Figures 5.139-5.141 show maximum inundation and water speeds for the 1:100 year remote tsunami for Hampden. Figures 5.142-5.144 show maximum inundation and water speeds for the 1:500 year remote tsunami for Hampden.

Hampden: Near-Field

- Trough arrives first approximately 95 minutes after fault rupture. Water level decreases 45 cm over 40 minutes.
- There is a small first arrival and then the first main has amplitude 1.7 m and arrives 2.8 hours after fault rupture.
- There is one other wave with amplitude over 1 m (1.5 m) which arrives 4 hours after fault rupture.
- Predominant period of wave arrivals: 25, 30 and 40 minutes.
- Maximum runup: up to 2.5 metres.
- There is some land inundated along the coast and inland beside the two streams that flow through the township. This inundation is more significant in the sea level rise scenarios.
- Erosion may be an issue for the sea level rises too as the maximum speeds are higher.

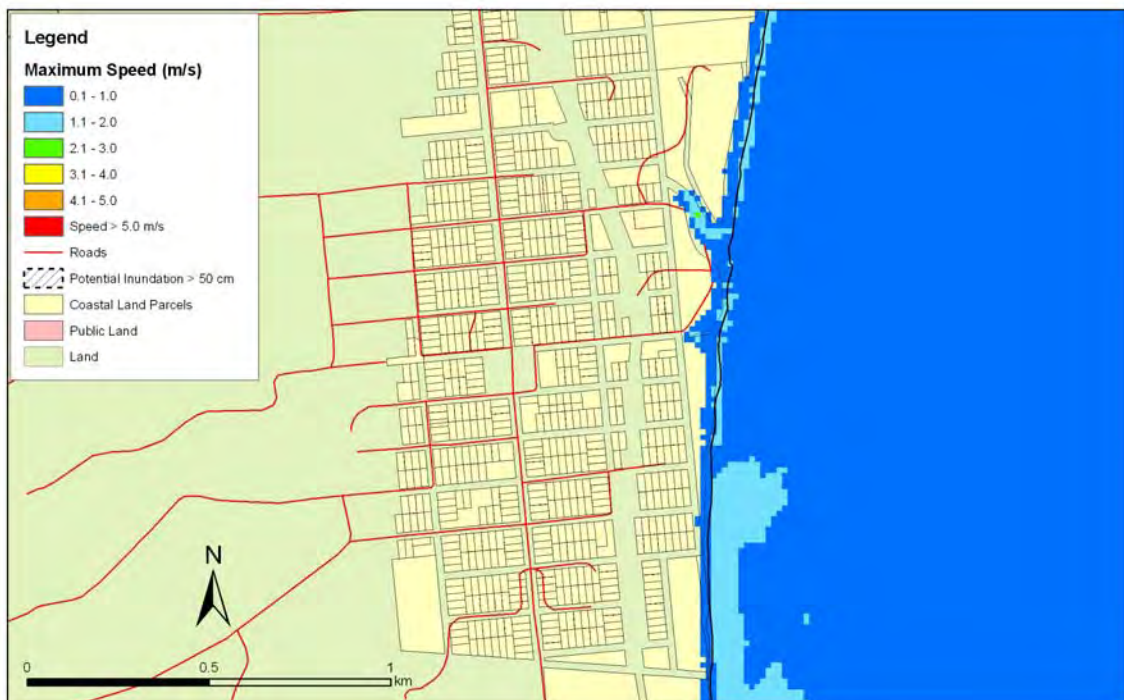
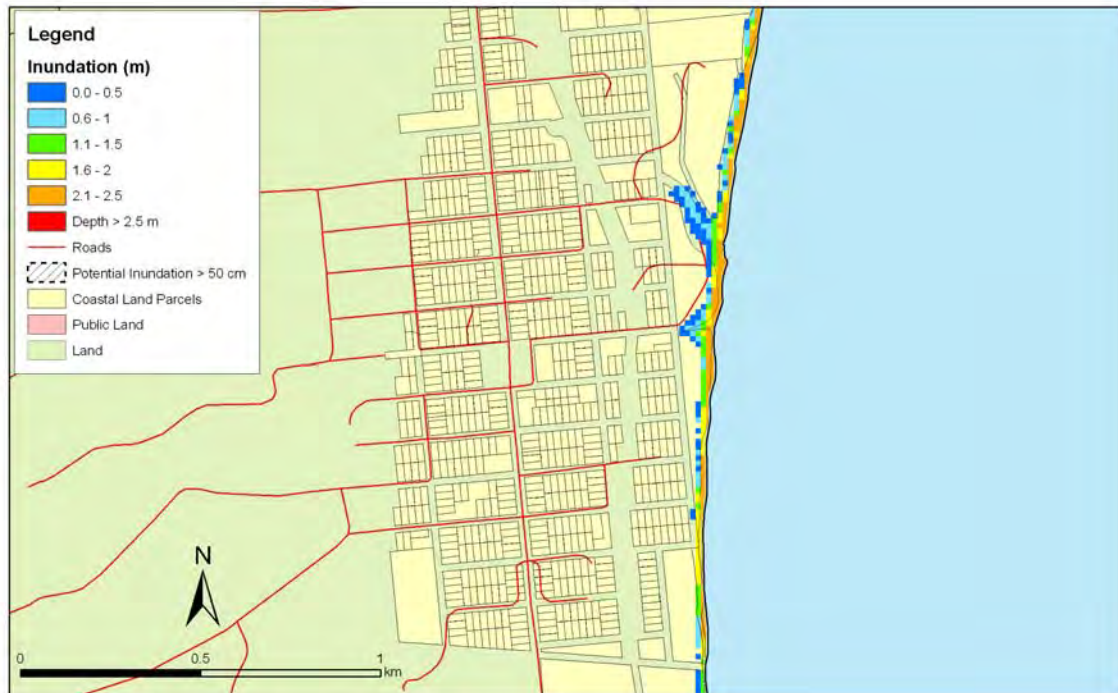


Figure 5.136: Hampden – Puysegur tsunami: Maximum water depth for inundated land (top) and maximum speed (bottom) for MHWS.

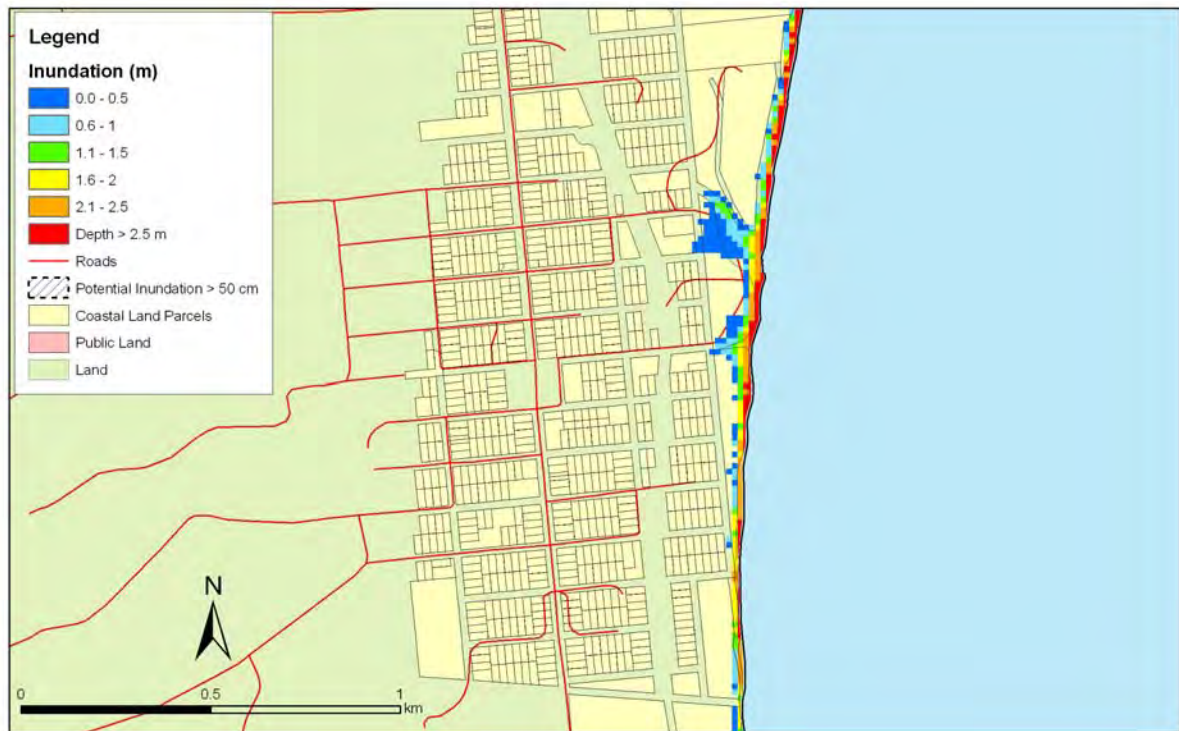


Figure 5.137: Hampden – Puysegur tsunami: Maximum water depth for inundated land (top) and maximum speed (bottom) for MHWS with a sea level rise of 30 cm.

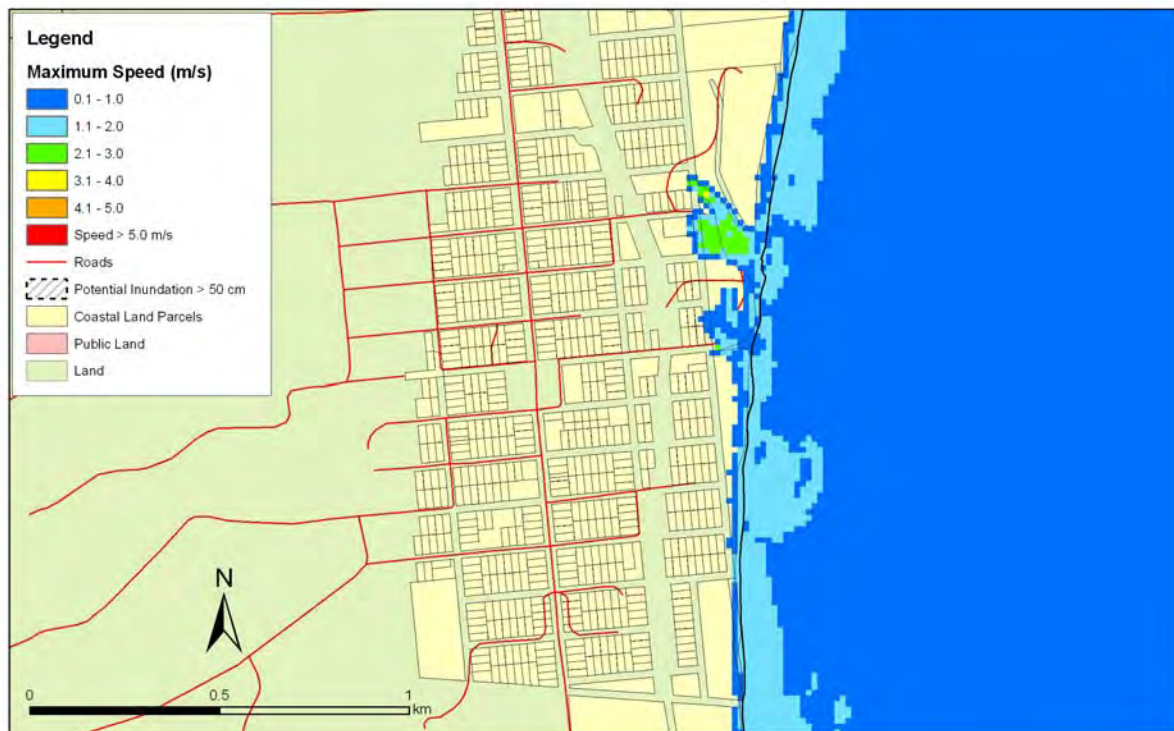
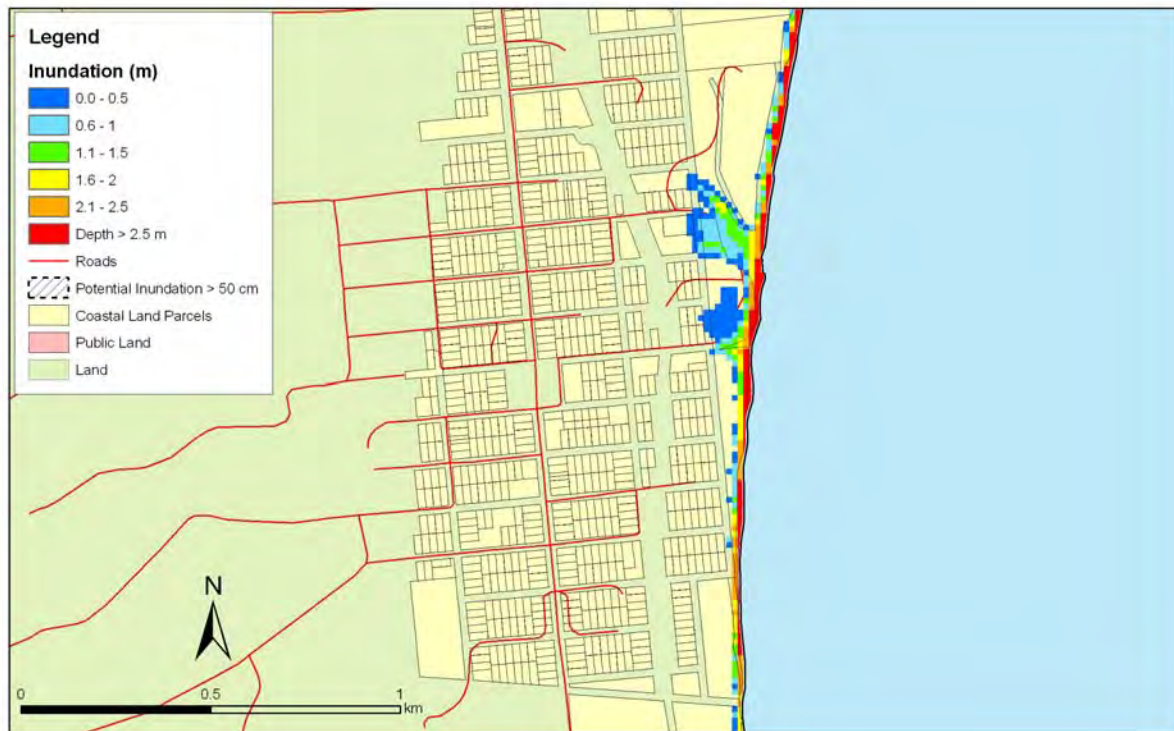


Figure 5.138: Hampden – Puysegur tsunami: Maximum water depth for inundated land (top) and maximum speed (bottom) for MHWS with a sea level rise of 50 cm.

Hampden: Far-Field

- Both remote tsunamis begin with an increase in the water level.
- Second wave is highest with amplitude 1.2m, total height 2.4m for 1:100 year tsunami and amplitude 1.8m, total height 3.6m for the 1:500 year tsunami.
- Big waves well after the main arrivals – up to 12 hours – with smaller waves after that.
- Resonance period around 105 minutes and also 80 minutes.
- Maximum runup: up to 2.2 metres for the 1:100 year tsunami and 2.8 metres for the 1:500 year tsunami.
- The inundation is similar to that of the Puysegur tsunami for the 1:100 year tsunami and its associated sea level rise scenarios. For the 1:500 year tsunami the inundation reaches further inland but following the same pattern as the other tsunamis.
- The maximum water speeds are lower than for the Puysegur tsunami and thus the risk of erosion is also less.

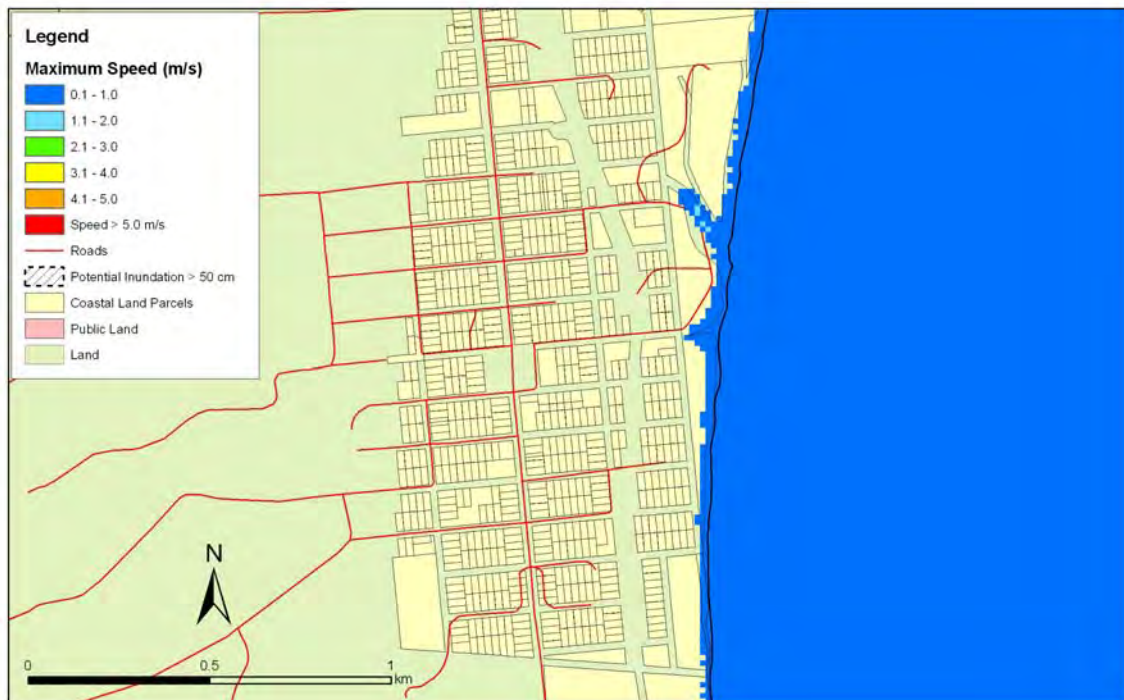
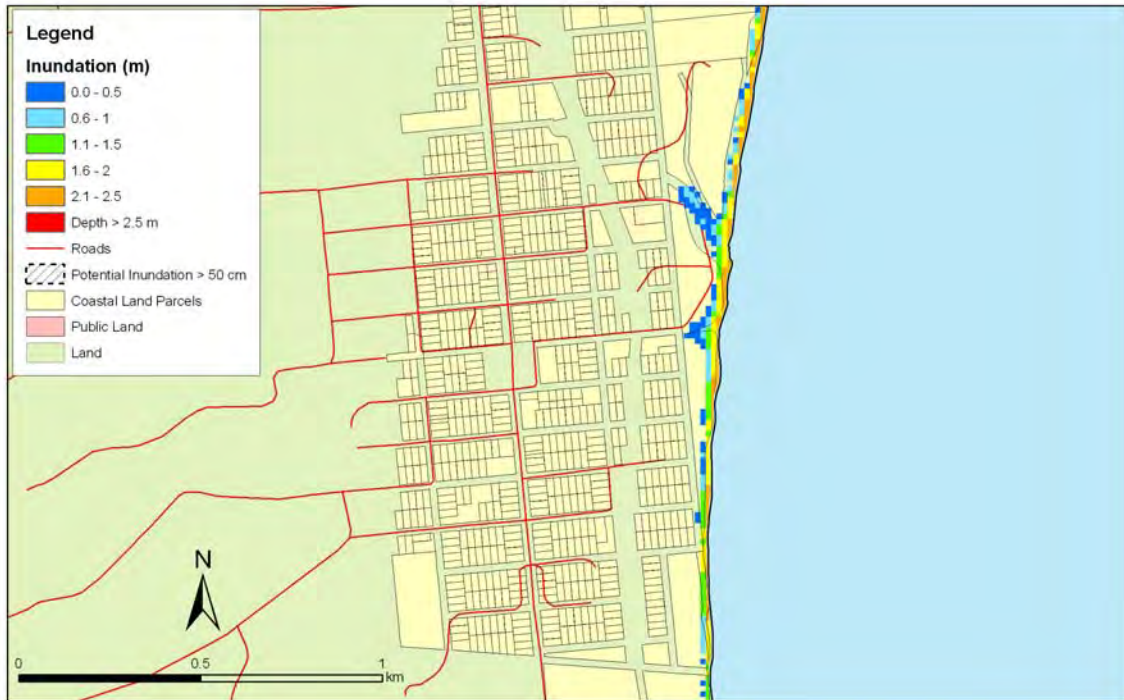


Figure 5.139: Hampden – 1:100 year remote tsunami: Maximum water depth for inundated land (top) and maximum speed (bottom) for MHWS.

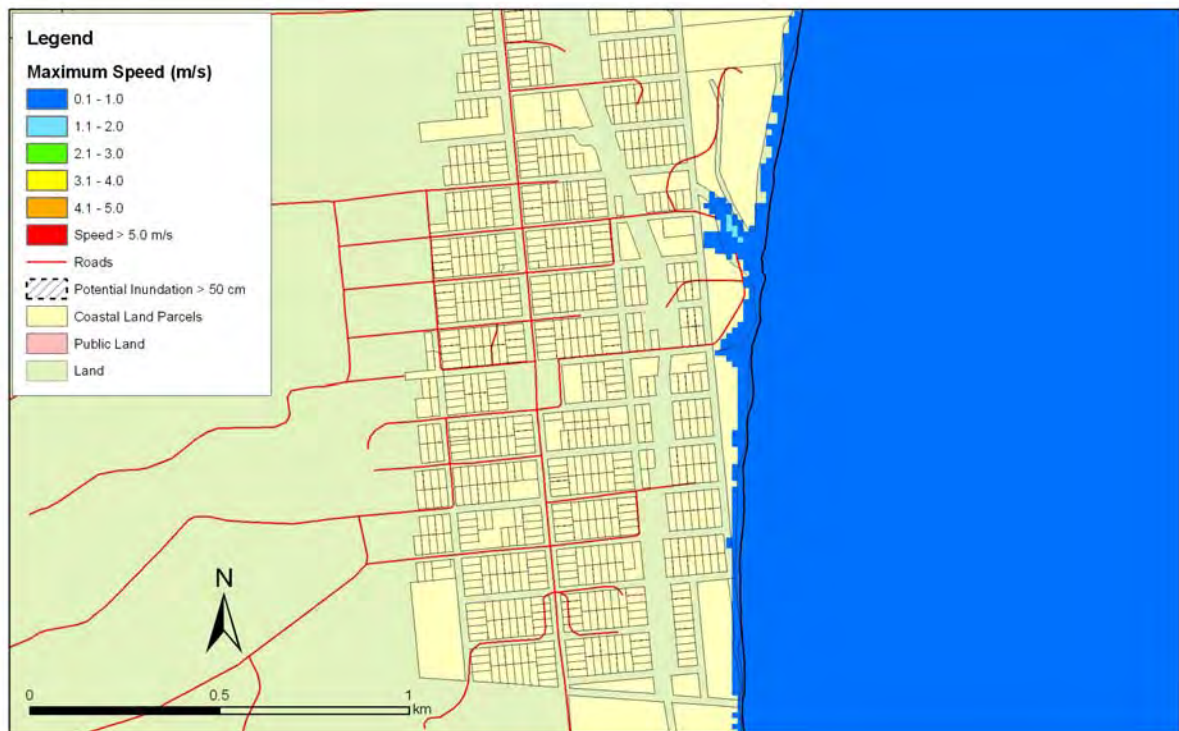
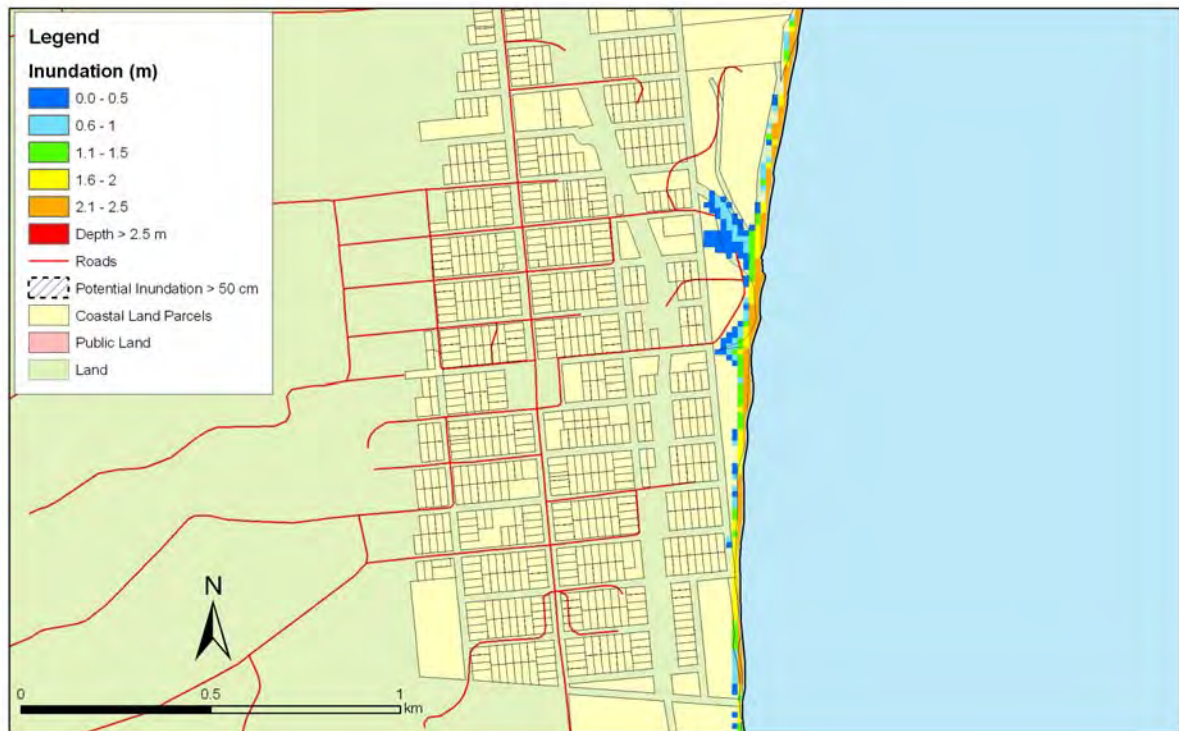


Figure 5.140: Hampden – 1:100 year remote tsunami: Maximum water depth for inundated land (top) and maximum speed (bottom) for MHWS with a sea level rise of 30 cm.

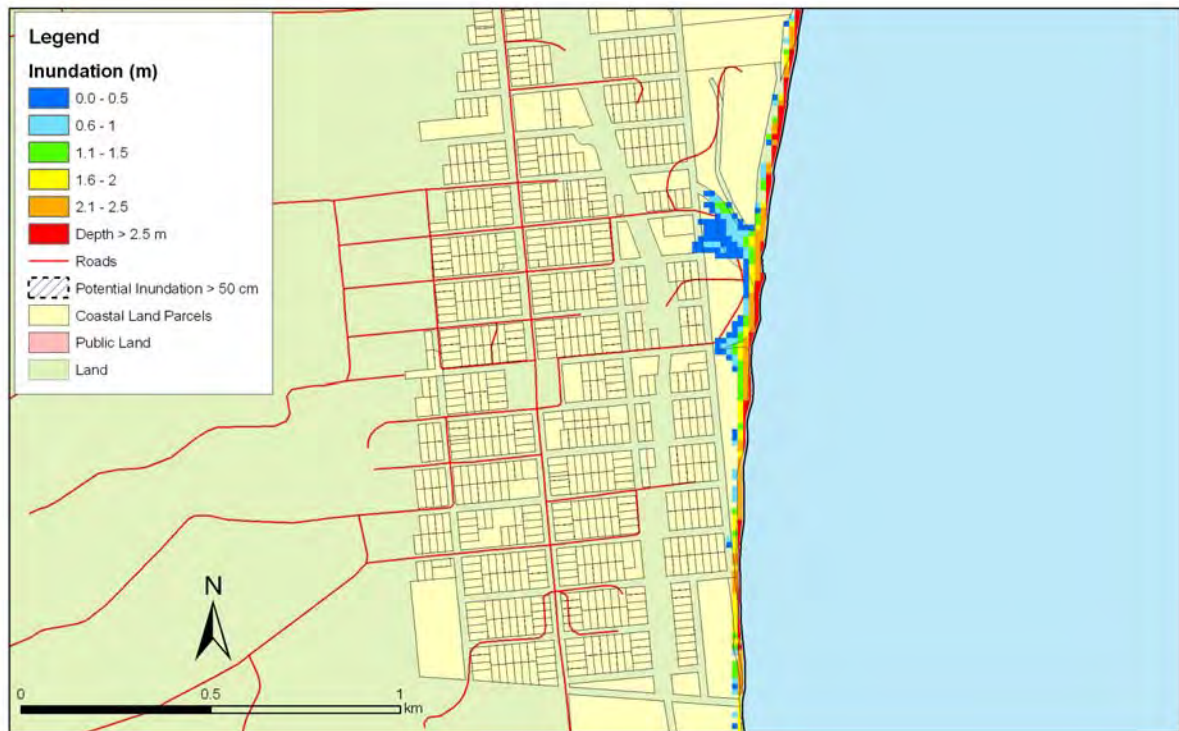


Figure 5.141: Hampden – 1:100 year remote tsunami: Maximum water depth for inundated land (top) and maximum speed (bottom) for MHWS with a sea level rise of 50 cm.

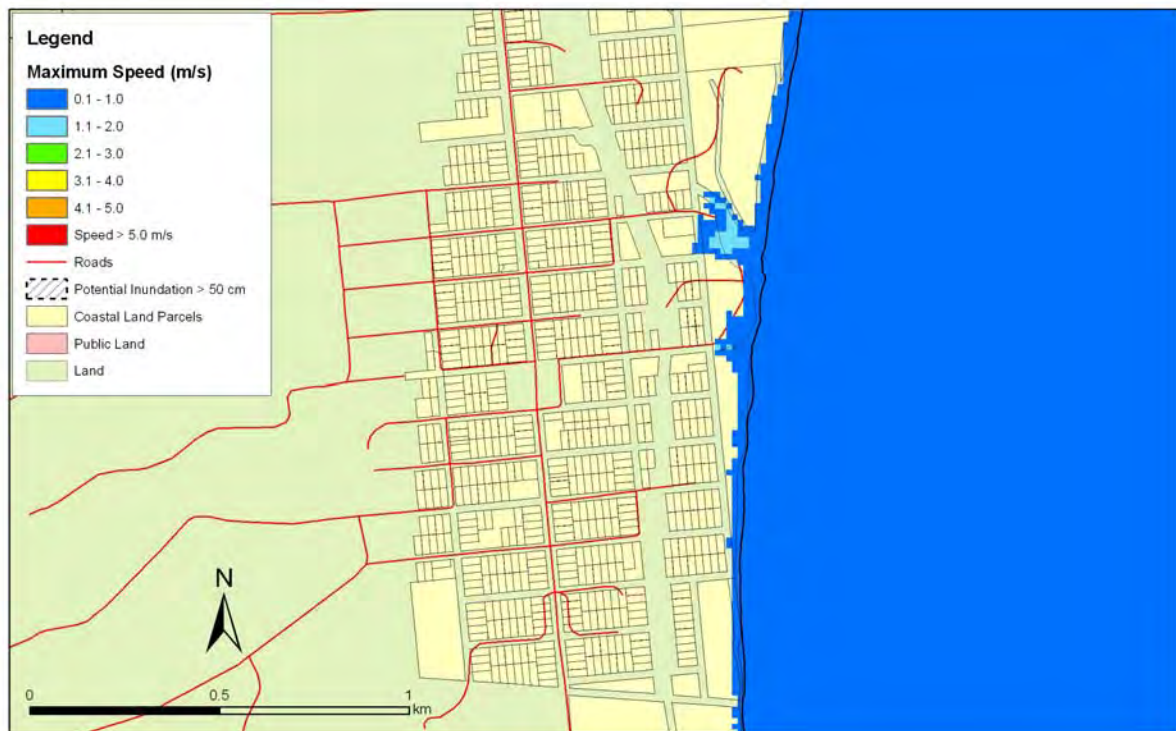
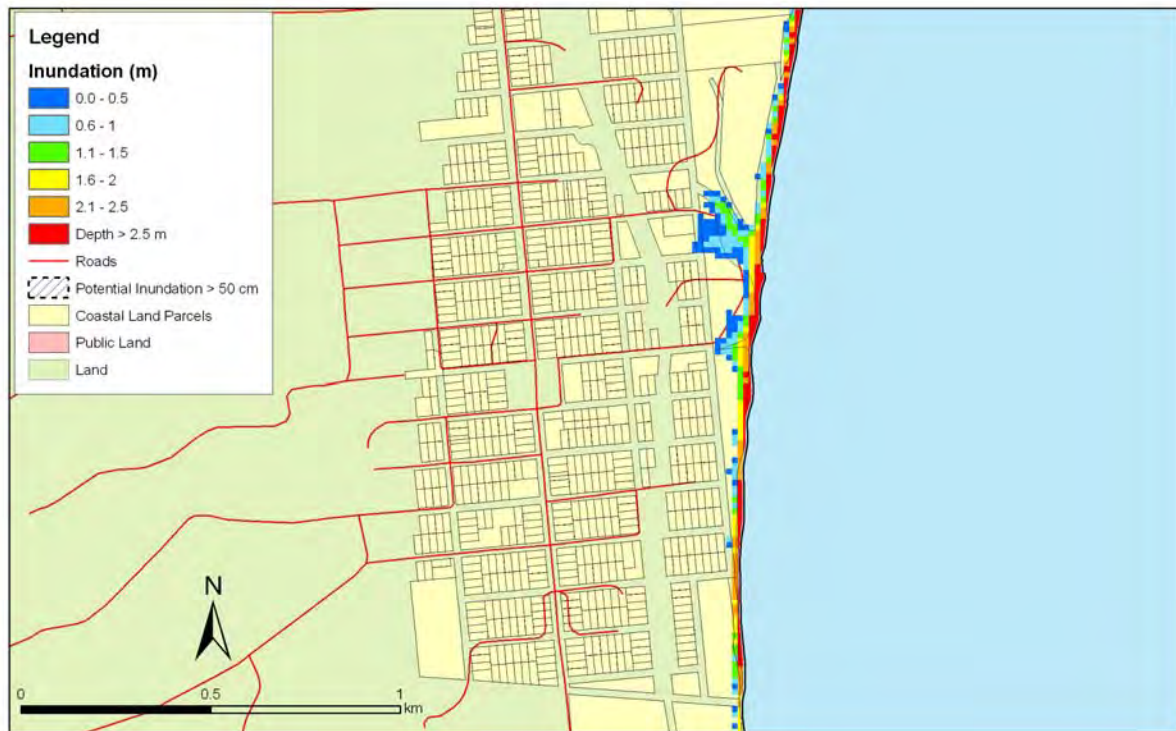


Figure 5.142: Hampden – 1:500 year remote tsunami: Maximum water depth for inundated land (top) and maximum speed (bottom) for MHWS.

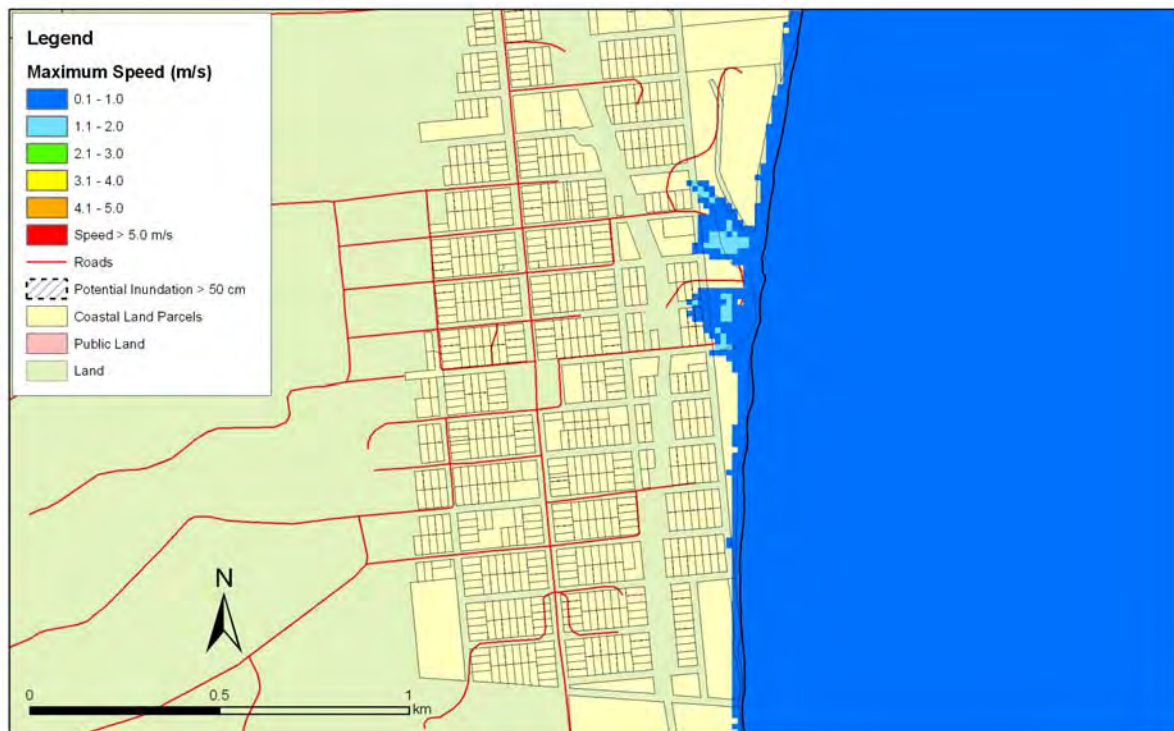
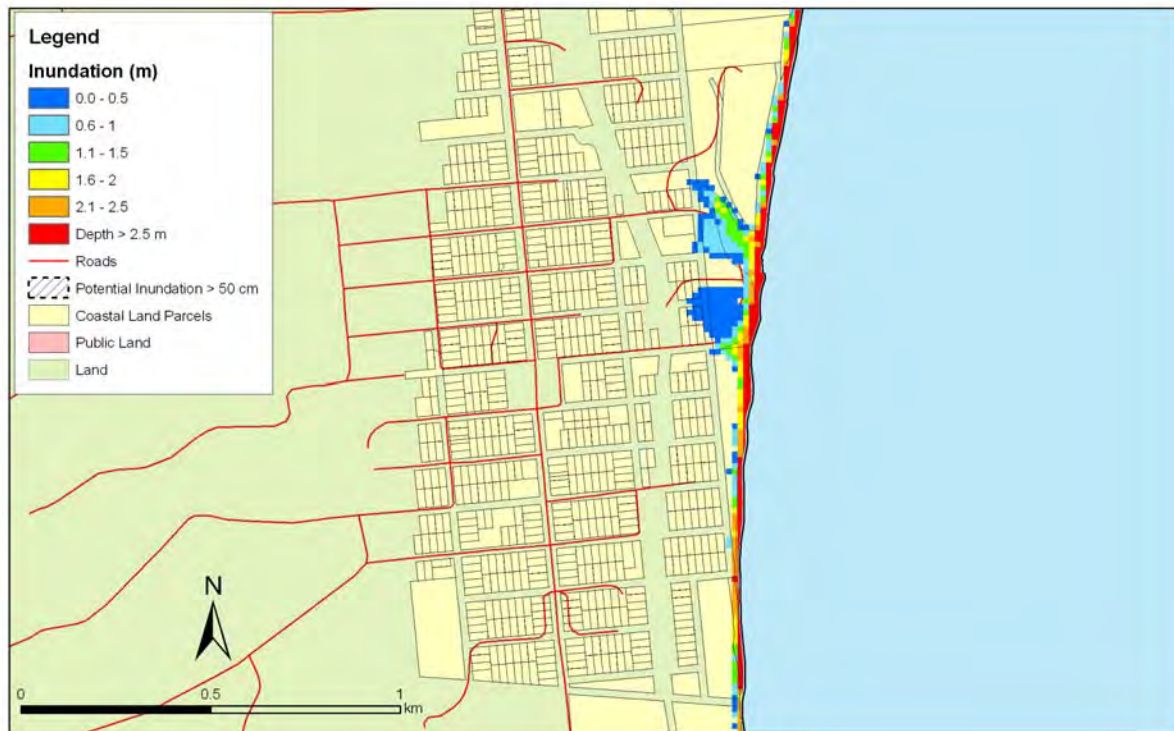


Figure 5.143: Hampden – 1:500 year remote tsunami: Maximum water depth for inundated land (top) and maximum speed (bottom) for MHWS with a sea level rise of 30 cm.

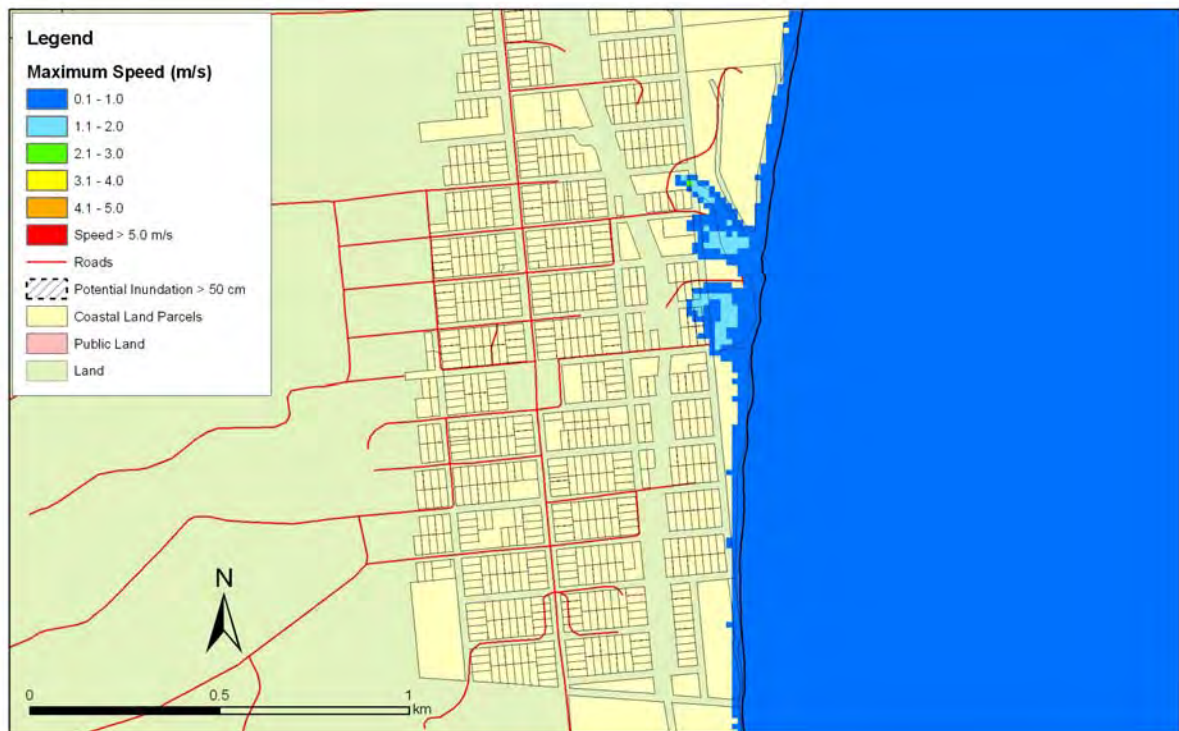
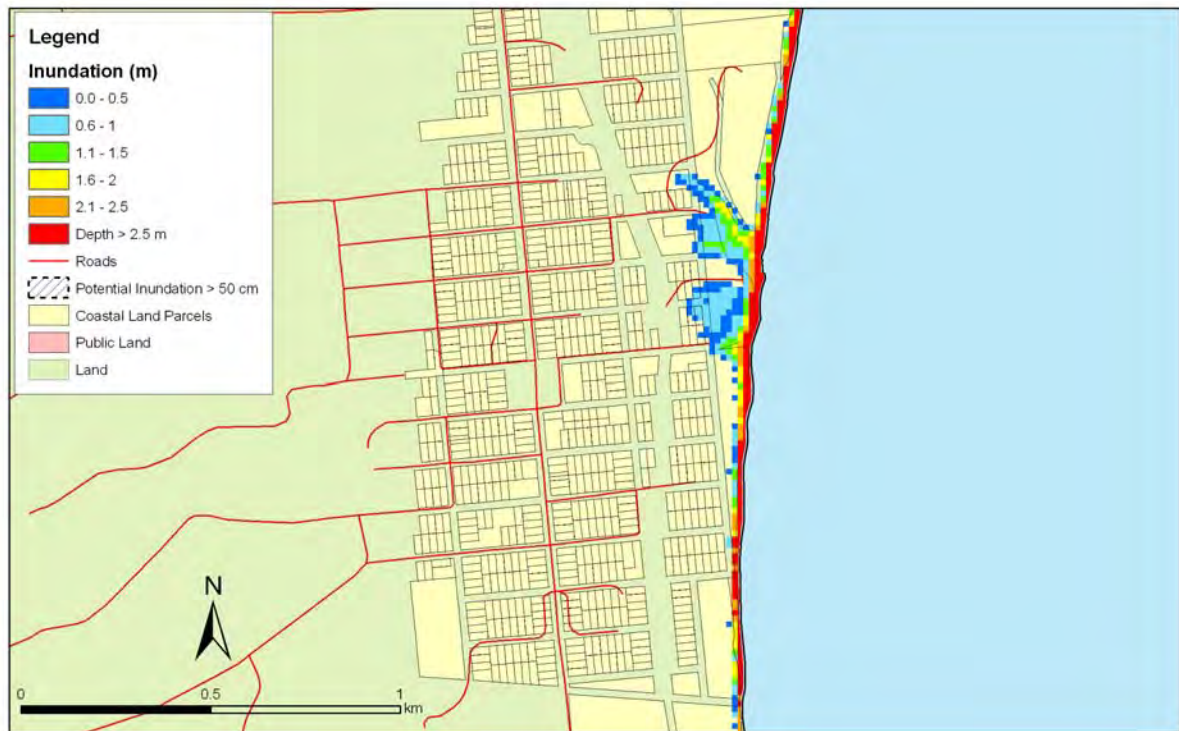


Figure 5.144: Hampden – 1:500 year remote tsunami: Maximum water depth for inundated land (top) and maximum speed (bottom) for MHWS with a sea level rise of 50 cm.

5.3.16 Taranui and Kakanui

5.145 – 5.147 show maximum inundation and water speed for the near-field (Puysegur) tsunami scenarios for this area. Figures 5.148-5.150 show maximum inundation and water speeds for the 1:100 year remote tsunami for Taranui and Kakanui. Figures 5.151-5.153 show maximum inundation and water speeds for the 1:500 year remote tsunami for Taranui and Kakanui.

Taranui and Kakanui: Near-Field

- Trough arrives first approximately 100 minutes after fault rupture. Water level decreases 35 cm over 40 minutes.
- First main wave is the biggest. Arrives around 2.9 hours after fault rupture. Amplitude 0.9 m.
- Several other waves with amplitude around 50 cm.
- Predominant period of wave arrivals: 100 minutes and also 25 minutes.
- Maximum runup: up to 2 metres.
- There is some land that lies right on the coast or the banks of the river that is inundated in the current sea level scenario. The spit at the entrance to the Kakanui River is over topped.
- The inundation is considerably increased in the two sea level rise scenarios – especially the 50 cm rise. Maximum speed at the mouth of the Kakanui River is also considerably higher meaning that the erosion risk is higher.

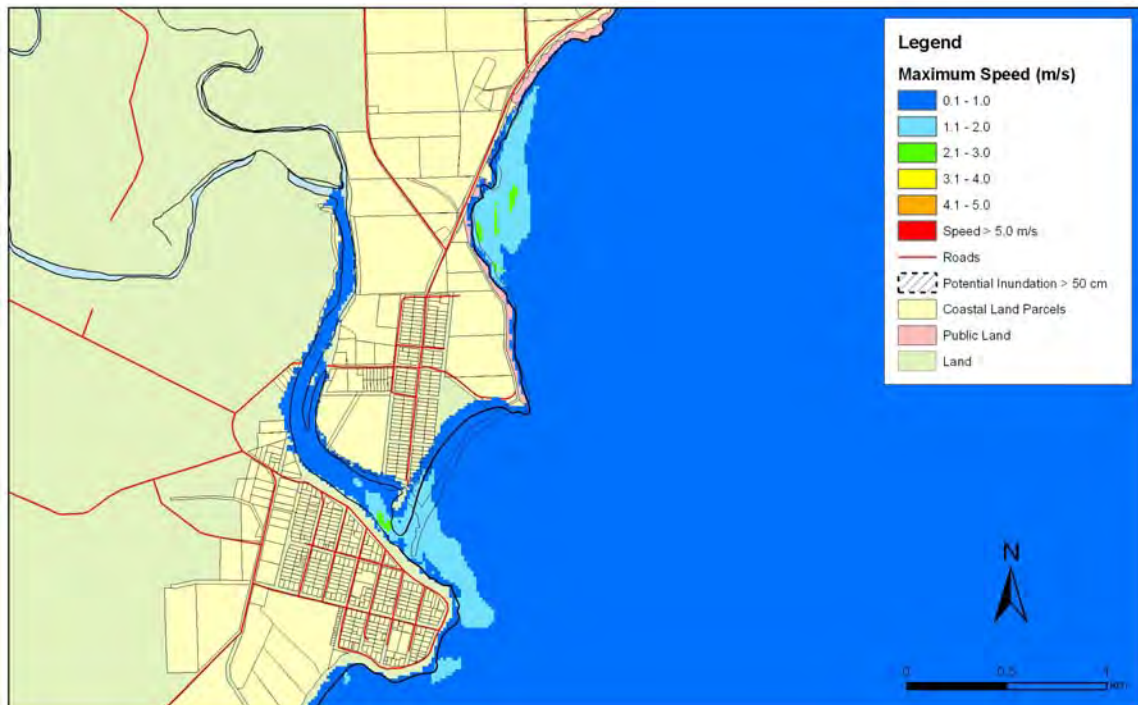


Figure 5.145: Taranui and Kakanui – Puysegur tsunami: Maximum water depth for inundated land (top) and maximum speed (bottom) for MHWS.

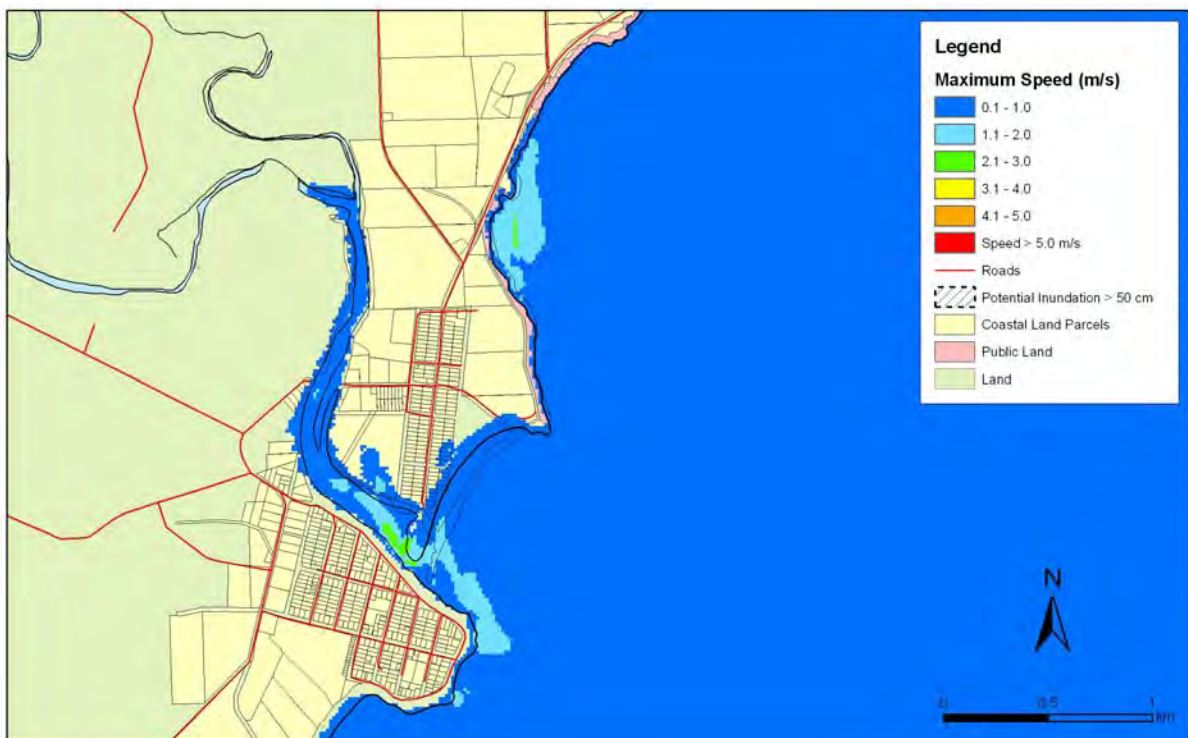


Figure 5.146: Taranui and Kakanui – Puysegur tsunami: Maximum water depth for inundated land (top) and maximum speed (bottom) for MHWS with a sea level rise of 30 cm.

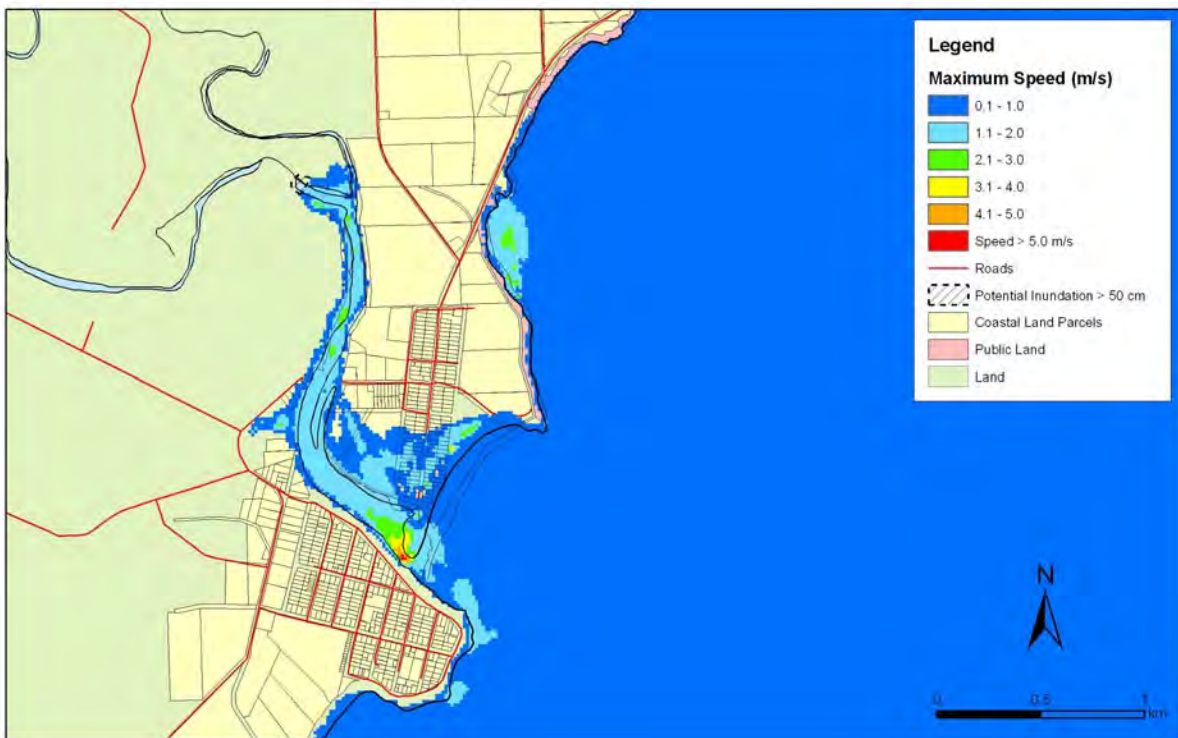
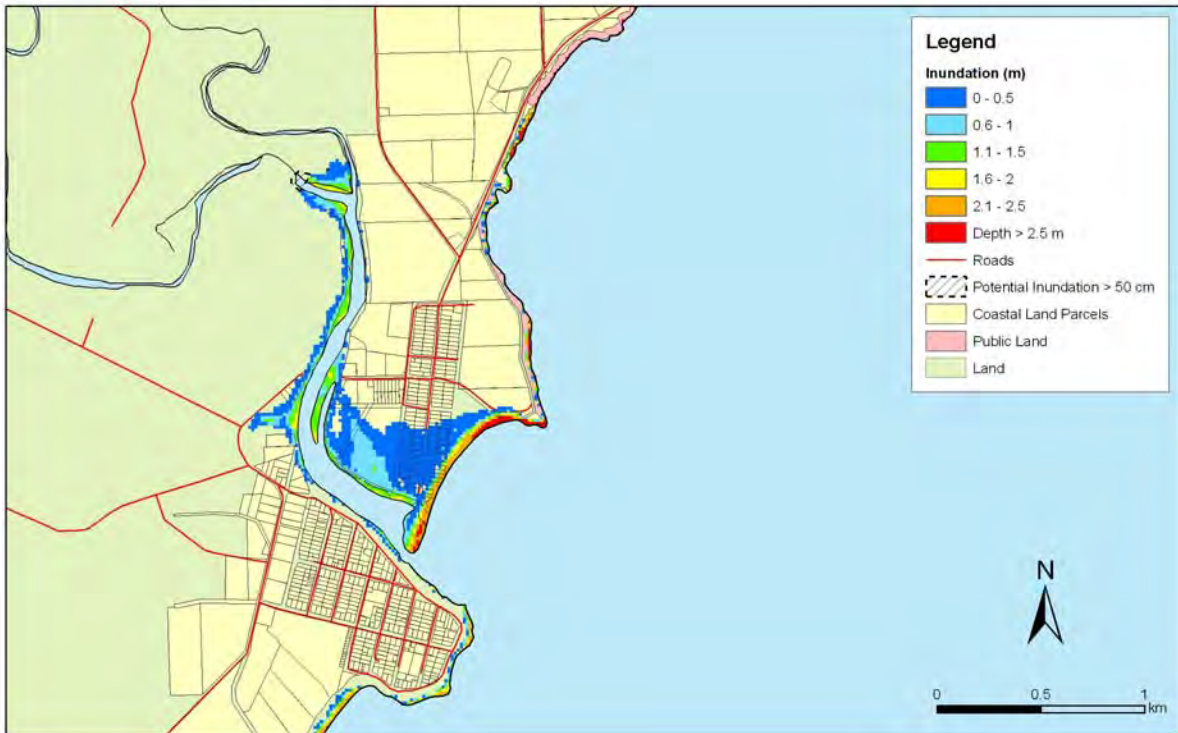


Figure 5.147: Taranui and Kakanui – Puysegur tsunami: Maximum water depth for inundated land (top) and maximum speed (bottom) for MHWS with a sea level rise of 50 cm.

Taranui and Kakanui: Far-Field

- Both remote tsunamis begin with an increase in the water level.
- Second wave is highest with amplitude 1.2m, total height 2.2m for the 1:100 year tsunami and amplitude 1.8m, total height 3.6m for the 1:500 year tsunami.
- Big waves well after the main arrivals – up to 12 hours – with smaller waves after that.
- Resonance period around 105 minutes and also 80 minutes.
- Maximum runup: up to 2.1 metres for 1:100 year tsunami and 2.8 metres for 1:500 year tsunami.
- Land on the north side of the Kakanui River is inundated by the 1:100 year tsunami at MHWS. Also land on the Taranui side near the bend in the river is inundated. This inundation is increased for the sea level rise scenarios and also the 1:500 year tsunami scenarios (The 1:500 year tsunami adding approximately 50 cm onto the water height of the 1:100 year tsunami).
- The sand spit is overtopped and there is risk of erosion there, especially for the larger tsunami scenarios.

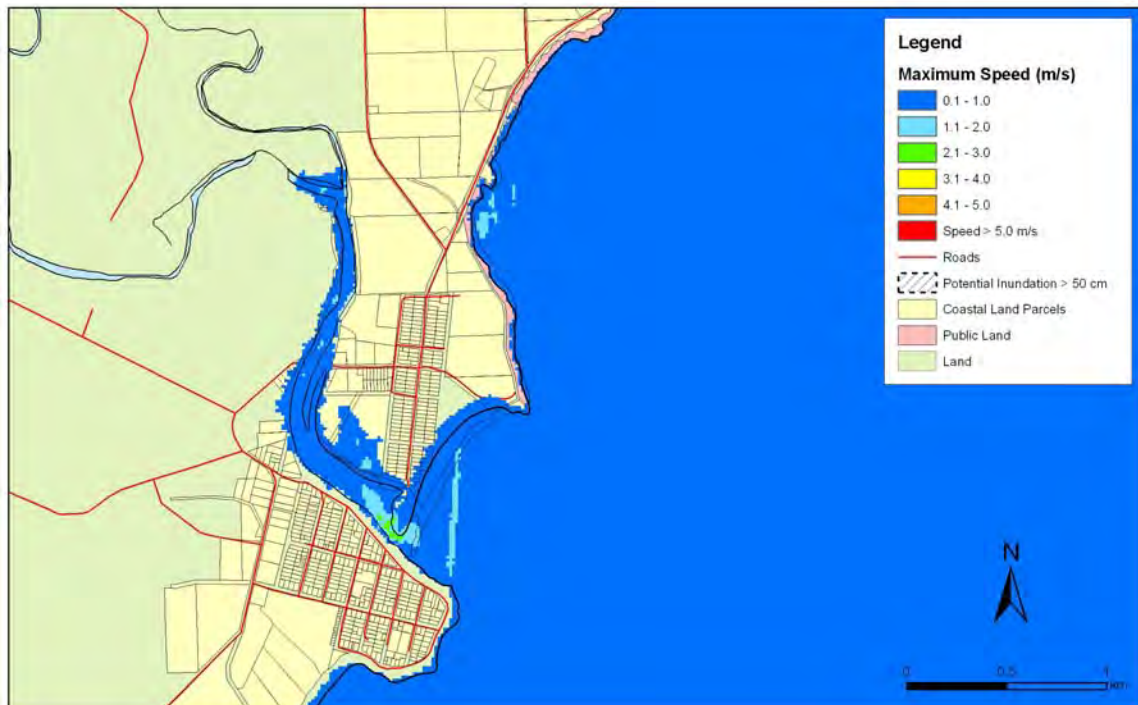
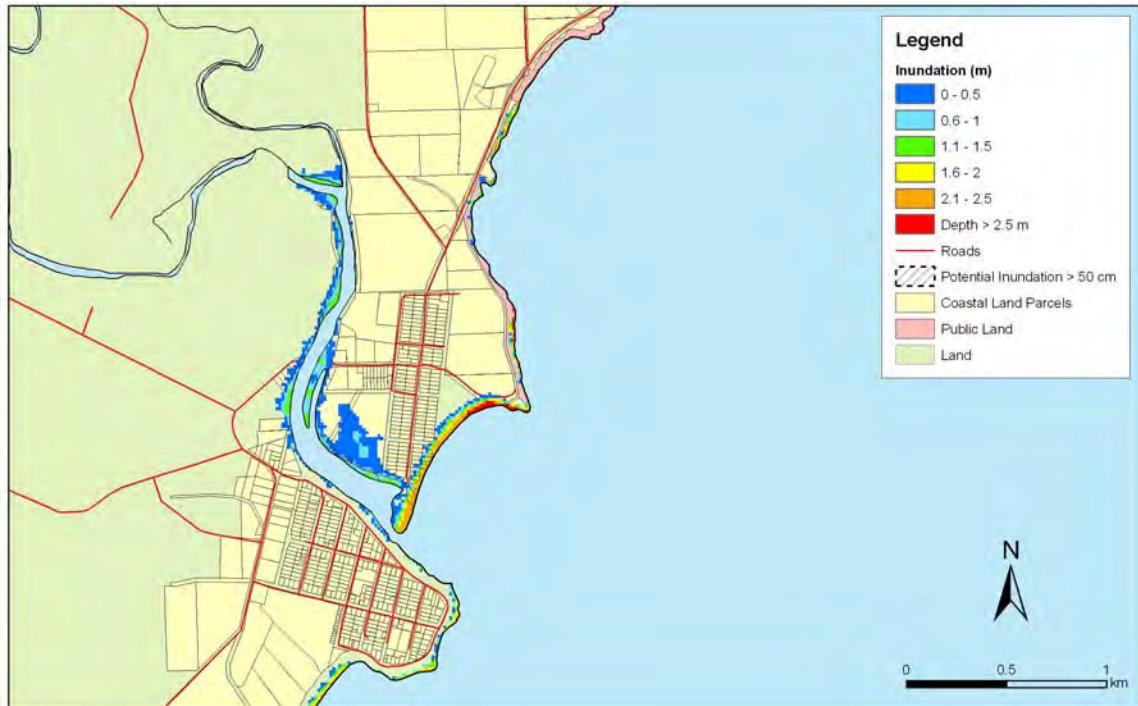


Figure 5.148: Kakanui and Taranui – 1:100 year remote tsunami: Maximum water depth for inundated land (top) and maximum speed (bottom) for MHWS.

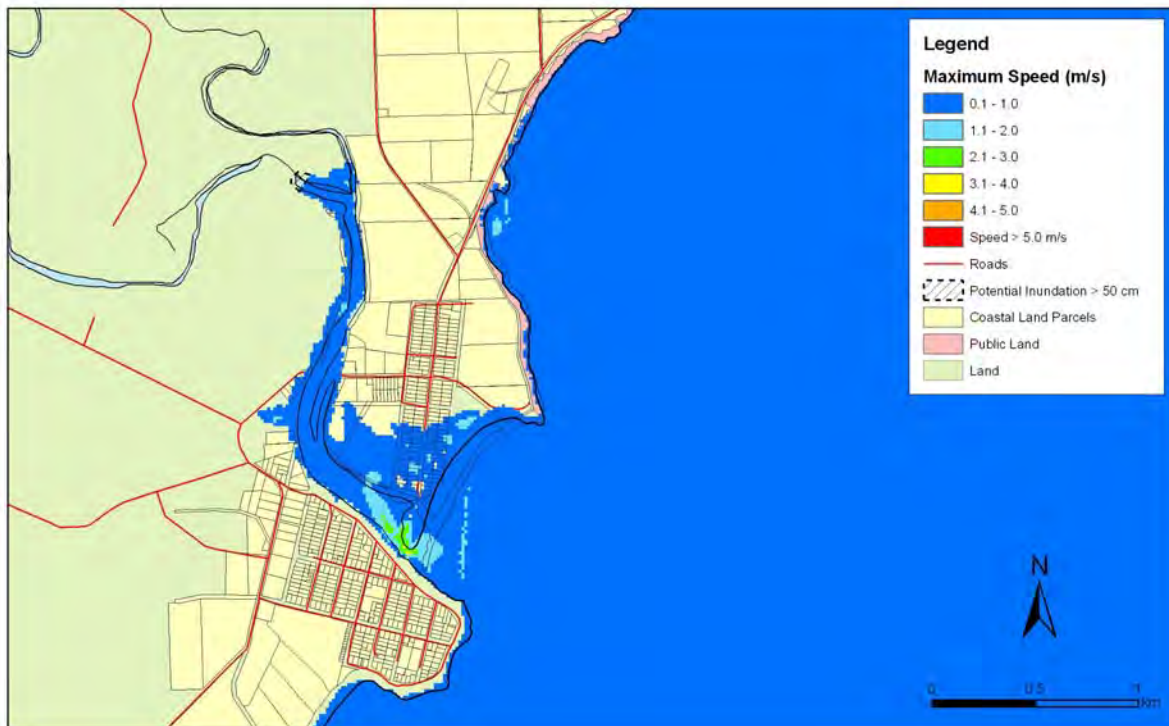


Figure 5.149: Kakanui and Taranui – 1:100 year remote tsunami: Maximum water depth for inundated land (top) and maximum speed (bottom) for MHWS with a sea level rise of 30 cm.

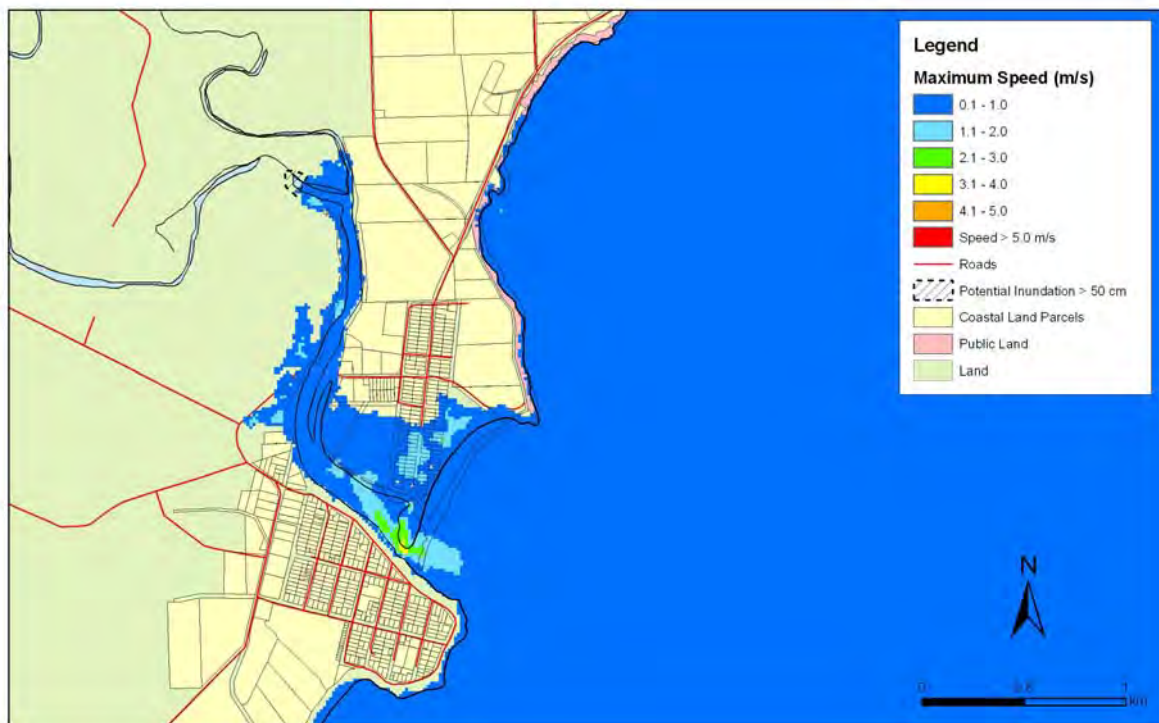
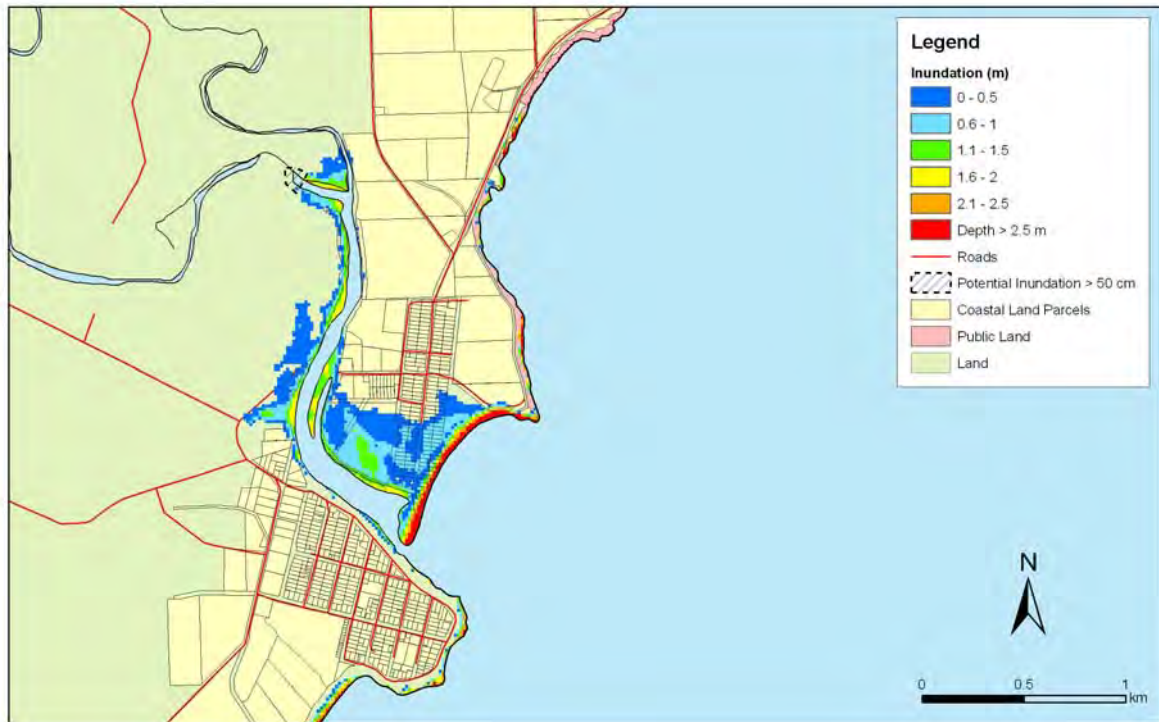


Figure 5.150: Kakanui and Taranui – 1:100 year remote tsunami: Maximum water depth for inundated land (top) and maximum speed (bottom) for MHWS with a sea level rise of 50 cm.

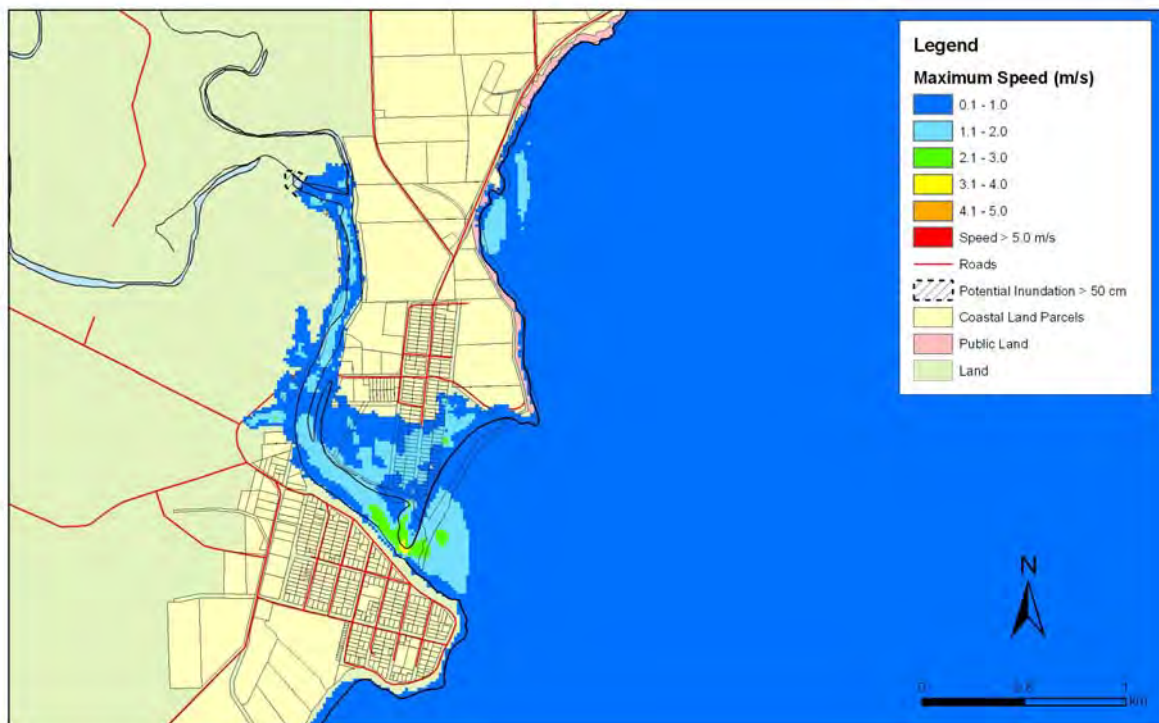
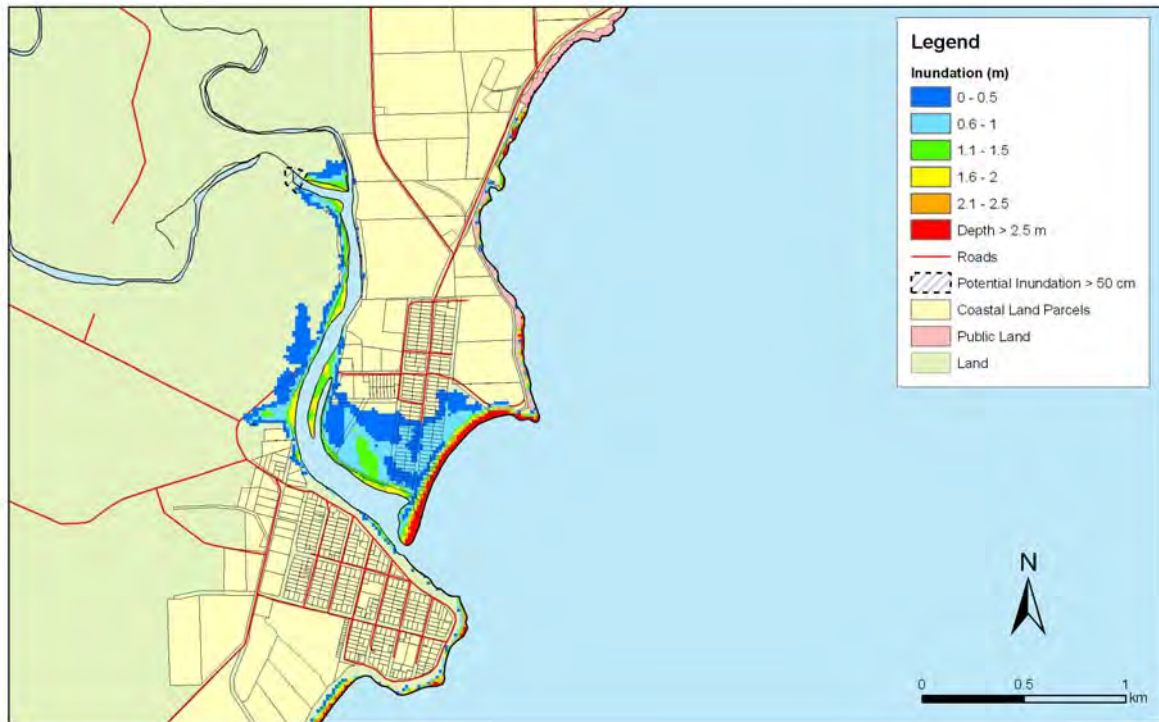


Figure 5.151: Kakanui and Taranui – 1:500 year remote tsunami: Maximum water depth for inundated land (top) and maximum speed (bottom) for MHWS.

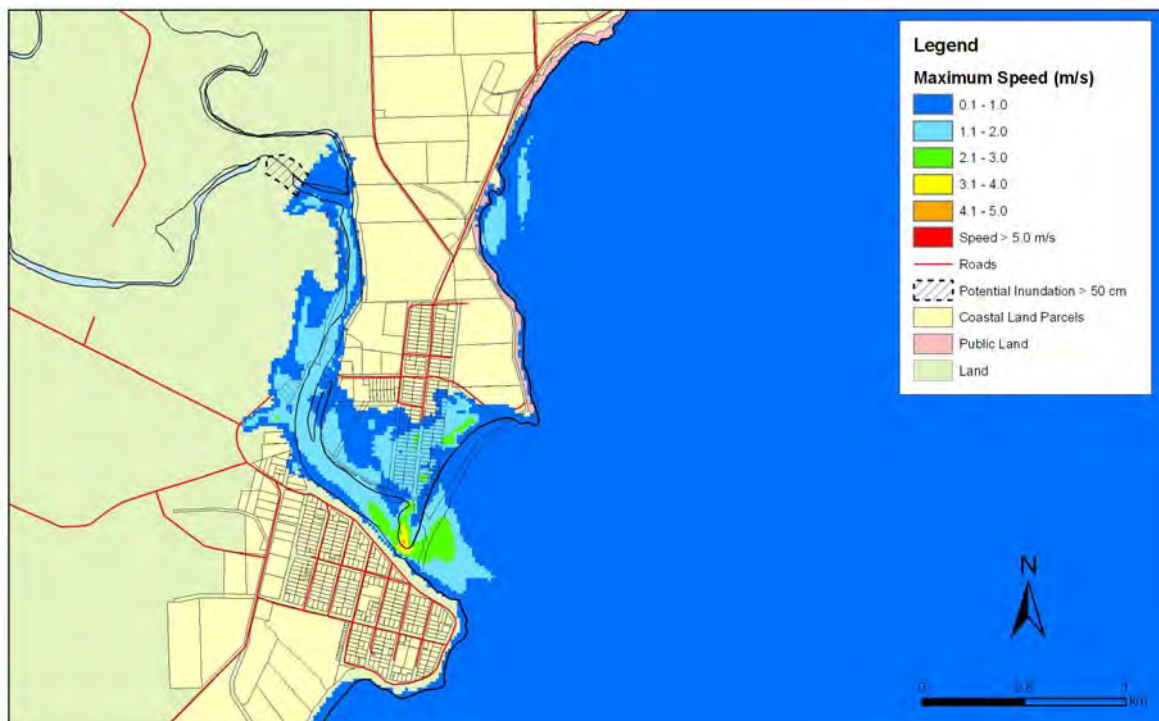
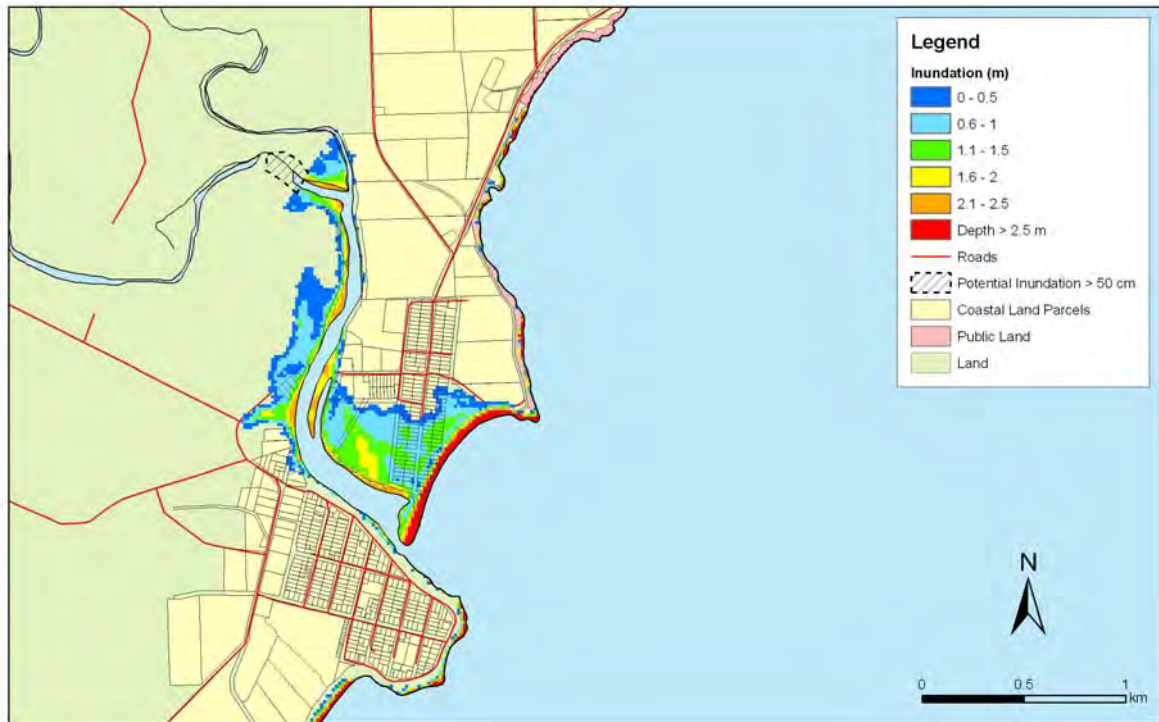


Figure 5.152: Kakanui and Taranui – 1:500 year remote tsunami: Maximum water depth for inundated land (top) and maximum speed (bottom) for MHWS with a sea level rise of 30 cm.

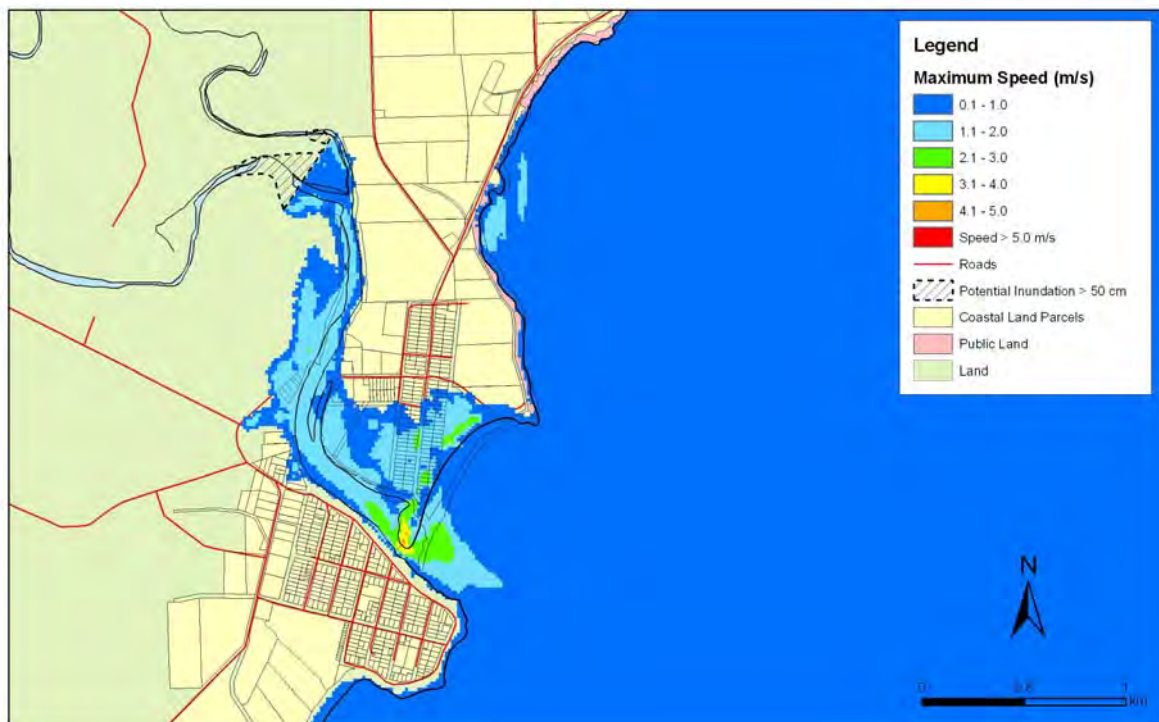
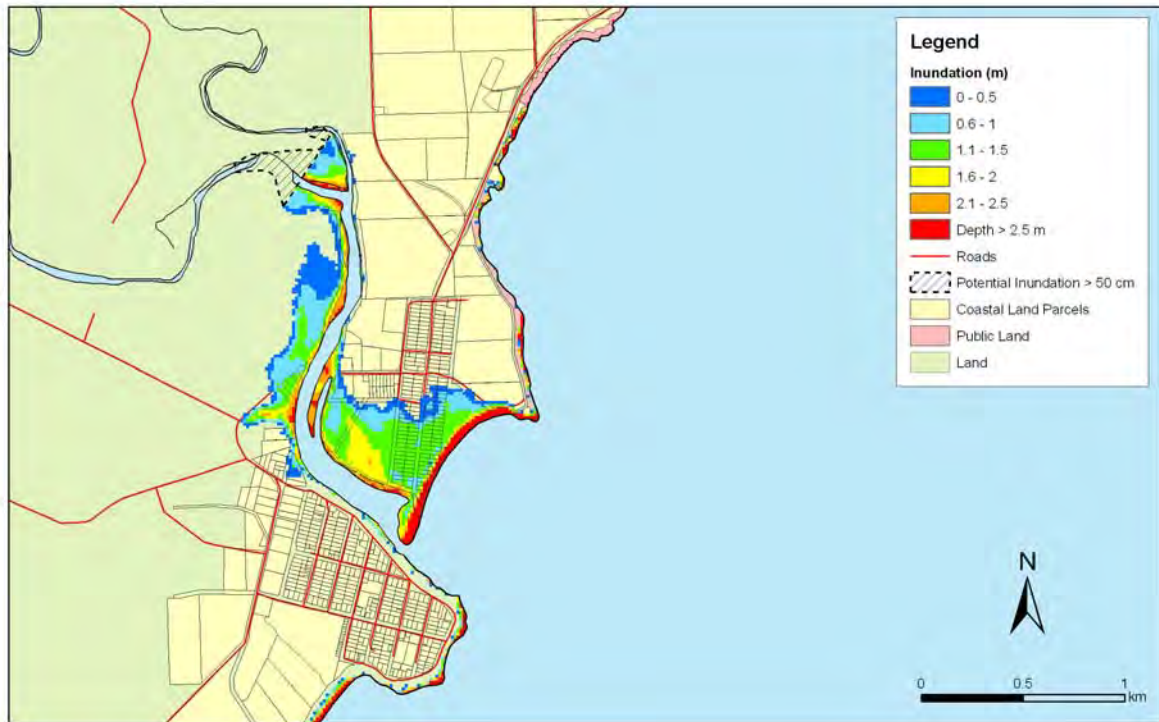


Figure 5.153: Kakanui and Taranui – 1:500 year remote tsunami: Maximum water depth for inundated land (top) and maximum speed (bottom) for MHWS with a sea level rise of 50 cm.

5.3.17 Oamaru

It should be noted that the inundation scenarios for Oamaru are based upon the 2004 LIDAR survey. The modelling therefore does not take account for any subsequent changes to the geomorphology of the coast.

Figures 5.154 – 5.156 show maximum inundation and water speed for the near-field (Puysegur) tsunami scenarios for this area. Figures 5.157-5.159 show maximum inundation and water speeds for the 1:100 year remote tsunami for Oamaru. Figures 5.160-5.162 show maximum inundation and water speeds for the 1:500 year remote tsunami for Oamaru.

Oamaru: Near-Field

- Trough arrives first approximately 105 minutes after fault rupture. Water level decreases 45 cm over 40 minutes.
- Small arrival before first main wave. First main wave is the biggest. Arrives around 3 hours after fault rupture. Amplitude 1.6 m.
- Several other wave arrivals with amplitude greater than 50 cm.
- Predominant period of wave arrivals: 100 minutes and 25 minutes.
- Maximum runup: up to 2.6 metres
- Inundation is confined to the coastline.
- The sea level rise scenarios increase the inundation but do not significantly change the outcome.



Figure 5.154: Oamaru – Puysegur tsunami: Maximum water depth for inundated land (top) and maximum speed (bottom) for MHWS.



Figure 5.155: Oamaru – Puysegur tsunami: Maximum water depth for inundated land (top) and maximum speed (bottom) for MHWS with a sea level rise of 30 cm.



Figure 5.156: Oamaru – Puysegur tsunami: Maximum water depth for inundated land (top) and maximum speed (bottom) for MHWS with a sea level rise of 50 cm.

Oamaru: Far-Field

- Both remote tsunamis begin with an increase in the water level.
- Second wave is highest with amplitude 1.2 m, total height 2.2 m for the 1:100 year tsunami and amplitude 1.6m, total height 3.2m for the 1:500 year tsunami.
- Big waves continue well after main arrivals – up to 12 hours – with smaller waves after that. Resonance period around 105 minutes and also 80 minutes.
- Maximum runup: up to 2.1 metres for 1:100 year and up to 2.6 metres for 1:500 year remote tsunami.
- Land right on the coast may be inundated, especially for the 1:500 year tsunami and for the sea level rise cases. The inundation is confined to the coastline in all cases though.

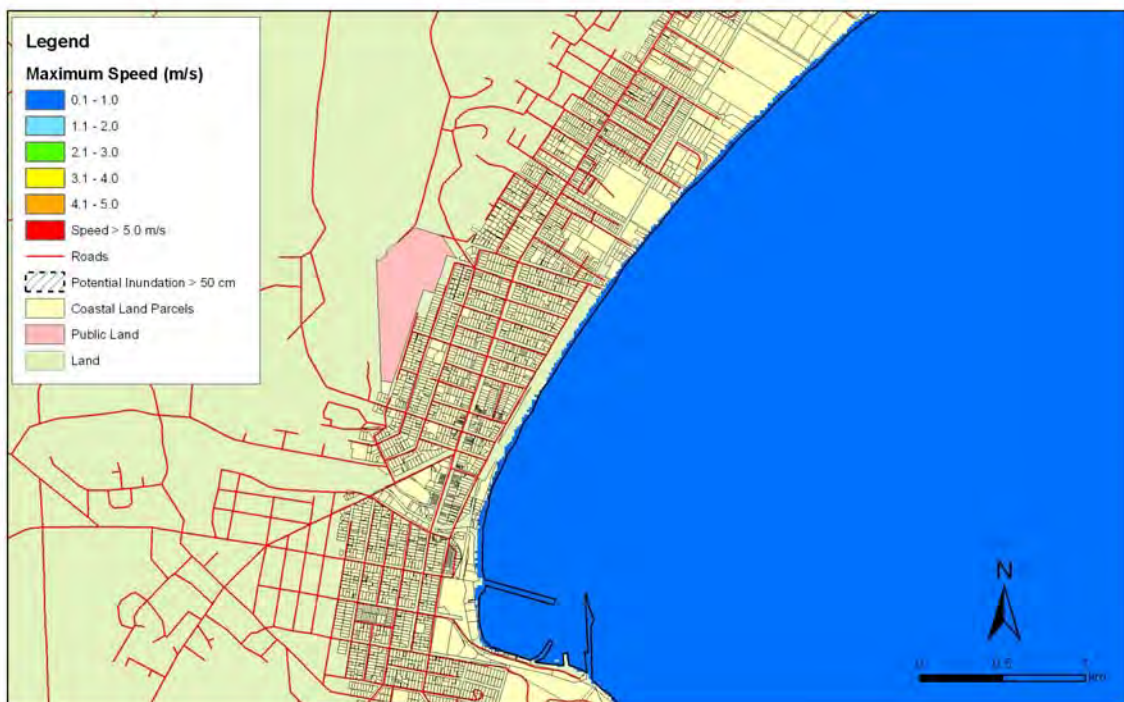


Figure 5.157: Oamaru – 1:100 year remote tsunami: Maximum water depth for inundated land (top) and maximum speed (bottom) for MHWS.

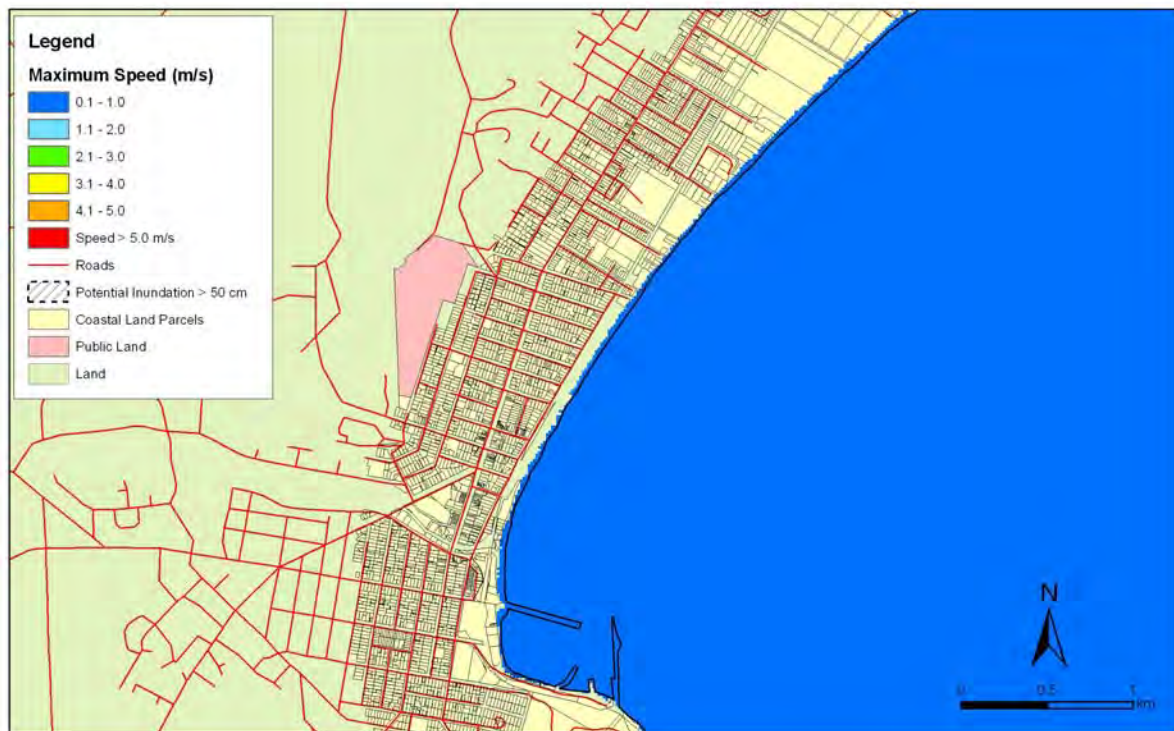


Figure 5.158: Oamaru – 1:100 year remote tsunami: Maximum water depth for inundated land (top) and maximum speed (bottom) for MHWS with a sea level rise of 30 cm..

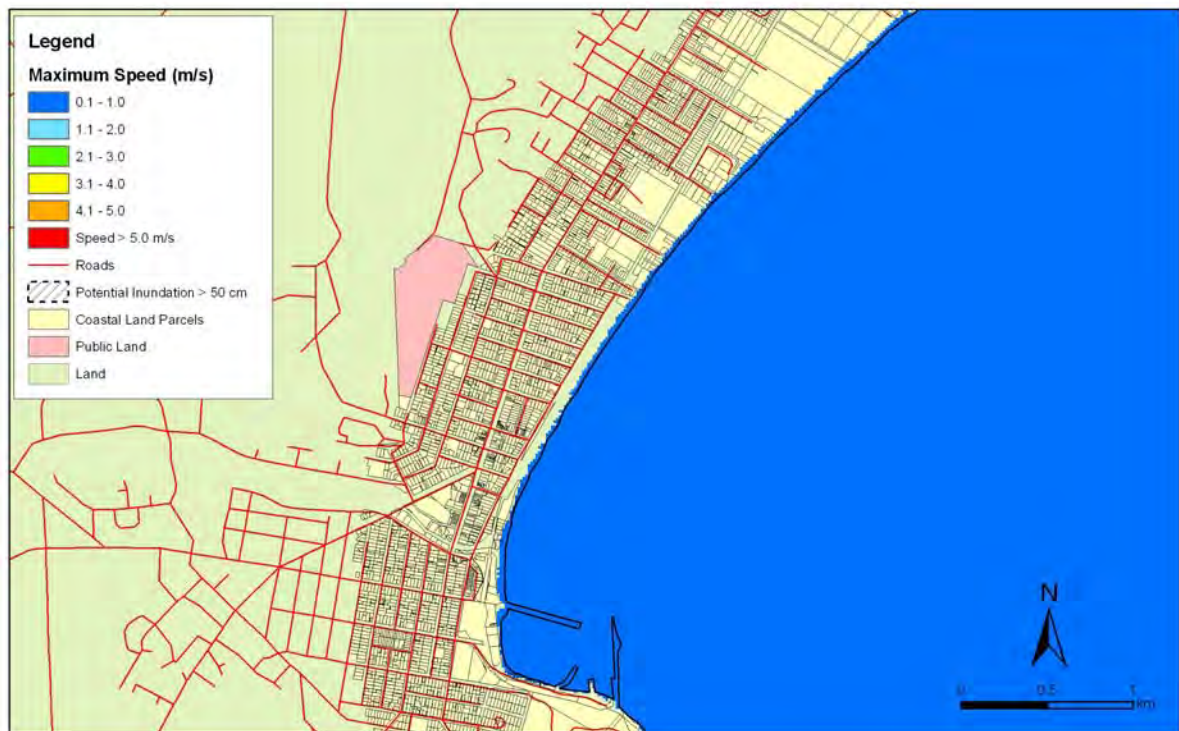


Figure 5.159: Oamaru – 1:100 year remote tsunami: Maximum water depth for inundated land (top) and maximum speed (bottom) for MHWS with a sea level rise of 50 cm.



Figure 5.160: Oamaru – 1:500 year remote tsunami: Maximum water depth for inundated land (top) and maximum speed (bottom) for MHWS.

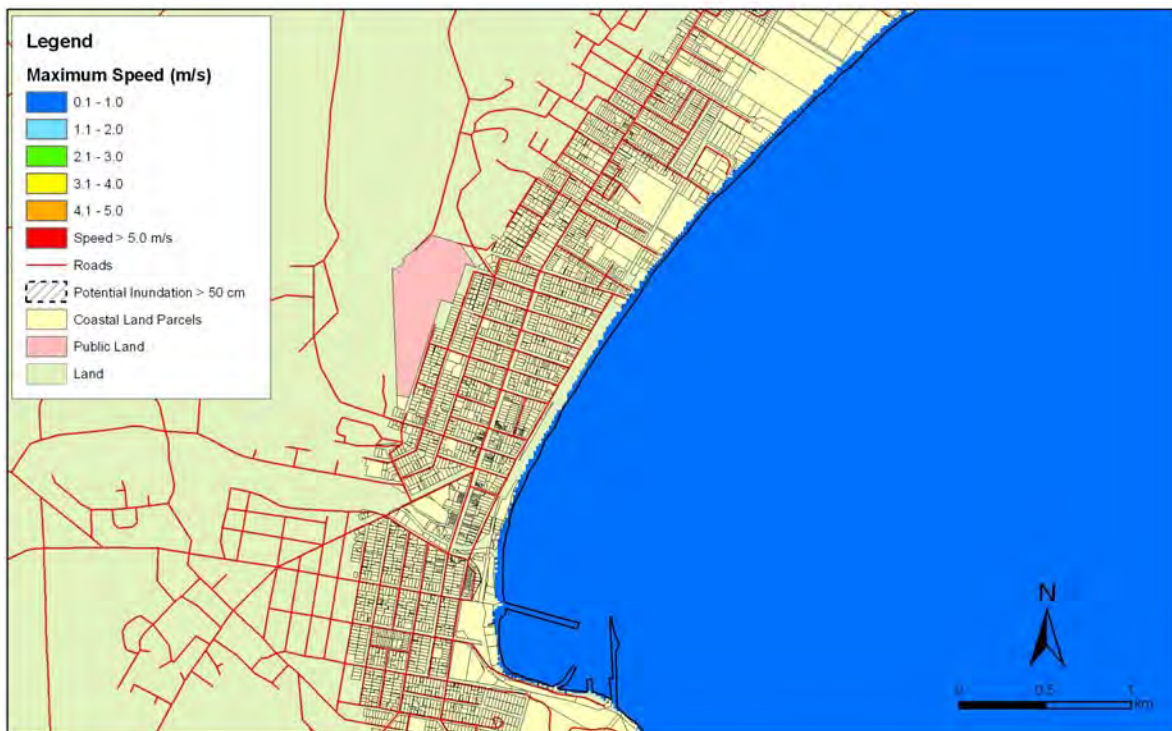


Figure 5.161: Oamaru – 1:500 year remote tsunami: Maximum water depth for inundated land (top) and maximum speed (bottom) for MHWS with a sea level rise of 30 cm.

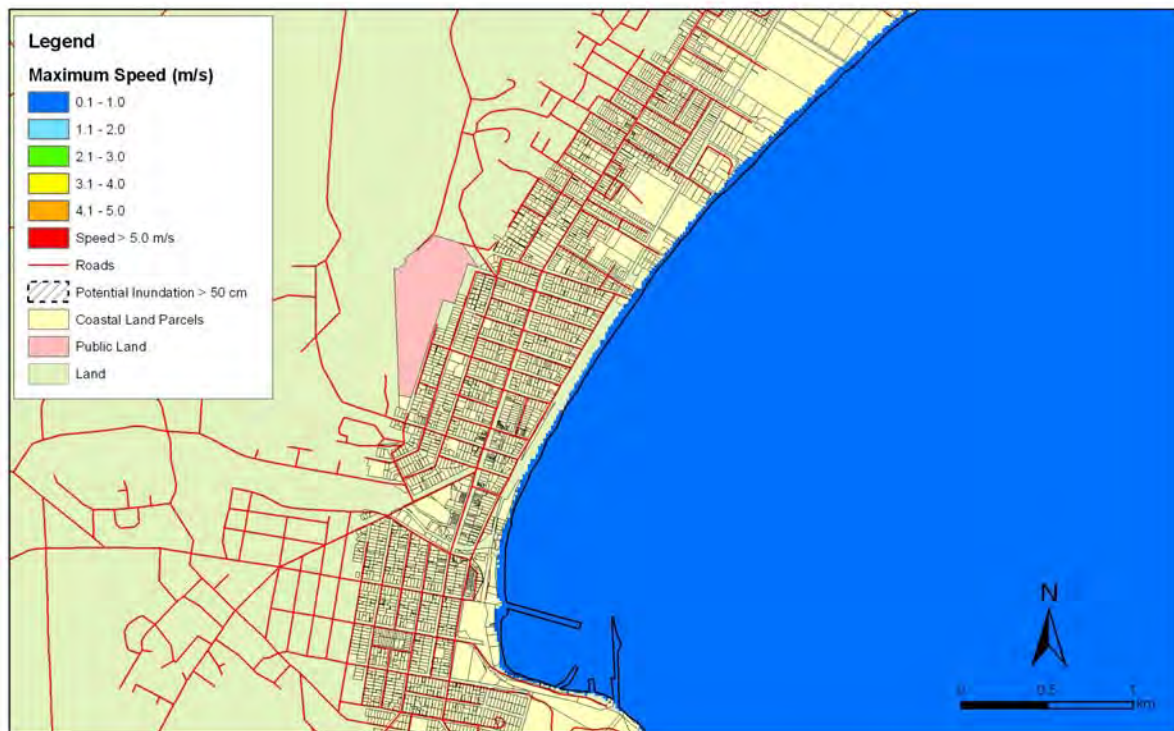


Figure 5.162: Oamaru – 1:500 year remote tsunami: Maximum water depth for inundated land (top) and maximum speed (bottom) for MHWS with a sea level rise of 50 cm.

6. Discussion

6.1 Near-field

There is no evidence of a near-field tsunami affecting the Otago coast since records began in 1840, however, 165 years is not long enough for the Otago coastline to have experienced the full range of possible events that may occur. For instance, in the historical record for Otago there are no local volcanic events, no large local or regional plate interface earthquakes (e.g. along the Puysegur subduction zone) and only a few earthquakes have occurred on a small number of the many local sources.

Local source submarine landslides can cause localised tsunamis. The initial displacement may be large but because they have far smaller wavelengths and have to travel over the continental shelf before reaching land, their effect is considerably reduced. The landslide modelled here was the largest likely to occur in this area. The maximum water level at the coast was around 2 m (indicating a wave amplitude of 1.1 m above the undisturbed level of sea) and this did not occur in the regions of interest. Thus submarine landslide generated tsunamis were not seen as a significant risk to these communities.

A large subduction zone earthquake on the Puysegur fault (especially one that does not rupture the surface) can however cause a significant tsunami on the Otago coastline. It is especially large for the southern part of the coast but can cause waves up to 1.7 metres high even in Oamaru because of trapped waves travelling up the coast. A tsunami of this kind would inundate many areas along the Otago coast.

The earthquake on the Puysegur fault would need to be at least magnitude M_w 7.8 or bigger to generate a tsunami of note given that a magnitude M_w 7.1 earthquake that occurred on the Puysegur fault in 2004 did not generate an identifiable tsunami on the sea level record and a magnitude M_w 7.4-7.7 earthquake in 1945 did not produce a historically recorded tsunami (although this might have been a strike-slip event). Large subduction zone earthquakes on the Puysegur fault have a return period in the order of 600 years. The nature of the fault tends towards infrequent large earthquakes, which also suggests that there are unlikely to be smaller Puysegur-generated tsunamis. In other words, a shorter return period event is unlikely.

This modelling represents a marked advance in our knowledge of near-field tsunami risk on the Otago coastline. Before this only general 'likely sources' had been identified. Here we clearly demonstrate that the Puysegur fault poses significant tsunami risk to the Otago coastline whereas submarine landslides are unlikely to have

much impact. The inundation caused by a Puysegur fault tsunami correlates well with evidence for a large tsunami that occurred in the Otago region in the 14th century (an event that was originally tentatively linked to submarine landsliding; Goff et al., 2006). This is strong evidence for the Puyusegur fault having a significant rupture (earthquake) at this time given that we have demonstrated that submarine landslides in the area unlikely to cause a large-scale tsunamis.

6.2 Far-field

There have been several remote tsunamis that have occurred within recorded history, most notably the 1868, 1877 and 1960 Chilean earthquakes which all generated tsunamis on the New Zealand coast. The 1868 tsunami caused the most widespread damage due to its source geometry guiding it directly towards New Zealand. While the 1960 earthquake was significantly larger its source geometry was such that the tsunami it generated passed mostly to the north of New Zealand. Limited observation data from these events on wave period, number of tsunami waves, variability along coast, etc, make it difficult to replicate tsunami wave trains and fully validate models. This far-field tsunami model however, has been checked against results of the historical tsunamis that exist for Lyttelton Harbour. This showed that RiCOM was able to satisfactorily replicate the behaviour and resonances of the tsunamis with the coastal geography.

The sizes of the waves generated by the remote tsunamis were similar along the entire Otago coastline. The differences were mainly due to the local geography and topography of the areas in question. The 1:500 year tsunami produced similar results to the 1:100 year tsunami with the wave amplitudes being around 50% bigger.

7. Conclusions

This study has investigated the effects of near- and far-field tsunamis on the Otago coastline. The numerical modelling carried out for this study has identified that the largest tsunami that the Otago region faces is one generated by a large subduction zone earthquake on the Puysegur fault.

The Puysegur tsunami is especially large for the southern portion of the Otago coastline. Further north, around the Otago Peninsula, its effects are comparable with a 1:100 year remote tsunami. North of the Otago Peninsula, remote events may cause more inundation than Puysegur tsunamis although the latter are still significant.

While inundation from the 1:100 year remote tsunami is relatively small in many places, this sort of event occurs more frequently and thus the associated risks and cumulative effects associated should not be overlooked.

Sea level rise exacerbates the effect of all of the tsunamis. When interpreting the sea level rise results from this tsunami modelling it must be remembered that some areas may be inundated at times simply because of the sea level rises and the ordinary tidally- and atmospherically-forced sea level fluctuations. Furthermore, sea level rise will cause erosion and changes to the coastline of its own which will also influence the inundation caused by the tsunamis.

Results for the inundation of private land in this report are only preliminary given the apparent problems with the accuracy of the information specifying private land provided to us. Furthermore, the resolutions of the model, coastline and GIS data mean that, especially right at the coast, areas of minor inundation are equivocal.

Even in regions where no inundation is indicated caution should be exercised in the event of a tsunami. The succession of incoming and outgoing tsunami waves can still be dangerous if you are on the beach or in an estuary or river mouth. Tsunamis have also been known to cause cliff erosion and rapid currents in rivers amongst their other hazards. Dunedin Harbour is well sheltered from tsunamis and although sea level fluctuations are observed they are no more than can ordinarily be seen due to tidal and atmospheric forcing, although some changes in current speed may be experienced.

This work represents a best estimate of the inundation on the Otago coastline caused by near- and far-field tsunamis. While every effort has been made to ensure accurate results, these are based upon our current state of knowledge.

8. References

- Assier Rzadkiewicz, S.; Mariotti, C.; Heinrich, P. (1997). Numerical simulation of submarine landslides and their hydraulic effects, *Journal of Waterway, Port, Coastal, and Ocean Engineering*, 123, 149-157.
- Beanland, S.; Berryman, K. (1989). Style and episodicity of late Quaternary activity on the Pisa-Grandview Fault Zone, Central Otago, New Zealand. *NZ Journal of Geology & Geophysics* 32: 451-461.
- Berryman, K. (2005). Review of Tsunami Hazard and Risk in New Zealand. Prepared for Ministry of Civil Defence and Emergency Management. Institute of Geological & Nuclear Sciences (GNS) client report 2005/104. (www.mcdem.govt.nz/)

memwebsite.nsf/Files/Tsunami_Hazard_report/\$file/Final_Hazard_and_Risk_Report-web.pdf)

Carter, L.; Carter, R.M. (1988). Late Quaternary development of left-bank-dominant levees in the Bounty Trough, New Zealand. *Marine Geology* 78: 185-197.

Carter, R.M. (1988). Post-breakup stratigraphy of the Kaikoura Synthem (Cretaceous-Cenozoic), continental margin, southeastern New Zealand. *NZ Journal of Geology & Geophysics* 31: 405-429.

Carter, R.M.; Carter, L. (1987). The Bounty Channel system: A 55-Million-Year-Old Sediment Conduit to the Deep Sea, Southwest Pacific Ocean. *Geo-Marine Letters* 7: 183-190.

Carter, R.M.; Carter, L. (1996). The abyssal Bounty Fan and lower Bounty Channel: evolution of a rifted-margin sedimentary system. *Marine Geology* 130: 181-202.

Casulli, V.; Cattani, E. 1994. Stability, accuracy, and efficiency of a semi-implicit method for three-dimensional shallow water flow. *Computers Mathematical Applications* 27(4): 99-112.

Cisternas, M.; Atwater, B.F.; Torrejón, F.; Sawai, Y.; Machuca, G.; Lagos, M.; Eipert, A.; Youlton, C.; Salgado, I.; Kamataki, T.; Shishikura, M.; Rajendran, C.P.; Malik, J.K.; Rizal, Y.; Husni, M. (2005). Predecessors to the giant 1960 Chile earthquake: *Nature* 437: 404-407.

De Lange, W.P.; Healy, T.R. (1986). New Zealand tsunamis 1840-1982. *NZ Journal of Geology & Geophysics* 29: 115-134.

Downes, G.; Cochran, U.; Wallace, L.; Reyners, M.; Berryman, K.; Walters, R.; Callaghan, F.; Barnes, P.; Bell, R. (2005). EQC Project 03/490 – Understanding local source tsunami: 1820s Southland tsunami. Prepared for EQC Research Foundation. (GNS client report 2005/153, NIWA client report HAM2005-135).

Doser, D.I.; Webb, T.H.; Maunder, D.E. (1999). Source parameters of large historical (1918-1962) earthquakes, South Island, New Zealand. *Journal of Geophys. Int.* 136: 769-794.

Dunedin City Council dangerous, insanitary and earthquake-prone buildings policy.
http://www.cityofdunedin.com/city/?page=policy_epbuilding

Dunedin City Lifelines Project Report. December 1998,

http://www.cityofdunedin.com/city/?page=cd_lifelines

Elverhøi, A.; Harbitz, C.; Dimaks, P.; Mohrig, D.; Marr, J.; Parker, G. (2000). On the dynamics of subaqueous debris flows, *Oceanography*, 13, 109-117.

Gersonde, R.; Kyte, F.T.; Bleil, U.; Diekmann, B.; Flores, J.A.; Gohl, K.; Grahl, G.; Hagen, R.; Kuhn, G.; Sierro, F.J.; Völker, D.; Abelman, A.; Bostwick, J.A. (1997). Geological record and reconstruction of the late Pliocene impact of the Eltanin asteroid in the Southern Ocean. *Nature* 390: 357-363.

Goff, J.R.; Hicks, D.M.; Hurren, H. (2006). Tsunami geomorphology in New Zealand. National Institute of Water & Atmospheric Research Technical Report 128.

Han, G.; Wang, D. (1996). Numerical modelling of Anhui debris flow, *Journal of Hydraulic Engineering (ASCE)*, 122, 262-265.

Heath, R.A. (1976). The response of several New Zealand harbours to the 1960 Chilean Tsunami. Tsunami Research Symposium 1974. *Royal Society of New Zealand Bulletin* 15: 71-82.

Henry, R.F.; Walters, R.A. (1993). A geometrically-based, automatic generator for irregular triangular networks. *Communications in Numerical Methods in Engineering* 9: 555-566.

Iverson, R.M.; Denlinger, R.P. (2001). Flow of variably fluidized granular masses across three-dimensional terrain: 1. Coulomb mixture theory. *Journal of Geophysical Research* 106 (B1), 537-552.

Johnstone, T. (1990). A seismic reflection investigation of the extent and geometry of recent northeast-trending faults of the Otago shelf. Unpublished MSc thesis, lodged in the library, University of Otago, Dunedin, New Zealand.

Lamarche, G.; Lebrun, J-F. (2000). Transition from strike-slip faulting to oblique subduction: active tectonics at the Puysegur Margin, South New Zealand. *Tectonophysics* 316 :67-89.

Litchfield, N.J.; Norris, R.J. (2000). Holocene motion on the Akatore Fault, south Otago coast, New Zealand. *NZ Journal of Geology & Geophysics* 43:405-418.

- Liu, Z.; Bird, P. (2002). Finite element modeling of neotectonics in New Zealand. *Journal of Geophysical Research* 107(B12), 2328, doi:10.1029/2001JB001075, 2002.
- Lynett P.; Liu P. (2002). A numerical study of submarine-landslide-generated waves and run-up. *Proceedings of the Royal Society of London A*, 458: 2885-2910.
- McCue, K. Seismic hazard mapping in Australia, the Southwest Pacific and Southeast Asia. Australian Geological Survey Organisation, GPO Box 378 Canberra ACT 2601, Australia (<http://www.seismo.ethz.ch/gshap/swpacific/swpacific.html>).
- NGDC Tsunami Database. National Geophysical Data Center. Website http://www.ngdc.noaa.gov/seg/hazard/tsevsrch_idb.shtml
- NGDC Significant Earthquake Database. National Geophysical Data Center. Website <http://www.ngdc.noaa.gov/nndc/struts/form?t=101650&s=1&d=1>
- New Zealand Nautical Almanac 2006/07. LINZ. website: <http://www.hydro.linz.govt.nz/nautical-almanac/index.asp>
- Norris, R.J.; Litchfield, N. (1996). Map of Offshore Quaternary Faults, Shag Point – Nugget Point Region and accompanying report “*Late Quaternary Faults offshore from East Otago*”. Prepared for Tonkin & Taylor Ltd.
- Sadek, E.A. (1980). A scheme for the automatic generation of triangular finite elements. *International Journal of Numerical Methods in Engineering* 15: 1813-1822.
- Staniforth, A.; Côté, J. (1991). Semi-Lagrangian integration schemes for atmospheric models—A review. *Mon. Weather Review* 119: 2206-2223.
- Stelling, G.; Zijlema, M. (2003). An accurate and efficient finite-difference algorithm for non-hydrostatic free-surface flow with application to wave propagation. *International Journal for Numerical Methods in Fluids* 43: 1-23.
- Walters, R.A. (2002). From River to Ocean: A Unified Modeling Approach. pp. 683-694. *In: Estuarine and Coastal Modeling: Proceedings off the 7th International Conference*. M.L.Spaulding, M.L. (Ed.). ASCE.

- Walters, R.A. (2004). Tsunami generation, propagation, and runup. Pp. 423-438. *In: Estuarine and Coastal Modeling: Proceedings of the 8th International Conference*. Spaulding, M.L. (Ed.). ASCE: 423-438.
- Walters, R.A. (2005a). Coastal Ocean models: Two useful finite element methods. *Continental Shelf Research* 25(7-8): 775-793.
- Walters, R.A. (2005b). A semi-implicit finite element model for non-hydrostatic (dispersive) surface waves. *International Journal for Numerical Methods in Fluid*. 49: 721-737.
- Walters, R.A.; Barnes, P.; Goff, J. (2006a). Locally generated tsunami along the Kaikoura coastal margin: Part 1. Fault ruptures. *New Zealand Journal of Marine and Freshwater Research* 40(1): 1-17.
- Walters, R.A.; Barnes, P.; Lewis, K.; Goff, J., Fleming, J (2006b). Locally generated tsunami along the Kaikoura coastal margin: Part 2. Submarine landslides. *New Zealand Journal of Marine and Freshwater Research* 40 (1): 18-34.
- Walters, R.; Callaghan, F. (2005). Understanding local source tsunamis: 1820s Southland tsunami. Prepared for Institute of Geological and Nuclear Sciences (IGNS). *NIWA Client Report CHC2005-035*.
- Walters R.A.; Casulli, V. (1998). A robust, finite element model for hydrostatic surface water flows. *Comm. in Numerical Methods in Engineering* 14: 931-940.
- Walters, R.; Wild, M.; Fleming, J.; Hurren, H.; Duncan, M.; Willsman, A. (2004). Kaikoura District engineering lifelines project: tsunami hazard assessment (Part 1b). Prepared for Environment Canterbury. NIWA Client Report CHC2004-004/Ecan Report U04/11.

Glossary

M_w	Moment magnitude. This is a logarithmic measure of seismic energy (i.e. an increase in magnitude of 1 is equivalent to recorded wave amplitudes that are 10 times larger, and approximately 30 times the energy). M_w is proportional to slip along the fault \times area of fault surface that slips.
Pliocene	The period in the geologic timescale that extends from 5.332 million to 1.806 million years before present.
Rheology	Study of the deformation and flow of matter under the influence of an applied stress.
Reverse fault	Occur as a result of compression - the hanging wall fault block moves up along the fault surface relative to the footwall fault block.
Subduction zone	Plate boundary where one tectonic plate slides under another, as the two plates move towards each other.
Strike-slip fault	Plate boundary where fault surface is usually almost vertical, and the plate motion is parallel to the fault surface (or strike of the fault). This means movement is predominantly horizontal.
Tsunami amplitude	Vertical height of wave from undisturbed level of sea to crest.
Tsunami height	Vertical crest-to-trough height of waves. This increases substantially as the wave approaches the shoreline.
Tsunami period	Time between successive wave peaks. This can fluctuate during an event and vary at different locations. The period is smaller for a near-field versus a far-field tsunami source.
Tsunami runup	Vertical height the seawater reaches above the mean sea level. Runup is dependent on the type of wave and local bathymetry.

APPENDIX A: Observations from South American Tsunamis

Table A.1: Summary of observations along the Otago coast for 1868, 1877 & 1960 South American tsunamis

Tsunami parameter	Event		
	1868	1877	1960
Source location	Northern Chile	Northern Chile	Southern Chile
Tsunami magnitude ¹	4	4	4
Total water level fluctuation			
Oamaru	4.6-6.1 m	2.5-3.0 m	3.0-4.3 m every 2 hrs with fluctuations of up to 2.1m every 5 mins. Max fluctuation between 4:30-6 am on 24 May when WL rose approx 1.37 m in 20 mins followed by a 2.97 m drop in an hour. Surges of 7-12 ft (2.1-3.7 m), lasting 20 mins occurred approx every hour (de Lange & Healy 1986).
Otago Heads	At 9 am, water rose 1.5 m to the normal high water mark.		
Port Chalmers	0.3-0.4 m	0.4-0.5 m fluctuations within 7-10 minutes at piers at 9:30 am.	Approx 1.3m. Max fluctuation between 8:30-9 pm on 23 May when water fell approx 0.53 m in 15 mins followed by a 0.59 m rise (excl. tides = 0.94 m variation over 1.5 hrs)
Otago Harbour	Less than at harbour entrance.		At 3:25 am at Dunedin a 0.3-0.6 m rise and fall in sea level occurred for 30 mins (de Lange & Healy 1986).
Clutha mouth		0.5 m surge at 10 am, followed by a 1.2 m rise in river level which receded 20 mins later.	0.82 m during high tide on afternoon of 24 th . Generally above 0.5 m until 26 th .
Pounaweia Inlet			Approx 0.5 m fluctuations observed.
(Timaru)	30 ft (9.1 m)		1.8 m
(Bluff)			0.63 m
Maximum water level			
Oamaru	0.6-0.75 m depth in Govt Landing Service Building	Approx 0.8 m above MHWS.	1 m from embankment in front of petrol

Tsunami parameter	Event		
	1868	1877	1960
Source location	Northern Chile	Northern Chile	Southern Chile
Tsunami magnitude¹	4	4	4
	(at noon)	At approx 8 am (low water) water rose. Within 10 mins WL was 1 ft below high water.	installations. 1 m above MHWS at 3 am (1.25 m above predicted tide)
Port Chalmers			0.45 m above high water for 18 minutes. 0.6 m above predicted tide at 9:30 pm.
Otago Harbour			0.3 m above MHWS at 4:20 am (0.35 m above predicted tide level)
Clutha mouth			0.55 m above pre-tsunami tide levels.
Minimum water level			
Oamaru	2.6-3.4 m below OLW (3.4 m is from moored boat being aground). Seabed exposed for 122 m from the shoreline.		1 m below MLWST, could walk out to the end of Holmes Wharf. 0.57 m below MLWS at 8 am (0.53 m below predicted tide level). 1.37 m below predicted tide at 2:15 am.
Otago Harbour			0.2 m below predicted tide at 3:30 am.
Clutha mouth			0.30 m below pre-tsunami tide levels.
Wave period			
Oamaru	Many rapid fluctuations in tide during day with time between rise & fall being as little as 5 minutes.		Onset of tsunami at 10 pm on 23 May with a negative wave of 1.67 m in 20 mins, followed by fluctuations of 1-2 m amplitude at 30-50 min periods.
Otago Heads	Rose to high water mark without breaking, remained at this level for 2 mins, then fell rapidly.		Onset of tsunami at 2:50 am on 23 May with a negative wave of 0.23 m in 50 mins, followed by 0.37 m rise in 40 mins by 4:20 am.
Port Chalmers			Onset of tsunami at 7:40 pm on 23 May with a negative wave of 0.48 m in 20 mins, followed by fluctuations of 0.3-0.5m amplitude at 15-20 min periods.
Clutha mouth		River rose hourly until	Ranged from 30-40 mins

Tsunami parameter	Event		
	1868	1877	1960
Source location	Northern Chile	Northern Chile	Southern Chile
Tsunami magnitude ¹	4	4	4
Bluff		2pm.	(35-45 mins). Tide on 24 th reported to fluctuate every half hour along with normal tide oscillations. Between 12:15 & 3pm the tide rose and fell 7 times (de Lange & Healy, 1986).
Miscellaneous			
Oamaru		At low tide (approx 8am) WL rose 1 m in 10 minutes. Small variations in WL up to noon, then a large wave overtopped the breakwater.	Water level fluctuations of 0.9-2.8m for 30 hrs from 9 am on 24 May. Tidal velocity out of harbour approx 4-5 knots, and quicker into harbour.
Otago Heads	Rate of up-rush at "lower red buoy" of 7 knots. Similar rise & fall of tide as recorded at Oamaru.		Fluctuations of up to 0.65 m approx 8-12 hours after the tsunami peak. Water rise of 0.9-1.2 m when wave hit at 3:15 am.
Port Chalmers	Water level rose and fell short periods all day, with drop of 0.4 m in 2 mins.		
Otago Harbour	Tide rose at 7 ft/hr in inner harbour.		
Taiari mouth	Sudden great rise & reflux of water 16.6 km up Taiari River.		
Clutha mouth			Fluctuations started at (9:30 pm) 10:30 pm on 23 May, and continued at measurable level until 5 pm on 26 May.

¹ Run-up near source of at least 16 m.

APPENDIX B: Background geological information for Otago faults

Takapu Fault Zone - Waipounamou Fault System

Liu & Bird (2002) used a “thin-shell finite element method” (incorporating faults, realistic rheology (see Glossary), laterally varying heat flow and topography, and plate velocity boundary conditions) to simulate neotectonic deformation of New Zealand. Figure B1 shows the fault slip rates derived from this modelling exercise.

Figure B1 includes north-west (NW) and south-east (SE) “hypothesized” coastal faults along the South Island. These faults (that are incorporated in the model), were selected to help explain the shape of bathymetric contours between the Campbell plateau and the South Island continental shelf.

As the SE coastal fault is immediately off the Otago coast, this fault is of particular interest for this tsunami study, especially since detailed seismic data (Carter, 1988) established that the southern part of this coastal fault coincides with the north-eastern part of the Waipounamou Fault System.

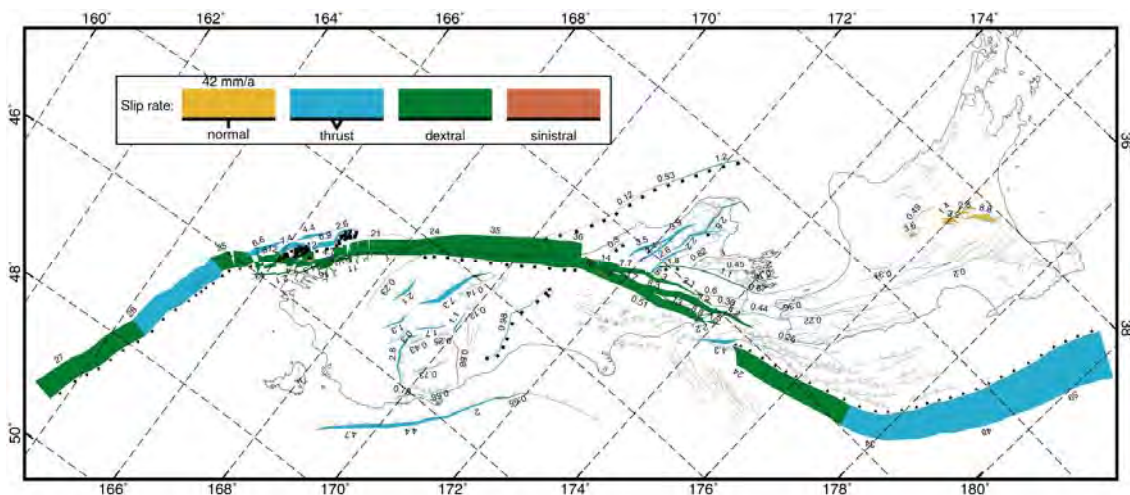


Figure B1: Long-term average fault slip rates predicted by preferred model NZT001 (Mercator projection). The width of each ribbon plotted beside a fault is proportional to long-term slip rate, which is also given by numbers in mm/yr. Faults with very small slip rates are locked and not marked by slip rates in the figure (Liu & Bird, 2002)

The Waipounamou Fault System consists of a series of faults similar to those occurring onshore, and can be observed from south of latitude 49°S to offshore from Dunedin, around latitude 45°50'S (Carter, 1988). Two faults within this fault system (with the most inshore fault being the Takapu Fault), are located approximately 30 km seawards of the Akatore Fault, and can be traced for about 50 km.

In the Liu & Bird (2002) modelling, a single offshore fault represented all the Waipounamou faults. This meant that the interaction and distribution of the slip between the individual faults (that make up the fault system) was not possible - only an estimate of the overall slip accommodated.

APPENDIX C: RiCOM model description

The numerical model used in this study is a general-purpose hydrodynamics and transport model known as RiCOM (River and Coastal Ocean Model). The model has been under development for several years and has been evaluated and verified continually during this process (Walters and Casulli 1998; Walters 2002, 2004, 2005a, 2005b). The hydrodynamics part of this model was used to derive the results described in this report.

The model is based on the Reynolds-averaged Navier-Stokes equations (RANS) that are time-averaged over turbulent time scales. For the simulation of weakly dispersive surface waves, these equations are averaged over water depth to derive a set of equations similar to the standard shallow water equations but contain additional terms that describe non-hydrostatic forces (Stelling and Zijlema 2003; Walters 2005b).

The free surface equation is derived from vertically integrating the continuity equation

$$\frac{\partial \eta}{\partial t} + \nabla \cdot (H\mathbf{u}) = 0 \quad (1)$$

where $\eta(x,y,t)$ is the water-surface elevation measured from the vertical datum, ∇ is the horizontal gradient operator, $h(x,y)$ is the land elevation measured from the vertical datum, and $H = \eta(x,y,t) - h(x,y)$ is the water depth. The vertical datum is arbitrary, but is usually set equal to the average water surface elevation (sea level). This choice minimizes truncation errors in the calculation of the water surface gradients.

After depth-averaging, the horizontal momentum equation becomes

$$\begin{aligned} \frac{D\mathbf{u}}{Dt} + \mathbf{f} \times \mathbf{u} = & -g\nabla\eta - \frac{1}{2}\nabla(q) - \frac{q}{2H}(\nabla\eta + \nabla h) \\ & + \frac{1}{H}\nabla \cdot (HA_h\nabla\mathbf{u}) - \frac{\tau_b}{\rho H} \end{aligned} \quad (2)$$

where D/Dt is a material derivative, \mathbf{u} is the depth-averaged velocity, \mathbf{f} is a vector representation of the Coriolis parameter, q is dynamic pressure which varies linearly in the vertical with $q = 0$ at the free surface, A_h is horizontal eddy viscosity, and τ_b is bottom friction. Surface stress and atmospheric pressure have been neglected. Bottom friction is written as

$$\frac{\tau_b}{\rho H} = \frac{C_D |\mathbf{u}| \mathbf{u}}{H} = \gamma \mathbf{u} \quad (3)$$

where C_D is a drag coefficient and γ is defined by (3). Equations (1) and (2) with $q = 0$ form the classical shallow water equations.

Next, the vertical momentum equation and the continuity equation must be depth averaged to derive governing equations for vertical velocity w and dynamic pressure q . The former is

$$\frac{Dw}{Dt} = -\frac{(q_\eta - q_h)}{H} = \frac{q_h}{H} \quad (4)$$

where w is the depth-averaged vertical velocity, q_η is dynamic pressure at the free surface, q_h is dynamic pressure at the bottom, and the vertical viscous terms have been neglected. The vertically integrated continuity equation is expressed as

$$\int_h^\eta \nabla \cdot \mathbf{u} dz + w_\eta - w_h = 0 \quad (5)$$

This equation is written in finite volume form when it is discretized.

In order to allow flexibility in the discretization of the model grid across the continental shelf, finite elements with unstructured triangular and quadrilateral elements of varying-size and shape are used for the spatial approximation. The time marching algorithm is a semi-implicit scheme that removes stability constraints on gravity wave propagation (Casulli and Cattani, 1994). The advection scheme is semi-Lagrangian which is robust, stable, and efficient (Staniforth and Côté, 1991). Wetting and drying of intertidal or flooded areas occurs naturally with this formulation and is a consequence of the finite volume form of the continuity equation and method of calculating fluxes through the element faces. At open (sea) boundaries, a radiation condition is enforced so that the outgoing wave will not reflect back into the modelled area.

The equations are solved with a split-step method. In the first step, the equations are solved with $q=0$ to derive an approximate solution for the dependent variables (Walters and Casulli, 1998). In the second step, an equivalent of a pressure Poisson equation is solved for q and the velocity solution from step one is corrected (Walters, 2005b).

This method can be expanded in a straightforward manner to 3 dimensions when greater accuracy is required (Stelling and Zijlema, 2003) and provides an alternative to the Boussinesq equations which use higher order velocity and geometry correction terms in the momentum equation (Lynnett and Liu, 2002).

APPENDIX D: Background geological information for Otago submarine landslide

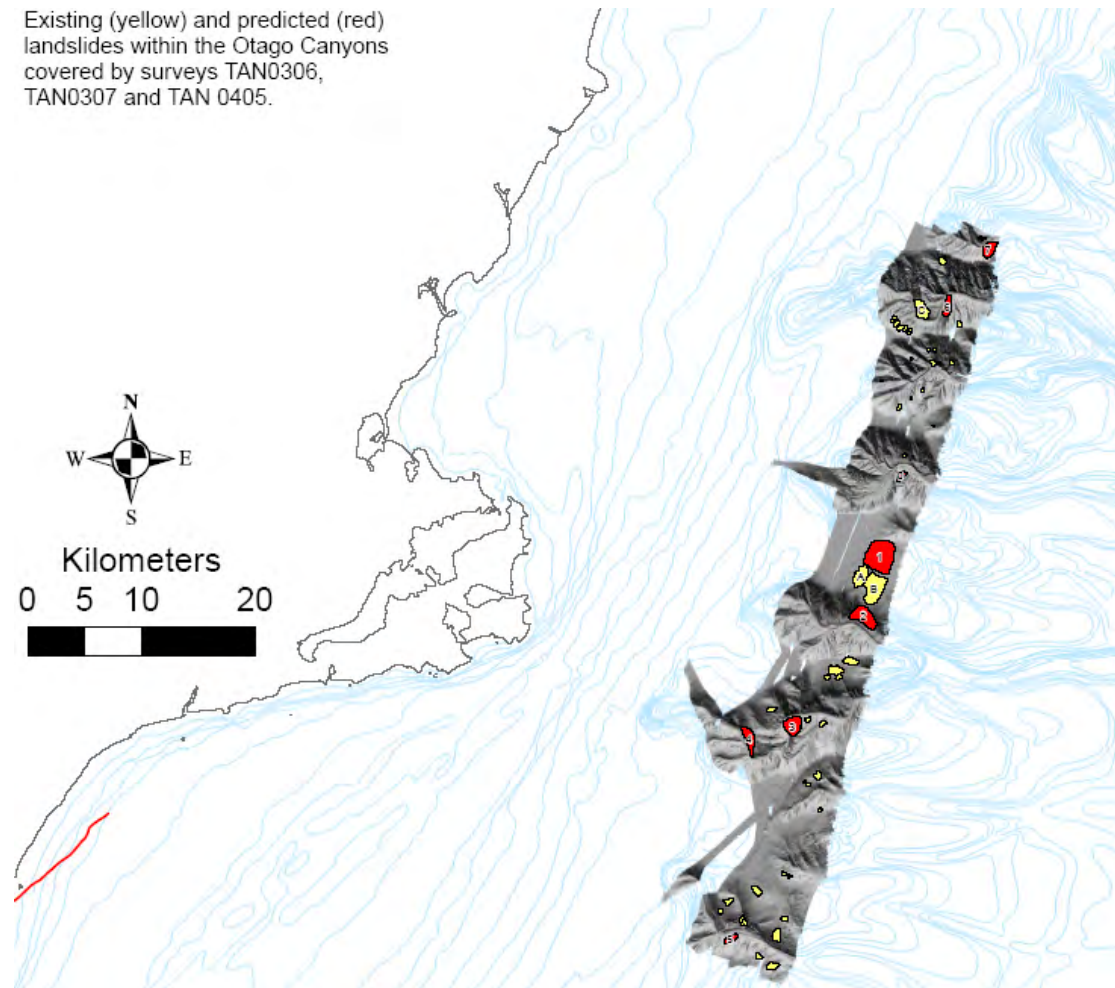


Figure D1: Existing (yellow) and predicted (red) landslides within the surveyed area of the Otago fan complex.

Table D1: Description of existing and predicted submarine failures.

Landslide	ID	Volume (cubic metres)	Bathymetry (m)	Downslope Length (m)	Alongslope Length (m)	movement Quadrant	X (merc41)	Y (merc41)	Failure style
Existing	A	35,000,000	243	1000	2000	SE	5981547.8	-4325442.2	Shallow (20m) deep sheet slide, debris expected to fluidise
Existing	B	60,000,000	344	1700	2500	SE	5982745.32	-4326467.85	Shallow (20m) deep sheet slide, debris expected to fluidise
Existing	C	160,000,000	850	1000	2000	SW	5986899.48	-4302007.26	Translational/Rotational slump style collapse. Horizontal movement approximately 200m.
Potential	0	45,000,000	779	400	1000	NW	5985107.89	-4316591.92	Translational/Rotational slump style collapse.
Potential	1	120,000,000	310	2700	2500	E	5983286.35	-4323674.63	Shallow (20m) deep sheet slide, debris expected to fluidise
Potential	2	550,000,000	581	1200	2400	SW	5981845.32	-4328986.76	Translational/Rotational slump style collapse.
Potential	3	200,000,000	790	1500	1500	W	5975603.2	-4338527.6	Translational/Rotational slump style collapse.
Potential	4	150,000,000	634	850	2000	W	5971763.8	-4339714.46	Translational/Rotational slump style collapse.
Potential	5	50,000,000	692	400	1300	NW	5970141.62	-4357237.87	Translational/Rotational slump style collapse.
Potential	6	100,000,000	969	500	1850	W	5989185.64	-4301755	Translational/Rotational slump style collapse.
Potential	7	120,000,000	590	850	1500	NW	5992867.03	-4296715.82	Translational/Rotational slump style collapse.

APPENDIX E: Velocity vectors for the Clutha Delta

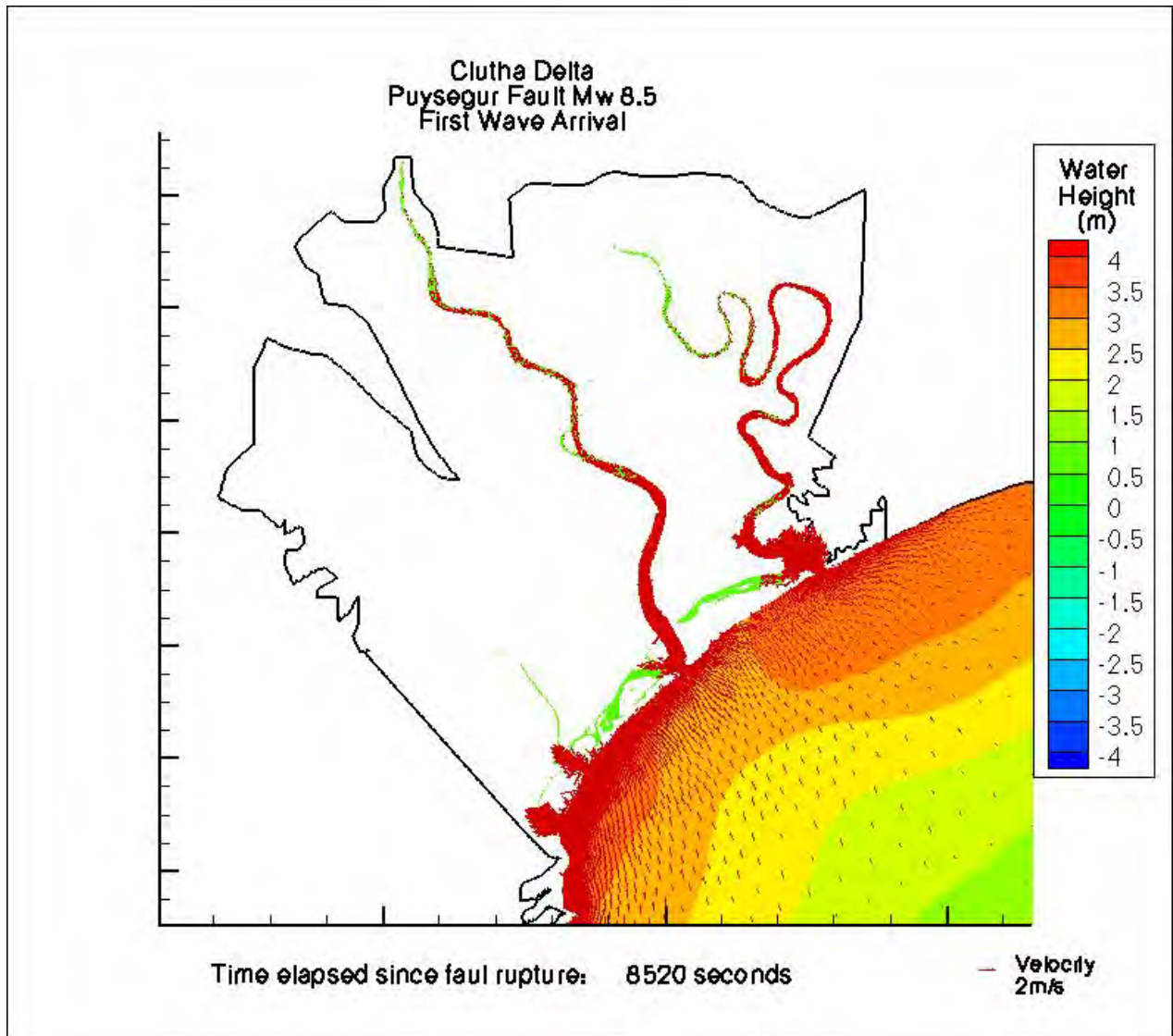


Figure E1: Kaka Point and Clutha – Puysegur 1:100 tsunami: Screen shot from animation showing first large wave arriving at the Clutha Delta with velocity vectors - at MHWS.

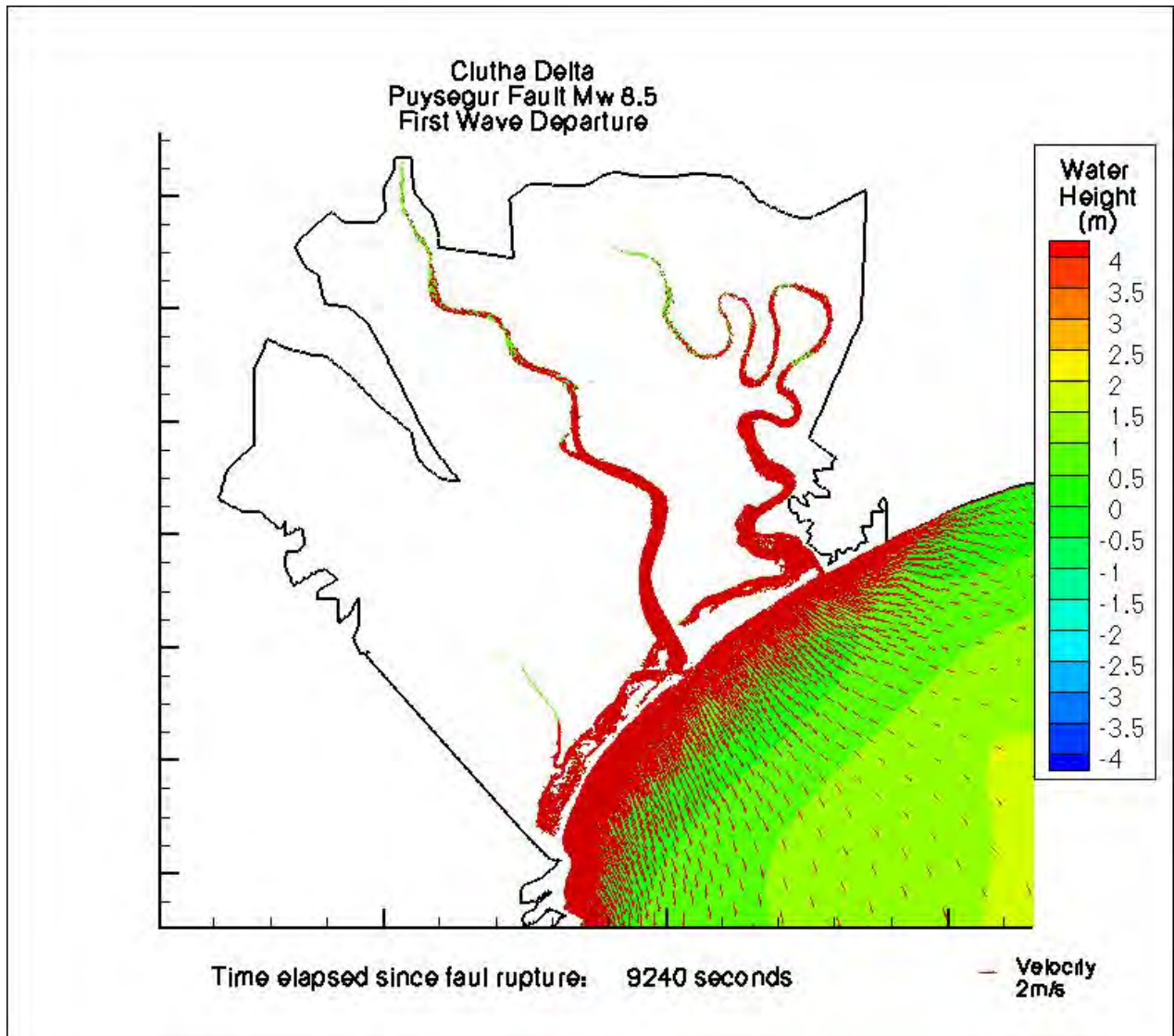


Figure E2: Kaka Point and Clutha – Puysegur 1:100 tsunami: Screen shot from animation showing drawdown following first large wave at the Clutha Delta with velocity vectors - at MHWS.